

Sorption Studies with Sedimentary Rock under Saline Conditions

NWMO TR-2013-22

December 2014

Peter Vilks and Neil H. Miller

Atomic Energy of Canada Limited

nwmo

NUCLEAR WASTE
MANAGEMENT
ORGANIZATION

SOCIÉTÉ DE GESTION
DES DÉCHETS
NUCLÉAIRES

Nuclear Waste Management Organization
22 St. Clair Avenue East, 6th Floor
Toronto, Ontario
M4T 2S3
Canada

Tel: 416-934-9814
Web: www.nwmo.ca

Sorption Studies with Sedimentary Rock under Saline Conditions

NWMO TR-2013-22

December 2014

Peter Vilks and Neil H. Miller
Atomic Energy of Canada Limited

This report has been prepared under contract to NWMO. The report has been reviewed by NWMO, but the views and conclusions are those of the authors and do not necessarily represent those of the NWMO.

All copyright and intellectual property rights belong to NWMO.

Document History

Title:	Sorption Studies with Sedimentary Rock under Saline Conditions		
Report Number:	NWMO TR-2013-22		
Revision:	R000	Date:	December 2014
Atomic Energy of Canada Limited			
Authored by:	Peter Vilks, Neil H. Miller		
Verified by:	Sim Stroes-Gascoyne		
Approved by:	Paul Thompson		
Nuclear Waste Management Organization			
Reviewed by:	Tammy Yang, Frank Garisto, Sarah Hirschorn, Paul Gierszewski		
Accepted by:	Mark Jensen		

ABSTRACT

Title: Sorption Studies with Sedimentary Rock under Saline Conditions
Report No.: NWMO TR-2013-22
Author(s): Peter Vilks and Neil H. Miller
Company: Atomic Energy of Canada Limited
Date: December 2014

Abstract

The purpose of this work was to improve the understanding of sorption processes in brine solutions where high salt concentrations (Na, Ca, Mg, K) may reduce cation sorption through mass action effects, and high ionic strengths may affect chemical reactions in solution and on mineral surfaces. Batch sorption tests were performed for the elements Li(I), Ni(II), Cu(II), Pb(II), Zr(IV) and U(VI) with Canadian sedimentary rocks (shale and limestone) and bentonite and the SR-270 reference brine solution (TDS = 275 g/L). The SR-270 brine contains Na, Ca, Cl, K, Mg, and a number of other minor elements to approximate natural brine. Batch sorption tests were also performed with a dilute reference solution (TDS = 0.49 g/L), containing millimolar amounts of Na, Ca, Cl and HCO₃, to provide a reference case to investigate the effect of salinity on sorption in clays and sedimentary rocks. The studied elements Li(I), Ni(II), Pb(II), and Zr(IV) are not redox sensitive. Although Cu and U are redox sensitive, this study focused on characterizing the sorption behaviour of Cu(II) and U(VI), which are the stable forms of these elements under oxidizing conditions. The sorption data obtained from this study contribute to the development of a database of sorption coefficients (K_d) for Canadian sedimentary rocks and bentonite in highly saline solutions.

Batch sorption tests were performed for time periods up to 127 days using solutions containing single elements (U and Zr) and multiple elements (Li, Ni, Cu, Pb and U). The sorption K_d values of divalent elements Ni, Cu and Pb were 1 to 3 orders of magnitude lower in the reference brine solution than in the dilute reference solution. Short term (1h) sorption tests showed that the sorption of U(VI), Cu(II) and Zr(IV) increased with pH in the range of 5-8. Desorption tests performed for U(VI) indicated that although desorption does occur, the sorption process is not completely reversible. When desorption was initiated, the apparent K_d values were factors of 5 to 7 higher than before desorption. After 55 days of desorption, these apparent K_d values remained at a factor of 2 higher than before desorption.

Using montmorillonite and illite to approximate bentonite and shale (with 60% illite), surface complexation modelling was performed for these minerals using a 2-site protolysis non-electrostatic surface complexation and cation exchange model. In the SR-270 reference brine, where sorption is dominated by surface complexation, the literature derived surface complexation constants for Ni produced simulated K_d values for bentonite and shale (7.0 cm³/g and 1.5 cm³/g) that matched measured values. In the cases where surface complexation constants were estimated using linear free energy relationships (LFER), simulated respective K_d values for bentonite and shale in brine solution were 73 cm³/g and 29 cm³/g for Cu, 6.1 cm³/g and 0.9 cm³/g for Pb, and 1350 cm³/g and 809 cm³/g for Zr. In the dilute reference water, the simulated respective K_d values for bentonite and shale were 1103 cm³/g and 787 cm³/g for Cu, 1089 cm³/g and 89 cm³/g for Pb, and 1544 cm³/g and 801 cm³/g for Zr. The simulated values in brine and dilute solutions differed from measured values by factors of 1.2 to 3.4. The agreement between simulated and measured K_d values provides confidence that sorption models might be used to provide a reasonable estimate of the sorption properties of elements for which experimental sorption data are not yet available in brines.

A diffusive mass transport test was performed with a Queenston shale sample and the SR-270 brine to study the sorption and migration properties of Li, Ni, Cu, Pb and U in shale. The K_d values derived from the batch tests were consistent with K_d values estimated from the diffusive mass transport experiments in shale, providing confidence that the sorption K_d values obtained from the batch sorption tests can be applied to account for sorption in mass transport within shale. The diffusion test was very effective at determining K_d values of weakly sorbing elements (e.g., Li, Ni, Pb) whose K_d values may at times be difficult to determine by batch techniques due to analytical interferences from high salt concentrations. Therefore, diffusive mass transport tests are a valuable complement to batch tests because they provide confidence in the equilibrium approach using K_d values to simulate diffusive mass transport in rock, and they provide another tool for determining K_d values of weakly sorbing elements.

In brine solutions it was discovered that Li is weakly sorbed (K_d values of 0.016 to 0.065 cm³/g on shale) and would be transported about 4 to 5 times slower than groundwater in shale. Ni and Pb are also weakly sorbed on limestone, shale and bentonite; Cu and U are moderately sorbed; Zr is moderately sorbed on limestone and strongly sorbed on bentonite and shale with retardation factors of 17,900 to 19,700.

TABLE OF CONTENTS

	<u>Page</u>
ABSTRACT.....	iii
1. INTRODUCTION.....	1
2. BATCH SORPTION EXPERIMENTS	4
2.1 GENERAL METHODS.....	5
2.2 URANIUM	9
2.2.1 Uranium Sorption as function of pH.....	9
2.2.2 Long Term Uranium Sorption Tests	11
2.2.3 Uranium Desorption Tests.....	13
2.3 ZIRCONIUM	15
2.3.1 Zirconium Sorption Variation with pH	15
2.3.2 Zirconium Sorption with Time	17
2.4 MULTI-ELEMENT (Li, Ni, Cu, Pb, U) SORPTION TESTS.....	19
2.4.1 Long Term Tests in Brine Solution	20
2.4.1.1 Li.....	21
2.4.1.2 Ni.....	23
2.4.1.3 Cu.....	26
2.4.1.4 Pb.....	29
2.4.1.5 U.....	32
2.4.2 Long Term Tests in Dilute Reference Solution.....	36
2.4.3 Short Term Sorption Tests to Evaluate pH Effects on Sorption in Brine Solution.....	43
2.5 SUMMARY	48
3. SORPTION MODELLING	51
3.1 SURFACE COMPLEXATION AND CATION EXCHANGE MODEL	51
3.2 NICKEL	54
3.3 COPPER	57
3.4 LEAD.....	60
3.5 ZIRCONIUM.....	63
3.6 SUMMARY	66
4. DIFFUSIVE MASS TRANSPORT EXPERIMENTS	67
4.1 DEFINITIONS.....	67
4.2 EXPERIMENTAL THEORY	70
4.3 METHOD.....	72
4.4 RESULTS.....	75
5. MASS TRANSPORT MODELLING	79
5.1 METHOD.....	79
5.2 DIFFUSIVE TRANSPORT RESULTS.....	82
5.3 SUMMARY	88
6. SUMMARY AND CONCLUSIONS.....	90
ACKNOWLEDGEMENTS	93

REFERENCES94
APPENDIX A: DATA FROM BATCH SORPTION AND TRANSPORT TESTS 97

LIST OF TABLES

	<u>Page</u>
Table 1: Experimental Solutions Used for Sorption Tests	3
Table 2: Solids Used in Sorption Experiments.....	4
Table 3: Element Concentrations Used in Sorption Tests	6
Table 4: Uranium Sorption Variation with pH by One Hour Short Time Sorption Tests.....	10
Table 5: Uranium Sorption in the SR-270 Brine with Time	12
Table 6: Uranium Desorption with Time.....	15
Table 7: Zirconium Sorption Variation in SR-270 Brine with pH and Time	16
Table 8: Zirconium Sorption in SR-270 Brine with Time	18
Table 9: Lithium Sorption in SR-270 Brine – Normal Conditions	21
Table 10: Lithium Sorption in SR-270 Brine – Sterile Conditions	22
Table 11: Nickel Sorption in SR-270 Brine – Normal Conditions	24
Table 12: Nickel Sorption in SR-270 Brine – Sterile Conditions	25
Table 13: Copper Sorption in SR-270 Brine – Normal Laboratory Conditions.....	27
Table 14: Copper Sorption in SR-270 Brine – Sterile Laboratory Conditions	28
Table 15: Lead Sorption in SR-270 Brine Under Normal Laboratory Conditions.....	30
Table 16: Lead Sorption in SR-270 Brine Under Sterile Laboratory Conditions	31
Table 17: Uranium Sorption in SR-270 Brine – Normal Conditions	33
Table 18: Uranium Sorption in SR-270 Brine – Sterile Conditions	34
Table 19: Lithium Sorption in Reference Dilute Water.....	37
Table 20: Nickel Sorption in Reference Dilute Water.....	38
Table 21: Copper Sorption in Reference Dilute Water.....	40
Table 22: Lead Sorption in Reference Dilute Water	41
Table 23: Uranium Sorption in Reference Dilute Water.....	42
Table 24: Sorption Variation with pH in SR-270 Brine by One Hour Short Term Sorption Tests.....	45
Table 25: Summary of Sorption Coefficients (cm^3/g) for Experimental Reference SR-270 Brine and Reference Dilute Solution	49
Table 26: Surface Protolysis Reactions and Constants for Na-illite and Montmorillonite	52
Table 27: Nickel Surface Complexation Reactions and Surface Complexation Constants	54
Table 28: Calculated Ni K_d Values for Montmorillonite and Illite	55
Table 29: Copper Surface Complexation Reactions and Surface Complexation Constants and Hydrolysis Constants.....	57
Table 30: Calculated Cu K_d Values for Montmorillonite and Illite.....	58
Table 31: Lead Surface Complexation Reactions and Surface Complexation Constants Estimated with LFER and Hydrolysis Constants	60
Table 32: Calculated Pb K_d Values for Montmorillonite and Illite	61
Table 33: Zirconium Surface Complexation Reactions and Surface Complexation Constants and Hydrolysis Constants.....	63
Table 34: Calculated Zr K_d Values on Montmorillonite and Illite	64
Table 35: Tracer Properties Used in Diffusion Test.....	73
Table 36: Parameters Used for Diffusive Mass Transport Modelling with AMBER.....	81
Table 37: Sorption Coefficients and Retardation Factors for Shale	89
Table 38: Sorption Coefficients (cm^3/g) in Brine Solutions Derived from Different Approaches	92

LIST OF FIGURES

	<u>Page</u>
Figure 1: Effect of pH on Uranium Sorption in SR-270 Brine by One Hour Short Time Sorption Tests	11
Figure 2: Variation of Uranium Sorption in SR-270 Brine with Time	13
Figure 3: Uranium Desorption Experiment after a Sorption Time of 112 Days	14
Figure 4: Effect of pH on Zr Sorption in SR-270 Brine, Based on One Hour Sorption Tests ...	17
Figure 5: Effect of Time on Zr Sorption in SR-270 Brine	18
Figure 6: Lithium Sorption in SR-270 Brine as a Function of Time Under Normal and Sterile Laboratory Conditions	23
Figure 7: Nickel Sorption in SR-270 Brine as a Function of Time Under Normal and Laboratory Conditions	26
Figure 8: Copper Sorption in SR-270 Brine as a Function of Time Under Normal and Sterile Laboratory Conditions	29
Figure 9: Lead Sorption in SR-270 Brine as a Function of Time Under Normal and Sterile Laboratory Conditions	32
Figure 10: Uranium Sorption in SR-270 Brine as a Function of Time Under Normal and Sterile Laboratory Conditions	35
Figure 11: Lithium Sorption in Dilute Reference Water as a Function of Time	38
Figure 12: Nickel Sorption in Dilute Reference Water as a Function of Time	39
Figure 13: Copper Sorption in Dilute Reference Water as a Function of Time	41
Figure 14: Lead Sorption in Dilute Reference Water as a Function of Time	42
Figure 15: Uranium Sorption in Dilute Reference Water as a Function of Time	43
Figure 16: Effect of pH on Lithium and Nickel Sorption in SR-270 Brine Using One Hour Short Term Sorption Tests	46
Figure 17: Effect of pH on Copper and Lead Sorption in SR-270 Brine Using One Hour Short Term Sorption Tests	47
Figure 18: Effect of pH on Uranium Sorption in SR-270 Brine Using One Hour Short Term Sorption Tests	48
Figure 19: Simulated Nickel Sorption in SR-270 Reference Brine and in Reference Dilute Solution Under Different pH Values	56
Figure 20: Simulated Copper Sorption in SR-270 Brine and in Dilute Solution Under Different pH Values	59
Figure 21: Simulated Lead Sorption in SR-270 Brine and Dilute Solution Under Different pH Values	62
Figure 22: Simulated Zirconium Sorption in SR-270 Brine and Dilute Water Under Different pH Values	65
Figure 23: Example of Tracer Mass Diffusion in a Through-diffusion Experiment	71
Figure 24: Schematic Diagram of Diffusion Cell	74
Figure 25: Sampling Shale Core to Determine Tracer Diffusion Profiles	74
Figure 26: Lithium Mass Diffusion through Shale Sample after 141 Days of Through Diffusion Test	75
Figure 27: Lithium Diffusion Profile in Shale after 141 Days of Through Diffusion Test	76
Figure 28: Nickel and Lead Diffusion Profiles in Shale after 141 Days of Through Diffusion Test	77
Figure 29: Uranium and Copper Diffusion Profiles in Shale after 141 Days of Through Diffusion Test	78
Figure 30: Simulated Lithium Diffusion Profile after 141 Days of Through Diffusion Test	83
Figure 31: Simulated Nickel Diffusion Profiles after 141 Days of Through Diffusion Test	84
Figure 32: Simulated Lead Diffusion Profiles after 141 Days of Through Diffusion Test	85

Figure 33: Simulated Copper Diffusion Profiles after 141 Days of Through Diffusion Test 86
Figure 34: Simulated Uranium Diffusion Profiles after 141 Days of Through Diffusion Test..... 87

1. INTRODUCTION

In Canada, Adaptive Phased Management (APM) is the federally approved approach for the long-term management of Canada's used nuclear fuel. From a technical perspective, APM involves the emplacement of used nuclear fuel within a Deep Geologic Repository (DGR) within a suitable crystalline or sedimentary rock formation (NWMO, 2005). At typical repository depths (~500 mBGS), sedimentary rocks in Canada may contain Na-Ca-Cl brines with a total dissolved solid (TDS) concentration ranging between 200 and 375 g/L (NWMO, 2011). In the process of assessing long-term DGR performance and safety, the radionuclide sorption properties of shales and limestone, and of clay-based engineered barrier systems, within such deep-seated saline groundwater systems are of interest. To this end, a literature review was undertaken to gather information on sorption processes in highly saline solutions and to develop a database of sorption values for Canadian sedimentary rocks in saline, near neutral pH settings (Vilks, 2011). Gaps in sorption data for saline waters were identified in NWMO's review of sorption in highly saline waters (Vilks, 2009). To address these gaps and to develop a methodology for performing sorption tests in highly saline solutions, sorption experiments in highly saline Na-Ca-Cl solutions (with TDS of 10-300 g/L) and Na-Cl solution (with TDS of 100 g/L) were initiated (Vilks et al., 2011). Sorption experiments have been performed for Ni (can be an analog for transition metals and Pb), Cu, Eu (as an analog to trivalent actinides) and U. These tests confirmed that in brine solutions, transition elements and actinides do sorb by surface complexation.

The purpose of this work is to further the understanding of sorption of radionuclides/elements in brine solutions that will contribute to the continuing development of a sorption database for Canadian sedimentary rocks (and bentonite) in highly saline waters. The strategy of this experimental program was to use a combination of static batch and mass transport sorption tests to characterize sorption reactions and to evaluate their role in mass transport. The sorption studies focused on U(VI), Zr(IV), Pb(II), Cu(II), Ni(II), and Li(I) and a new reference brine solution SR-270-PW (Table 1). The following sorption tests were conducted:

- (1) Batch tests studied sorption as a function of time to identify reaction times required to achieve equilibrium or steady state;
- (2) Desorption tests were performed to evaluate the reversibility of sorption to the dilution of tracer concentrations in solution (keeping in mind that reactions that are too slow under lab conditions may be reversible over geologic time scales);
- (3) Batch tests compared sorption in a reference dilute solution to a brine solution in order to illustrate the effect of salinity on sorption and to help in the testing of sorption models by providing an extreme range in solution compositions;
- (4) Parallel sorption tests were performed under normal laboratory conditions and under sterile conditions to determine whether laboratory tests with brine solutions could be affected by the presence of microbes;
- (5) Sorption experiments were performed using multiple elements for comparison to single-element test to determine whether trace elements compete for the sorption sites;
- (6) Sorption tests in brine solutions were performed with different pH values to characterize the variation in sorption with pH. This information is valuable in formulating sorption

models. Since pH buffers were not used to control pH, the duration of these tests were limited to 1 hour because the solution pH value higher or lower than 6.2 to 6.5 was not stable due to the pH buffering attributed to the rock samples; and

- (7) Diffusive mass transport test was performed to study the migration of Li (conservative tracer), Ni, Cu, Pb and U in shale. The sorption coefficients obtained from the diffusive mass transport experiment are compared to sorption values determined from batch sorption tests to determine whether the sorption coefficients derived from batch testing can be applied to account for sorption effects (i.e., retardation) during mass transport of the element through the rock matrix. Zirconium was not used in the diffusion test because of initial concerns that Zr might interfere with the sorption of the other elements.

Batch sorption measurements were performed with shale and limestone supplied by NWMO, and with bentonite supplied by AECL. The Queenston shale and Cobourg limestone samples were taken from cored borehole samples (DGR1-459.27 mBGS and DGR3-689.02 mBGS) at the Bruce nuclear site in southwestern Ontario. The mineralogical compositions of these solids are summarized in Table 2. Sorption tests were performed in a reference brine solution SR-270, based on the SR-270-PW reference groundwater, and a reference freshwater (Table 1).

Table 1: Experimental Solutions Used for Sorption Tests

Water Name	Natural Reference Brine SR-270-PW	Experimental Reference Brine SR-270	Experimental Reference Dilute Solution
Nominal pH Redox state Eh (mV)	6.0 Reducing -200	6.3 to 6.5 Oxidizing 800	8.0 to 8.2 Oxidizing 800
Solutes	(mol/L)	(mol/L)	(mol/L)
Na	2.179	2.179	0.0042
K	0.320	0.320	-
Ca	0.798	0.798	0.0018
Mg	0.337	0.337	-
HCO ₃	0.0018	0.0018	0.0018
SO ₄	0.00458	0.00458	-
Cl	4.753	4.753	0.0060
Br	0.0213	0.0213	-
Sr	0.0137	0.0137	-
Li	0.00072	0.00072	-
F	0.000105	0.000105	-
I	0.000024	0.000024	-
B	0.0074	-	-
Si	0.00014	0.00014	-
Fe	0.00054	-	-
NO ₃	<0.0002	-	-
PO ₄	-	-	-
TDS (g/L)	275	275	0.49
Water type	Na-Ca-Cl	Na-Ca-Cl	Na-Ca-Cl
*Ionic Strength (mol/L)	6.0	6.0	0.010

* Ionic strength was calculated using PHREEQC, version 2.18.5570 and the SIT database (released on August 15, 2011) (Parkhurst and Appelo, 1999). The ionic strength of SR-270-PW and SR-270 is 6.7 mol/L calculated with Pitzer.dat incorporated in PHREEQC.

Table 2: Solids Used in Sorption Experiments

Geologic Material	Reference	Major Minerals	Expected Properties
Cobourg argillaceous limestone	NWMO, 2011	calcite (81 wt%) dolomite (8 wt%) sheet silicate (6 wt%) quartz (3 wt%)	low CEC surface sites <ul style="list-style-type: none"> • CO₃ major • Si-O minor • Al-O minor
Queenston Shale (Used in batch and diffusion mass transport tests.)	Barone et al., 1990	Illite (40 wt %) chlorite (10 wt %) quartz (26 wt %) calcite (13 wt %) dolomite (5 wt %) feldspar (4 wt %) hematite (trace)	CEC = 12.5 meq/100 g surface sites <ul style="list-style-type: none"> • Si-O major • Al-O major • Fe-O minor • CO₃ minor
Queenston Shale from Bruce nuclear site. (Used mass transport test with hydraulic gradient.)	NWMO, 2011	sheet silicate (40 wt%) quartz (17 wt%) calcite (24 wt%) dolomite (14 wt%) gypsum (trace) anhydrite (trace) halite (trace) hematite (trace) goethite (trace)	surface sites <ul style="list-style-type: none"> • Si-O major • Al-O major • Fe-O minor • CO₃ minor
Wyoming Sodium Bentonite	Lajudie et al., 1995 Liu and Neretnieks, 2006	montmorillonite (75 wt %) quartz (15.2 wt %) feldspar (5 to 8 wt %) calcite (1.4 wt %) kaolinite < 1 wt % illite (< 1 wt %)	CEC = 79 to 85 meq/100 g edge sites (OH)=2.8 meq/100g surface sites <ul style="list-style-type: none"> • Si-O major • Al-O major • CO₃ minor

2. BATCH SORPTION EXPERIMENTS

The batch sorption experiments described in this work measured the sorption properties of Li, Ni, Cu, Zr, Pb and U in the experimental SR-270 reference brine solution. Initially sorption tests were performed with the single elements U and Zr to evaluate the effects of sorption time and pH. Next, sorption tests with multiple elements (Li, Ni, Cu, Pb and U) were performed in a brine solution in both sterile and normal laboratory conditions to study sorption as a function of time and to determine whether microbes affect sorption measurements in brine solutions. Multi-element tests were also performed in a reference dilute solution (Table 1) to highlight the effect of brine on sorption and to help in the testing of sorption models. The multi-element tests were

also used to study the effect of pH on the sorption in brine solutions. The measured sorption coefficients contribute sorption values for elements Ni, Cu, Zr, Pb and U to the sorption database for sedimentary rocks in brines, and provide a comparison to sorption properties observed in mass transport experiments in shale.

2.1 GENERAL METHODS

The shale and limestone samples were first crushed and powdered in the laboratory. Because the bentonite was received in a granular form, its grain size was reduced by gentle grinding with a mortar and pestle. The shale, limestone and bentonite were dry sieved to collect a size fraction between 100 and 200 μm for use in the sorption experiments.

The solutions used in the sorption tests are summarized in Table 1. The experimental reference brine was derived from the natural reference brine (SR-270-PW) composition. The experimental solution was formulated to include most elements from the reference brine. With the exception of U, the elements used for sorption tests in this study are not redox sensitive, and the sorption properties determined under normal atmospheric O_2 concentrations are applicable to subsurface reducing conditions. Uranium exists as U(VI) under atmospheric conditions and as U(IV) under the strong reducing conditions given for the natural reference brine. Since the intent of this work was to study the sorption properties of U(VI), no attempt was made to achieve reducing conditions. The achievement of strong reducing conditions with a pe of -3.4 was beyond the scope of this work. Fe was not included in the reference brine because under oxidizing conditions Fe(II) would be oxidized to Fe(III), resulting in the precipitation of most Fe. The experimental brine also did not contain B because Cu could form B complexes. The dilute reference solution (Table 1) contains millimolar amounts of ions Na, Cl, Ca, and HCO_3 to reflect dilute surface waters, with the HCO_3 concentration set equal to that in the brine. Upon contact with distilled water, minerals will quickly release salts to the water (from porewater and mineral dissolution), and using a starting solution that already contains some ions (as opposed to using distilled water) will minimize changes to water chemistry during sorption tests. The carbonate content of brine and dilute water were identical, to remove the impact of carbonate complexes when comparing sorption results from these two water types. The range of experimental pH values corresponded to the pH conditions imposed on the solutions by bentonite, shale and limestone. Any attempt to alter the pH of an experimental suspension by the addition of acid or base would be temporary as the modified pH would drift back to equilibrium values in a matter of hours. The difference in equilibrium pH between brine and dilute waters is attributed to ionic strength effects, particularly on the activity coefficient of the hydrogen ion.

Copper was obtained as $\text{CuCl}_2 \cdot 2\text{H}_2\text{O}$ (J.T. Baker, Baker analyzed reagent grade). Nickel was added as $\text{NiCl}_2 \cdot 6\text{H}_2\text{O}$ (J.T. Baker, Baker analyzed reagent grade). Lithium tracer solutions were prepared by dissolving $\text{LiOH} \cdot 2\text{H}_2\text{O}$ (Anachemia AC-5474, UN-2680). Lead solutions were prepared by dissolving metallic lead with 50% HNO_3 , and converting the lead to chloride solutions by evaporating to dryness and redissolving in dilute HCl. Uranium solutions were prepared from uranyl nitrate hexahydrate ($\text{N}_2\text{O}_8\text{U} \cdot 6\text{H}_2\text{O}$), supplied by Fluka Chemie AG. Zirconium tracer was prepared by dissolving zirconyl chloride octahydrate ($\text{Cl}_2\text{OZr} \cdot 8\text{H}_2\text{O}$), Sigma-Aldrich (lot#09696APV), into 0.1 mol/L HCl.

Uranium concentration was determined colorimetrically as its bromo-PADAP complex at pH of 7.85 (Johnson and Florence, 1971; Marczenko and Balcerzak, 2000). The uranium detection limit with this method was approximately 7×10^{-7} mol/L. An attempt was made to analyze Zr using the bromo-PDAP spectroscopic method with solutions containing 1×10^{-5} mol/L Zr.

However, early tests indicated that to avoid issues with low Zr solubility, it was necessary to perform experiments with less than 5×10^{-6} mol/L Zr. This was below the practical detection limit of the spectroscopic method. Therefore, Zr concentration was determined with inductively coupled plasma mass spectroscopy (ICP-MS). If samples were diluted by a factor of 5 to reduce salt concentration, ALS Environmental Labs (Winnipeg, MB) could analyze Zr with a detection limit of 2.7×10^{-7} mol/L. However, part way through the sorption studies, ALS changed their analytical protocols (due to problems with high salt concentrations) and the detection limit for Zr increased to unacceptable levels. The analytical protocol was then changed to diluting brine samples by a factor of 101, and sending samples to Activation Laboratories Ltd. (ACTLABS), in Ancaster, ON, for analysis by high resolution ICP-MS. High resolution ICP-MS was also used to measure Li, Ni, Cu, Pb and U in all multi-element batch and mass transport tests. Taking into account the dilution factor, the respective detection limits for Li, Ni, Cu, Pb, U and Zr were 2.9×10^{-4} mol/L, 3.4×10^{-5} mol/L, 1.6×10^{-6} mol/L, 4.4×10^{-7} mol/L, 4.2×10^{-7} mol/L, and 1.1×10^{-6} mol/L. The element concentrations (Table 3) used to initiate sorption tests were determined by both the element analytical detection limits and solubility considerations. Solubility limits for Cu and Zr were 5×10^{-5} mol/L and 5×10^{-6} mol/L, respectively. Solubility limits for Li, Ni, Pb and U were higher than 1×10^{-3} mol/L, and were not a limiting factor.

Table 3: Element Concentrations Used in Sorption Tests

Li(I) (mol/L)	Ni(II) (mol/L)	Cu(II) (mol/L)	Pb(II) (mol/L)	Zr(IV) (mol/L)	U(VI) (mol/L)
2×10^{-2}	1×10^{-4}	1×10^{-5}	5×10^{-5}	1×10^{-6}	1×10^{-5}

The pH of sample solutions was determined with a Radiometer Analytical SAS combined pH electrode (pH C2401-8). The pH electrode was calibrated with NBS reference buffer solution with an ionic strength of 0.1 mol/L (Wu et al. 1988). It is recognized that pH measurements in brine solutions (in neutral pH ranges) may be affected by changes in liquid junction potentials as a result of higher salt concentrations (Hinds et al. 2009; Baumann 1973). A standard procedure of measuring pH was adopted that consisted of determining pH in unstirred samples after the majority of solids had settled out of suspension.

Sorption tests were performed using two different approaches. The first approach involved using a relatively small sample volume (10 or 20 mL) for each test to produce a single sorption measurement. In the second approach the solution volume was increased to 200 mL. This provided the ability to take multiple samples from the same sorption test at various time intervals and to have better control over pH. These methods are described in greater detail in the Appendix (A.1 and A.2) of Vilks et al. (2011).

The reaction vessels used in the small volume tests were polycarbonate, 30 mL volume Oak Ridge type centrifuge tubes. The experimental solid/liquid ratios were varied by using solid weights of 0.1 to 0.5 g, and solution volumes of 20 mL. Mineral solids were first weighed into each centrifuge tube. Then the brine solutions with different element concentrations were

added to each tube. Centrifuge tubes with no minerals were used as blanks to check for sorption on centrifuge tube walls and to serve as a measure of the amount of each element that was available for sorption. Sorption tests were performed with either single elements to avoid competition for sorption sites by different elements, or as multi-element tests to check for the possibility of element competition for sorption sites.

Sorption experiments were performed in contact with the atmosphere, which has a partial CO₂ pressure of 3.3×10^{-4} atm, and a partial O₂ pressure of 0.21 atm (Stumm and Morgan, 1981). The experimental time frame for the small volume tests varied from 1 h to 14 d. Samples were shaken once a day for 15 seconds. At the end of the reaction period, the solids were separated from solution by centrifuging for 15 minutes at 20000 rpm. The supernatant solutions were decanted into clean plastic vials. After measuring pH, the water samples were acidified to pH of 2 with 1 mol/L HNO₃ to ensure that the tested elements remained in solution. This procedure was also performed for the blank solutions.

The larger volume tests were performed using 250 mL, polypropylene Nalgene wide-mouth bottles. The starting solution volume was 200 mL. Depending upon the element and the type of rock, the mass of solids was varied from 1 g (bentonite) to 2 g (shale) and to 5 g (limestone) to optimize the change in element solution concentration produced by the sorption process. The target was to have 40 to 60 percent of the total element sorbed to ensure optimum accuracy in measuring the amount sorbed and the amount left in solution. If the amount of sorption approaches 100 percent, the concentration of the sorbing element in solution approaches zero and likely falls below the detection limit. The resulting uncertainty in the "equilibrium" element concentration in solution will result in a very high uncertainty in the derived sorption coefficient. Furthermore, if sorption is slow to reach equilibrium, and if there is a very large drop in solution concentration, the amount of element sorbed may not have had a chance to equilibrate with the element's lower concentration in solution. In that case the amount of sorbed element may represent equilibrium with a higher dissolved element concentration than is measured. Since sorption coefficients are a ratio of sorbed element concentration divided by dissolved element concentration, the low measured dissolved concentration could produce a sorption coefficient value that is too high.

After weighing out the rock sample into the reaction vessel, reference brine solution without the testing tracer element was added and the rock samples were conditioned in the brine solution for at least one week. During this period, the pH was periodically checked. After the conditioning period, one half of the brine solution (by volume) was removed and replaced with an equal volume of brine containing the element of interest for the sorption test. This step initiated the sorption test. 5 mL of solution was sampled at selected times from the sorption reaction vessel. The samples were centrifuged and a portion (0.2 or 2.5 mL) was removed and acidified with 20 mL of HNO₃. As previously mentioned, the sample volume of 2.5 mL had to be reduced to 0.2 mL to decrease the amount of salt in the samples being analyzed by high resolution ICP-MS. The remaining sample volume was used to determine the pH at the time of sampling.

Blank tests were performed with identical solution volumes and element concentrations, except that they contained no solids. The blank tests were sampled immediately after the sorption test was initiated to confirm the initial concentration of the element being studied. These samples were acidified without centrifuging. Afterwards, the blank tests were sampled every time that the samples were taken for sorption measurements. These samples were centrifuged and acidified in the same way as samples from the sorption experiments. The pH values of blank tests were adjusted to bracket the pH values observed in the reaction vessels with solids.

When test solutions contact with solids, they tend to reach an equilibrium pH value within 1 to 3 days. The equilibrium pH value depends mainly upon the type of solution. Measured pH values decrease with increasing salt concentration, which may be explained to some degree by the increase in the H⁺ ion activity coefficient with higher ionic strength (Wiesner et al., 2006). In most cases the equilibrium solution pH values of bentonite are slightly higher than those of shale and limestone, which are identical. Previous attempts to manipulate experimental pH by the addition of an acid or a base failed to produce steady-state pH values that were significantly different from the equilibrium pH values. Attempts to reduce high solution pH values in sorption experiments included the reduction of solid/liquid ratios, conditioning solids at lower pH and increasing total dissolved carbonate concentration to reduce calcite dissolution. The problem with adding concentrated acid to maintain pH is that the acid will keep dissolving carbonate, thereby changing the solid and solution composition. The use of pH buffers is a possibility, but their use was avoided in this study due to potential effects on sorption reactions.

Sorption results were expressed as sorption coefficients (K_d) and as percent sorbed. Sorption coefficients were calculated as follows:

$$K_d = \frac{S}{C} = \frac{(C_0 - C) \times Vol}{C \times m} \times 1000 \quad (\text{cm}^3/\text{g}) \quad (1)$$

Where: C_0 = initial concentration of sorbate (mol/L) determined from blank solutions
 C = equilibrium concentration of sorbate measured in solution (mol/L)
 S = concentration of sorbate on the solid (mol/g)
 Vol = total volume of solution (L)
 m = mass of sorbing solid in the system (g)
 Conversion factor: 1000 cm³/L

The percent sorbed is defined as

$$\text{percent sorbed} = \frac{\text{mass sorbate removed from solution} \times 100\%}{\text{total sorbate available for sorption}} \quad (2)$$

If sorption measurements are being performed on rock coupons in which the sorbate does not significantly penetrate into the mass of the coupon and sorption occurs mainly on the surface, it is better to report sorption in terms of sorbed mass per specific surface area (A_{sp}). The specific surface area has units of area per mass solid (cm²/g), and may be estimated by BET (Brunauer, Emmett and Teller) measurements. The specific surface areas for the solids were previously determined by BET measurements and were reported by Vilks et al. (2011) to be 249,810 cm²/g, 115,160 cm²/g, and 28,940 cm²/g for bentonite, shale and limestone, respectively. In this case the concentration of sorbate on the solid (S_A) has units of mol/cm², and the sorption coefficient is defined as K_a where

$$K_a = \frac{S_A}{C} \times 1000 \quad (\text{cm}) \quad (3)$$

The value of K_a is related to K_d by the following:

$$K_a = \frac{K_d}{A_{sp}} \quad (4)$$

2.2 URANIUM

The purpose of this chapter is to investigate U(VI) sorption in the experimental reference SR-270 brine solution as a function of pH (Section 2.2.1) and of sorption time (Section 2.2.2). The sorption tests described in this chapter were performed with the single U element. At the completion of the long term sorption experiment, the sorption solution was diluted in order to investigate the reversibility of U sorption (Section 2.2.3). U analyses were performed with the colorimetric bromo-PADAP method. Uranium sorption was also studied as part of multi-element tests in which all tracers were determined by ICP-MS. These latter experiments are described in Chapter 2.4.

Although U may occur in the IV, V and VI oxidation states, only the VI species are likely to be present under the oxidizing conditions of these sorption experiments. In the experimental reference brine solution, the dominant U species predicted by PHREEQC (version 1.18.5570 with SIT database) are $(\text{UO}_2)_2(\text{CO}_3)(\text{OH})_3^-$ (42%), $\text{UO}_2(\text{CO}_3)_3^{-4}$ (34%), $\text{UO}_2(\text{CO}_3)$ (12%) and $\text{UO}_2(\text{CO}_3)_2^{-2}$ (9%). The dominant U species in the dilute water are predicted to be $\text{UO}_2(\text{CO}_3)_2^{-2}$ (89%) and $\text{UO}_2(\text{CO}_3)_3^{-4}$ (9%). Solubility is limited by schoepite, $\text{UO}_2(\text{OH})_2 \cdot \text{H}_2\text{O}$. The dominant solution species and the solubility limiting solid suggest that U would sorb to oxygen sites coordinated to Si or Al, and possibly to carbonate sites.

2.2.1 Uranium Sorption as function of pH

The response of sorption to changes in pH is of interest because it is of use for interpreting the results of sorption models, particularly those involving complexation to amphoteric surface sites. Due to the pH buffering of solutions by the minerals, the sorption time of tests at high and low pH values was only 1 hour. The short reaction times likely do not represent equilibrium conditions. Therefore, the results of these tests can be used to describe sorption trends with pH, but they should not be used for direct comparison to thermodynamic modelling. The initial sorption experiments performed to characterize U sorption as a function pH used the small volume (20 mL) tests in Oak Ridge type centrifuge tubes. The respective weights of bentonite, shale and limestone used in these tests were 0.1, 0.2 and 0.5 g. Preliminary tests showed that since the experimental duration was only 1 h, the observed U sorption was very low in the SR-270 reference brine. Therefore, the carbonate concentration was reduced by a factor of 10 (from 0.0018 to 0.00018 mol/L) to increase the amount of U sorption, thereby facilitating the sorption measurements. Before doing sorption experiments, the solid samples were preconditioned with 20 mL of SR-270 brine for 1 week. Sorption tests were initiated by removing 10 mL of conditioning solution and replacing it with 10 mL of brine containing U, to produce an initial U concentration of 1×10^{-5} mol/L. The pH for each test was set by adjusting the pH of the tracer solution before adding it to the reaction vessel containing solids. The amount of HCl or NaOH required to achieve a desired pH shift was previously determined by trial and error. After 1 h the samples were centrifuged and sampled. A portion of the sample was used for U analysis (acidified with HCl) and the other portion was used to measure pH.

The experimental results are summarized in Table 4 and illustrated in Figure 1. Table A1 in the Appendix provides more information on sorption measurements. Uranium sorption did not change significantly in the pH range of 6 to 7. However, above pH 7 there was a steep increase in sorption with higher pH, with percent sorbed reaching 90% by pH 8. These results show that within the expected pH ranges for the brine solution in contact with sedimentary rocks, U

sorption will not be significantly affected by pH. However, models developed to simulate U sorption should be able to reproduce the significant increase in sorption above pH 7. The purpose of these tests was to illustrate trends in U sorption with pH variation. Since the tests are short term, the reported sorption values are significantly less than equilibrium values. In those cases where the percent sorbed is very high (88% and higher) there is a possibility that the calculated sorption coefficients are too high since the amount of sorbed U was determined by a higher dissolved U concentration than was measured at the end of the test. As indicated by desorption tests (Chapter 2.2.3), these values could be a factor 2 to 7 higher than equilibrium values.

Table 4: Uranium Sorption Variation with pH by One Hour Short Time Sorption Tests

Solid	pH	K_d (cm^3/g)	K_a (cm)	% sorbed
bentonite	2.9	20	8.0×10^{-5}	9
	3.0	18	7.3×10^{-6}	8
	5.8	10	4.2×10^{-5}	5
	6.8	14	5.7×10^{-5}	7
	6.9	18	7.3×10^{-5}	8
	6.9	14	5.7×10^{-5}	7
	7.0	14	5.7×10^{-5}	7
	7.4	95	3.8×10^{-4}	32
	7.5	103	4.1×10^{-4}	34
	7.9	1432	5.7×10^{-3}	88
shale	5.3	3	2.2×10^{-5}	3
	6.0	4	3.8×10^{-5}	4
	6.1	8	7.0×10^{-5}	8
	6.9	9	7.9×10^{-5}	8
	7.0	11	9.7×10^{-5}	10
	7.0	5	4.6×10^{-5}	5
	7.7	92	8.0×10^{-4}	48
	7.7	113	9.9×10^{-4}	53
	8.0	1775	1.5×10^{-2}	95
	8.0	1066	9.3×10^{-3}	91
limestone	5.5	1	3.5×10^{-5}	3
	5.5	0	0	0
	6.0	3	1.1×10^{-4}	8
	6.0	4	1.3×10^{-4}	8
	6.8	4	1.4×10^{-4}	9
	7.1	7	2.4×10^{-4}	15
	7.2	6	2.1×10^{-4}	13
	8.0	970	3.4×10^{-2}	96
	8.0	324	1.1×10^{-2}	89
	8.1	533	1.8×10^{-2}	93

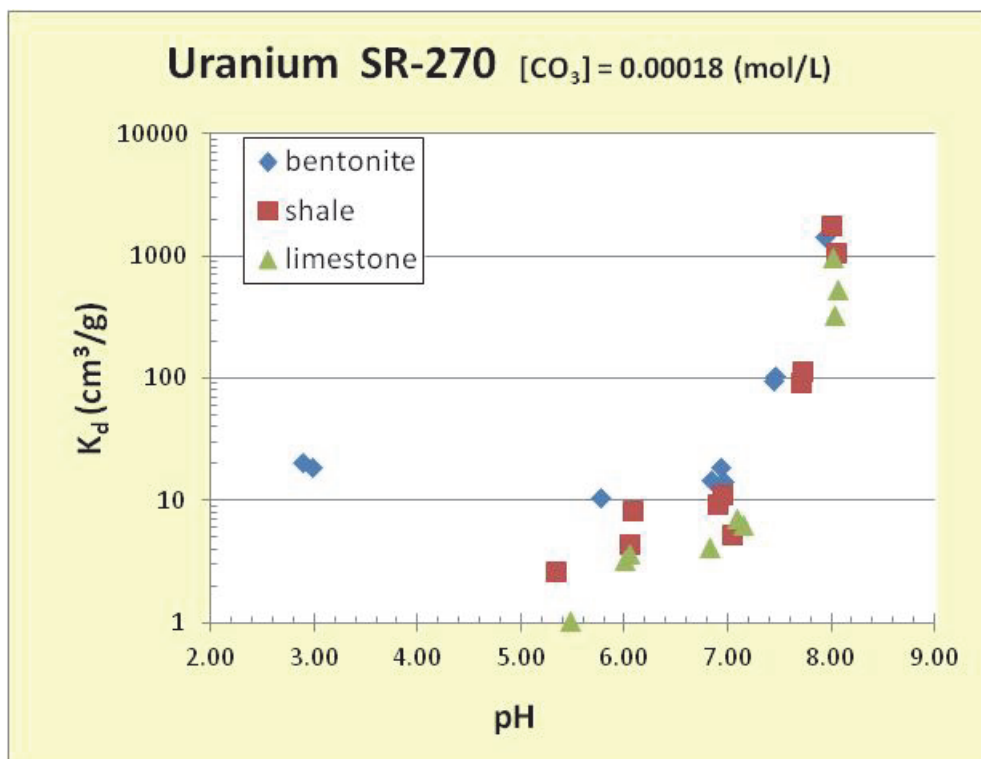


Figure 1: Effect of pH on Uranium Sorption in SR-270 Brine by One Hour Short Time Sorption Tests

2.2.2 Long Term Uranium Sorption Tests

The long term U sorption experiments were performed as large volume tests with initial 200 mL solution volumes. The starting weights of bentonite, shale and limestone were 1.0, 2.0 and 5.0 g, respectively. The total concentration of HCO_3^- in these tests was 0.0018 mol/L, which is standard for the reference SR-270 brine solution. All solids were conditioned for 1 week with U-free brine before starting sorption tests. Sorption tests were initiated by removing 100 mL of conditioning brine and replacing it with 100 mL of brine with tracer U, giving an initial U concentration of 1×10^{-5} mol/L. After shaking the reaction vessels, 5 mL solution samples were removed after sorption reaction times of 1, 7, 14, 28, 42, 56 and 112 days. After measuring the pH of each sample, they were acidified with HCl and saved for U analyses by the colorimetric bromo-PADAP method. The final pH values of the test brines at 112 days, as determined by the sorbing solids, were 6.4 for bentonite, 6.3 for shale and 6.2 for limestone.

The results of the long term uranium sorption tests are summarized in Table 5 and illustrated in Figure 2. Table A2 in the Appendix provides more information on individual sorption measurements, which were used to calculate the average values in Table 5. The values in Table 5 and Figure 2 represent the average of 3 measurements, with reported errors being standard deviations. The percent of total U sorbed ranged from 3 to 16 %. Sorption on

bentonite reached steady state after 14 days. Sorption on shale and limestone continued to increase up to 112 days, suggesting that steady state was not achieved. Considering the longest reaction time (112 d), average U sorption K_d values for bentonite, shale and limestone were 28 ± 6 , 19 ± 1 and 3.8 ± 0 cm^3/g , respectively. Uranium sorption K_d values determined for the SR-270 brine were a factor of 3 to 50 lower than those determined for a 300 g/L Na-Ca-Cl brine (Vilks et al., 2011), which contained only 5×10^{-5} mol/L carbonate (a factor of 36 less than in SR-270 which had 1.8×10^{-4} mol/L carbonate). The pH values of 300 g/L Na-Ca-Cl and SR-270 brines for U sorption tests are very similar. This illustrates that the carbonate concentration has a major impact on U(VI) sorption. PHREEQC calculations indicate that in the SR-270 brine (total carbonate = 0.0018 mol/L) the fraction of U associated with carbonate is 97% and the fraction of hydroxyl species is 3%. In the 300 g/L brine, 21% of U species are carbonate, while 49% are hydroxyl species. The remaining U is associated with neutral and negatively charged chloride species. The factor of 16 higher fraction of hydroxyl species and the reduction in the negatively charged carbonate species, helps to explain why U sorption was higher in the 300 g/L Na-Ca-Cl brine.

Table 5: Uranium Sorption in the SR-270 Brine with Time

Solid	Time (day)	pH	K_d (cm^3/g)	K_a (cm)	% sorbed
Bentonite	1	6.3	13 ± 7	$(5.3 \pm 2.7) \times 10^{-5}$	6 ± 3
	7	6.3	25 ± 6	$(1.0 \pm 0.2) \times 10^{-4}$	11 ± 2
	14	6.4	28 ± 5	$(1.1 \pm 0.2) \times 10^{-4}$	12 ± 2
	28	6.5	27 ± 7	$(1.1 \pm 0.3) \times 10^{-4}$	12 ± 3
	42	6.4	27 ± 4	$(1.1 \pm 0.2) \times 10^{-4}$	12 ± 2
	56	6.4	27 ± 4	$(1.1 \pm 0.2) \times 10^{-4}$	12 ± 2
	112	6.4	28 ± 6	$(1.1 \pm 0.2) \times 10^{-4}$	12 ± 2
Shale	1	6.3	7.6 ± 1.0	$(6.6 \pm 0.8) \times 10^{-5}$	7 ± 1
	7	6.2	13 ± 1	$(1.1 \pm 0.1) \times 10^{-4}$	11 ± 1
	14	6.3	14 ± 0.4	$(1.2 \pm 0.0) \times 10^{-4}$	12 ± 0
	28	6.3	16 ± 2	$(1.4 \pm 0.1) \times 10^{-4}$	11 ± 1
	42	6.3	15 ± 0	$(1.3 \pm 0.0) \times 10^{-4}$	13 ± 0
	56	6.3	17 ± 1	$(1.4 \pm 0.0) \times 10^{-4}$	14 ± 0
	112	6.3	19 ± 1	$(1.6 \pm 0.0) \times 10^{-4}$	16 ± 0
Limestone	1	6.2	1.1 ± 0.2	$(3.8 \pm 0.6) \times 10^{-5}$	3 ± 0
	7	6.2	2.1 ± 0.5	$(7.2 \pm 0.2) \times 10^{-5}$	5 ± 1
	14	6.3	2.7 ± 0	$(9.5 \pm 0.0) \times 10^{-5}$	6 ± 0
	28	6.3	3.3 ± 1.1	$(1.1 \pm 0.4) \times 10^{-4}$	7 ± 2
	42	6.2	3.0 ± 0.2	$(1.1 \pm 1.0) \times 10^{-4}$	7 ± 0
	56	6.2	3.4 ± 0.1	$(1.2 \pm 0.0) \times 10^{-4}$	8 ± 0
	112	6.2	3.8 ± 0	$(1.3 \pm 0.0) \times 10^{-4}$	9 ± 0

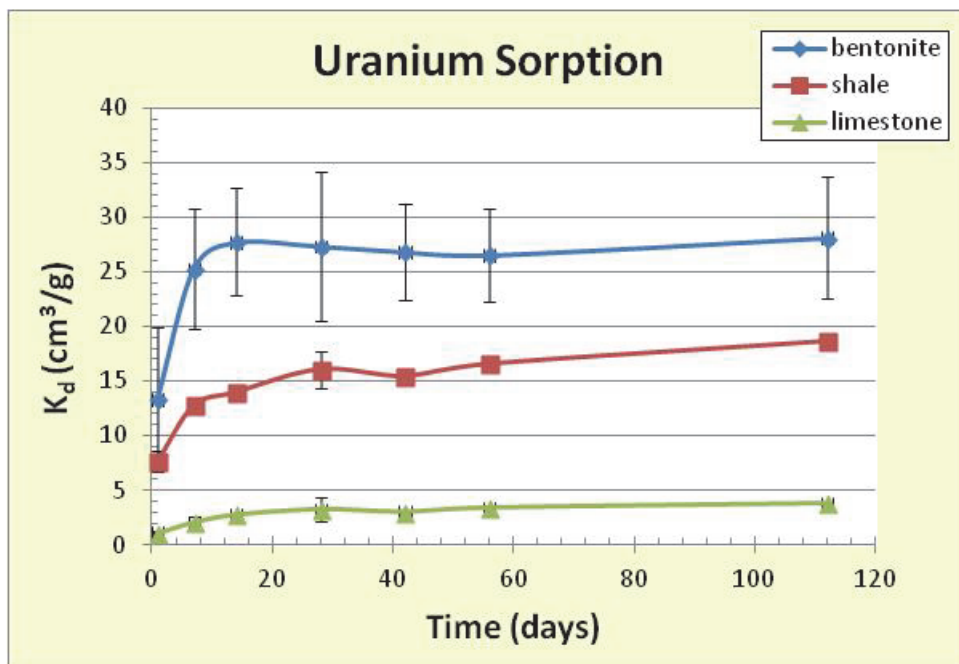


Figure 2: Variation of Uranium Sorption in SR-270 Brine with Time

2.2.3 Uranium Desorption Tests

The purpose of the desorption test was to evaluate the reversibility of U sorption on laboratory time scales. This could be of interest when evaluating the results of mass transport tests performed on comparable time scales. Any irreversibility identified in the lab may not be proof of irreversibility on geologic time scales. The desorption tests were performed after U had sorbed for a total of 112 days. The strategy was to reduce the concentration of U in solution and measure sorption coefficients as a function of time to determine whether the sorption coefficients would return to values observed before desorption was initiated. To achieve this, the contents of each reaction vessel were quantitatively transferred to centrifuge tubes. After ultracentrifuging, the supernatant was removed and replaced with 25 mL of U-free brine solution. The solids on the bottom of each centrifuge tube were dispersed by sonification and immediately 2.5 mL solution was removed for centrifuging and subsequent U analysis. This determines the U concentration immediately after dilution. After 1 h, the sorption test tubes were shaken and sampled again (2.5 mL). This sampling procedure was repeated after 2, 7, 14, 28 and 56 days.

The calculation of sorption coefficients for the desorption phase must account for the removal of dissolved U when 100 mL of solution was replaced with 25 mL of sorbate-free ionic medium.

The basic approach to calculating K_d values during desorption is to determine the mass of U that has desorbed, based on the increase in dissolved U concentration in solution. The K_d value at the time of desorption is calculated by dividing the concentration of sorbate remaining on the solid (S_n) by dissolved sorbate concentration (C_n). The sorption coefficient (nK_d) for desorption interval n (where n is a number 1, 2, etc.) becomes:

$${}^nK_d = \frac{S_n}{C_n} \times 1000 \quad (\text{cm}^3/\text{g}) \quad (5)$$

Where: $S_n = S_{n-1} - \text{des}S_n$ (mol/g)

S_{n-1} = total concentration of sorbate on solid in previous sampling period (mol/g)

$\text{des}S_n$ = desorbed sorbate concentration at sampling interval n

$$= \text{vol}_n \times (C_n - C_{n-1})/m \quad (\text{mol/g})$$

vol_n = total volume in reaction vessel at interval n before sample removed (L)

$$= \text{vol}_{n-1} - \text{vol}_{\text{samp}}$$

vol_{n-1} = volume in reaction vessel at previous sampling event (L)

C_n = dissolved sorbate concentration at interval n (mol/L)

C_{n-1} = dissolved sorbate concentration in previous interval (mol/L)

The results of the U desorption tests are summarized in Table 6 and illustrated in Figure 3. Table A3 in the Appendix provides more information on individual desorption measurements, which were used to calculate the average values in Table 6. The values in Table 6 represent the average of 3 measurements and the error bars shown are standard deviations. The first sorption coefficients determined 3 h after desorption was initiated were a factor of 4.7 to 6.9 higher than the sorption coefficient (K_d^0) measured just before desorption. The drop in K_d/K_d^0 values showed that U desorption from all solids was very rapid during the first day, and then slowed down significantly, particularly after the first week. Uranium desorption from bentonite may continue at a very slow rate after 56 days. Uranium desorption from shale appears to have stopped after 14 days. Since K_d/K_d^0 was still around 2, it seems that a portion of the U is permanently fixed on shale. Desorption from limestone appears to continue after 56 days. Perhaps the ongoing slow desorption rate is due to U diffusing out of limestone porosity. In the original sorption experiment with U sorbing on limestone, sorption did not achieve a steady state within the experimental time frame perhaps because the low porosity of the limestone limited access to sorption sites within rock particles and the rate of sorption to these internal sites was diffusion controlled.

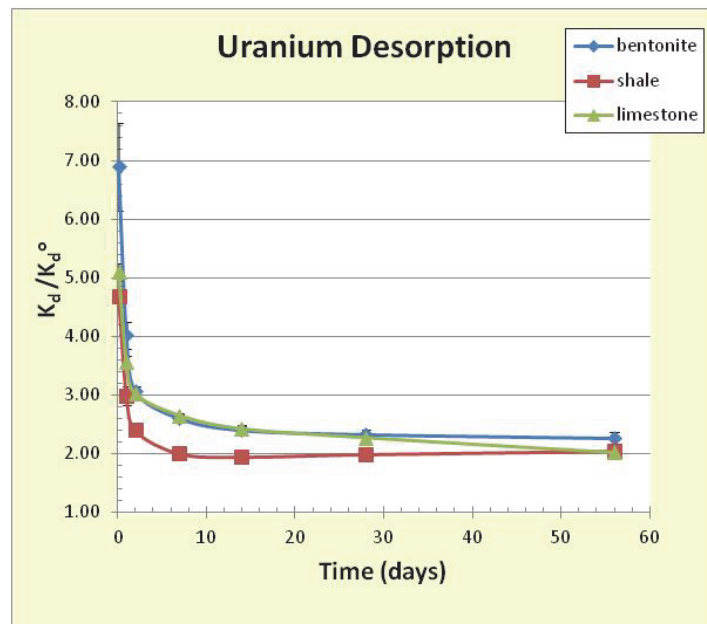


Figure 3: Uranium Desorption Experiment after a Sorption Time of 112 Days

Table 6: Uranium Desorption with Time

Solid	Desorption Time (day)	K_d (cm^3/g)	K_d/K_d^0
Bentonite	0.13	193 ± 32	6.89 ± 0.74
	1	112 ± 17	4.02 ± 0.23
	2	86 ± 15	3.07 ± 0.09
	7	73 ± 12	2.60 ± 0.07
	14	68 ± 12	2.40 ± 0.06
	28	65 ± 11	2.33 ± 0.07
	56	64 ± 10	2.27 ± 0.11
Shale	0.13	87 ± 4	4.68 ± 0.17
	1	56 ± 4	2.99 ± 0.16
	2	45 ± 3	2.39 ± 0.08
	7	37 ± 2	2.00 ± 0.03
	14	36 ± 1	1.94 ± 0.05
	28	37 ± 1	1.98 ± 0.02
	56	38 ± 1	2.04 ± 0.05
Limestone	0.13	19 ± 1	5.10 ± 0.15
	1	14 ± 0	3.56 ± 0.11
	2	11 ± 0	3.02 ± 0.09
	7	10 ± 0	2.65 ± 0.04
	14	9.2 ± 0.2	2.43 ± 0.05
	28	8.6 ± 0.2	2.27 ± 0.05
	56	7.6 ± 0.3	2.02 ± 0.08

2.3 ZIRCONIUM

Zirconium is a transition metal with an oxidation state of IV. PHREEQC (SIT database) predicts that the neutral $\text{Zr}(\text{OH})_4$ will be the only Zr species present in the reference brine solution. Zirconium has a low solubility and is expected to sorb by surface complexation due to its tendency to form hydrolysis species. Zirconium was the only sorbing tracer used in these tests, and Zr was not studied as part of the multi-element tests described later.

2.3.1 Zirconium Sorption Variation with pH

The initial sorption experiments performed to characterize Zr sorption as a function of pH used the small volume (20 mL) tests in Oak Ridge type centrifuge tubes. The respective weights of bentonite, shale and limestone used in these tests were 0.1, 0.2 and 0.5 g. Before starting the sorption experiments, the solid samples were preconditioned with 20 mL of SR-270 brine for 1 week. Sorption tests were initiated by removing 10 mL of conditioning solution and replacing it with 10 mL of brine containing Zr, to produce an initial Zr concentration of 1×10^{-6} mol/L. The

pH for each test was set by adjusting the pH of the tracer solution before adding it to the reaction vessel containing solids. The amount of HCl or NaOH required to achieve a desired pH shift was previously determined by trial and error. After 1 h the solution samples were centrifuged and sampled. A portion of the solution sample was used for Zr analysis (acidified with HNO₃) and the other portion was used to measure pH. Zirconium analysis was done by ICP-MS (ALS Environmental Labs). Several tests at equilibrium solution pH values were performed for 1 and 14 days to obtain a preliminary estimate of the impact of time on Zr sorption.

The results of these sorption tests are summarized in Table 7 as single point measurements. Table A4 in the Appendix provides more information on sorption measurements, which are displayed in Table 7. Zirconium sorption increased significantly on all solids over the 14-day period. The percentage of total Zr that was sorbed increased to as high as 95% for shale. Given the analytical detection limit and Zr solubility limit, the ability to determine sorption values may be limited when the percent sorbed is very high because of difficulties in accurately measuring very low Zr concentrations. In future sorption tests, the ratios of solids to liquids will be significantly decreased to reduce the percent sorbed value and increase the accuracy of measured Zr concentrations. The variation with pH is shown in Figure 4. Zirconium sorption between pH values of 6.5 and 7.0 does not change significantly. However, as the pH approached 8, Zr sorption values increased by a factor of 1.3 to 1.8. Compared to pH effects on U sorption, this was a minor change.

Table 7: Zirconium Sorption Variation in SR-270 Brine with pH and Time

Solid	Time (day)	pH	K _d (cm ³ /g)	K _a (cm)	% sorbed
Bentonite	0.042	6.5	35	1.4 x 10 ⁻⁴	15
	0.042	7.0	36	1.4 x 10 ⁻⁴	16
	0.042	7.8	64	2.6 x 10 ⁻⁴	25
	1	6.6	172	6.9 x 10 ⁻⁴	46
	14	6.6	979	3.9 x 10 ⁻³	83
Shale	0.042	6.5	82	7.1 x 10 ⁻⁴	46
	0.042	7.0	84	7.3 x 10 ⁻⁴	45
	0.042	7.8	138	1.2 x 10 ⁻³	58
	1	6.5	370	3.2 x 10 ⁻³	78
	14	6.4	1967	1.7 x 10 ⁻²	95
Limestone	0.042	6.4	13	8.3 x 10 ⁻⁴	24
	0.042	6.9	12	8.3 x 10 ⁻⁴	24
	0.042	7.9	18	1.1 x 10 ⁻³	31
	1	6.4	47	1.6 x 10 ⁻³	55
	14	6.3	179	6.2 x 10 ⁻³	82

Small volume (20 mL) sorption tests

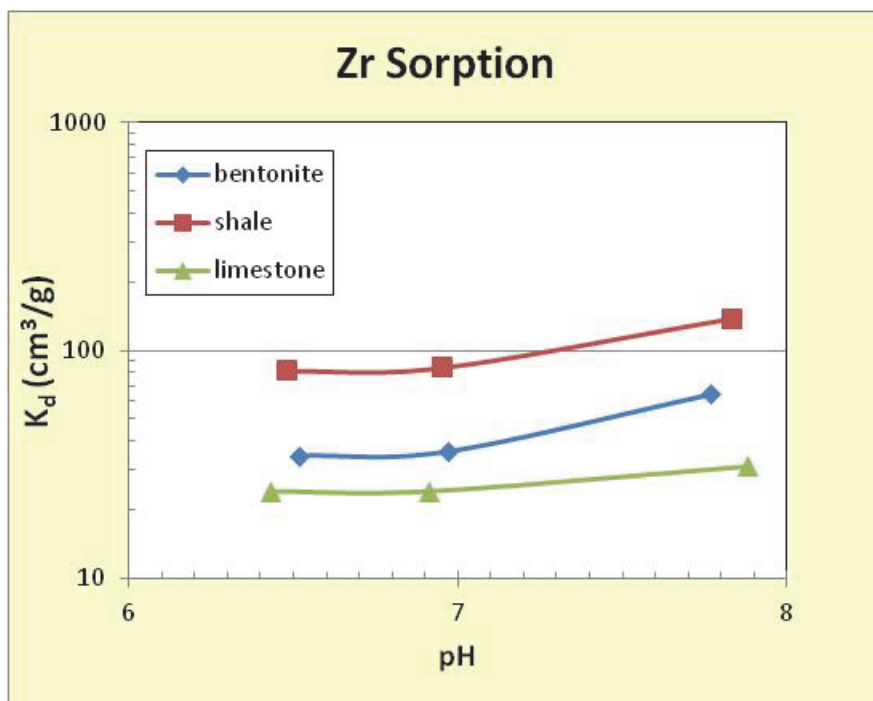


Figure 4: Effect of pH on Zr Sorption in SR-270 Brine, Based on One Hour Sorption Tests

2.3.2 Zirconium Sorption with Time

The long term Zr sorption experiments were performed as large volume tests with initial 200 mL solution volumes. The starting weights of bentonite, shale and limestone were 1.0, 2.0 and 5.0 g, respectively. All solids were conditioned with Zr free brine for 1 week before starting sorption tests. Sorption tests were initiated by removing 100 mL of conditioning brine and replacing it with 100 mL of brine with tracer Zr, giving an initial Zr concentration of 1×10^{-6} mol/L. After shaking the reaction vessels, 5 mL solution samples were removed to determine sorption values after reaction times of 1, 3, 7 and 14 days. After measuring the pH of each sample, they were acidified with HNO_3 and saved for Zr analyses by ICP-MS. Sorption values for longer time periods are not available because ALS changed their analyses protocol, and by the time the new high resolution ICP-MS method was employed the dissolved Zr had fallen below detection limits. The final pH values of the test brine solutions, as determined by the sorbing solids, were 6.6 for bentonite, 6.4 for shale and 6.3 for limestone.

The results of Zr sorption tests with time are summarized in Table 8 and illustrated in Figure 5. The results are reported as average values from 3 measurements, and error bars are standard deviations. In one case for limestone (with no reported errors), the reported value is from a single measurement. Table A5 in the Appendix provides more information on individual Zr sorption measurements, which were used to calculate the average values in Table 8. The total average percentage of Zr sorbed in these tests varied from 25% to 83%. Sorption on bentonite continued to increase till 14 days, and likely would have increased with additional time. Sorption on shale appeared to reach steady state after 7 days. Zirconium sorption on limestone did not

reach a steady state within 14 days. Since the best data for Zr sorption in brine solutions were from the 14 day sorption tests, the final Zr sorption values adopted by this report were derived from these tests. As stated before, future Zr sorption experiments should use a significantly lower solid to liquid ratio to reduce the percentage of sorbed Zr.

Table 8: Zirconium Sorption in SR-270 Brine with Time

Solid	Time (day)	pH	K_d (cm^3/g)	K_a (cm)	% sorbed
Bentonite	1	6.4	70 ± 25	$(2.8 \pm 1.0) \times 10^{-4}$	25 ± 7
	3	6.5	164 ± 31	$(6.6 \pm 0.1) \times 10^{-4}$	45 ± 4
	7	6.5	339 ± 29	$(1.4 \pm 0.1) \times 10^{-3}$	63 ± 2
	14	6.6	454 ± 66	$(1.8 \pm 0.3) \times 10^{-3}$	69 ± 3
Shale	1	6.4	182	1.6×10^{-3}	65
	3	6.4	333 ± 29	$(2.9 \pm 0.2) \times 10^{-3}$	77 ± 2
	7	6.4	494 ± 0	$(4.3 \pm 0.0) \times 10^{-3}$	83 ± 0
	14	6.4	494 ± 0	$(4.3 \pm 00) \times 10^{-3}$	83 ± 0
Limestone	1	6.3	53 ± 21	$(1.8 \pm 0.7) \times 10^{-3}$	55 ± 11
	3	6.3	50 ± 1	$(1.7 \pm 0.0) \times 10^{-3}$	55 ± 0
	7	6.3	89 ± 16	$(3.1 \pm 0.5) \times 10^{-3}$	69 ± 4
	14	6.3	144 ± 31	$(5.0 \pm 1.1) \times 10^{-3}$	78 ± 4

Large volume (200 mL) sorption test

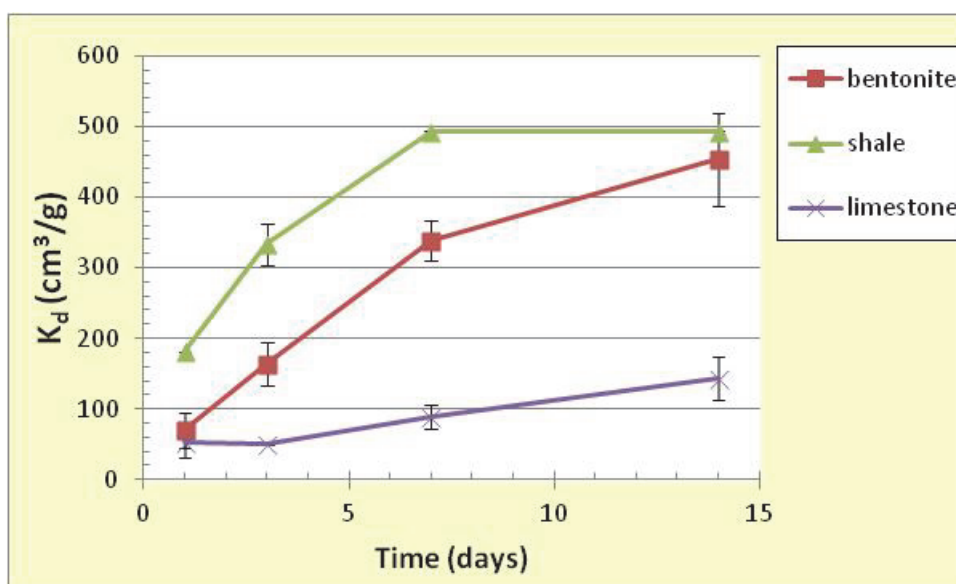


Figure 5: Effect of Time on Zr Sorption in SR-270 Brine

2.4 MULTI-ELEMENT (Li, Ni, Cu, Pb, U) SORPTION TESTS

One of the reasons for performing multi-element tests was to determine to what extent sorbing elements may compete for the same sorption sites. This can be done by comparing the sorption coefficients of U obtained by the multi-element sorption test with the U sorption coefficients obtained with the single element test described in Chapter 2.2.2. The sorption results for Ni and Cu can be compared to previously reported values (Vilks et al., 2011) measured in 300 g/L Na-Ca-Cl brine. Multi-element tests are possible because ICP-MS can determine the concentration of a number of different elements in the same analysis. Multi-element tests are therefore less expensive than single-element tests. The experiments described in this chapter include tests with the experimental reference SR-270 brine, as well as the reference dilute solution.

The element selection for multi-element sorption tests was based on having a range of sorption values from very weak to moderately strong. Zirconium was not included because its sorption coefficient is very high and preliminary calculations with surface complexation models indicated that there was a possibility that Zr could affect the sorption of some of the other elements.

The predicted solution chemistry of the sorbing elements is expected to have a significant impact on their sorption properties. The cation Li^+ is the only Li species expected to be present in brine and dilute solutions. Since Li does not form significant complexes with oxygen-containing anions its ability to form surface complexes is limited. Also, since it has the largest hydrated radius of the Group 1 elements, its ability to compete with other cations in brine solutions is expected to be small. Therefore, Li is not expected to sorb to any significant extent but was included in the multi-element tests to evaluate its sorption properties and determine its suitability for use as a conservative tracer in mass transport experiments described later in this report.

In the reference brine solution, the dominant soluble Ni species are predicted to be NiCl^+ (65%) and Ni^{2+} (35%), while in the reference dilute water, the dominant species are Ni^{2+} (88%), and NiCO_3 (6%). Solubility limiting solids for Ni in brine and dilute solution are Ni(OH)_2 and $\text{NiCO}_3 \cdot 5.5\text{H}_2\text{O}$, suggesting that Ni has an affinity for carbonate and oxygen sites coordinated with Si, Al or another metal. Nickel is expected to sorb by a combination of surface complexation and cation exchange, although the latter is probably limited in brine solutions due to the mass action of salts. Since Ni^{2+} has a relatively simple chemistry and a higher solubility than other elements such as Cu^{2+} , it is relatively simple to use experimentally.

Copper is a transition element, which will be present as a divalent cation under oxidizing conditions. The dominant copper species in the reference SR-270 brine solution used in this study are predicted to be CuCl_2 (49%), CuCl^+ (40%) and Cu^{+2} (10%). In the reference dilute solution the dominant species are Cu(OH)_2 (87%) and CuCO_3 (11%). Solubility in both solutions is limited by Cu(OH)_2 and to a lesser extent by CuCO_3 . Therefore, Cu chemistry will be affected by pH and total carbonate concentration. Furthermore, Cu is likely to sorb to exposed oxygen sites on silicate minerals, and carbonate sites in calcite or dolomite. Although Cu could be expected to sorb by a combination of surface complexation and cation exchange, the latter is probably suppressed in brine solutions due to the mass action of salts.

Lead is a Group 14 metal, which is expected to be in the II oxidation state. PHREEQC (version 2.18.5570, SIT database) predicts that in the reference brine Pb aqueous chemistry will be dominated by the anionic chloride species PbCl_4^{-2} (92%) and PbCl_3^- (6%). In the dilute water,

the dominant Pb species is PbCO_3 (91%), with lesser amounts of PbOH^+ (4%), Pb^{+2} (2%) and $\text{Pb}(\text{CO}_3)_2^{-2}$ (2%). The dominance of anionic chloride species and the lack of Pb^{+2} in brine suggests that Pb would probably not sorb as strongly as Ni and Cu. However, as will be seen later from the results of sorption measurements and modelling, the Ni and Pb sorption K_d values for brine are similar. This indicates that an examination of solution species alone, does not provide the whole story for sorption processes.

As previously mentioned, the dominant U species in the experimental reference SR-270 brine solution predicted by PHREEQC (version 1.18.5570 with SIT database) are $(\text{UO}_2)_2(\text{CO}_3)(\text{OH})_3^-$ (42%), $\text{UO}_2(\text{CO}_3)_3^{-4}$ (34%), $\text{UO}_2(\text{CO}_3)$ (12%) and $\text{UO}_2(\text{CO}_3)_2^{-2}$ (9%). The dominant U species in the dilute solution are predicted to be $\text{UO}_2(\text{CO}_3)_3^{-4}$ (89%) and $\text{UO}_2(\text{CO}_3)_3^{-4}$ (9%).

2.4.1 Long Term Tests in Brine Solution

The long term multi-element sorption experiments were performed as large volume tests with initial 200 mL solution. The starting weights of bentonite, shale and limestone were 1.0, 2.0 and 5.0 g, respectively. All solids were conditioned with tracer free brine for 1 week before starting sorption tests. Sorption tests were initiated by removing 100 mL of conditioning brine and replacing it with 100 mL of brine containing tracers. The starting tracer concentrations were 2×10^{-2} mol/L Li, 1×10^{-4} mol/L Ni, 1×10^{-5} mol/L Cu, 5×10^{-5} mol/L Pb, and 1×10^{-5} mol/L U. After shaking the reaction vessels, 5 mL samples were removed to determine sorption values after reaction times of 1 to 127 days. After measuring the pH of each solution sample, they were acidified with HNO_3 and saved for concentration analyses by ICP-MS. The final pH values of the test solutions after the reaction time of 127 days, as determined by the sorbing solids, were 6.5 for bentonite, 6.4 for shale and 6.3 for limestone.

Since all the sorption tests were conducted in the standard laboratory conditions, the potential effect of microbes existing in the laboratory conditions that may affect the element sorption behaviour in brine solution was investigated by performing two parallel sets of experiments. One set was performed with standard laboratory protocols without any additional steps to remove microbes. The other set was performed under sterile conditions. The purpose of these sorption test comparisons was to evaluate the potential effect of microbes in the laboratory and was not intended to investigate the effect of microbes on the sorption of elements in brine solutions under in-situ conditions in the geosphere which is expected to be negligible. After weighing out the solids into the reaction vessels, the solids and vessels were sterilized by autoclaving at 121°C for 20 minutes. The solids were allowed to cool for 2 days, after which the autoclaving was repeated to kill any spores that may have survived the first autoclaving. The brine solutions and tracers were autoclaved once for 15 minutes at 121°C . The sorption process was initiated for both sample sets as described above. The sterile tests were sampled with sterile needles and syringes.

The results of the multi-element sorption tests are summarized in Table 9 to Table 18. The data tables for normal and sterile are grouped together for each element to facilitate comparisons. Values in the tables represent the average of 3 measurements, and the errors are standard deviations. The results are illustrated in Figure 6 to Figure 10. See Table A6 to Table A10 in the Appendix which provide the results of individual measurements for each element.

2.4.1.1 Li

As expected, Li sorption was very weak, with the total percentage of sorbed Li varying from 0% to 6% (Table 9, Table 10 and Table A6). The variation in Li sorption values did not show any clear trends with time (Figure 6). Focusing on the sorption values determined with times of 3 days and longer, under normal conditions, the respective sorption coefficients for bentonite, shale and limestone were 2 ± 2 , 2 ± 4 , and $1 \pm 1 \text{ cm}^3/\text{g}$. Under sterile conditions, the respective sorption coefficients for bentonite, shale and limestone were 3 ± 4 , 2 ± 3 , and $0 \pm 1 \text{ cm}^3/\text{g}$. Microbes in the laboratory did not have any effect on Li sorption. Considering both normal and sterile conditions, the average sorption K_d values for bentonite, shale and limestone were 2 ± 3 , 2 ± 3 , and $1 \pm 1 \text{ cm}^3/\text{g}$. The low sorption value for shale suggests that Li might be a good candidate for use as a conservative tracer in mass transport experiments in shale. However, sorption values higher than 0 were observed in a number of cases (Tables 9 and 10), suggesting that Li is weakly sorbed, with a low sorption coefficient that was difficult to measure accurately in these tests. The precision of Li sorption measurements could be improved by significantly increasing the solid/liquid ratio to provide more sorption sites, and by reducing the Li concentration in the experimental solutions.

Table 9: Lithium Sorption in SR-270 Brine – Normal Conditions

Solid	Time (day)	pH	K_d (cm^3/g)	K_a (cm)	% sorbed
Bentonite	1	6.5	5 ± 3	$(1.9 \pm 1.3) \times 10^{-5}$	2 ± 2
	3	6.5	2 ± 3	$(0.7 \pm 1.0) \times 10^{-5}$	1 ± 2
	7	6.5	0 ± 0	0	0 ± 0
	16	6.5	0 ± 0	0	0 ± 0
	71	6.5	2 ± 4	$(0.8 \pm 1.0) \times 10$	1 ± 2
	99	6.5	2 ± 2	$(0.7 \pm 0.8) \times 10$	1 ± 1
	127	6.5	4 ± 2	$(1.6 \pm 0.6) \times 10^{-5}$	2 ± 1
Shale	1	6.5	2 ± 1	$(1.6 \pm 1.0) \times 10^{-5}$	2 ± 1
	3	6.5	0 ± 5	0	1 ± 3
	7	6.5	0 ± 0	0	0 ± 0
	16	6.3	6 ± 9	$(5.1 \pm 7.5) \times 10^{-5}$	5 ± 7
	71	6.3	2 ± 3	$(1.5 \pm 2.6) \times 10^{-5}$	2 ± 3
	99	6.3	0 ± 1	0	0 ± 1
	127	6.36	0 ± 1	0	0 ± 1
Limestone	1	6.4	0 ± 0	0	0 ± 1
	3	6.3	0 ± 0	0	0 ± 0
	7	6.3	1 ± 1	$(3.1 \pm 4.8) \times 10^{-5}$	2 ± 3
	16	6.3	2 ± 3	$(7.0 \pm 11) \times 10^{-5}$	4 ± 7
	71	6.3	0 ± 0	$(1.3 \pm 1.2) \times 10^{-5}$	1 ± 1
	99	6.3	0 ± 1	$(0.9 \pm 0.9) \times 10^{-5}$	1 ± 1
	127	6.38	0 ± 0	$(0.8 \pm 0.7) \times 10^{-5}$	1 ± 1

Table 10: Lithium Sorption in SR-270 Brine – Sterile Conditions

Solid	Time (day)	pH	K_d (cm³/g)	K_a (cm)	% sorbed
Bentonite	1	6.57	0 ± 0	(0.3 ± 0.6) × 10 ⁻⁵	0 ± 0
	3	6.50	3 ± 2	(1.5 ± 1.0) × 10 ⁻⁵	1 ± 1
	7	6.54	0 ± 0	0	0 ± 0
	16	6.56	0 ± 1	0	0 ± 0
	64	6.51	10 ± 2	(4.2 ± 0.9) × 10 ⁻⁵	5 ± 1
	93	6.49	4 ± 6	(1.5 ± 2.4) × 10 ⁻⁵	2 ± 3
	121	6.53	3 ± 4	(1.2 ± 1.5) × 10 ⁻⁵	2 ± 2
Shale	1	6.53	0 ± 0	0	0 ± 0
	3	6.41	3 ± 4	(2.2 ± 3.1) × 10 ⁻⁵	1 ± 1
	7	6.41	4 ± 4	(3.6 ± 3.8) × 10 ⁻⁵	4 ± 4
	16	6.42	0 ± 0	0	0 ± 0
	64	6.36	1 ± 2	(1.2 ± 1.5) × 10 ⁻⁵	1 ± 2
	93	6.37	1 ± 1	(0.7 ± 1.2) × 10 ⁻⁵	1 ± 1
	121	6.38	1 ± 2	(1.0 ± 1.4) × 10 ⁻⁵	1 ± 2
Limestone	1	6.49	3 ± 4	(9.8 ± 12) × 10 ⁻⁵	6 ± 8
	3	6.38	0 ± 0	0	0 ± 0
	7	6.38	1 ± 1	(4.4 ± 4.3) × 10 ⁻⁵	3 ± 3
	16	6.36	0 ± 0	0	0 ± 0
	64	6.33	1 ± 1	(2.0 ± 2.3) × 10 ⁻⁵	1 ± 2
	93	6.31	0 ± 0	(0.8 ± 1.3) × 10 ⁻⁵	1 ± 1
	121	6.34	0 ± 0	0	0 ± 0

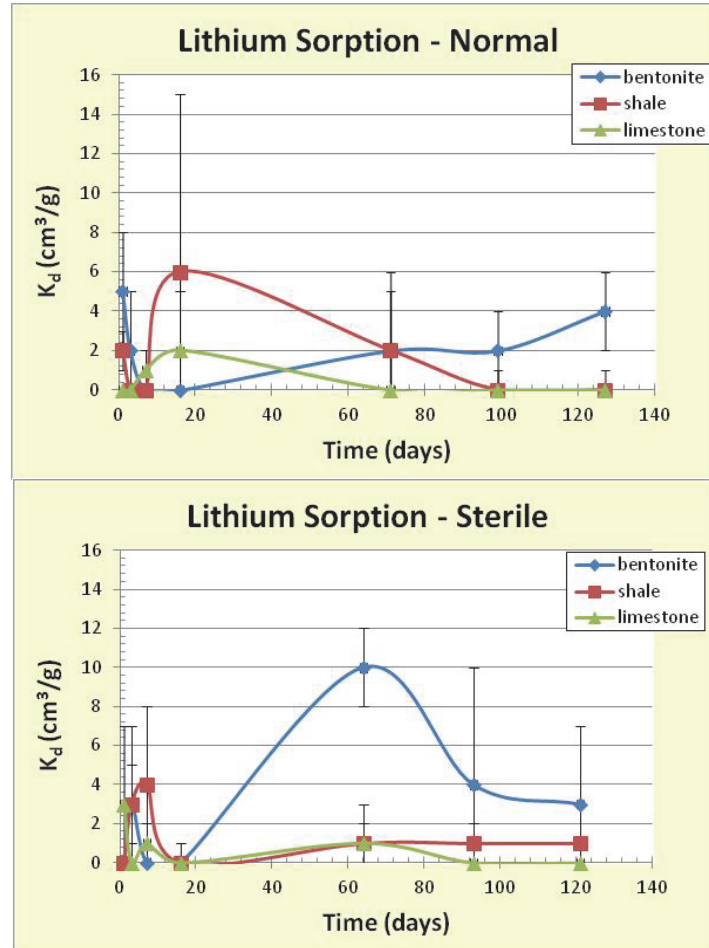


Figure 6: Lithium Sorption in SR-270 Brine as a Function of Time Under Normal and Sterile Laboratory Conditions

2.4.1.2 Ni

Nickel sorption in SR-270 brine (Table 11, Table 12 and Table A7) was also rather weak, with the total percent sorbed varying from 0% to 6%. Under normal laboratory conditions, Ni sorption values were 7 cm³/g for bentonite and 3 cm³/g for shale within the first day of the sorption reaction, but dropped to 0 by 99 days for bentonite and 71 days for shale (Figure 7). Sorption on limestone was consistently low. Under sterile laboratory conditions, Ni sorption values for bentonite had also dropped to 0 at around 64 days, but then increased after 93 days. Under sterile conditions, a sorption steady state appeared to be established for bentonite and limestone at 93 days. However, given the variability in sorption values it is difficult to make definitive conclusions regarding the achievement of steady-state. Therefore, the entire set of sorption values was used to calculate average sorption values, without any attempt to identify steady-state. Under normal conditions the respective sorption coefficients for bentonite, shale and limestone were 3 ± 4 , 2 ± 3 , and 1 ± 1 cm³/g. Under sterile conditions, the respective sorption coefficients for bentonite, shale and limestone were 8 ± 9 , 3 ± 3 , and 2 ± 2 cm³/g. Given the variability in average sorption coefficients, it seems that microbial action in the lab did not have an effect on Ni sorption. Considering data from both normal and sterile conditions,

average Ni sorption values for SR-270 brine for bentonite, shale and limestone were 5 ± 5 , 2 ± 3 , and 1 ± 2 cm^3/g , respectively. Previous Ni sorption measurements under normal laboratory conditions in a 300 g/L Na-Ca-Cl brine, using the same Ni concentration of 1×10^{-4} mol/L and a 7 day sorption reaction time, produced respective sorption coefficients for bentonite, shale and limestone of 34 ± 1 , 6 ± 0 , and 0.4 ± 0.2 cm^3/g (Vilks et al., 2011). The dominant Ni species in the SR-270 brine were similar to those in the 300 g/L Na-Ca-Cl brine, which contained NiCl^+ (75%) and Ni^{+2} (25%). The reason for the higher sorption in the 300 g/L Na-Ca-Cl brine compared to that in the synthetic SR-270 brine has not been identified.

Table 11: Nickel Sorption in SR-270 Brine – Normal Conditions

Solid	Time (day)	pH	K_d (cm^3/g)	K_a (cm)	% sorbed
Bentonite	1	6.5	7 ± 2	$(2.9 \pm 0.9) \times 10^{-5}$	4 ± 1
	3	6.5	0 ± 0	0	0 ± 0
	7	6.5	4 ± 4	$(1.7 \pm 1.6) \times 10^{-5}$	2 ± 2
	16	6.5	9 ± 0	$(3.4 \pm 0.0) \times 10^{-5}$	4 ± 0
	71	6.5	8 ± 13	$(3.1 \pm 5.3) \times 10^{-5}$	3 ± 6
	99	6.5	0 ± 0	0	0 ± 0
	127	6.5	0 ± 0	0	0 ± 0
Shale	1	6.5	4 ± 5	$(3.2 \pm 4.4) \times 10^{-5}$	3 ± 5
	3	6.5	0 ± 0	0	0 ± 0
	7	6.5	4 ± 4	$(3.4 \pm 3.7) \times 10^{-5}$	4 ± 4
	16	6.3	3 ± 3	$(2.7 \pm 2.8) \times 10^{-5}$	3 ± 3
	71	6.3	0 ± 0	0	0 ± 0
	99	6.3	0 ± 0	0	0 ± 0
	127	6.4	0 ± 0	0	0 ± 0
Limestone	1	6.4	1 ± 1	$(3.4 \pm 2.6) \times 10^{-5}$	2 ± 2
	3	6.3	0 ± 0	0	0 ± 0
	7	6.3	0 ± 1	$(1.5 \pm 2.5) \times 10^{-5}$	1 ± 2
	16	6.3	1 ± 0	$(2.5 \pm 0.7) \times 10^{-5}$	2 ± 1
	71	6.3	2 ± 3	$(5.3 \pm 9.2) \times 10^{-5}$	3 ± 6
	99	6.3	0 ± 0	0	0 ± 0
	127	6.3	0 ± 0	0	0 ± 0

Table 12: Nickel Sorption in SR-270 Brine – Sterile Conditions

Solid	Time (day)	pH	K_d (cm ³ /g)	K_a (cm)	% sorbed
Bentonite	1	6.6	1 ± 2	$(0.4 \pm 0.6) \times 10^{-5}$	0 ± 1
	3	6.5	11 ± 0	$(4.4 \pm 0.0) \times 10^{-5}$	5 ± 0
	7	6.5	4 ± 4	$(1.4 \pm 1.5) \times 10^{-5}$	2 ± 2
	16	6.6	11 ± 0	$(4.4 \pm 0.0) \times 10^{-5}$	5 ± 0
	64	6.5	0 ± 0	0	0 ± 0
	93	6.5	13 ± 23	$(5.3 \pm 9.2) \times 10^{-5}$	6 ± 10
	121	6.5	13 ± 0	$(5.3 \pm 0.0) \times 10^{-5}$	6 ± 0
Shale	1	6.5	1 ± 2	$(1.3 \pm 2.2) \times 10^{-5}$	1 ± 2
	3	6.4	6 ± 0	$(4.8 \pm 0.0) \times 10^{-5}$	5 ± 0
	7	6.4	1 ± 1	$(1.0 \pm 1.2) \times 10^{-5}$	1 ± 1
	16	6.4	4 ± 3	$(3.2 \pm 2.8) \times 10^{-5}$	4 ± 3
	64	6.4	0 ± 0	0	0 ± 0
	93	6.4	0 ± 0	0	0 ± 0
	121	6.4	7 ± 0	$(5.8 \pm 0.0) \times 10^{-5}$	6 ± 0
Limestone	1	6.5	1 ± 2	$(3.5 \pm 6.0) \times 10^{-5}$	2 ± 4
	3	6.4	2 ± 0	$(7.7 \pm 0.0) \times 10^{-5}$	5 ± 0
	7	6.4	2 ± 1	$(6.1 \pm 2.2) \times 10^{-5}$	4 ± 1
	16	6.4	1 ± 1	$(5.1 \pm 4.4) \times 10^{-5}$	4 ± 3
	64	6.3	0 ± 0	0	0 ± 0
	93	6.3	3 ± 5	$(9.2 \pm 16) \times 10^{-5}$	6 ± 10
	121	6.3	3 ± 0	$(9.2 \pm 0.0) \times 10^{-5}$	6 ± 0

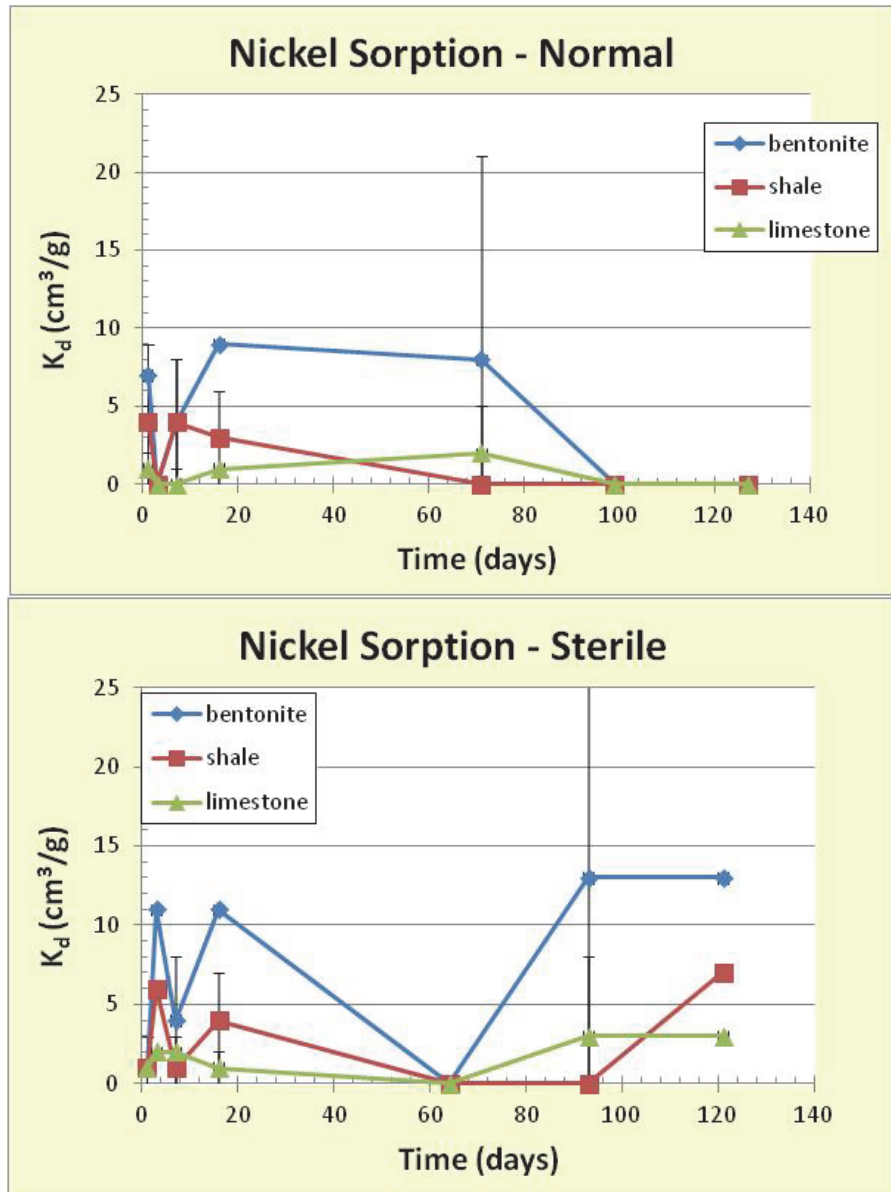


Figure 7: Nickel Sorption in SR-270 Brine as a Function of Time Under Normal and Laboratory Conditions

2.4.1.3 Cu

Copper sorption in SR-270 brine (Table 13, Table 14 and Table A8) was significantly stronger than Ni, with the total percentage of sorbed Cu varying from 0% to 47%. Under normal laboratory conditions, Cu sorption values for the 3 solids were slightly high within the first day of the sorption reaction, but dropped by day 3 (Table 13 and Figure 8). Sorption on bentonite and shale then increased, with sorption on bentonite reaching steady-state after 99 days. It could be noted that even though there is a trend of increasing sorption on shale with time, the average

sorption value at 127 days is not significantly different from that at 99 days, given the standard deviation of the average. Therefore, for the purposes of calculating average sorption values for shale, steady state is considered to be achieved by 71 days. Sorption on limestone appeared to reach steady state after 71 days. Under sterile laboratory conditions, Cu sorption values appeared to reach steady state after 16 days for bentonite and limestone, and after 64 days for shale. Focusing on the sorption values determined after 71 days, under normal laboratory conditions, the respective sorption coefficients for bentonite, shale and limestone were 112 ± 38 , 67 ± 36 , and 11 ± 7 cm³/g. Under sterile laboratory conditions, respective sorption coefficients for bentonite, shale and limestone were 103 ± 5 , 38 ± 17 , and 9 ± 6 cm³/g. These latter values were calculated using sorption values determined after 16 days. Given the variability in measured sorption values, the difference between tests performed under normal and sterile laboratory conditions was not significant. Considering data from both normal and sterile conditions, average Cu sorption values for SR-270 brine for bentonite, shale and limestone are 107 ± 25 , 52 ± 31 , and 11 ± 6 cm³/g, respectively. Sorption values previously determined for Cu in a 300 g/L Na-Ca-Cl brine under normal laboratory conditions, with the same Cu concentration of 1×10^{-5} mol/L, similar pH conditions and a 7 day sorption reaction time 6.5, 0, and 0.2 cm³/g for bentonite, shale and limestone, respectively (Vilks et al., 2011). The dominant Cu species in the SR-270 brine were similar to those in the 300 g/L Na-Ca-Cl brine, which contained CuCl₂ (59%), CuCl⁺ (33%) and Cu⁺² (5%). The sorption values reported for the 300 g/L brine were lower than the values reported for 7 days in this study for bentonite (23 cm³/g) and shale (10 cm³/g). Perhaps the lower sorption in the 300 g/L Na-Ca-Cl brine can be partially explained by the lower concentration of uncomplexed Cu⁺² species (5%), which was about half that in the SR-270 brine (10% of the total Cu).

Table 13: Copper Sorption in SR-270 Brine – Normal Laboratory Conditions

Solid	Time (day)	pH	K _d (cm ³ /g)	K _a (cm)	% sorbed
Bentonite	1	6.5	51 ± 7	(2.1 ± 0.3) × 10 ⁻⁴	21 ± 2
	3	6.5	50 ± 0	(2.0 ± 0) × 10 ⁻⁴	20 ± 0
	7	6.5	23 ± 4	(9.2 ± 1.7) × 10 ⁻⁵	10 ± 2
	16	6.5	29 ± 11	(1.2 ± 0.5) × 10 ⁻⁴	13 ± 4
	71	6.5	77 ± 48	(3.1 ± 1.9) × 10 ⁻⁴	27 ± 12
	99	6.5	133 ± 0	(5.3 ± 0) × 10 ⁻⁴	40 ± 0
	127	6.5	133 ± 0	(5.3 ± 0) × 10 ⁻⁴	40 ± 0
Shale	1	6.5	13 ± 7	(1.1 ± 0.6) × 10 ⁻⁴	11 ± 5
	3	6.5	8 ± 14	(0.7 ± 1.2) × 10 ⁻⁴	7 ± 12
	7	6.5	10 ± 7	(8.4 ± 6.5) × 10 ⁻⁵	9 ± 6
	16	6.3	16 ± 9	(1.4 ± 0.8) × 10 ⁻⁴	13 ± 7
	71	6.3	53 ± 24	(4.6 ± 2.1) × 10 ⁻⁴	33 ± 12
	99	6.3	53 ± 24	(4.6 ± 2.1) × 10 ⁻⁴	33 ± 12
	127	6.4	94 ± 48	(8.2 ± 4.2) × 10 ⁻⁴	47 ± 12
Limestone	1	6.4	4 ± 1	(1.4 ± 0.3) × 10 ⁻⁴	9 ± 2
	3	6.3	0 ± 0	0	0 ± 0
	7	6.3	0 ± 0	0	0 ± 0
	16	6.3	0 ± 0	0	0 ± 0
	71	6.3	12 ± 13	(4.2 ± 4.7) × 10 ⁻⁴	20 ± 20
	99	6.3	10 ± 0	(3.5 ± 0.0) × 10 ⁻⁴	20 ± 0
	127	6.3	10 ± 0	(3.4 ± 0.0) × 10 ⁻⁴	20 ± 0

Table 14: Copper Sorption in SR-270 Brine – Sterile Laboratory Conditions

Solid	Time (day)	pH	K_d (cm³/g)	K_a (cm)	% sorbed
Bentonite	1	6.6	31 ± 10	(1.2 ± 0.4) × 10 ⁻⁴	13 ± 4
	3	6.5	85 ± 45	(3.4 ± 1.8) × 10 ⁻⁴	29 ± 12
	7	6.5	47 ± 11	(1.9 ± 0.4) × 10 ⁻⁴	19 ± 4
	16	6.6	111 ± 0	(4.4 ± 0.0) × 10 ⁻⁴	36 ± 0
	64	6.5	100 ± 0	(2.7 ± 2.3) × 10 ⁻⁴	33 ± 0
	93	6.5	100 ± 0	(4.0 ± 0.0) × 10 ⁻⁴	33 ± 0
	121	6.5	100 ± 0	(4.0 ± 0.0) × 10 ⁻⁴	33 ± 0
Shale	1	6.5	6 ± 1	(5.5 ± 0.7) × 10 ⁻⁵	6 ± 1
	3	6.4	17 ± 0	(1.4 ± 0.0) × 10 ⁻⁴	14 ± 0
	7	6.4	4 ± 3	(3.3 ± 2.3) × 10 ⁻⁴	4 ± 2
	16	6.4	30 ± 22	(2.6 ± 1.9) × 10 ⁻⁴	21 ± 12
	64	6.4	50	(1.6) × 10 ⁻⁴	33
	93	6.4	40 ± 17	(3.5 ± 1.5) × 10 ⁻⁴	28 ± 10
	121	6.4	40 ± 17	(3.5 ± 1.5) × 10 ⁻⁴	28 ± 10
Limestone	1	6.5	2 ± 3	(0.6 ± 1.2) × 10 ⁻⁴	5 ± 6
	3	6.4	7 ± 0	(2.3 ± 0.0) × 10 ⁻⁴	14 ± 0
	7	6.4	3 ± 1	(9.6 ± 4.3) × 10 ⁻⁵	6 ± 3
	16	6.4	12 ± 9	(4.1 ± 3.1) × 10 ⁻⁴	21 ± 12
	64	6.3	10 ± 14	(2.3 ± 4.0) × 10 ⁻⁴	17 ± 24
	93	6.3	12 ± 7	(4.1 ± 2.4) × 10 ⁻⁴	22 ± 10
	121	6.3	8 ± 0	(2.8 ± 0.0) × 10 ⁻⁴	17 ± 0

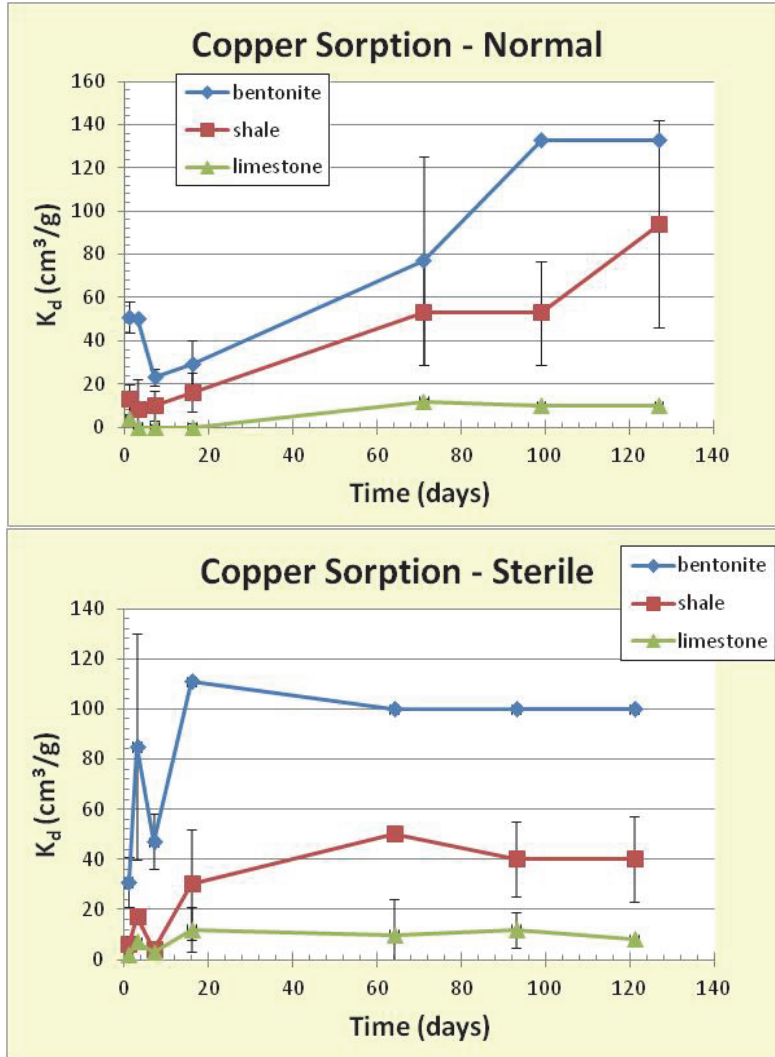


Figure 8: Copper Sorption in SR-270 Brine as a Function of Time Under Normal and Sterile Laboratory Conditions

2.4.1.4 Pb

Lead sorption in SR-270 brine (Table 15, Table 16 and Table A9) was relatively low, with the total percentage of sorbed Pb varying from 0% to 6%. The standard deviations of average Pb sorption coefficients indicate a relatively high variability in measured sorption values. To get more precise measurements with less variability, Pb sorption should be investigated using solid to liquid ratios that are probably an order of magnitude higher. The variation in Pb sorption did not display any clear trends with time under both normal and sterile laboratory conditions (Figure 9). Focusing on the sorption values determined with times longer than 16 days, under normal conditions, the respective Pb sorption coefficients for bentonite, shale and limestone were 5 ± 4 , 3 ± 2 , and 1 ± 1 cm³/g. Under sterile conditions, the respective sorption coefficients for bentonite, shale and limestone were 3 ± 3 , 3 ± 3 , and 1 ± 1 cm³/g. Given the variability in measured sorption values, the sorption tests performed under both normal and sterile conditions

produced identical results. Considering data from both normal and sterile conditions, average Pb sorption K_d values for SR-270 brine for bentonite, shale and limestone are 5 ± 4 , 3 ± 3 , and 1 ± 1 cm^3/g , respectively.

Table 15: Lead Sorption in SR-270 Brine Under Normal Laboratory Conditions

Solid	Time (day)	pH	K_d (cm^3/g)	K_a (cm)	% sorbed
Bentonite	1	6.5	3 ± 5	$(1.1 \pm 2.0) \times 10^{-5}$	1 ± 2
	3	6.5	1 ± 1	$(0.3 \pm 0.5) \times 10^{-5}$	0 ± 1
	7	6.5	7 ± 3	$(2.7 \pm 1.3) \times 10^{-5}$	3 ± 1
	16	6.5	4 ± 3	$(1.6 \pm 1.4) \times 10^{-5}$	2 ± 2
	71	6.5	1 ± 1	$(2.6 \pm 4.5) \times 10^{-6}$	0 ± 1
	99	6.5	5 ± 5	$(1.0 \pm 2.0) \times 10^{-5}$	2 ± 2
	127	6.5	9 ± 1	$(3.6 \pm 5.6) \times 10^{-5}$	4 ± 1
Shale	1	6.5	1 ± 2	$(1.0 \pm 1.5) \times 10^{-5}$	1 ± 2
	3	6.5	2 ± 1	$(1.4 \pm 1.2) \times 10^{-5}$	2 ± 1
	7	6.5	6 ± 2	$(5.1 \pm 2.1) \times 10^{-5}$	6 ± 2
	16	6.3	3 ± 3	$(2.5 \pm 3.5) \times 10^{-5}$	3 ± 3
	71	6.3	2 ± 1	$(1.4 \pm 1.2) \times 10^{-5}$	2 ± 1
	99	6.3	3 ± 3	$(2.6 \pm 2.6) \times 10^{-5}$	3 ± 3
	127	6.4	5 ± 1	$(4.6 \pm 1.1) \times 10^{-5}$	5 ± 1
Limestone	1	6.4	0 ± 1	$(1.5 \pm 2.3) \times 10^{-5}$	1 ± 2
	3	6.3	1 ± 1	$(2.3 \pm 2.9) \times 10^{-5}$	2 ± 2
	7	6.3	2 ± 1	$(5.8 \pm 3.2) \times 10^{-5}$	4 ± 2
	16	6.3	2 ± 2	$(6.5 \pm 7.5) \times 10^{-5}$	5 ± 4
	71	6.3	1 ± 1	$(2.3 \pm 2.9) \times 10^{-5}$	2 ± 2
	99	6.3	0 ± 0	0	0 ± 1
	127	6.3	2 ± 0	$(6.3 \pm 0.9) \times 10^{-5}$	4 ± 1

Table 16: Lead Sorption in SR-270 Brine Under Sterile Laboratory Conditions

Solid	Time (day)	pH	K_d (cm ³ /g)	K_a (cm)	% sorbed
Bentonite	1	6.6	3 ± 6	(1.3 ± 2.3) × 10 ⁻⁵	2 ± 3
	3	6.5	2 ± 1	(1.0 ± 4.6) × 10 ⁻⁵	1 ± 1
	7	6.5	0 ± 0	0	0 ± 0
	16	6.6	2 ± 1	(0.7 ± 0.5) × 10 ⁻⁵	1 ± 1
	64	6.5	0 ± 0	0	0 ± 0
	93	6.5	6 ± 0	(2.3 ± 0.0) × 10 ⁻⁵	3 ± 0
	121	6.5	4 ± 1	(1.6 ± 0.6) × 10 ⁻⁵	2 ± 1
Shale	1	6.5	0 ± 0	0	0 ± 0
	3	6.4	3 ± 2	(2.5 ± 1.4) × 10 ⁻⁵	3 ± 1
	7	6.4	1 ± 1	(0.4 ± 0.8) × 10 ⁻⁵	1 ± 1
	16	6.4	1 ± 2	(1.0 ± 1.7) × 10 ⁻⁵	1 ± 2
	64	6.4	3 ± 2	(2.1 ± 1.9) × 10 ⁻⁵	2 ± 2
	93	6.4	7 ± 2	(2.1 ± 1.9) × 10 ⁻⁵	6 ± 2
	121	6.4	1 ± 1	(1.1 ± 1.0) × 10 ⁻⁵	1 ± 1
Limestone	1	6.5	0 ± 1	(1.1 ± 1.8) × 10 ⁻⁵	1 ± 1
	3	6.4	2 ± 0	(6.7 ± 0.7) × 10 ⁻⁵	5 ± 0
	7	6.4	0 ± 0	0	1 ± 1
	16	6.4	1 ± 1	(2.1 ± 2.9) × 10 ⁻⁵	1 ± 2
	64	6.3	1 ± 1	(1.9 ± 2.7) × 10 ⁻⁵	1 ± 2
	93	6.3	1 ± 1	(5.2 ± 3.0) × 10 ⁻⁵	4 ± 2
	121	6.3	0 ± 1	(1.4 ± 1.9) × 10 ⁻⁵	1 ± 1

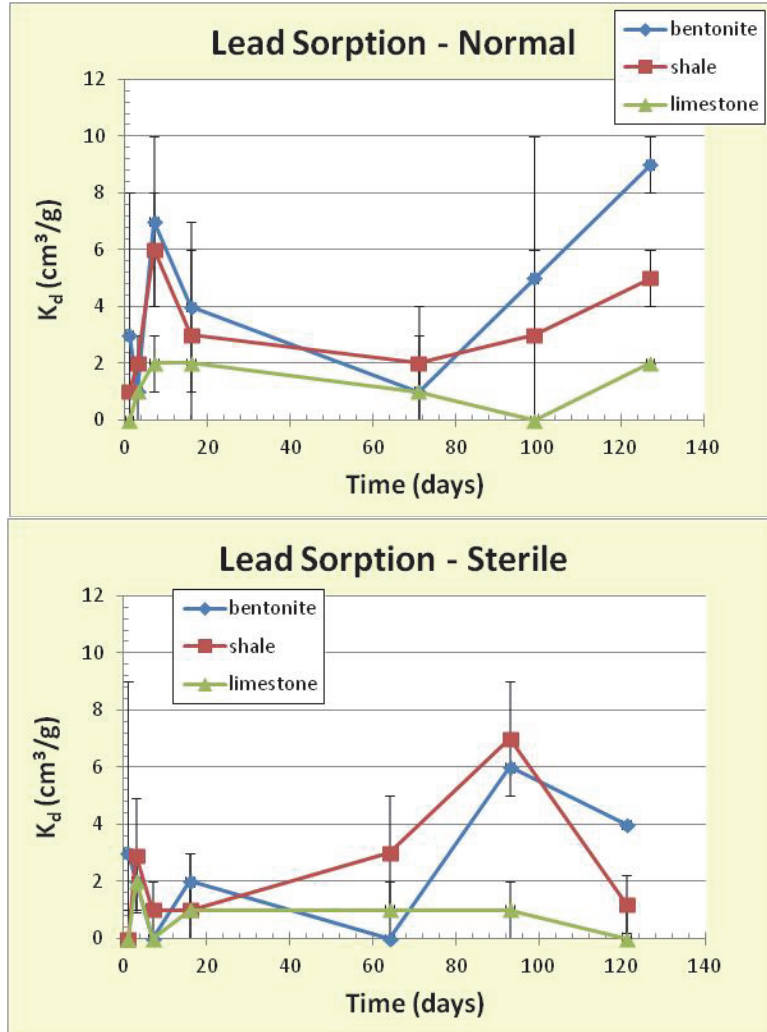


Figure 9: Lead Sorption in SR-270 Brine as a Function of Time Under Normal and Sterile Laboratory Conditions

2.4.1.5 U

Uranium sorption in SR-270 brine (Table 17, Table 18 and Table A10) was moderate, with the total percentage of sorbed U varying from 1% to 28%. The variation in U sorption with time is illustrated in Figure 10. Sorption on bentonite reached a steady state after 71 and 64 days under normal and sterile laboratory conditions respectively. Under normal laboratory conditions, steady-state conditions were close to being achieved for shale and limestone after 71 days, except for the small increase in sorption at 127 days suggesting that sorption might continue to increase. Under sterile laboratory conditions, steady state was achieved for shale after 93 days and for limestone after 64 days. Focusing on the sorption values determined after 71 days, under normal laboratory conditions the respective U sorption coefficients for bentonite, shale and limestone were 34 ± 8 , 27 ± 4 , and 8 ± 0 cm³/g. Under sterile laboratory conditions, using reaction times of 64 days and longer for bentonite and limestone and times of 93 days and longer for shale, the respective sorption coefficients for bentonite, shale and limestone were

44 ± 6 , 38 ± 4 , and 13 ± 2 cm^3/g . The measured U sorption coefficients for bentonite measured under normal and sterile conditions were not significantly different. Uranium sorption on shale and limestone was about a factor of 1.4 - 1.5 higher under sterile conditions. The U sorption coefficients determined in the single element tests of Chapter 2.2.2 were a factor of 1.3 to 2.4 lower than those measured in these multi-element experiments. The difference may be due to experimental variability or the use of different analytical techniques (spectroscopic method versus ICP-MS). It is certainly not due to the competition of sorption sites from the other tracer elements used in the sorption tests. Considering uranium sorption coefficients determined under steady-state conditions, the average sorption values from single-element and multi-element tests (normal and sterile) for bentonite, shale and limestone were 34 ± 9 , 28 ± 9 , and 10 ± 4 cm^3/g , respectively.

Table 17: Uranium Sorption in SR-270 Brine – Normal Conditions

Solid	Time (day)	pH	K_d (cm^3/g)	K_a (cm)	% sorbed
Bentonite	1	6.5	4 ± 3	$(1.7 \pm 3.0) \times 10^{-5}$	2 ± 4
	3	6.5	7 ± 0	$(3.0 \pm 0.0) \times 10^{-5}$	4 ± 0
	7	6.5	6 ± 3	$(1.5 \pm 1.6) \times 10^{-5}$	1 ± 3
	16	6.5	26 ± 18	$(1.0 \pm 0.7) \times 10^{-4}$	11 ± 8
	71	6.5	35 ± 9	$(1.4 \pm 0.4) \times 10^{-4}$	15 ± 3
	99	6.5	30 ± 9	$(1.2 \pm 0.3) \times 10^{-4}$	13 ± 3
	127	6.5	37 ± 9	$(1.5 \pm 0.4) \times 10^{-4}$	16 ± 3
Shale	1	6.5	5 ± 4	$(4.3 \pm 0.3) \times 10^{-5}$	5 ± 3
	3	6.5	6 ± 4	$(5.0 \pm 3.0) \times 10^{-5}$	5 ± 3
	7	6.5	9 ± 0	$(7.5 \pm 0.2) \times 10^{-5}$	8 ± 0
	16	6.3	20 ± 7	$(1.7 \pm 0.6) \times 10^{-4}$	17 ± 5
	71	6.3	26 ± 5	$(2.2 \pm 0.4) \times 10^{-4}$	20 ± 3
	99	6.3	26 ± 5	$(2.2 \pm 0.4) \times 10^{-4}$	20 ± 3
	127	6.4	31 ± 0	$(2.7 \pm 0.0) \times 10^{-4}$	24 ± 0
Limestone	1	6.4	1 ± 1	$(4.4 \pm 3.8) \times 10^{-5}$	3 ± 3
	3	6.3	2 ± 1	$(7.9 \pm 4.9) \times 10^{-5}$	5 ± 3
	7	6.3	1 ± 0	$(4.8 \pm 1.2) \times 10^{-5}$	3 ± 1
	16	6.3	7 ± 4	$(2.5 \pm 1.3) \times 10^{-4}$	15 ± 7
	71	6.3	8 ± 0	$(2.8 \pm 0.0) \times 10^{-4}$	17 ± 0
	99	6.3	8 ± 0	$(2.8 \pm 0.0) \times 10^{-4}$	17 ± 0
	127	6.3	9 ± 0	$(3.0 \pm 0.0) \times 10^{-4}$	18 ± 0

Table 18: Uranium Sorption in SR-270 Brine – Sterile Conditions

Solid	Time (day)	pH	K_d (cm ³ /g)	K_a (cm)	% sorbed
Bentonite	1	6.6	11 ± 15	(5.8 ± 4.4) × 10 ⁻⁵	7 ± 5
	3	6.5	24 ± 0	(9.4 ± 0.0) × 10 ⁻⁵	11 ± 0
	7	6.5	25 ± 4	(1.0 ± 0.2) × 10 ⁻⁴	11 ± 2
	16	6.6	33 ± 8	(1.3 ± 0.3) × 10 ⁻⁴	14 ± 3
	64	6.5	49 ± 0	(2.0 ± 0.0) × 10 ⁻⁴	20 ± 0
	93	6.5	40 ± 0	(1.6 ± 0.0) × 10 ⁻⁴	17 ± 0
	121	6.5	42 ± 9	(1.7 ± 0.4) × 10 ⁻⁴	17 ± 3
Shale	1	6.5	6 ± 3	(4.9 ± 0.2) × 10 ⁻⁵	5 ± 2
	3	6.4	10 ± 4	(8.4 ± 3.1) × 10 ⁻⁵	9 ± 3
	7	6.4	7 ± 7	(6.0 ± 5.8) × 10 ⁻⁵	6 ± 6
	16	6.4	14 ± 8	(1.2 ± 0.7) × 10 ⁻⁴	12 ± 6
	64	6.4	30 ± 5	(2.6 ± 0.4) × 10 ⁻⁴	23 ± 3
	93	6.4	38 ± 0	(3.3 ± 0.0) × 10 ⁻⁴	28 ± 0
	121	6.4	37 ± 6	(3.2 ± 0.6) × 10 ⁻⁴	27 ± 3
Limestone	1	6.5	3 ± 0	(8.8 ± 0.7) × 10 ⁻⁵	6 ± 0
	3	6.4	5 ± 0	(1.6 ± 0.0) × 10 ⁻⁴	11 ± 0
	7	6.4	4 ± 2	(1.3 ± 0.6) × 10 ⁻⁴	9 ± 4
	16	6.4	6 ± 2	(1.9 ± 0.6) × 10 ⁻⁴	12 ± 3
	64	6.3	12 ± 2	(4.2 ± 0.7) × 10 ⁻⁴	23 ± 3
	93	6.3	14 ± 2	(4.9 ± 0.8) × 10 ⁻⁴	26 ± 3
	121	6.3	12 ± 2	(4.2 ± 0.8) × 10 ⁻⁴	23 ± 3

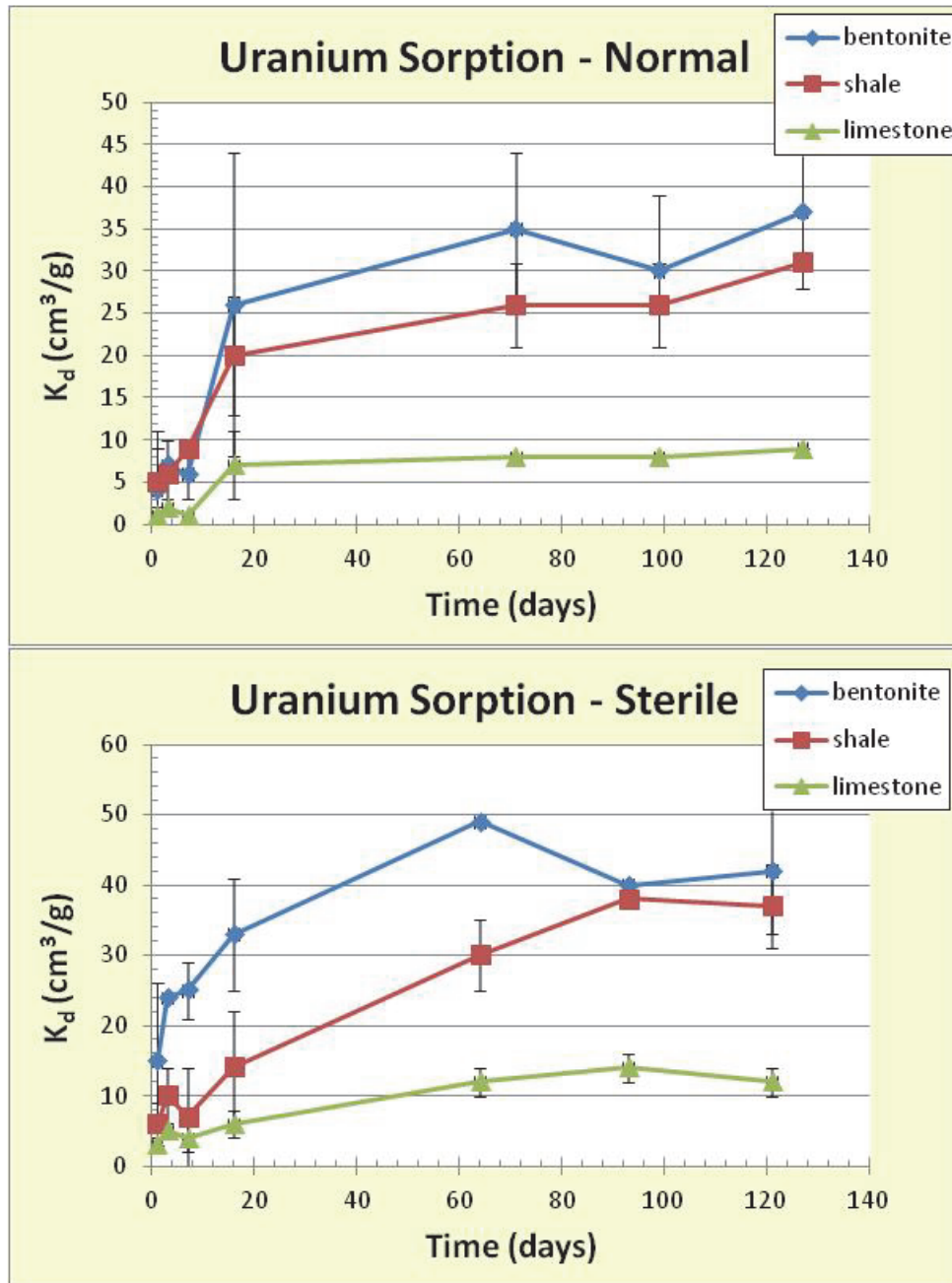


Figure 10: Uranium Sorption in SR-270 Brine as a Function of Time Under Normal and Sterile Laboratory Conditions

2.4.2 Long Term Tests in Dilute Reference Solution

As with the sorption tests in the brine solution, the multi-element sorption experiments in dilute reference solution were performed using large volume solution of 200 mL. The starting weights of bentonite, shale and limestone were 1.0, 2.0 and 5.0 g, respectively. All solids were conditioned with tracer free dilute reference water for 1 week before starting sorption tests. Sorption tests were initiated by removing 100 mL of conditioning water and replacing it with 100 mL of dilute reference solution containing tracers. The starting tracer concentrations were 2×10^{-2} mol/L Li, 1×10^{-4} mol/L Ni, 1×10^{-5} mol/L Cu, 5×10^{-5} mol/L Pb, and 1×10^{-5} mol/L U, the same as being used in the experimental reference SR-270 brine. After shaking the reaction vessel, 5 mL solution samples were removed for analyses after sorption reaction times of 1, 2, 7, 14 and 63 days. After measuring the pH for each solution samples, they were acidified with HNO_3 and saved for tracer analyses by ICP-MS. The final pH values of the test solutions at 63 days, as determined by the sorbing solids, were 8.1 for bentonite, 8.0 for shale, and 8.1 for limestone.

The results of Li sorption in dilute reference water are summarized in Table 19 and Table A11, and illustrated in Figure 11. Lithium sorption was low, with the percentage sorbed of total Li varying from 0% to 5%. Sorption on bentonite reached a steady state within 1 day. Sorption variation with time on shale and limestone was not clear, given the very low sorption values, with relatively large variabilities. The average sorption values for Li were calculated from measurements with sorption reaction times of 1 to 63 days. The respective sorption K_d values for bentonite, shale and limestone are 8 ± 5 , 2 ± 2 , and 0 ± 1 cm^3/g . On a mass basis, the salt content of the dilute water is a factor of 430 lower than that of the brine solution. Lithium sorption K_d value on bentonite was only a factor of 4 higher than in brine, and since sorption on shale and limestone was not significantly different from 0, Li sorption in the dilute solution was very similar to that in brine. This indicates that the millimolar quantities of dissolved Na^+ and Ca^{+2} were able to compete with Li^+ for cation exchange sites, even though the Li^+ concentration was about a factor of 3 to 11 higher than these competing cations. Sodium is sorbed more strongly than Li^+ because it has a smaller hydrated radius, while Ca^{+2} is sorbed more strongly because it is a divalent cation.

The results of Ni sorption in dilute reference water are summarized in Table 20 and Table A12, and illustrated in Figure 12. Nickel sorption was high, with the percentage sorbed of total Ni varying from 17% to 97%. Sorption values continued to increase with time, never reaching a steady state for any of the solids within 63 days. This indicates that a slow reaction, which has not been identified, is contributing to Ni sorption. Had the sorption tests been extended to over 100 days, a steady state would eventually have been achieved as the percent sorbed approached 100%, likely for all solids. The problem with having a high percent sorbed Ni (say > 90%) is that there is a higher uncertainty in the calculated sorption value due to the uncertainty in the equilibrium dissolved Ni concentration. To obtain a better measurement of Ni sorption in the dilute solution, the solid/liquid ratio would need to be reduced in the future sorption tests to get percent sorbed values closer to 50 %. The uncertainty in the sorption values measured at 14 days is less than that measured after 63 days, yet the sorption values measured at 14 days are probably less than the steady state or equilibrium sorption values. Therefore, the adopted approach to calculating the average Ni sorption values for the dilute solution is to average the sorption data measured at 14 and 63 days for bentonite and limestone (sorption value for shale is averaged over sorption data measured at 7, 14, and 63 days). The respective sorption K_d values for bentonite, shale and limestone are 1580 ± 850 , 1620 ± 1090 , and 230 ± 160 cm^3/g . These values are 2 orders of magnitude higher than that determined in brine solution, where Ni

sorption was suppressed by the mass action of the salt and possible competition with Ca^{+2} in the surface complexation reactions (discussed later in chapter 4.1.2). The Ni sorption coefficient for shale was higher compared to bentonite, which was not the case in brine solution. The reason why the Ni sorption coefficient was higher on the solid with a smaller surface area has not been identified.

Table 19: Lithium Sorption in Reference Dilute Water

Solid	Time (day)	pH	K_d (cm^3/g)	K_a (cm)	% sorbed
Bentonite	0.042	8.2	2 ± 1	$(0.6 \pm 0.5) \times 10^{-5}$	1 ± 1
	1	8.1	8 ± 8	$(3.4 \pm 3.1) \times 10^{-5}$	4 ± 4
	2	8.2	8 ± 4	$(3.0 \pm 1.8) \times 10^{-5}$	4 ± 2
	7	8.2	5 ± 3	$(2.2 \pm 1.4) \times 10^{-5}$	3 ± 2
	14	8.2	8 ± 8	$(3.2 \pm 3.3) \times 10^{-5}$	4 ± 4
	63	8.1	11 ± 3	$(4.4 \pm 1.3) \times 10^{-5}$	5 ± 1
Shale	0.042	8.0	0 ± 0	0	0 ± 0
	1	8.0	3 ± 2	$(2.9 \pm 1.7) \times 10^{-5}$	3 ± 2
	2	8.1	3 ± 3	$(2.6 \pm 3.0) \times 10^{-5}$	3 ± 3
	7	8.1	1 ± 1	$(0.7 \pm 1.0) \times 10^{-5}$	1 ± 1
	14	8.1	0 ± 0	0	0 ± 0
	63	8.0	3 ± 4	$(2.4 \pm 3.4) \times 10^{-5}$	3 ± 4
Limestone	0.042	8.1	2 ± 1	$(7.9 \pm 4.3) \times 10^{-5}$	5 ± 3
	1	8.1	1 ± 1	$(2.3 \pm 2.7) \times 10^{-5}$	2 ± 2
	2	8.2	2	5.2×10^{-5}	4
	7	8.1	0 ± 0	0	0 ± 0
	14	8.1	0 ± 1	0	1 ± 2
	63	8.1	0 ± 1	0	1 ± 1

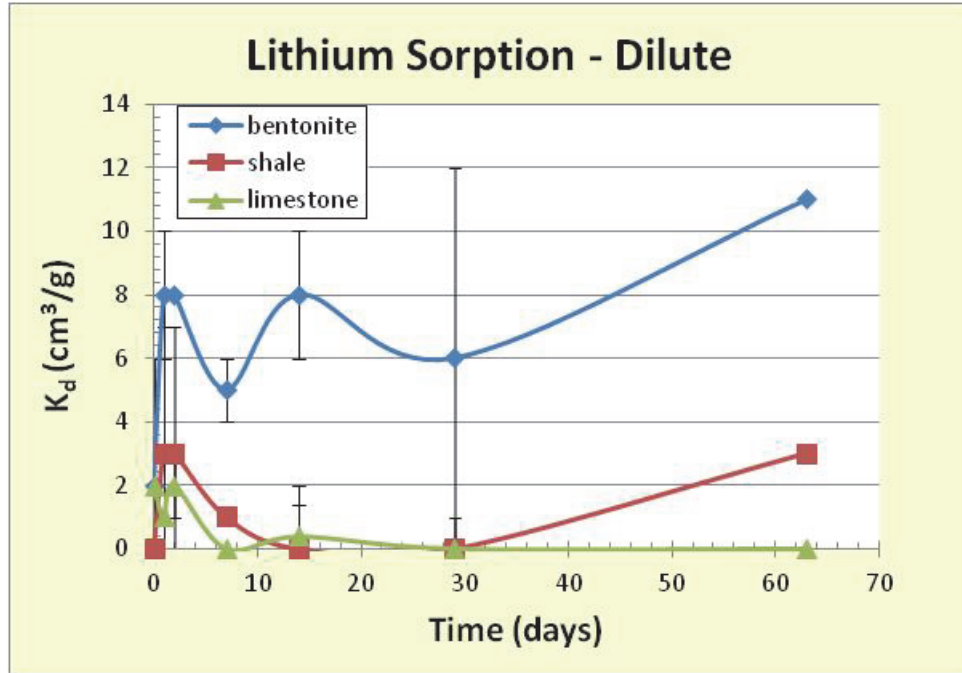


Figure 11: Lithium Sorption in Dilute Reference Water as a Function of Time

Table 20: Nickel Sorption in Reference Dilute Water

Solid	Time (day)	pH	K_d (cm ³ /g)	K_a (cm)	% sorbed
Bentonite	0.042	8.2	283 ± 12	$(1.1 ± 0.0) × 10^{-3}$	59 ± 1
	1	8.1	381 ± 34	$(1.5 ± 0.1) × 10^{-3}$	66 ± 2
	2	8.2	388 ± 66	$(1.6 ± 0.3) × 10^{-3}$	66 ± 4
	7	8.2	628 ± 64	$(2.5 ± 0.3) × 10^{-3}$	76 ± 2
	14	8.2	825 ± 0	$(3.3 ± 0.0) × 10^{-3}$	80 ± 0
	63	8.1	2333 ± 314	$(9.3 ± 1.3) × 10^{-3}$	92 ± 1
Shale	0.042	8.1	41 ± 5	$(3.6 ± 0.4) × 10^{-4}$	29 ± 3
	1	8.1	114 ± 0	$(9.9 ± 0.0) × 10^{-4}$	53 ± 0
	2	8.1	189 ± 11	$(1.6 ± 0.0) × 10^{-3}$	65 ± 1
	7	8.1	496 ± 1	$(4.3 ± 0.0) × 10^{-3}$	83 ± 0
	14	8.1	1028 ± 1	$(8.9 ± 0.0) × 10^{-3}$	91 ± 0
	63	8.0	2759 ± 2	$(2.4 ± 0.0) × 10^{-2}$	97 ± 0
Limestone	0.042	8.1	8 ± 1	$(2.9 ± 0.2) × 10^{-4}$	17 ± 1
	1	8.1	20 ± 1	$(7.1 ± 0.4) × 10^{-4}$	34 ± 1
	2	8.2	41	$1.4 × 10^{-3}$	50
	7	8.1	56 ± 5	$(1.9 ± 0.2) × 10^{-3}$	58 ± 2
	14	8.1	88 ± 4	$(3.0 ± 0.2) × 10^{-3}$	69 ± 1
	63	8.1	370 ± 42	$(1.3 ± 0.1) × 10^{-2}$	90 ± 1

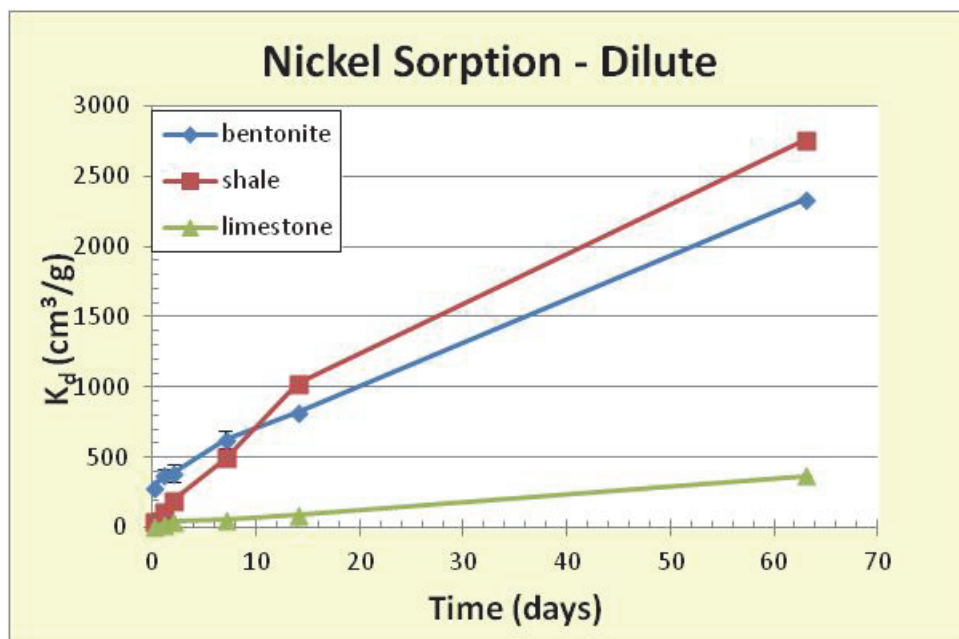


Figure 12: Nickel Sorption in Dilute Reference Water as a Function of Time

The results of Cu sorption in dilute reference water are summarized in Table 21 and Table A13, and illustrated in Figure 13. Copper sorption was high, with the percentage sorbed of total Cu varying from 77% to 94%. Sorption reached a steady state within 14 days for all solids. As discussed with Ni, the very high percent sorbed Cu values observed after 14 days are analytically difficult due to the uncertainty in the dissolved Cu concentration used to calculate sorption values. Using the same approach as with Ni, sorption data determined at 7 days was combined with data determined at 14 and 63 days to calculate the average sorption values for Cu. The respective average sorption K_d values for bentonite, shale and limestone were 2380 ± 960 , 1190 ± 450 , and $480 \pm 180 \text{ cm}^3/\text{g}$. Compared to the sorption measurements in brine solution, sorption K_d values on bentonite and shale were factors of 22 and 23 higher, while sorption on limestone was a factor of 48 higher. The sorption K_d values of Cu and Ni were similar in the dilute water, while in brine Ni sorption K_d values were a factor of 9 to 22 less than that of Cu.

Lead sorption in dilute reference solution is summarized in Table 22 and Table A14, and illustrated in Figure 14. Lead sorption was high, with the percentage sorbed of total Pb varying from 64% to 76%. Sorption on bentonite was relatively rapid, reaching a high K_d value at 14 days, and then decreasing to a K_d value that was not significantly different from the value observed at 2 days. Steady-state sorption was achieved for shale at 14 days, and 7 days for limestone. Average sorption values for Pb were calculated from measurements with sorption reaction times corresponding to steady-state conditions. The respective sorption K_d values for bentonite, shale and limestone were 523 ± 108 , 293 ± 13 , and $106 \pm 17 \text{ cm}^3/\text{g}$. Lead sorption K_d values in the dilute reference solution were approximately 2 orders of magnitude higher compared with brine solution.

The results of U sorption in dilute reference water are summarized in Table 23 and illustrated in Figure 15. Moderate amounts of U were sorbed in the dilute reference solution, with the percentage sorbed of total U varying from 10% to 26% for bentonite, 16% to 60% for shale and 11% to 69% for limestone. Uranium sorption on bentonite and shale reached maximum values at 14 days, followed by small decreases at 63 days. Sorption on limestone continued to increase with time, indicating that a steady state was not achieved and that the sorption coefficient determined at 63 days is a minimum value. The average U sorption K_d value for bentonite was calculated using sorption measurements from 2 to 63 days because values at 2 days were not significantly different from those at 63 days. Average U sorption K_d values for shale were calculated from sorption measurements at reaction times of 14 and 63 days. The K_d value for limestone was based on measurements made at 63 days. Respective sorption values for bentonite, shale and limestone are 57 ± 12 , 144 ± 8 , and 88 ± 5 cm^3/g . Compared to brine, U sorption coefficients in the reference dilute water were higher for bentonite, shale and limestone by a factor of 1.5, 4.5 and 8, respectively. These differences are small compared to the significantly higher sorption K_d values observed in dilute water for the transition metals Ni, Cu and Pb.

Table 21: Copper Sorption in Reference Dilute Water

Solid	Time (day)	pH	K_d (cm^3/g)	K_a (cm)	% sorbed
Bentonite	0.042	8.2	940 ± 0	$(3.8 \pm 0.0) \times 10^{-3}$	82 ± 0
	1	8.1	960 ± 92	$(3.8 \pm 0.4) \times 10^{-3}$	83 ± 1
	2	8.2	1147 ± 89	$(4.6 \pm 0.4) \times 10^{-3}$	85 ± 1
	7	8.2	1224 ± 0	$(4.9 \pm 0.0) \times 10^{-3}$	86 ± 0
	14	8.2	3197 ± 1	$(8.5 \pm 7.4) \times 10^{-3}$	94 ± 0
	63	8.1	2997 ± 1	$(1.2 \pm 0.0) \times 10^{-2}$	94 ± 0
Shale	0.042	8.1	475 ± 65	$(4.1 \pm 0.6) \times 10^{-3}$	82 ± 2
	1	8.1	454 ± 0	$(3.9 \pm 0.0) \times 10^{-3}$	82 ± 0
	2	8.1	574 ± 45	$(5.0 \pm 0.4) \times 10^{-3}$	85 ± 1
	7	8.1	612 ± 0	$(5.3 \pm 0.0) \times 10^{-3}$	86 ± 0
	14	8.1	1458 ± 245	$(1.3 \pm 0.2) \times 10^{-2}$	93 ± 1
	63	8.0	1500 ± 1	$(1.3 \pm 0.0) \times 10^{-2}$	94 ± 0
Limestone	0.042	8.1	137 ± 17	$(4.7 \pm 0.6) \times 10^{-3}$	77 ± 2
	1	8.1	173 ± 14	$(6.0 \pm 0.5) \times 10^{-3}$	81 ± 1
	2	8.2	219 ± 18	$(7.6 \pm 0.6) \times 10^{-3}$	85 ± 1
	7	8.1	245 ± 0	$(8.5 \pm 0.0) \times 10^{-3}$	86 ± 0
	14	8.1	583 ± 98	$(2.0 \pm 0.3) \times 10^{-2}$	93 ± 1
	63	8.1	600 ± 0	$(2.1 \pm 0.0) \times 10^{-2}$	94 ± 0

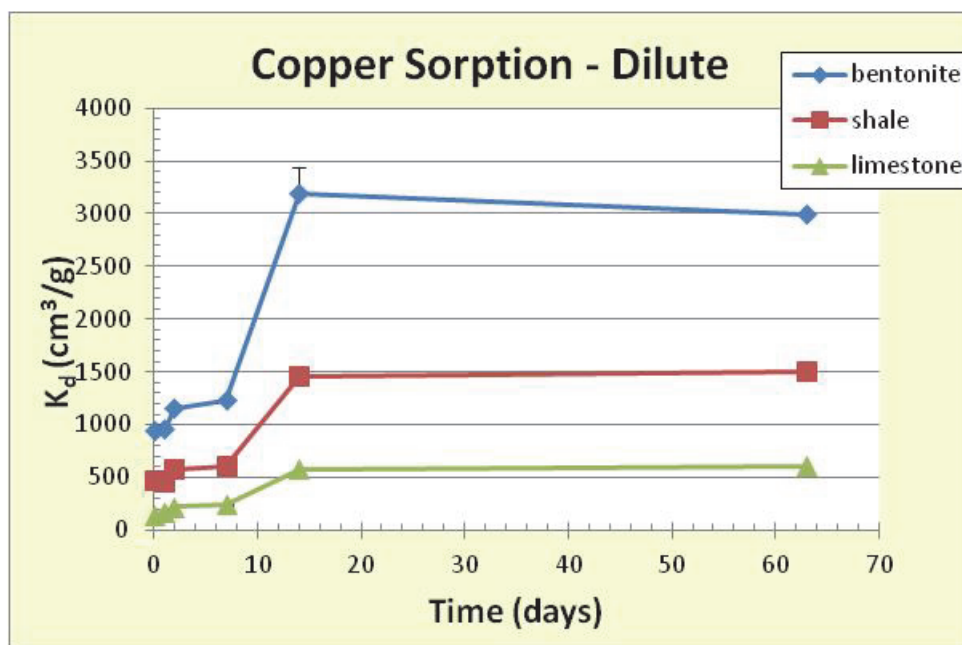


Figure 13: Copper Sorption in Dilute Reference Water as a Function of Time

Table 22: Lead Sorption in Reference Dilute Water

Solid	Time (day)	pH	K_d (cm^3/g)	K_a (cm)	% sorbed
Bentonite	0.042	8.2	396 ± 31	$(1.6 \pm 0.1) \times 10^{-3}$	66 ± 2
	1	8.1	379 ± 33	$(1.5 \pm 0.1) \times 10^{-3}$	65 ± 2
	2	8.2	472 ± 10	$(1.9 \pm 0.0) \times 10^{-3}$	70 ± 0
	7	8.2	536 ± 12	$(2.1 \pm 0.0) \times 10^{-3}$	73 ± 0
	14	8.2	623 ± 0	$(2.5 \pm 0.0) \times 10^{-3}$	76 ± 0
	63	8.1	462 ± 198	$(1.8 \pm 0.8) \times 10^{-3}$	67 ± 12
Shale	0.042	8.1	214 ± 5	$(1.9 \pm 0.0) \times 10^{-3}$	68 ± 1
	1	8.1	184 ± 7	$(1.6 \pm 0.0) \times 10^{-3}$	65 ± 1
	2	8.1	245 ± 5	$(2.1 \pm 0.0) \times 10^{-3}$	71 ± 0
	7	8.1	262 ± 5	$(2.3 \pm 0.0) \times 10^{-3}$	72 ± 0
	14	8.1	295 ± 19	$(2.6 \pm 0.2) \times 10^{-3}$	75 ± 1
	63	8.0	291 ± 8	$(2.5 \pm 0.0) \times 10^{-3}$	74 ± 1
Limestone	0.042	8.1	81 ± 0	$(2.8 \pm 0.0) \times 10^{-3}$	67 ± 0
	1	8.1	72 ± 4	$(2.5 \pm 0.2) \times 10^{-3}$	64 ± 1
	2	8.2	80 ± 25	$(2.8 \pm 0.9) \times 10^{-3}$	65 ± 8
	7	8.1	102 ± 6	$(3.5 \pm 0.2) \times 10^{-3}$	72 ± 1
	14	8.1	107 ± 31	$(3.7 \pm 0.1) \times 10^{-3}$	72 ± 7
	63	8.1	108 ± 9	$(3.7 \pm 0.3) \times 10^{-3}$	73 ± 2

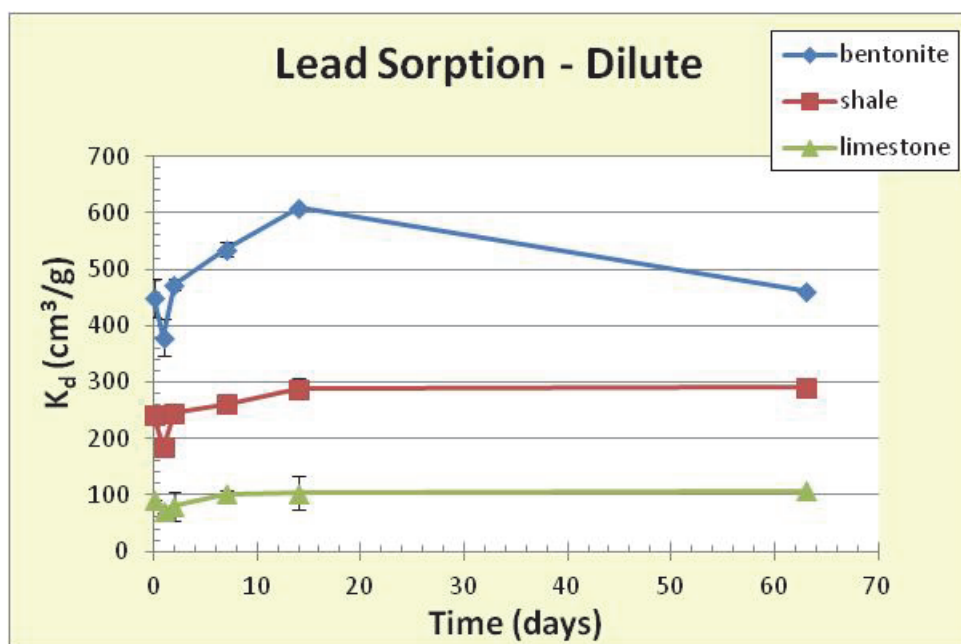


Figure 14: Lead Sorption in Dilute Reference Water as a Function of Time

Table 23: Uranium Sorption in Reference Dilute Water

Solid	Time (day)	pH	K_d (cm^3/g)	K_a (cm)	% sorbed
Bentonite	0.042	8.2	23 ± 7	$(9.2 \pm 2.7) \times 10^{-5}$	10 ± 3
	1	8.1	44 ± 3	$(1.8 \pm 0.1) \times 10^{-4}$	18 ± 1
	2	8.2	48 ± 11	$(1.9 \pm 0.5) \times 10^{-4}$	19 ± 4
	7	8.2	58 ± 9	$(2.3 \pm 0.4) \times 10^{-4}$	22 ± 3
	14	8.2	71 ± 2	$(2.8 \pm 0.0) \times 10^{-4}$	26 ± 1
	63	8.1	49 ± 7	$(2.0 \pm 0.3) \times 10^{-4}$	20 ± 2
Shale	0.042	8.1	19 ± 3	$(1.7 \pm 0.3) \times 10^{-4}$	16 ± 2
	1	8.1	50 ± 4	$(4.3 \pm 0.3) \times 10^{-4}$	33 ± 2
	2	8.1	71 ± 0	$(6.2 \pm 0.0) \times 10^{-4}$	42 ± 0
	7	8.1	122 ± 0	$(2.3 \pm 0.4) \times 10^{-4}$	55 ± 0
	14	8.1	150 ± 5	$(1.3 \pm 0.0) \times 10^{-3}$	60 ± 1
	63	8.0	138 ± 5	$(1.2 \pm 0.4) \times 10^{-3}$	58 ± 1
Limestone	0.042	8.1	5 ± 1	$(1.7 \pm 0.4) \times 10^{-4}$	11 ± 2
	1	8.1	15 ± 2	$(5.1 \pm 0.6) \times 10^{-4}$	27 ± 2
	2	8.2	18	6.3×10^{-4}	31
	7	8.1	39 ± 4	$(1.4 \pm 0.1) \times 10^{-3}$	49 ± 2
	14	8.1	55 ± 5	$(1.9 \pm 0.2) \times 10^{-3}$	58 ± 2
	63	8.1	88 ± 5	$(3.0 \pm 0.2) \times 10^{-3}$	69 ± 1

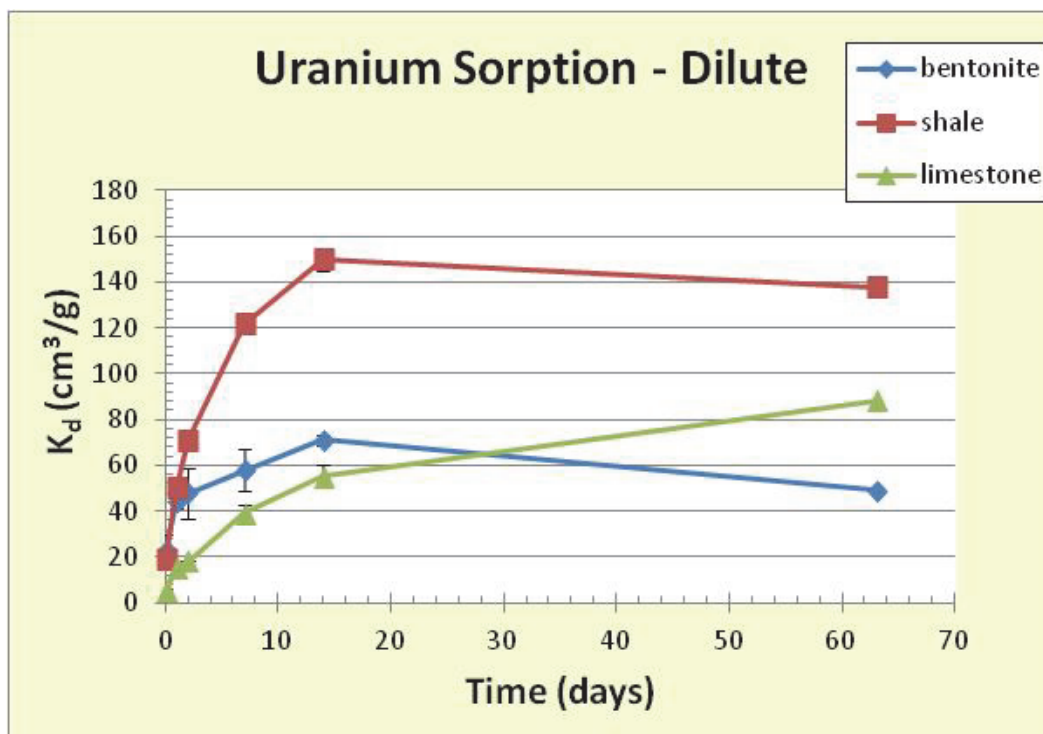


Figure 15: Uranium Sorption in Dilute Reference Water as a Function of Time

2.4.3 Short Term Sorption Tests to Evaluate pH Effects on Sorption in Brine Solution

Sorption experiments were performed to characterize Li, Ni, Cu, Pb and U sorption as a function of pH using the small volume (20 mL) tests in Oak Ridge type centrifuge tubes. The respective weights of bentonite, shale and limestone used in these tests were 0.1, 0.2 and 0.5 g. Before the sorption experiments, the solid samples were preconditioned with 20 mL of SR-270 brine for 1 week. Sorption tests were initiated by removing 10 mL of conditioning solution and replacing it with 10 mL of brine containing tracers. The starting tracer concentrations were 2×10^{-2} mol/L Li, 1×10^{-4} mol/L Ni, 1×10^{-5} mol/L Cu, 5×10^{-5} mol/L Pb, and 1×10^{-5} mol/L U, the same as in the other multi-element sorption tests. The pH for each test was set by adjusting the pH of the tracer solution before adding it to the reaction vessel containing solids. The amount of HCl or NaOH required to achieve a desired pH shift was previously determined by trial and error. After 1 h, the samples were centrifuged and solutions were sampled. A portion of the solution sample was used for ICP-MS analysis (acidified with HNO₃) and the other portion was used to measure pH. ICP-MS analysis was done by ACTLABS.

The variation in sorption coefficients with pH is summarized in Table 24, and given in more detail in Table A16 to Table A20 in the Appendix. Lithium sorption was weak, with percent sorbed values ranging from 0% to 7%. As shown in Figure 16, Li sorption did not display any clear trends with pH. The variability in Li sorption K_d values is typical of what has been seen in other tests in this study and is not related to pH. The 1 hour experimental time span was too

short to detect Ni sorption, except for one data point at a higher pH for bentonite and limestone (Figure 16). The experimental design needs to be modified by increasing the solid/liquid ratio to provide information on Ni sorption variability with respect to pH in brine solution. The 1 hour experimental time was sufficient to detect Cu sorption, with the percent sorbed values ranging from 0% to 43%. Copper sorption on bentonite displayed a gradual increase in sorption from pH 5 to pH 7, followed by a significant increase as the pH approached 8 (Figure 17). Copper sorption on shale did not display a significant increase with pH, while sorption on limestone did not change until the pH increased toward 8. Lead sorption values determined within a 1 hour period were low, with percent sorbed values ranging from 0% to 7%. Sorption on bentonite did not show a clear trend with pH, while sorption on shale and limestone increased as the pH approached 8 (Figure 17). For uranium, the percent sorbed values ranged from 0% to 80%. All solids displayed a significant increase in U sorption between pH 7 and 8 (Figure 18). The observed trends are similar to those observed in the single element U sorption tests (Figure 1) described previously. When comparing results with Figure 1, it is important to note that those tests were performed with a carbonate concentration that was reduced by a factor of 10 in the single element test to increase U sorption.

As previously mentioned, the time span of these sorption tests was kept to a minimum in an effort to minimize pH shifts caused by buffering from minerals. As a result these sorption values do not represent equilibrium conditions, and in many cases the amount of sorption in the 1 h time span was too low to determine good sorption values. These data can be used to describe sorption trends with pH but they are not appropriate for use in thermodynamic modelling. The only approach to extend sorption time is by using pH buffers.

Table 24: Sorption Variation with pH in SR-270 Brine by One Hour Short Term Sorption Tests

Solid	pH	Lithium K_d (cm^3/g)	Nickel K_d (cm^3/g)	Copper K_d (cm^3/g)	Lead K_d (cm^3/g)	Uranium K_d (cm^3/g)
Bentonite	5.0	0.0	0.0	14	0.5	27
	5.0	2.3	0.0	33	3.8	35
	6.0	5.3	0.0	32	7.4	5.3
	6.0	5.3	0.0	32	5.0	5.3
	6.6	6.2	0.0	38	4.2	11
	6.6	0.0	0.0	na	6.3	5.4
	7.2	3.1	0.0	na	0.0	0.0
	7.2	2.5	0.0	na	0.9	0.0
	7.6	0.0	0.0	na	0.0	0.0
	7.8	1.9	0.0	73	0.1	0.0
	8.0	4.3	10	52	1.0	31
Shale	5.8	0.0	0.0	17	1.3	2.8
	5.8	0.8	0.0	17	1.3	0.0
	6.0	1.6	0.0	16	0.0	0.0
	6.0	0.0	0.0	7	0.0	0.0
	6.5	0.0	0.0	20	0.4	2.8
	6.5	0.0	0.0	na	0.0	0.0
	7.2	0.6	0.0	na	1.4	1.5
	7.2	0.9	0.0	na	0.9	1.5
	7.6	0.0	0.0	na	0.0	12
	7.7	3.0	0.0	20	3.4	49
	7.7	1.0	0.0	20	1.9	50
Limestone	5.8	0.2	0.0	6.7	0.3	0.0
	5.8	0.0	0.0	6.6	0.0	0.0
	6.0	0.2	0.0	2.9	0.0	0.0
	6.0	1.6	0.0	2.9	0.5	0.0
	6.4	0.0	0.0	3.3	0.4	0.0
	6.4	1.1	0.0	3.3	0.5	1.1
	7.2	0.7	0.0	na	0.4	3.5
	7.2	0.0	0.0	na	0.0	3.5
	7.8	0.0	0.0	4.9	0.0	79
	7.8	0.0	0.0	na	0.0	80
	7.8	1.5	0.0	7.9	1.3	40
8.0	1.5	2.2	11	1.5	59	

- One hour experimental time
- Values represent single measurements
- na: not available

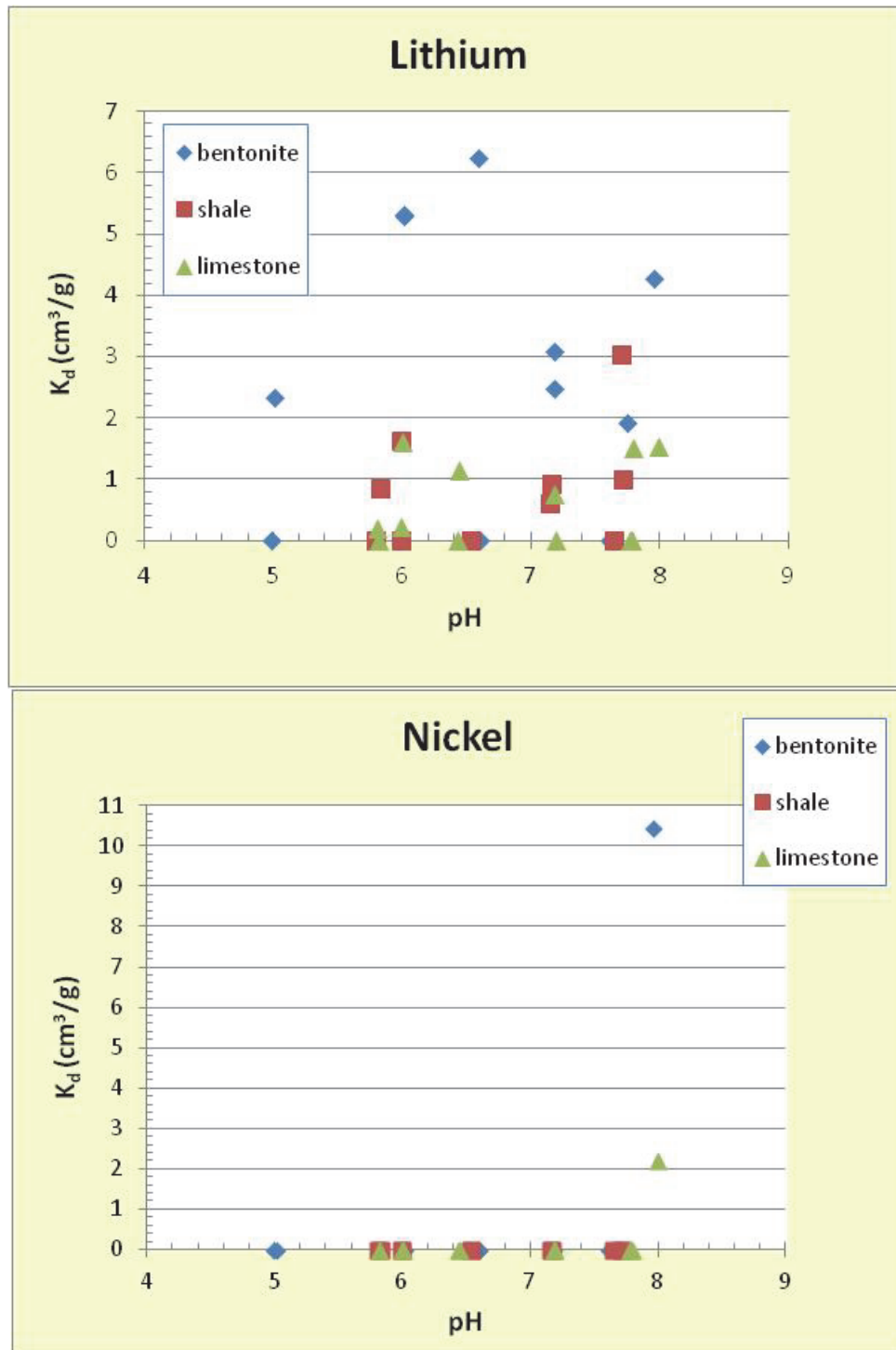


Figure 16: Effect of pH on Lithium and Nickel Sorption in SR-270 Brine Using One Hour Short Term Sorption Tests

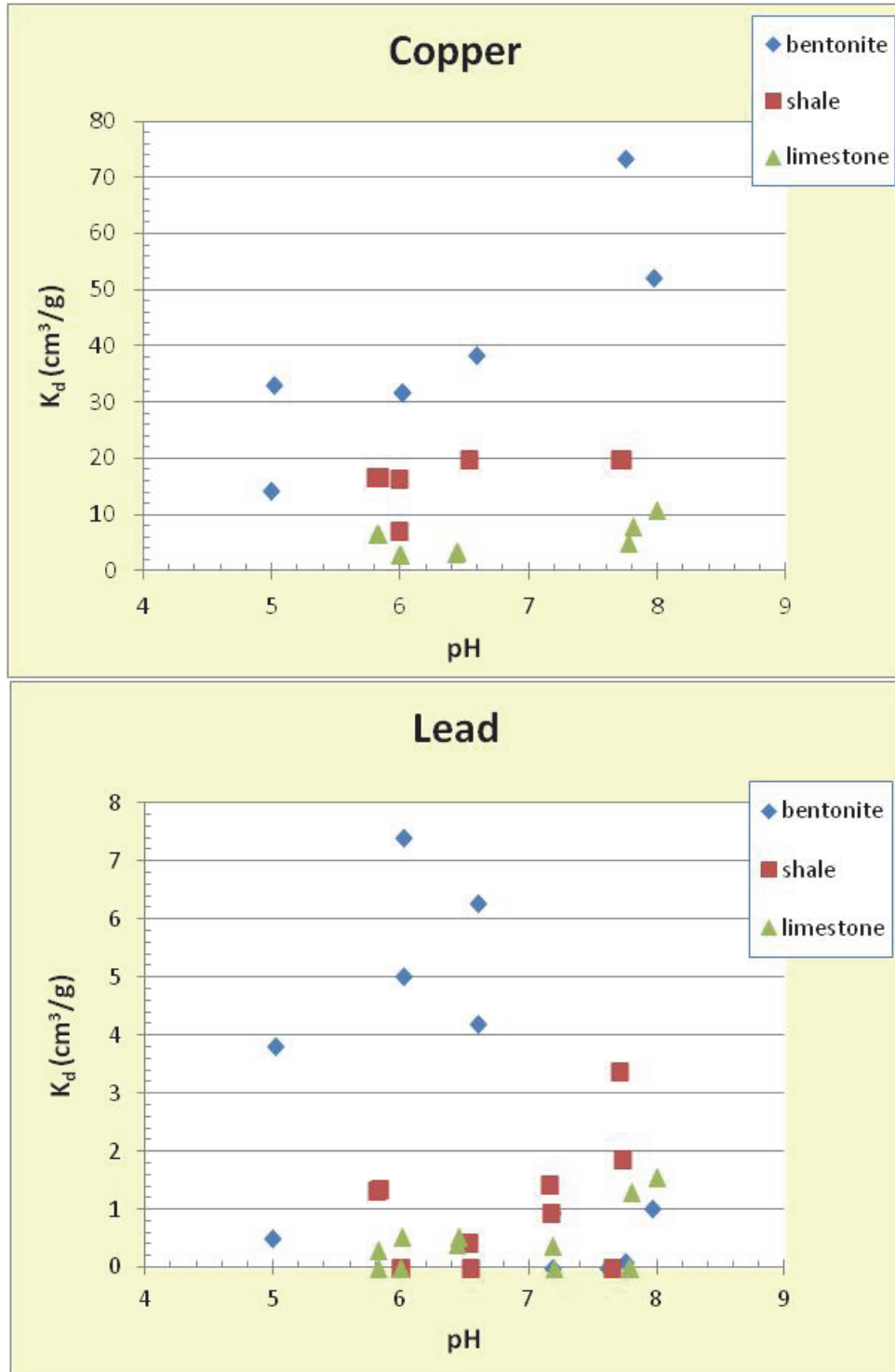


Figure 17: Effect of pH on Copper and Lead Sorption in SR-270 Brine Using One Hour Short Term Sorption Tests

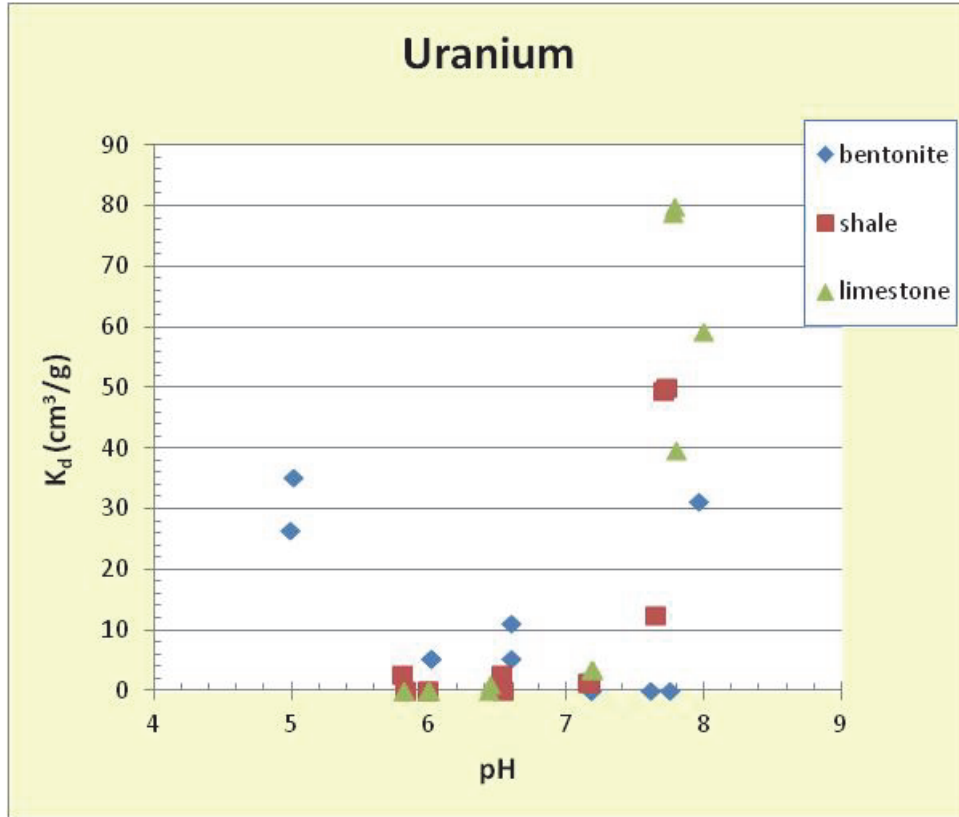


Figure 18: Effect of pH on Uranium Sorption in SR-270 Brine Using One Hour Short Term Sorption Tests

2.5 SUMMARY

The purpose of this section is to summarize the results of Chapter 2, focusing on presenting average K_d values in one location, describing how sorption varies with time, summarizing the desorption test, and discussing the effects of pH.

Sorption Coefficients: The results of sorption on bentonite, shale and limestone in the experimental reference SR-270 brine and the dilute reference solutions are summarized in Table 25. These values have been described and discussed in the previous chapters. Table 25 is intended to be a convenient, single-point reference, summarizing the results of all batch sorption tests. The sorption measurements used to calculate the average values were selected from experimental times that represent steady-state conditions. If a correlation between sorption and experimental time was not apparent, then most sorption measurements were included in the average calculation. If sorption increased with time and steady state was not achieved, measurements corresponding to the longest sorption times were selected. Table 25 includes the number of data points (n) used to calculate each average value.

Table 25: Summary of Sorption Coefficients (cm³/g) for Experimental Reference SR-270 Brine and Reference Dilute Solution

Element	SR-270 Reference Brine			Reference Dilute Solution		
	Bentonite	Shale	Limestone	Bentonite	Shale	Limestone
Li(I)	2 ± 3 (n = 31)	2 ± 3 (n = 36)	1 ± 1 (n = 36)	8 ± 5 (n = 15)	2 ± 2 (n = 10)	0 ± 1 (n = 13)
Ni(II)	5 ± 5 (n = 39)	2 ± 3 (n = 42)	1 ± 2 (n = 42)	1580 ± 850 (n = 6)	1620 ± 1090 (n = 6)	230 ± 160 (n = 6)
Cu(II)	107 ± 25 (n = 18)	52 ± 31 (n = 19)	11 ± 6 (n = 18)	2380 ± 960 (n = 8)	1190 ± 450 (n = 9)	480 ± 180 (n = 9)
Pb(II)	5 ± 4 (n = 15)	3 ± 3 (n = 18)	1 ± 1 (n = 18)	523 ± 108 (n = 12)	293 ± 13 (n = 6)	106 ± 17 (n = 9)
Zr(IV)	454 ± 66 (n = 3)	494 ± 0 (n = 3)	144 ± 31 (n = 3)	nd	nd	nd
U(VI)	34 ± 9 (n = 33)	28 ± 9 (n = 21)	10 ± 4 (n = 21)	57 ± 12 (n = 12)	144 ± 8 (n = 4)	88 ± 5 (n = 3)

Note: n is the number of measurements used to calculate average and the error is the standard deviation.

Effect of Sorption Time: Long term sorption tests were performed for sorption reaction times as long as 127 days for the reference brine and 63 days for the reference dilute solution. Lithium sorption did not show any correlation with time in the brine solution, but sorption on bentonite appeared to reach a steady state after 1 d in the dilute water. In the brine solution, nickel sorption did not show a good correlation with time under normal laboratory conditions, but a sorption steady state appeared to be established on bentonite and limestone at 93 days under sterile laboratory conditions. In dilute solution nickel sorption increased with time without achieving a steady state within the 63-day period. Copper sorption achieved steady state in the brine solution after 16 days under sterile laboratory conditions. Under normal laboratory conditions, Cu sorption in brine on bentonite achieved steady state after 99 days, while sorption on shale and limestone achieved steady state by 71 days. Copper sorption in the dilute solution achieved steady state after 14 days. However, the calculation of average copper sorption values included data from 7 days because of the uncertainty associated with high percent

sorbed values observed at 14 days. Lead sorption on all the three solids did not reach steady state in brine during the experimental time period. In the dilute reference solution, lead sorption achieved steady state after 2 days for bentonite, 14 days for shale, and 7 days for limestone. Zirconium sorption in brine reached a maximum sorption value at 14 days, but this could not be confirmed as steady state because sorption data were not available for sorption tests with longer experimental time periods. In the brine solution for multi-element sorption tests, uranium sorption on bentonite reached steady state after 71 days under normal laboratory conditions. Under sterile laboratory conditions sorption on shale reached steady state after 93 days and sorption on bentonite and limestone reached steady state after 64 days. In the brine solution for single element sorption tests, uranium sorption on bentonite reached steady state after 14 days, U sorption on shale and limestone didn't reach steady state after 112 days. In the dilute solution, U reached steady state after 2 days for bentonite and 14 days for shale, while for limestone, sorption continued to increase for the full 63-day time frame.

Desorption Tests: Uranium desorption experiments, initiated by diluting the concentration of dissolved U (at the end of the sorption test), showed that the initial sorption coefficients measured at 3 h after dilution were a factor of 4.7 to 6.9 higher than before desorption. Uranium desorption from all solids was very rapid during the first day, and then slowed down significantly, particularly after the first week. Uranium desorption from bentonite and limestone continued at a very slow rate up to and probably beyond 56 days. Uranium desorption from shale appears to have stopped after 14 days, suggesting that some U was permanently fixed on the shale.

Effect of pH: Short term, 1 h, sorption tests were performed to evaluate the effect of pH on sorption. Sorption reaction times were short because pH buffers were not used and pH values would not remain constant for long time periods due to the pH buffering properties of the solids. The buffering capacity of the sedimentary rocks is likely to limit the variability of pH values under field conditions compared to those values observed in the laboratory sorption tests. However, the response of sorption to changes in pH is of interest because it is of use for interpreting the results of sorption mechanisms, particularly those involving complexation to amphoteric surface sites. These sorption values do not represent equilibrium conditions. They can be used to describe sorption trends with pH and are not appropriate for use in thermodynamic modelling. The only approach to increasing sorption time to better approximate equilibrium is by the use of pH buffers.

The observed sorption of lithium and nickel within 1 h was weak and did not display any clear trends with pH. Copper sorption on bentonite displayed a gradual increase in sorption from pH 5 till pH 7, followed by a significant increase as the pH approached 8. Copper sorption on shale did not display a significant increase with pH, while sorption on limestone did not change until the pH increased toward 8. Lead sorption on bentonite did not show a clear trend with pH, while sorption on shale and limestone increased as the pH approached 8. Uranium sorption on all solids displayed a significant increase between pH 7 and 8. Zirconium sorption did not change significantly between pH values of 6.5 and 7.0. However, as the pH approached 8, zirconium sorption values increased by a factor of 1.3 to 1.8. Compared to uranium, this was a minor change. Note that the pH measurements in brine solution have uncertainties due to the lack of standard pH buffers for brine solutions. However, a more significant uncertainty in understanding sorption variation with pH was the pH buffering by the solids used in the sorption measurements, which limited the experimental sorption time at high and low pH to an hour. The only way to increase sorption times at these pH values is by the use of pH buffers and the assumption that the solid surfaces are stable at buffered high and low pH.

3. SORPTION MODELLING

3.1 SURFACE COMPLEXATION AND CATION EXCHANGE MODEL

Surface complexation modelling has the potential for estimating sorption values that are applicable for in-situ groundwater compositions based on sorption values reported in the literature or measured in the laboratory. Furthermore, for some elements, such as Cu, Pb and Zr, it may be able to derive sorption values based on surface site binding constants that are estimated from Linear Free Energy Relationships (LFER) (Bradbury and Baeyens, 2005b, 2009b). LFER assumes that for a given metal there is a relationship between the free energies of aqueous species and the corresponding surface metal complexes. This relationship is established for a given solid using measured sorption values for a number of metals. Measured surface binding constants are plotted against corresponding hydrolysis constants to derive relationships with which one can predict surface binding constants for other metals based on their aqueous hydrolysis constants.

PHREEQC can incorporate a 2-site protolysis non-electrostatic surface complexation and cation exchange model as described by Baeyens and Bradbury (1997) and Bradbury and Baeyens (1997, 2005b, 2009a). This model assumes that sorption occurring on oxygen sites associated with broken bonds (located on edge sites in clay minerals) can be described by strong and weak amphoteric surface sites. It is also assumed that different minerals may contain the same basic type of sites, except with different site densities (to determine capacities) and slightly different surface site binding constants. Site densities and binding constants are determined from acid-base titrations (Baeyens and Bradbury, 1997) of mineral surfaces. Examples of acid-base surface reactions and associated protolysis constants for Na-illite and montmorillonite are given in Table 26. Site binding constants are determined by fitting metal sorption data covering a range of pH conditions and metal concentrations. Model fitting is time consuming because values of site density, protolysis constants and binding constants must be consistent with acid-base titration and sorption edge data (Bradbury and Baeyens, 2005b).

If sorption isotherms are not linear over the range of metal concentrations used to derive experimental data, a combination of strong and weak sites is required to explain the sorption data. Although strong surface sites, $\equiv\text{S}^{\circ}\text{OH}$, have a small surface density, they sorb strongly and account for sorption at trace metal concentrations. The weak sites have a much higher capacity, but weaker binding constants. The role of the weak sites, $\equiv\text{S}^{\text{w}1}\text{OH}$ and $\equiv\text{S}^{\text{w}2}\text{OH}$, is to account for non-linear sorption behaviour in the presence of high metal concentrations. If the sorption isotherm is linear, the sorption model could be limited to only one type of site. However, even if sorption can be described by one type of site, three sites are required to explain the acid-base titration data for clays.

Surface complexation reactions for metals are formulated with the assumption that metals complex with surface oxygens in an analogous way to the formation of hydrolysis species in solution. The approach taken by Bradbury and Baeyens (1997) is to focus on the types of metal hydrolysis species that are present and then to formulate metal hydrolysis species as analogous surface species. For example, if the dominant hydroxyl Ni^{+2} species in solution is NiOH^+ , the corresponding surface species is $\equiv\text{S}^{\circ}\text{ONi}^+$. The surface species $\equiv\text{S}^{\circ}\text{ONi}(\text{OH})_2^-$ would be equivalent to $\text{Ni}(\text{OH})_3^-$. The surface species has one less hydroxyl than the equivalent solutions species. An example of surface complexation reactions and constants for Ni sorbing on montmorillonite is provided in Table 27. All surface complexation reactions are written with

respect to free ions (Ni^{+2} , Cu^{+2} , Pb^{+2} , and Zr^{+4}), despite the likelihood that other aqueous tracer species may be contributing to the sorption process in some way.

The general equation used to formulate surface complexation reactions with a metal, Me, having a charge z, is as follows:

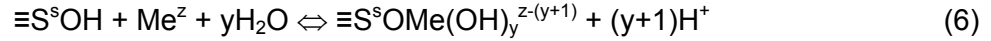


Table 26: Surface Protolysis Reactions and Constants for Na-illite and Montmorillonite

Surface Protolysis Reaction	^a log K _{protolysis} Na-illite	^b log K _{protolysis} montmorillonite
$\equiv\text{S}^{\text{s}}\text{OH} + \text{H}^+ \leftrightarrow \equiv\text{S}^{\text{s}}\text{OH}_2^+$	4.0	4.5
$\equiv\text{S}^{\text{s}}\text{OH} \leftrightarrow \equiv\text{S}^{\text{s}}\text{O}^- + \text{H}^+$	-6.2	-7.9
$\equiv\text{S}^{\text{w1}}\text{OH} + \text{H}^+ \leftrightarrow \equiv\text{S}^{\text{w1}}\text{OH}_2^+$	4.0	4.5
$\equiv\text{S}^{\text{w1}}\text{OH} \leftrightarrow \equiv\text{S}^{\text{w1}}\text{O}^- + \text{H}^+$	-6.2	-7.9
$\equiv\text{S}^{\text{w2}}\text{OH} + \text{H}^+ \leftrightarrow \equiv\text{S}^{\text{w2}}\text{OH}_2^+$	8.5	6.0
$\equiv\text{S}^{\text{w2}}\text{OH} \leftrightarrow \equiv\text{S}^{\text{w2}}\text{O}^- + \text{H}^+$	-10.5	-10.5

^a Bradbury and Baeyens (2009a)

^b Bradbury and Baeyens (2005b)

Sorption by coulombic cation exchange reactions can be described with the following exchange reaction describing the exchange of element B, having a charge of b, with sorbed element A, having a charge a, on an exchange site:



The thermodynamic exchange constant for the reaction can be defined as:

$${}^B_AK = \frac{(N_B)^a}{(N_A)^b} \times \frac{(f_B)^a}{(f_A)^b} \times \frac{[A]^b}{[B]^a} \times \frac{(\gamma_A)^b}{(\gamma_B)^a} = {}^B_AK_C \times \frac{(f_B)^a}{(f_A)^b} \quad (8)$$

The thermodynamic exchange constant is B_AK , and B_AK_C is the selectivity coefficient. The fractions of A and B located on the exchange sites are N_A and N_B . The total amount of cations in the exchange sites are determined by the Cation Exchange Capacity (CEC), given in terms of equivalents per mass of solid (kg). Aqueous concentrations are [A] and [B]. The surface activity coefficients are f_A and f_B , while the aqueous activity coefficients are γ_A and γ_B . Since surface activity coefficients are not well defined and may vary as the relative surface concentrations of elements A and B vary, the selectivity coefficient, B_AK_C , might only be considered a constant when one of the elements is present at trace concentration. The distribution ratio between solid and solution (${}^B R_d$) of element B that is attributed to cation exchange is defined as:

$${}^B R_d = \frac{\text{Amount of sorbate B on solid per unit mass}}{\text{Sorbate aqueous concentration}} \quad (9)$$

The value of ${}^B R_d$ can be related to the selectivity coefficient if the CEC is known and the solution activity coefficients are calculated, assuming that N_A has an approximate value of 1.

$${}^B_A K_c = ({}^B R_d)^a \times \frac{b^a}{CEC^a} \times [A]^b \times \frac{(Y_A)^b}{(Y_B)^a} \quad (10)$$

In practice it is assumed that the CEC of the sorbing solid is dominated by either Na or Ca. Selectivity coefficients with respect to Na or Ca are available for clay minerals for a number of elements. When cation exchange is included in sorption modelling with a program such as PHREEQC, it is apparent that cation exchange is most important when the concentrations of Na and Ca are low, and for lower pH values where the aqueous speciation of sorbing species is dominated by positively charged species. Cation exchange is not considered for elements dominated by neutral or anionic species.

Bradbury and Baeyens (2005b) used published and their “in-house” measured sorption data to derive surface complexation constants for a number of elements sorbing on montmorillonite (Mn(II), Co(II), Ni(II), Zn(II), Cd(II), Eu(III), Am(III), Sn(IV), Th(IV), Np(V) and U(VI)). They used the derived surface constants to find a correlation between the logarithms of the surface constants (${}^s K_{x-1}$ and ${}^{w1} K_{x-1}$) and the logarithms of the formation constants of their corresponding hydrolysis species (hydrolysis constant ${}^{OH} K_x$). The purpose of the correlation was to estimate surface complexation constants for elements whose sorption properties were not measured. The correlation obtained for the strong surface sites was:

$$\log {}^s K_{x-1} = 8.1 \pm 0.3 + (0.90 \pm 0.02) \log {}^{OH} K_x \quad (11)$$

R = 0.99

The correlation for the weak surface sites was:

$$\log {}^{w1} K_{x-1} = 6.2 \pm 0.8 + (0.98 \pm 0.09) \log {}^{OH} K_x \quad (12)$$

R = 0.98

The above correlations were used to estimate values of $\log {}^s K_{x-1}$ and $\log {}^{w1} K_{x-1}$ for a number of elements including Pd(II), Pb(II), Pu(III), Zr(IV), U(IV), Np(IV), Pu(IV) and Pa(V).

Bradbury and Baeyens (2009b) repeated the above exercise for Na-illite using experimental data for Ni(II), Co(II), Eu(III), Sn(IV), Am(III), Th(IV), Pa(V) and U(VI). Sorption on illite was modelled using one strong site, and the resulting surface site binding constants were correlated with hydrolysis constants. The correlation equation between the surface binding constant and the hydrolysis constant using this LFER approach for illite is given by equation 13. Any information on the sorption properties of illite provides insight into the sorption properties of shale.

$$\log {}^s K_{x-1} = 7.9 \pm 0.4 + (0.83 \pm 0.02) \log {}^{OH} K_x \quad (13)$$

R = 0.99

3.2 NICKEL

PHREEQC was used to simulate Ni sorption on Na-montmorillonite and illite using a 2-site protolysis non-electrostatic surface complexation and cation exchange model. The purpose of this exercise was to determine whether surface binding constants determined in 0.01 to 0.5 mol/L NaClO₄ solutions could be used to approximate sorption reactions in brine solutions. The assumptions are: (1) that the thermodynamic code, PHREEQC, can account for Ni interactions with brine salts; (2) that the surface complexation constants determined in diluted NaClO₄ solutions are not significantly different from that in brine solutions; and (3) that montmorillonite and illite can be used to approximate the sorption properties of bentonite and shale. The nickel selectivity coefficients for cation exchange of Ni⁺² for Na⁺ reported for Na-montmorillonite and illite are 3.1 and 12.6, respectively (Bradbury and Baeyens, 2005b, 2009b). The surface complexation reactions and constants for Ni sorption on montmorillonite and illite were determined by Bradbury and Baeyens (2005b, 2009b) using experimental results from 0.1 and 0.5 mol/L NaClO₄ solutions. These values are given in Table 27. Note that for illite, Ni sorption on weak sites is not included because Bradbury and Baeyens (2009a) did not need it to explain measured Ni sorption on illite as a function of dissolved Ni concentration. The CEC values for Na-montmorillonite and illite are 0.87 and 0.225 equivalents/kg (Bradbury and Baeyens, 2005b; Baeyens and Bradbury, 2004). The site capacities for both Na-montmorillonite and illite are 0.002 mol/kg for the strong site and 0.04 mol/kg for each of the two weak sites. Simulations were performed using a solid to liquid ratio of 0.54 g/L. The solid/liquid ratio determines the total sorption site capacity (CEC and complexation) for the system and what fraction of Ni in the system is associated with the solid. The sorption K_d value for Ni is calculated by summing the Ni concentrations in all of the solid sites (mol/kg) and dividing by the total Ni concentration in solution. The final K_d is not affected by the solid/liquid ratio.

Table 27: Nickel Surface Complexation Reactions and Surface Complexation Constants

Ni Surface Complexation Reaction	Mont. Strong Site log ^s K _{x-1}	Mont. Weak Site log ^{w1} K _{x-1}	Illite Strong Site log ^s K _{x-1}
$\equiv\text{S}^{\text{s}}\text{OH} + \text{Ni}^{+2} \leftrightarrow \equiv\text{S}^{\text{s}}\text{ONi}^{+} + \text{H}^{+}$	-0.6		0.7
$\equiv\text{S}^{\text{s}}\text{OH} + \text{Ni}^{+2} + \text{H}_2\text{O} \leftrightarrow \equiv\text{S}^{\text{s}}\text{ONi}(\text{OH})^0 + 2\text{H}^{+}$	-10		-8.2
$\equiv\text{S}^{\text{s}}\text{OH} + \text{Ni}^{+2} + 2\text{H}_2\text{O} \leftrightarrow \equiv\text{S}^{\text{s}}\text{ONi}(\text{OH})_2^{-} + 3\text{H}^{+}$	-20		-17.3
$\equiv\text{S}^{\text{w1}}\text{OH} + \text{Ni}^{+2} \leftrightarrow \equiv\text{S}^{\text{w1}}\text{ONi}^{+} + \text{H}^{+}$		-3.3	
$\equiv\text{S}^{\text{s}}\text{OH} + \text{Ca}^{+2} \leftrightarrow \equiv\text{S}^{\text{s}}\text{OCa}^{+} + \text{H}^{+}$	-3.4 ± 0.56		-2.71 ± 0.66
$\equiv\text{S}^{\text{w1}}\text{OH} + \text{Ca}^{+2} \leftrightarrow \equiv\text{S}^{\text{w1}}\text{OCa}^{+} + \text{H}^{+}$		-6.3 ± 1.69	

Note: The Ni surface complexation reactions and constants are from Bradbury and Baeyens (2005b, 2009b) determined at 0.1 and 0.5 mol/L NaClO₄ solutions, while the constants for Ca reactions were estimated using the LFER approach.

Initial simulations with the experimental reference brine SR-270 showed that $\equiv\text{S}^{\text{s}}\text{ONi}^{+}$ was the dominant surface species. However, the simulated sorption coefficient was approximately a factor of 4 higher than the measured. To explore the possibility that the high concentration of Ca⁺² in the brine may occupy some of the surface sites used by Ni⁺², surface complexation

reactions for Ca^{+2} were also included to the sorption model. The Ca^{+2} surface complexation constants were derived using the LFER approach (Bradbury and Baeyens, 2005b, 2009b) and assuming that the logarithm of the formation constant ($^{\text{OH}}K$) of CaOH^+ is -12.78. The surface complexation reactions for Ca^{+2} sorbing on montmorillonite and illite are given in Table 27. The inclusion of Ca^{+2} sorption reduced Ni^{+2} sorption in brine by a factor of 5. In a study of competing metal sorption on montmorillonite, Bradbury and Baeyens (2005a) observed that metals with similar chemistries, such as valence and hydrolysis behaviour, compete with one other in sorption reactions. However, metals with dissimilar chemistries do not compete in sorption reactions.

Table 28 and Figure 19 summarize the simulated Ni sorption values for montmorillonite and illite in the SR-270 reference brine and the dilute reference solution. In the brine solution the $\equiv\text{S}^{\text{O}}\text{Ni}^+$ surface species dominates, although the $\equiv\text{S}^{\text{O}}\text{NiOH}^0$ and $\equiv\text{S}^{\text{O}}\text{Ni}(\text{OH})_2^-$ species become more prominent at higher pH. However, in the dilute water the simulated sorption is dominated by cation exchange, with the surface complexation accounting for less than 1 percent of total sorption. The simulated Ni^{+2} sorption K_d values for montmorillonite and illite in SR-270 are in good agreement with the average experimentally derived K_d values for bentonite and shale (assuming 60% illite content). Simulated Ni^{+2} sorption K_d values for montmorillonite in dilute water is a factor of 2 higher than the measured sorption at a pH of 8 for bentonite, while the simulated value for shale (assuming 60% illite content) is a factor of 2.7 lower than the measured value. Since Ni^{+2} makes up 88 percent of aqueous Ni species in dilute water, the exchange of Ni^{+2} for Na^+ should provide a reasonable approximation of Ni sorbed by coulombic attraction. Sorption can be simulated for a range of pH values, but the actual measured K_d values that are representative of equilibrium or steady-state conditions are available only for a limited number of pH values which were in equilibrium with bentonite and shale. Therefore, the simulated values cannot be verified beyond pH conditions found in batch sorption tests. The tests described in Chapter 2.4.3 were an attempt to address this. However, the 1 h experimental duration was too short to produce comparable steady-state sorption K_d values for Ni.

Table 28: Calculated Ni K_d Values for Montmorillonite and Illite

pH	Reference SR-270 Brine			Reference Dilute Solution		
	Simulated K_d (cm^3/g)	Measured K_d (cm^3/g)		Simulated K_d (cm^3/g)	Measured K_d (cm^3/g)	
	Montmorillonite		Bentonite	Montmorillonite		Bentonite
5	0.8			2533		
6				2545		
6.5	7.0		5 ± 5			
7	12			3183		
8	17.6			3247		1580 ± 850
9	17.9			2856		
	Illite	60% of Illite	Shale	Illite	60% of Illite	Shale
5	2.5	1.5		974	584	
6				981	589	
6.3	2.5	1.5	2 ± 3			
7	2.5	1.5		991	595	
8	2.7	1.6		974	584	1620 ± 1090
8.5	3.0	1.8				
9.5				864	518	

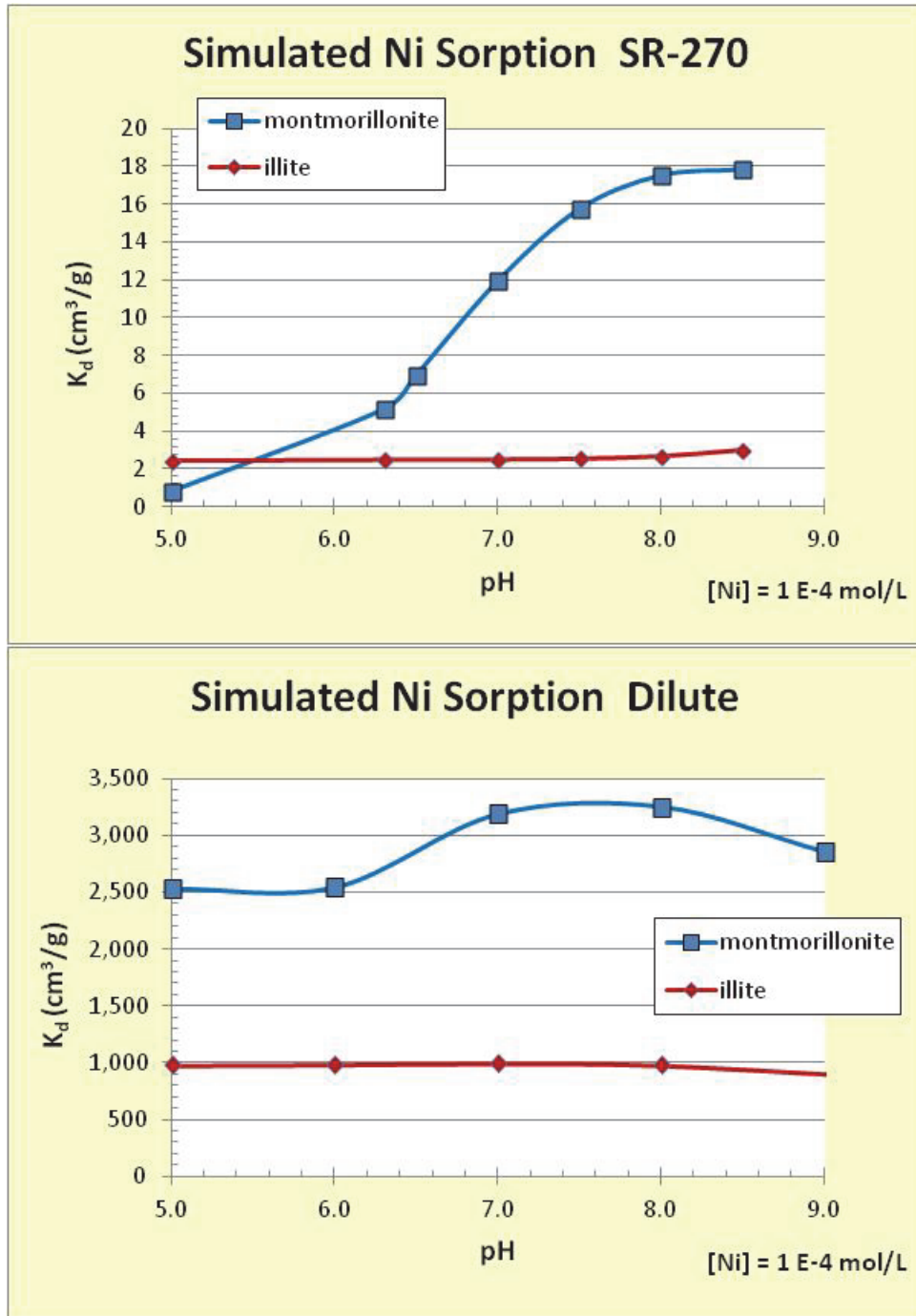


Figure 19: Simulated Nickel Sorption in SR-270 Reference Brine and in Reference Dilute Solution Under Different pH Values

3.3 COPPER

Since surface complexation constants for Cu were not available, the LFER approach was used to estimate surface complexation constants for Cu. These constants were derived assuming that the dominant Cu hydroxyl species in solution are CuOH^+ , Cu(OH)_2^0 , Cu(OH)_3^- , and Cu(OH)_4^{2-} . It should be remembered that in the reference brine solution (pH = 6.3), Cu speciation is dominated by chloride species, and the hydroxyl species make up less than 0.3 percent of all Cu species. The Cu hydrolysis constant $\text{Log}^{\text{OH}}K_x$ values were obtained from the MINTEQ thermodynamic database in PHREEQC. The estimated surface complexation constants and the hydrolysis constants for Cu hydroxyl species used to derive these constants are summarized in Table 29. As in the case with Ni, competition with Ca^{+2} was included in the sorption model simulations. The purpose of this exercise was to investigate whether the sorption parameters (i.e. surface sorption site binding constants) estimated by the LFER approach, using sorption parameters for other elements determined in diluted NaClO_4 solutions, could be used to approximate sorption reactions for Cu in brine solutions. As before, the assumptions are (1) that the thermodynamic code, PHREEQC, can account for Cu interactions with brine salts; (2) that the surface complexation constants determined in NaClO_4 solutions are not significantly different from those in brine solutions; and (3) that montmorillonite and illite can be used to approximate the sorption properties of bentonite and shale. Since Cu selectivity coefficients for the cation exchange of Cu^{+2} with Na^+ were not available, it was assumed that the selectivity coefficient of Ni^{+2} would be a reasonable approximation for Cu^{+2} , based on their similar charge and hydrated radii. The Ni selectivity coefficients used for Cu are 3.1 and 12.6 for Na-montmorillonite and illite, respectively (Bradbury and Baeyens 2005b, 2009b). The CEC values for Na-montmorillonite and illite are 0.87 and 0.225 equivalents/kg (Bradbury and Baeyens 2005b; Baeyens and Bradbury 2004). The site capacities for both Na-montmorillonite and illite are 0.002 mol/kg for the strong site, and 0.04 mol/kg for each of the two weak sites. The sorption K_d value for Cu is calculated by summing the Cu concentrations in all of the solid sites (mol/kg) and dividing the sum by the total Cu concentration in solution.

Table 29: Copper Surface Complexation Reactions and Surface Complexation Constants and Hydrolysis Constants

Cu Surface Complexation Reaction	Montmorillonite $\log^s K_{x-1}$ or $\log^{w1} K_{x-1}$	Illite $\log^s K_{x-1}$	Cu Hydrolysis $\text{Log}^{\text{OH}} K_x$
$\equiv\text{S}^{\text{s}}\text{OH} + \text{Cu}^{+2} \Leftrightarrow \equiv\text{S}^{\text{s}}\text{OCu}^+ + \text{H}^+$	0.9 ± 0.5	1.26 ± 0.6	-8.0
$\equiv\text{S}^{\text{s}}\text{OH} + \text{Cu}^{+2} + \text{H}_2\text{O} \Leftrightarrow \equiv\text{S}^{\text{s}}\text{OCu(OH)}^0 + 2\text{H}^+$	-4.21 ± 0.6	-3.45 ± 0.7	-13.68
$\equiv\text{S}^{\text{s}}\text{OH} + \text{Cu}^{+2} + 2\text{H}_2\text{O} \Leftrightarrow \equiv\text{S}^{\text{s}}\text{OCu(OH)}_2^- + 3\text{H}^+$	-16.1 ± 0.8	-14.4 ± 0.9	-26.9
$\equiv\text{S}^{\text{s}}\text{OH} + \text{Cu}^{+2} + 3\text{H}_2\text{O} \Leftrightarrow \equiv\text{S}^{\text{s}}\text{OCu(OH)}_3^{2-} + 4\text{H}^+$	-27.5 ± 1.1	$-25.0 \pm 0.1.2$	-39.6
$\equiv\text{S}^{\text{w1}}\text{OH} + \text{Cu}^{+2} \Leftrightarrow \equiv\text{S}^{\text{w1}}\text{OCu}^+ + \text{H}^+$	-1.64 ± 0.08		-8.0
$\equiv\text{S}^{\text{s}}\text{OH} + \text{Ca}^{+2} \Leftrightarrow \equiv\text{S}^{\text{s}}\text{OCa}^+ + \text{H}^+$	-3.4 ± 0.56	-2.71 ± 0.66	
$\equiv\text{S}^{\text{w1}}\text{OH} + \text{Ca}^{+2} \Leftrightarrow \equiv\text{S}^{\text{w1}}\text{OCa}^+ + \text{H}^+$	-6.3 ± 1.69		

Note: The constants for Cu and Ca reactions were estimated using LFER developed by Bradbury and Baeyens (2005b, 2009b). The uncertainties were estimated from uncertainties associated with the LFER equations. The Cu hydrolysis $\text{Log}^{\text{OH}}K_x$ values were obtained from the MINTEQ thermodynamic database in PHREEQC.

Table 30 and Figure 20 summarize the simulated Cu sorption K_d values for montmorillonite and illite in the SR-270 reference brine and the dilute reference solution. In the brine solution the $\equiv S^sOCu^+$ and $\equiv S^sOCu(OH)^0$ surface species dominate, with $\equiv S^sOCu(OH)^0$ becoming more important at higher pH. On montmorillonite, the weak site, $\equiv S^{w1}OCu^+$, is equally important. In the dilute solution the simulated Cu sorption is dominated by cation exchange. The simulated results illustrate that copper sorption by cation exchange decreases significantly with higher pH because of the decrease in Cu^{+2} concentration in solution due to the formation of Cu complexes with carbonate and hydroxyl. In the SR-270 reference brine, the simulated Cu sorption K_d value on montmorillonite is a factor of 1.5 lower than the average experimentally derived K_d value on bentonite, and simulated K_d value on shale (account for 60% illite) is a factor of 1.7 lower than the average experimentally derived K_d value. Compared to the measured K_d values for Cu sorption on bentonite and shale, the simulated sorption K_d value in dilute water is a factor of 2.2 lower than the measured value on bentonite and a factor of 1.5 lower than the measured value on shale. Reasons for the difference between simulated and measured Cu sorption in dilute solution could be that Ni^{+2} selectivity does not provide a perfect analog for Cu^{+2} selectivity, and $CuOH^+$ is another cationic Cu species not considered in the model.

Copper sorption can be simulated for a range of pH values, but the actual measured K_d values that are representative of equilibrium or steady-state conditions are available only for the limited number of pH values which were in equilibrium with bentonite and shale. Therefore, the simulated K_d values cannot be verified beyond pH conditions found in batch sorption tests. The sorption tests described in Chapter 2.4.3 were an attempt to address this. However, the 1 h experimental duration was too short to produce comparable steady-state K_d values for Cu. Nevertheless, the measured (1h) pattern of Cu sorption with respect to pH was similar to the simulated pattern for bentonite, but did not show the increased sorption above pH 6.3 that was simulated for illite.

Table 30: Calculated Cu K_d Values for Montmorillonite and Illite

pH	SR-270			Dilute Solution		
	Simulated K_d (cm ³ /g)	Measured K_d (cm ³ /g)		Simulated K_d (cm ³ /g)	Measured K_d (cm ³ /g)	
	Montmorillonite	Bentonite		Montmorillonite	Bentonite	
5	5.6			15807		
6				1412		
6.5	73	107 ± 25				
7	111			7160		
8	163			1103	2380 ± 960	
8.5	169			268		
	Illite	60% of Illite	Shale	Illite	60% of Illite	Shale
5	5.6	3.4		3905	2343	
6				6717	4030	
6.3	49	29	52 ± 11			
7	111	67		4601	2761	
8	163	98		1312	787	1190 ± 450
8.5	169	101				
9.0				317	190	

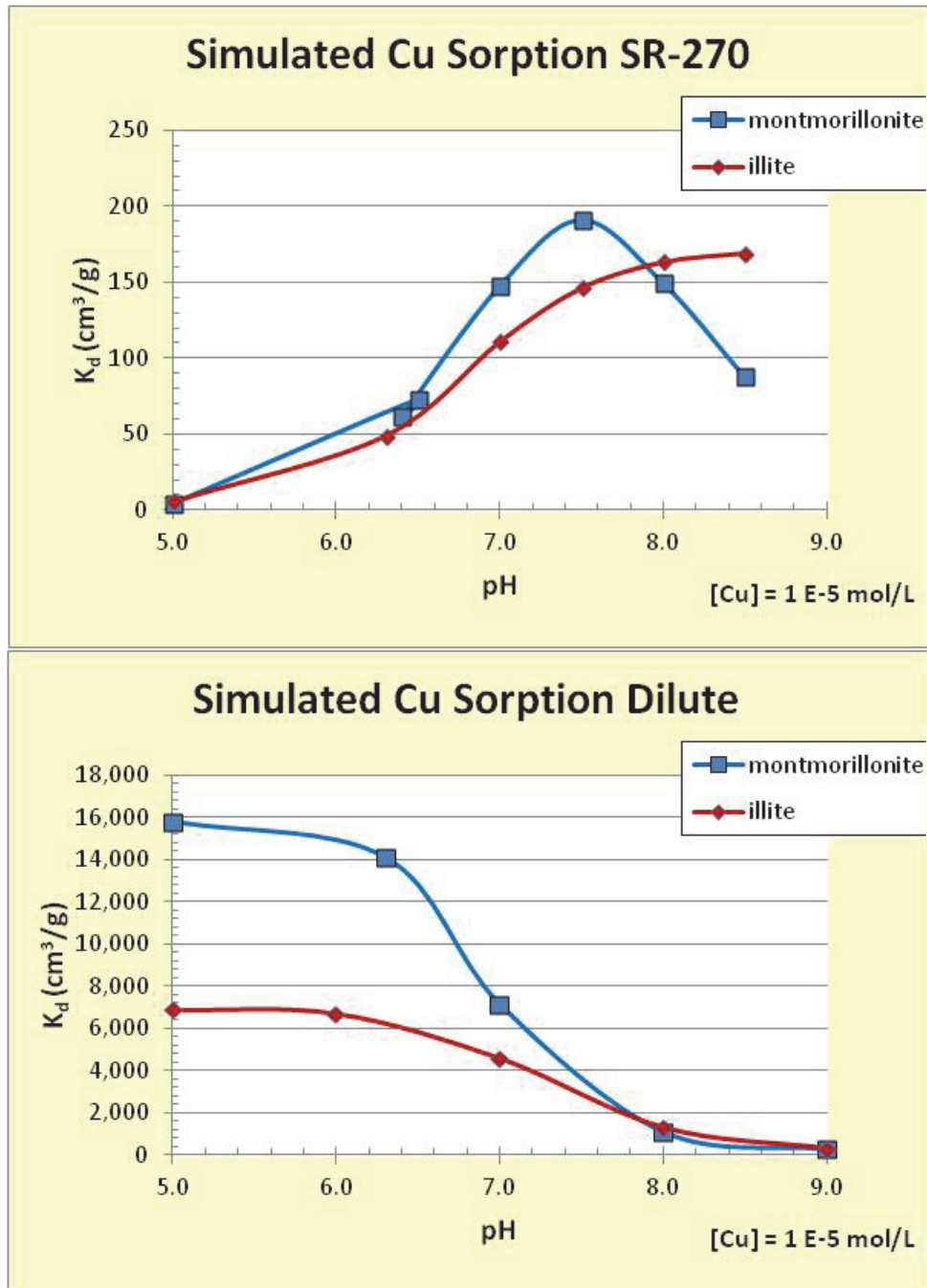


Figure 20: Simulated Copper Sorption in SR-270 Brine and in Dilute Solution Under Different pH Values

3.4 LEAD

Since surface complexation constants for lead sorption on montmorillonite and illite have not been determined by direct measurement, the LFER relations proposed by Bradbury et al. (2005b and 2009b) were used to estimate surface binding constants for Pb sorption on montmorillonite and illite. These constants were derived assuming that the dominant Pb hydroxyl species in reference SR-270 brine solution are PbOH^+ , Pb(OH)_2^0 , and Pb(OH)_3^- . As mentioned previously, the Pb aqueous chemistry in the SR-270 brine is dominated by chloride species, and the hydroxyl species comprise less than 0.2 percent of the total Pb in solution. The Pb hydrolysis constant $\text{Log}^{\text{OH}}K_x$ values were obtained from the PHREEQC thermodynamic database (phreeqc.dat, ver. 2.18.5570). The estimated surface complexation constants and the Pb hydrolysis constants for hydroxyl species used to derive these constants are summarized in Table 31. Competition with Ca^{+2} for sorption was included for montmorillonite, but not for illite. Competition with Ca^{+2} reduced simulated sorption K_d value on montmorillonite to be more in line with measured values, while simulated sorption on illite was below measured values even without considering competition from Ca. A good physiochemical reason why Ca would compete with Pb for sorption on Montmorillonite but not on illite has not been identified. The purpose of this exercise was to determine whether sorption parameters (i.e. sorption surface binding constants) estimated by the LFER approach, using sorption parameters for other elements determined in diluted NaClO_4 solutions, could be used to approximate sorption reactions for Pb in brine solutions. As before, the assumptions are (1) that the thermodynamic code, PHREEQC, can account for Pb interactions with brine salts; (2) that the surface complexation constants determined in NaClO_4 solutions are not significantly different from that in brine solutions; and (3) that montmorillonite and illite can be used to approximate the sorption properties of bentonite and shale.

The Pb^{+2} selectivity coefficients for cation exchange reported for Na-montmorillonite vary from 3.7 to 5.2 (Bradbury and Baeyens 2005b), and the value of 5.2 was used in this study. Selectivity coefficient for Pb^{+2} sorbing on illite was not reported. However, noting that the selectivity coefficient for Pb^{+2} on montmorillonite is a factor of 1.68 higher than that for Ni^{+2} sorbing on montmorillonite, the selectivity coefficient for Pb^{+2} sorbing on illite was estimated from the Ni^{+2} selectivity coefficient to be 21.

Table 31: Lead Surface Complexation Reactions and Surface Complexation Constants Estimated with LFER and Hydrolysis Constants

Cu Surface Complexation Reaction	Montmorillonite $\log^s K_{x-1}$ or $\log^{w1} K_{x-1}$	Illite $\log^s K_{x-1}$	Pb Hydrolysis $\text{Log}^{\text{OH}}K_x$
$\equiv\text{S}^s\text{OH} + \text{Pb}^{+2} \Leftrightarrow \equiv\text{S}^s\text{OPb}^+ + \text{H}^+$	1.17 ± 0.45	1.51 ± 0.55	-7.7
$\equiv\text{S}^s\text{OH} + \text{Pb}^{+2} + \text{H}_2\text{O} \Leftrightarrow \equiv\text{S}^s\text{OPb(OH)}^0 + 2\text{H}^+$	-7.3 ± 0.64	-6.29 ± 0.74	-17.1
$\equiv\text{S}^s\text{OH} + \text{Pb}^{+2} + 2\text{H}_2\text{O} \Leftrightarrow \equiv\text{S}^s\text{OPb(OH)}_2^- + 3\text{H}^+$	-17.2 ± 0.9	-15.42 ± 0.96	-28.1
$\equiv\text{S}^{w1}\text{OH} + \text{Pb}^{+2} \Leftrightarrow \equiv\text{S}^{w1}\text{OPb}^+ + \text{H}^+$	-1.35 ± 2.8		-7.7
$\equiv\text{S}^s\text{OH} + \text{Ca}^{+2} \Leftrightarrow \equiv\text{S}^s\text{OCa}^+ + \text{H}^+$	-3.4 ± 0.56		
$\equiv\text{S}^{w1}\text{OH} + \text{Ca}^{+2} \Leftrightarrow \equiv\text{S}^{w1}\text{OCa}^+ + \text{H}^+$	-6.3 ± 1.69		

Note: The constants for Pb and Ca reactions were estimated using LFER developed by Bradbury and Baeyens (2005b, 2009b). The uncertainties were estimated from uncertainties associated with the LFER equations.

Table 32 and Figure 21 summarize the simulated Pb sorption values for montmorillonite and illite in the SR-270 reference brine and the dilute reference solution. In the brine solution, the $\equiv\text{S}^{\circ}\text{OPb}^+$ surface species dominates sorption on illite up to pH values greater than 8, where the $\equiv\text{S}^{\circ}\text{OPb}(\text{OH})^0$ species becomes important. Simulated sorption on montmorillonite is dominated by the weak site, $\equiv\text{S}^{\text{w}1}\text{OPb}^+$. In the dilute solution, the simulated Pb sorption is dominated by cation exchange. As with Cu, Pb sorption by cation exchange decreases significantly with higher pH because of the decrease in Pb^{+2} concentration in solution due to the formation of Pb complexes with carbonate and hydroxyl. The simulated Pb sorption K_d values in SR-270 on montmorillonite were a factor of 1.2 higher than the average measured K_d value on bentonite, while simulated sorption K_d value on shale (account for 60% of illite sorption value) was a factor of 3.4 lower than measured sorption value. However, considering the uncertainty in the average measured values, the simulated values were not significantly different from measured values. The simulated sorption K_d value in dilute water is a factor of 2 higher than measured values for bentonite, but a factor of 3 lower than measured values for shale.

Lead sorption can be simulated for a range of pH values, but the actual measured K_d values that are representative of equilibrium or steady-state conditions are available only for the limited number pH values which were in equilibrium with bentonite and shale. Therefore, the simulated K_d values cannot be verified beyond pH conditions found in batch sorption tests. The tests described in Chapter 2.4.3 were an attempt to address this. However, the 1 h experimental duration was too short to produce comparable steady-state K_d values for Pb.

Table 32: Calculated Pb K_d Values for Montmorillonite and Illite

pH	SR-270			Dilute Solution		
	Simulated K_d (cm^3/g)	Measured K_d (cm^3/g)		Simulated K_d (cm^3/g)	Measured K_d (cm^3/g)	
	Montmorillonite	Bentonite		Montmorillonite	Bentonite	
5	0.05			2907		
6.5	6.08	5 ± 4		2670		
7	13.3			1798		
7.5	22.4			1287		
8	26			1089	523 ± 108	
8.5	27			1033		
	Illite	60% of Illite	Shale	Illite	60% of Illite	Shale
5	0.13	0.08		874	524	
6.3	1.47	0.88	3 ± 3	716	430	
7	2.60	1.56		325	195	
7.5	3.27	1.96		148	89	293 ± 13
8.0	4.39	2.63		78	47	
8.5	7.38	4.42		55	33	

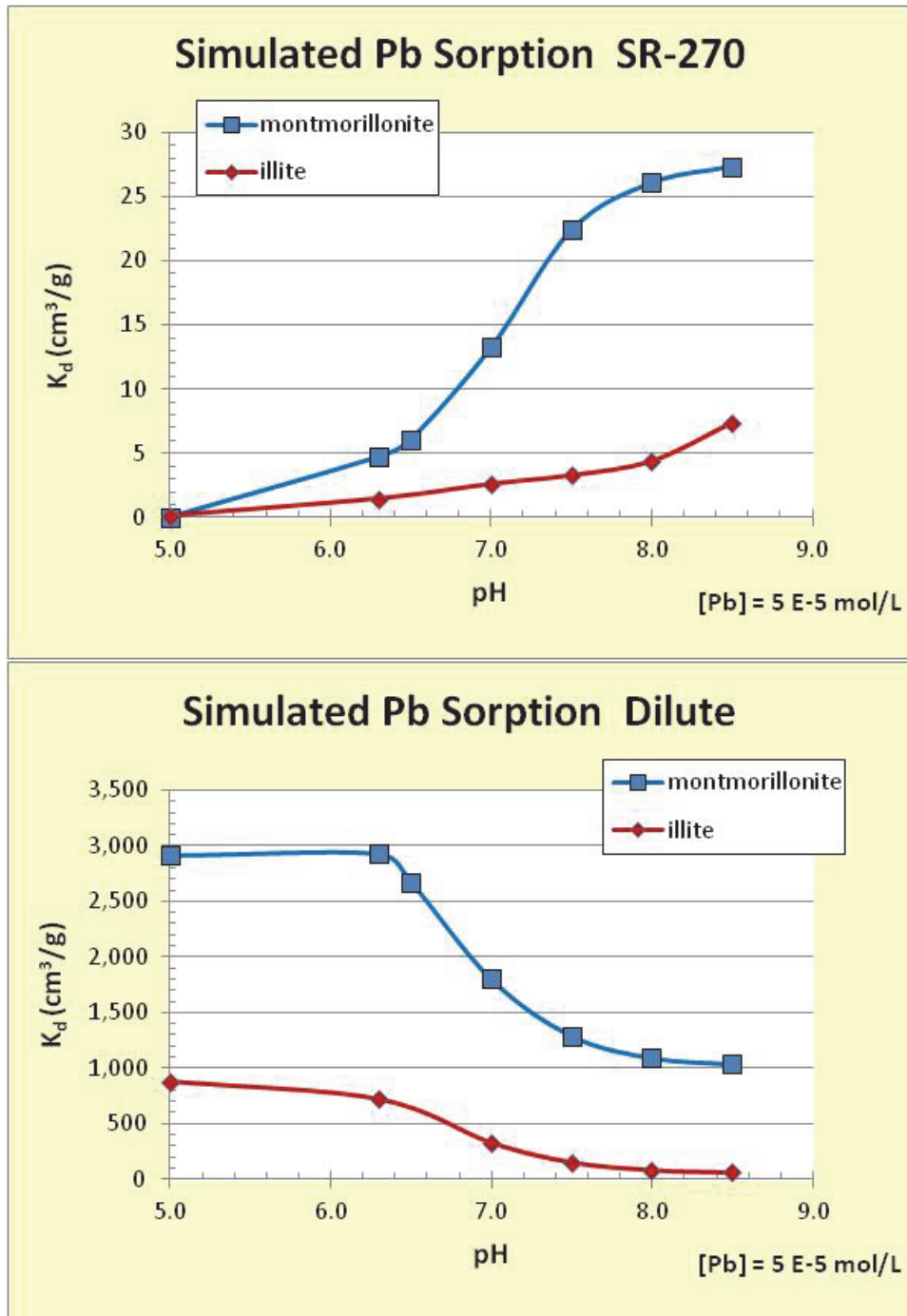


Figure 21: Simulated Lead Sorption in SR-270 Brine and Dilute Solution Under Different pH Values

3.5 ZIRCONIUM

Given the lack of Zr sorption data, the LFER relations proposed by Bradbury et al. (2005b and 2009b) were used to estimate surface binding constants for Zr sorption on montmorillonite and illite. The surface species and their associated surface binding constants derived using LFER are given in Table 33. Competition with Ca^{+2} was not included because its chemistry is not similar to that of Zr^{+4} . Since the dominant Zr species in solution is the neutral charged $\text{Zr}(\text{OH})_4^0$, cation exchange was not included in the Zr sorption model. The site capacities for both Na-montmorillonite and illite are 0.002 mol/kg for the strong site and 0.04 mol/kg for each of the two weak sites (Bradbury and Baeyens, 2005b, 2009b). The K_d value for Zr is calculated by summing the Zr concentrations in all of the solid sites (mol/kg) and being divided by the total Zr concentration in solution. The purpose of this exercise was to determine whether the sorption surface binding constants estimated by the LFER approach, using the sorption surface constants for other elements determined in diluted NaClO_4 solutions, could be used to approximate sorption reactions for Zr in brine solutions. As before, the assumptions are (1) that the thermodynamic code, PHREEQC, can account for Zr interactions with brine salts; (2) that the surface complexation constants determined in diluted NaClO_4 solutions are not significantly different from that in brine solutions; and (3) that montmorillonite and illite can be used to approximate the sorption properties of bentonite and shale.

Table 33: Zirconium Surface Complexation Reactions and Surface Complexation Constants and Hydrolysis Constants

Zr Surface Complexation Reaction	Montmorillonite $\log {}^sK_{x-1}$ or $\log {}^{w1}K_{x-1}$	Illite $\log {}^sK_{x-1}$	Zr Hydrolysis $\text{Log } {}^{\text{OH}}K_x$
$\equiv\text{S}^{\text{OH}} + \text{Zr}^{+4} \Leftrightarrow \equiv\text{S}^{\text{O}}\text{Zr}^{+3} + \text{H}^+$	8.39 ± 0.31	8.17 ± 0.41	-7.7
$\equiv\text{S}^{\text{OH}} + \text{Zr}^{+4} + \text{H}_2\text{O} \Leftrightarrow \equiv\text{S}^{\text{O}}\text{Zr}(\text{OH})^{+2} + 2\text{H}^+$	8.98 ± 0.32	8.71 ± 0.42	-17.1
$\equiv\text{S}^{\text{OH}} + \text{Zr}^{+4} + 3\text{H}_2\text{O} \Leftrightarrow \equiv\text{S}^{\text{O}}\text{Zr}(\text{OH})_3^0 + 4\text{H}^+$	6.13 ± 0.34	6.08 ± 0.36	
$\equiv\text{S}^{\text{OH}} + \text{Zr}^{+4} + 5\text{H}_2\text{O} \Leftrightarrow \equiv\text{S}^{\text{O}}\text{Zr}(\text{OH})_5^{-2} + 6\text{H}^+$	-18 ± 1	-16 ± 1	-28.1
$\equiv\text{S}^{\text{w1}}\text{OH} + \text{Zr}^{+4} \Leftrightarrow \equiv\text{S}^{\text{w1}}\text{OZr}^{+3} + \text{H}^+$	6.51 ± 0.8		-7.7

Note: The constants for Zr reactions were estimated using LFER developed by Bradbury and Baeyens (2005b, 2009b). The uncertainties were estimated from uncertainties associated with the LFER equations.

Simulations with the reference brine SR-270 indicated that $\equiv\text{S}^{\text{O}}\text{Zr}(\text{OH})_3^0$ was the only significant Zr surface species. This is not surprising since $\text{Zr}(\text{OH})_4^0$ is predicted to be the dominant Zr species in solution. Simulated Zr sorption coefficients for the reference brine SR-270 and the dilute reference water are presented in Figure 22 and Table 34, along with the measured sorption coefficients in SR-270. The simulated sorption coefficients for bentonite do not vary significantly with pH from a pH value of 4 to about 8, but decreased for illite above pH of 7. This contrasts with the trend in Zr sorption coefficients with pH (1 h duration tests) measured from pH of 5 to 7.8 (Figure 4) where the measured sorption value is higher at pH of 7.8. $\text{Zr}(\text{OH})_4^0$ is the dominant solution species in both reference waters, except below pH of 3.5

in the brine where Zr fluoride complexes become more important than hydroxyl complexes. The presence of fluoride complexes accounts for reduced sorption in brine at low pH. The simulated Zr sorption coefficient for montmorillonite is a factor of 3.0 higher than the average measured sorption coefficient for bentonite in SR-270. The simulated sorption coefficient for illite, reduced to account for the 60% illite content in shale, is a factor of 1.6 higher than the measured sorption value on shale. This provides confidence that the simulated Zr sorption K_d value, derived using LFER, provide a reasonable approximation of Zr sorption value in brine solutions. Zirconium sorption was not measured in dilute water. However, the simulations in Table 34 indicate that Zr sorption in dilute solution would be only 12% to 15% higher than that in brine solution at pH values of interest.

Table 34: Calculated Zr K_d Values on Montmorillonite and Illite

pH	SR-270			Dilute Water		
	Simulated K_d (cm ³ /g)	Measured K_d (cm ³ /g)		Simulated K_d (cm ³ /g)	Measured K_d (cm ³ /g)	
	Montmorillonite	Bentonite		Montmorillonite	Bentonite	
2	0			1511		
3	530			1537		
4	1324			1543		
5	1354			1546		
6.5	1349	454 ± 66		1546		
7	1348			1546		
8	1339			1544		
9	1283			1544		
	Illite	60% of Illite	Shale	Illite	60% of Illite	Shale
2	0	0		1491	895	
3	842	505		1534	920	
4	1349	809		1541	925	
5	1354	812		1538	923	
6.3	1349	809	494 ± 0	1515	909	
7	1324	794		1479	887	
8.0	1107	664		1335	801	
9.0	495	297		1083	650	

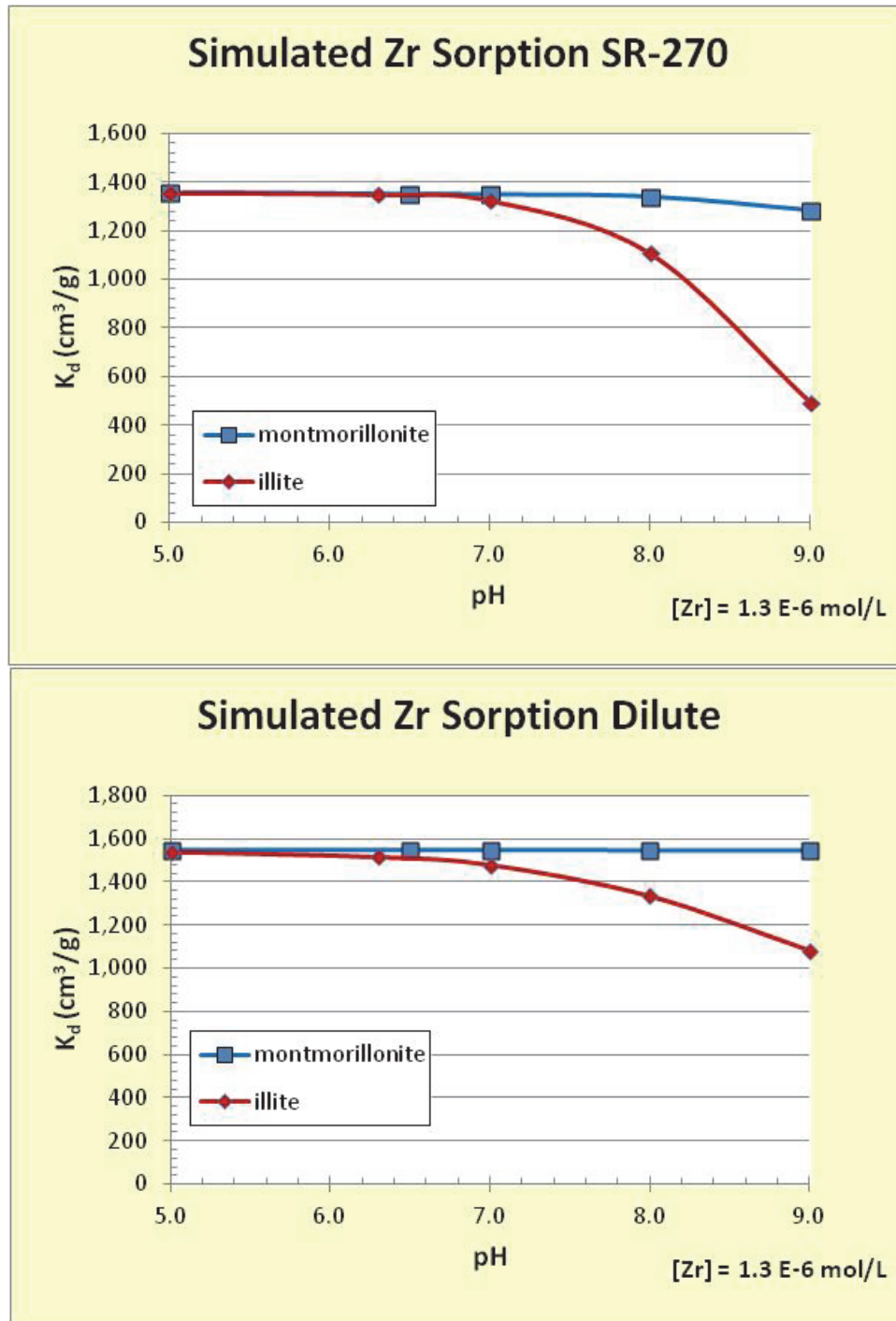


Figure 22: Simulated Zirconium Sorption in SR-270 Brine and Dilute Water Under Different pH Values

3.6 SUMMARY

Assuming that montmorillonite and illite can be used to approximate bentonite and shale, surface complexation modelling was performed for these minerals using a 2-site protolysis non-electrostatic surface complexation and cation exchange model. Acid-base properties, site densities, and cation exchange properties were obtained from the literature (Bradbury and Baeyens (2005b, 2009b)). Nickel surface complexation constants were obtained from the literature. Surface complexation constants for Cu, Pb and Zr were estimated using LFER and metal hydrolysis constants. Cation exchange selectivity coefficients for Ni were obtained from the literature (Bradbury and Baeyens, 2005b; Baeyens and Bradbury, 2004). Copper selectivity coefficients were based on Ni values. Lead selectivity coefficient for montmorillonite was obtained from the literature (Bradbury and Baeyens, 2005b), while the value for illite was based on the Ni value. Competition with Ca^{+2} for surface complexation sites was included for Ni, Cu and Pb, but not for Zr. Cation exchange was not included for Zr sorption reaction because its dominant aqueous species is the neutral $\text{Zr}(\text{OH})_4$. The simulated sorption K_d results could be compared to the measurements from two solutions with drastically different salt concentrations. The ability to compare simulated sorption results over a broad pH range with 1 hour short time sorption tests was limited because the sorption experimental time was too short to obtain equilibrium sorption values and for some elements such as Ni, the sorption K_d value measured after 1 hour was 0. Longer sorption times at higher and lower pH values can only be achieved with the use of pH buffers and the assumption that they do not affect the solid surfaces.

The simulated Ni sorption values were in very good agreement with measured values in brine solution, where sorption was dominated by surface complexation. In the dilute water, where sorption is dominated by cation exchange, the simulated sorption coefficient on montmorillonite was a factor of 2.0 higher than the measured, while simulated sorption coefficient on shale was a factor of 2.7 lower than the measured. In those cases where surface complexation parameters were estimated by LFER, the simulated sorption values were very close to measured values. Simulated Cu sorption coefficient on montmorillonite was a factor of 1.5 lower than the measured value on bentonite, simulated Cu sorption coefficient on shale (after accounting for 60% of illite in shale) was a factor of 1.7 lower than the measured value on shale. The simulated and measured Pb sorption values were not significantly different. Simulated Zr sorption coefficients on shale and montmorillonite were factors of 1.6 and 3 higher than measured. Given issues with detection limits, the measured sorption coefficient on bentonite could be a minimum value. In the dilute reference solution, simulated Cu sorption K_d values were factors of 2.2 and 1.5 lower than the measured values for bentonite and shale respectively. Compared to the measurements in the dilute solution, the simulated Pb sorption coefficient was a factor of 2 higher on bentonite, and a factor of 3 lower on shale.

It is encouraging that the sorption of certain elements can be predicted with sorption modelling, to obtain calculated K_d values that are within a factor of 3 of measured values. However, one should remember that although surface complexation models can be used to reproduce the results of sorption experiments over a wide range of conditions and to extrapolate the sorption values to different solution conditions, this does not prove the actual existence of the proposed surface reactions. The existence of the proposed surface species needs to be demonstrated by independent experimental methods. Nevertheless, sorption modelling remains a useful tool for furthering the understanding of sorption and extrapolating sorption results to new groundwater conditions.

4. DIFFUSIVE MASS TRANSPORT EXPERIMENTS

Understanding sorption and its role in the transport of radionuclides in Canadian sedimentary rocks under saline conditions requires a combination of batch sorption experiments and diffusive mass transport test to demonstrate that sorption coefficients (K_d) measured using batch sorption tests can be applied to explain mass transport results. Diffusion is the primary transport mechanism in the low permeability Ordovician shales and limestones. Therefore, a diffusive mass transport test was undertaken with sorbing tracers to improve the understanding of sorption in mass transport. This was intended to address aspects of specific surface areas, and sorption and desorption kinetics.

The diffusion test was performed with sorbing tracers to study the effect of sorption on diffusion-only transport in shale. The experimental configuration was a diffusion cell in which a rock coupon is sandwiched between a tracer reservoir and an elution reservoir (Vilks and Miller, 2007). Tracers would include one or more sorbing tracers along with a conservative tracer to characterize the physical, non-reactive diffusion properties of the rock. The diffusion properties of Queenston shale for non-sorbing tracers (iodide and tritium) has previously been determined (Vilks and Miller, 2007). The intent of the diffusion test was to determine the tracer sorption coefficients by comparing the apparent diffusion coefficients of sorbing tracers with those of the non-sorbing tracer. The diffusion of sorbing and non-sorbing tracers was characterized by (1) monitoring the breakthrough of tracers in the elution reservoir, and (2) characterizing the diffusion profiles of tracers within the rock core sample by cutting or grinding material from the core sample, leaching it to recover tracers and determining tracer concentrations as a function of core length. The diffusion profiles were intended to characterize the diffusion of those elements that may be sorbed too strongly to diffuse into the elution reservoir in sufficient quantities to be measurable.

4.1 DEFINITIONS

Diffusivity is a measure of the ability of a species to move through a medium under the influence of its concentration gradient. Diffusivity is quantified as a diffusion coefficient, D . Diffusivity can be measured under steady-state or transient conditions, and each has its advantages and area of applicability.

The processes of diffusion are described by Fick's first and second laws. In generalized situations, such as the conduction of heat in a solid, or the diffusion of species in a single phase medium such as water, Fick's first law states that the mass of a diffusing substance passing through a given cross section per unit of time is proportional to the concentration gradient. In one dimension,

$$J = -D \cdot \frac{\partial C}{\partial x} \quad (14)$$

where

- J is the mass flux [$\text{mol}/\text{m}^2\text{s}$],
- D is the diffusion coefficient [m^2/s],
- C is the species concentration [mol/m^3], and

$\partial C/\partial x$ is the concentration gradient.

Fick's second law relates concentration with both space and time. In one dimension,

$$\frac{\partial C}{\partial t} = D \cdot \frac{\partial^2 C}{\partial x^2} \quad (15)$$

When evaluating diffusion through a fluid in a two-phase system, such as groundwater in a porous rock, it becomes necessary to modify Fick's laws to account for the fact that water only occupies a fraction of the total volume occupied by the rock. The modification is applied by redefining the diffusion coefficient (D) to include factors such as the porosity and the pore geometry, which is defined by a combination of tortuosity and constrictivity.

The diffusion coefficients that are used in Equations 19 and 20 to describe diffusivity in heterogeneous media have been defined to account for various combinations of the effects of porosity, tortuosity and constrictivity. The type of diffusion coefficient used depends on the particular application.

Because species diffuse through water in pore spaces, all diffusion coefficients applied to heterogeneous media can be related to the free-water diffusion coefficients (D_w). Free-water diffusion coefficients have been measured for numerous cations and ions. Values of free-water diffusion coefficients for cations and anions vary between 1.03×10^{-9} and 9.59×10^{-9} m²/s (e.g., Harvey, 1996).

For certain applications, diffusion may be considered as a function of species concentration only in porewater. For example, this may be useful if diffusion data is available in the form of a diffusion profile, which shows changes in a species porewater concentration as a function of distance (e.g., Gimmi and Waber, 2004). Diffusion in porewater is commonly described with a porewater diffusion coefficient, which accounts for the effects of tortuosity (τ) and constrictivity (δ) within connected pore spaces. This type of diffusion coefficient may be used as one of the input parameters in certain computer models that have porosity and diffusion as separate input parameters. The porewater diffusion coefficient (D_p) is defined as follows (Ohlsson and Neretnieks, 1995):

$$D_p = \frac{D_w \delta}{\tau^2} \quad (16)$$

Diffusion can also be treated by considering a volume of rock as a whole. In this case, the connected porosity must be included in the calculation of the diffusive flux to account for the small volume of connected pore space compared to the volume of the whole rock. The effective or empirical diffusion coefficient (D_e) is commonly used to describe diffusive fluxes. Some authors (Bradbury et al., 1982) have also referred to this as the intrinsic diffusion coefficient (D_i). The effective diffusion coefficient is defined as (Choi and Oscarson, 1996; Skagius and Neretnieks, 1982; and Ohlsson and Neretnieks, 1995):

$$D_e = \frac{D_w \delta \epsilon_t}{\tau^2} \quad (17)$$

The through-transport porosity (ε_t) determines the diffusive flux through rock when steady state has been achieved. However, the storage capacity of the rock must also be considered. The storage capacity results from the dead end porosity (ε_d), and sorption for those species that are likely to adsorb onto mineral surfaces. The storage capacity is quantified by the rock capacity factor (α), which has been defined as (Bradbury and Green, 1985):

$$\alpha = \varepsilon_c + \rho \cdot K_d \quad (18)$$

where ρ is the bulk density of the rock, K_d is the sorption coefficient, and the total connected porosity (ε_c) is given by:

$$\varepsilon_c = \varepsilon_t + \varepsilon_d \quad (19)$$

The rock capacity term can be incorporated into Fick's second law to describe concentration variation with space and time within a rock:

$$\frac{\partial C}{\partial t} = \frac{D_e}{\alpha} \cdot \frac{\partial^2 c}{\partial x^2} \quad (20)$$

The apparent diffusion coefficient (D_a) has been defined as (Bradbury and Green, 1985; Choi and Oscarson, 1996; Oscarson and Hume, 1994; and Ohlsson and Neretnieks, 1995):

$$D_a = \frac{D_e}{\alpha} = \frac{D_p \varepsilon_t}{(\varepsilon_c + \rho K_d)} \quad (21)$$

In the case of a non-sorbing tracer, such as iodide, the rock capacity term (α) is equal to the total connected porosity (ε_c). If the transport porosity (ε_t) is the same as the ε_c , the apparent diffusion coefficient for the non-sorbing tracer will be the same as the porewater diffusion coefficient (D_p).

The constrictivity (δ) and tortuosity (τ) are difficult, if not impossible, to be determined separately by experimental means. Because of the difficulty in separating δ and τ , the term 'tortuosity' is often found in experimental work to have been used to describe the quantity $\tau / \sqrt{\delta}$. Melnyk and Skeet (1987) and Katsube et al. (1986) referred to the quantity $\tau / \sqrt{\delta}$ as an 'effective tortuosity' (τ_D) and defined it as:

$$\tau_D^2 = \frac{\tau^2}{\delta} \quad (22)$$

The effective tortuosity values can be calculated from measured values of effective diffusion coefficients and estimated values of transport porosity, using equation 17, and assuming that ε_t and ε_c are identical. Effective tortuosity values may vary depending upon the tracer because the porosity used for diffusion may vary from one tracer to another. The porosity value used in equation 17 could be derived from water immersion or from rock capacity factors derived with conservative tracers in diffusion experiments.

In this report the convention for reporting effective tortuosity focuses on the increased path length a solute must diffuse. By this convention, the diffusion coefficient is reduced by effective tortuosity values greater than one.

4.2 EXPERIMENTAL THEORY

In through-diffusion cell experiments, a rock sample is positioned between two solution reservoirs of equal hydraulic head. A concentration gradient is then established across the rock sample by addition of tracers to one of the reservoirs. Once the system has reached a steady state, the flux of tracer across the sample is measured and the effective diffusion coefficient of the tracer in the rock sample is determined. Vilks et al. (1999) have described a method used to estimate diffusion parameters from laboratory experiments on crystalline rocks, which is based on the work of Cramer et al. (1997), Bradbury et al. (1982), Wadden and Katsube (1982), Skagius and Neretnieks (1982), and Katsube et al. (1986). Following the initial breakthrough of tracer, the amount of tracer (conservative or weakly sorbing) diffusing through the sample into the elution reservoir eventually reaches a steady state, provided that the physical properties of the rock remain constant during the diffusion experiment (Figure 23). The mass of tracer (M_t) diffusing through the sample under steady-state conditions at time (t) is described by the following equation:

$$M_t = D_e(C_o A/L) t - \alpha(ALC_o/6) \quad (23)$$

where

- D_e = effective diffusion coefficient for a given tracer in the rock sample;
- A = surface area through which the tracer diffuses;
- L = diffusion path length (i.e., thickness of rock sample);
- C_o = concentration of a given tracer in the tracer reservoir; and
- α = rock capacity factor.

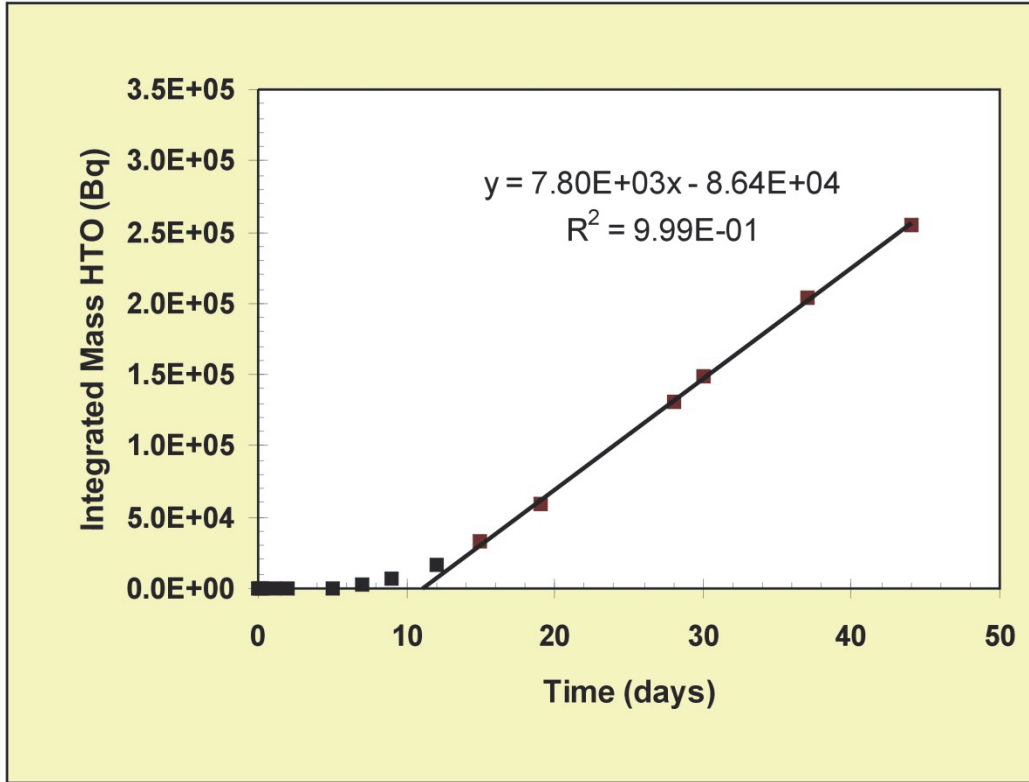


Figure 23: Example of Tracer Mass Diffusion in a Through-diffusion Experiment

When steady state has been achieved, a plot of M_t versus time will produce a straight line with a slope:

$$\text{Slope} = D_e(C_o A/L) \quad (24)$$

and an intercept:

$$\text{Intercept} = -\alpha(ALC_o/6) \quad (25)$$

Because C_o , A and L are known, the slope of the line can be used to calculate D_e . The intercept of the straight line can be used to calculate the dimensionless rock capacity factor (α), which represents the amount of tracer retained in the rock sample before steady state is achieved. The magnitude of α depends upon the total connected porosity accessed by the tracer (ε_c) and on the amount of tracer that is adsorbed by the rock sample. Therefore, D_e and α are the basic parameters that can be estimated from through-diffusion data, without additional assumptions.

The error associated with estimated values of D_e is estimated from the uncertainty in the diffusive flux, which is obtained from the slope of the linear portion of the M_t versus time plot. This uncertainty is calculated from linear regression analysis. The error associated with values of rock capacity determined from diffusion experiments can also be estimated from the uncertainty of the intercept of the M_t versus time plots using linear regression analysis.

4.3 METHOD

The sample of Queenston shale used for this test was obtained from archived drill core from Niagara Falls, Ontario. The sample core depth was 98.9 m below ground surface. The core diameter was 62.5 mm and its thickness was 9.75 mm. The properties of Queenston shale from Niagara Falls have been previously studied with diffusion experiments using iodide and tritium (Vilks and Miller, 2007). The porosity of this sample of Queenston shale determined by water immersion is 0.0663 ± 0.0048 , while the iodide rock capacity is 0.037 ± 0.011 and the tritium rock capacity is 0.096 ± 0.032 . The rock capacities provide an indication of how much porosity is occupied by a non-sorbing tracer. The effective tortuosity (τ_D) based on tests with iodide is 9.89 ± 2.62 . The core sample was installed in the diffusion cell (Figure 24) by cementing it into the sample holder with silicon rubber adhesive sealant (RTV 108, Momentive performance materials). The diffusion cell contains a 950 cm³ volume tracer reservoir, contacting one side of the sample, and a 155 cm³ elution reservoir contacting the other side. Initially both reservoirs were filled with SR-270 reference brine solution (no tracers) and the sample core was allowed to saturate with brine for a period of 6 days. During the conditioning period, the water level on the tracer reservoir side was higher than on the elution reservoir side to promote water flow through the sample. At the completion of the conditioning period the conditioning solution was removed from both reservoirs. Both reservoirs were rinsed with fresh brine solution.

To initiate the diffusion test, tracer-free brine was added to the elution reservoir. Next a brine solution with tracers was added to the tracer reservoir and care was taken to make sure that both reservoirs were at the same hydraulic level. The injected tracer concentrations, free-water diffusion coefficients and expected sorption properties of the tracer elements based on batch sorption tests are summarized in Table 35. Both reservoirs were exposed to the same atmospheric pressure. The elution reservoir was sampled several times during a week to determine if tracer had diffused through the shale sample. During sampling, a 5 cm³ volume solution was removed and immediately replaced it with the same volume of tracer-free brine to ensure that both the tracer and elution reservoirs remain at the same level. The sampling rate was kept to a minimum because the diffusion process was expected to be very slow and a faster sampling rate would not allow tracer concentrations to build up to a measurable rate within the elution reservoir. As tracers diffuse through the rock, eventually a steady-state diffusive flux across the sample will be achieved. The time frame required to achieve steady state for a given element depends upon its free-water diffusion coefficient and sorption properties. Past experience has indicated that it may take 5 to 10 days to achieve steady state for a non-sorbing tracer (iodide or tritium) diffusing through a 10 mm thick shale sample, and considerably longer for a sorbing tracer. The duration of this diffusion test was 141 days. The pH of the elution reservoir (6.56 ± 0.04) remained constant for the duration of the diffusion test.

Since some of the tracers will sorb onto the shale, it is possible that they will not be eluted in sufficient quantities to be detected during the time frame of the diffusion test (141 days). Therefore, it is important to determine how far into the shale each tracer has been able to diffuse. After the diffusion test was terminated, the tracer and elution reservoirs were emptied and the diffusion cell was taken apart to remove the shale sample. Once removed from the cell, the shale core was stored in a humid environment to minimize evaporative losses and possible migration of tracers in the core caused by redistribution of porewater due to evaporation. In order to determine tracer concentration as a function of distance from the tracer reservoir side, a section of core (approximately one quarter) was removed for sampling purposes. The sample section was chosen to avoid core edges, in case they were affected by drilling. Starting from the tracer side, the core sample was sanded using 100 grit wet/dry sandpaper (Figure 25).

During the sanding process the remaining core thickness and weight were checked to monitor the amount of shale removed. The sampled shale layers varied in thickness from 0.1 to 1.3 mm, with thickness increasing away from the tracer side. A total of 18 samples were collected. A reference shale sample, not exposed to tracer solution, was also sanded to determine background tracer concentrations. The shale samples were leached overnight with 2.5 cm³ volumes of 2% (by volume) HNO₃ acid. The leached samples were centrifuged for 15 minutes using an IEC clinical centrifuge at the maximum setting of 7. Then 2 cm³ of supernatant were removed and diluted to 20 cm³ before being submitted to analyses by ICP-MS. The measured background concentrations of Li, Ni, Cu, Pb and U in the reference shale sample were 8.4×10^{-5} , 5.0×10^{-6} , 2.5×10^{-6} , 7.5×10^{-7} , and 9.2×10^{-8} mol/kg, respectively.

Table 35: Tracer Properties Used in Diffusion Test

Element	Concentration (mol/L)	Free-Water Diffusion Coefficient (D_w) (m^2/a)	K_d Values from Batch Experiments for Shale (cm^3/g)
Li ⁺	2×10^{-2}	0.032	2 ± 3
Ni ⁺²	1×10^{-4}	0.042	2 ± 3
Cu ⁺²	1×10^{-5}	0.045	52 ± 31
Pb ⁺²	5×10^{-5}	0.060	3 ± 3
UO ₂ ⁺²	1×10^{-5}	0.269	28 ± 9

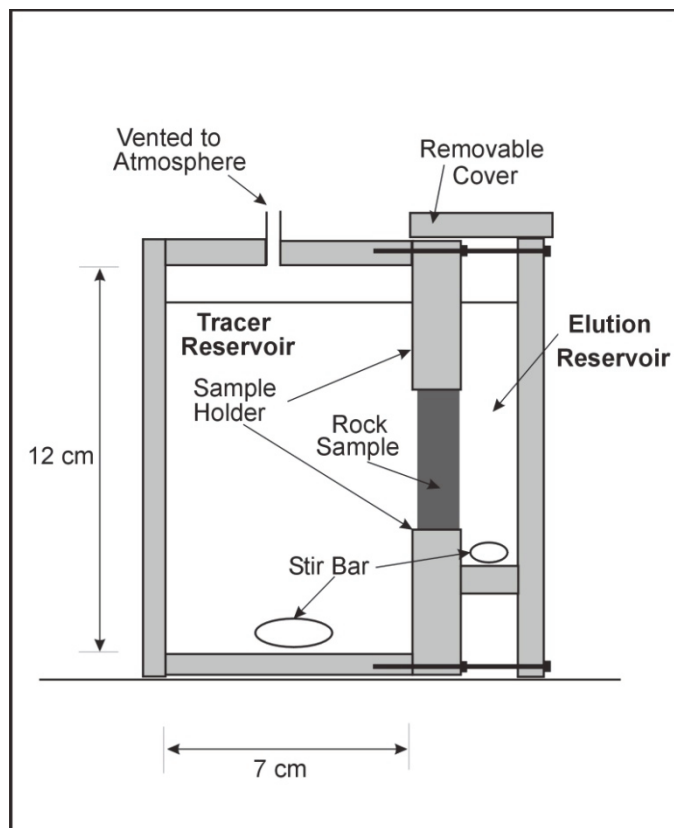


Figure 24: Schematic Diagram of Diffusion Cell

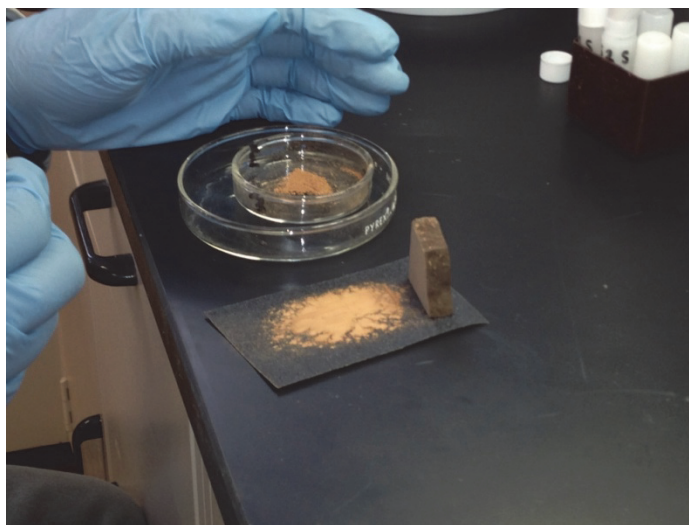


Figure 25: Sampling Shale Core to Determine Tracer Diffusion Profiles

4.4 RESULTS

Analyses of brine solution from the elution reservoir showed that Li was diffusing through the shale. However, breakthrough of Ni, Pb and U was not detected during the experiment. The initial Cu concentrations observed in the elution reservoir were too high to be attributed to the tracer, and were interpreted to result from the leaching of Cu from the shale. Therefore, only the diffusion properties of Li could be analysed from the tracer breakthrough data. Figure 26 illustrates the integrated mass of Li that has diffused through shale sample as a function of time. The regression line (and its equation) is based on data points measured after 84 days and longer in order to better approximate steady-state conditions. The calculated lithium effective diffusion coefficient (D_e) was $1.45 \times 10^{-12} \text{ m}^2/\text{s}$, and the rock capacity for Li was estimated to be 0.108 (by equation 25). The estimated effective tortuosity was 6.0. The data for Figure 26 are presented in Table A21 in the Appendix A.

Equation 18 can be used to estimate the K_d value for Li from the Li rock capacity value. Assuming that the water immersion derived shale porosity (0.0663, reported by Vilks and Miller 2007), is the appropriate porosity to use, and that the bulk rock density is 2.608 g/cm^3 , the estimated K_d value for Li is $0.016 \text{ cm}^3/\text{g}$. If the average iodide rock capacity (0.037, reported by Vilks and Miller 2007), is a better estimate of porosity used by Li then the estimated K_d would be $0.027 \text{ cm}^3/\text{g}$. If the tritium rock capacity (0.096, reported by Vilks and Miller 2007), is more appropriate, the K_d value would be significantly lower, $0.0046 \text{ cm}^3/\text{g}$.

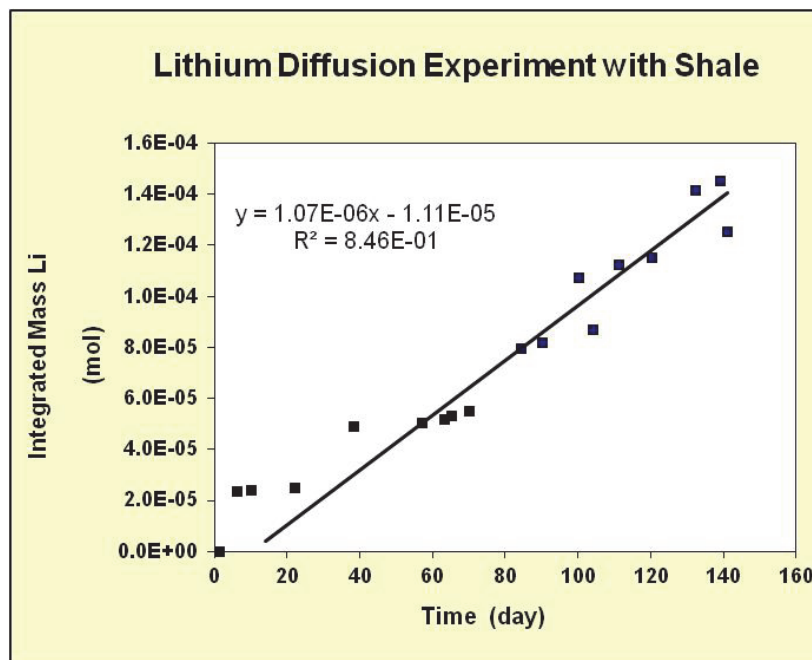


Figure 26: Lithium Mass Diffusion through Shale Sample after 141 Days of Through Diffusion Test

The Li diffusion profile through the shale sample, illustrating Li distribution after 141 days, is illustrated in Figure 27. With the exception of lower Li concentrations at 2 to 3 mm, the concentration profile is fairly straight, approximating steady-state conditions. The Li

concentrations within 0.5 mm of the contact with tracer solution are slightly high, possibly due to a small amount of Li sorption. The data for the diffusion profiles for Li and the other tracers are presented in Table A22 of the Appendix A.

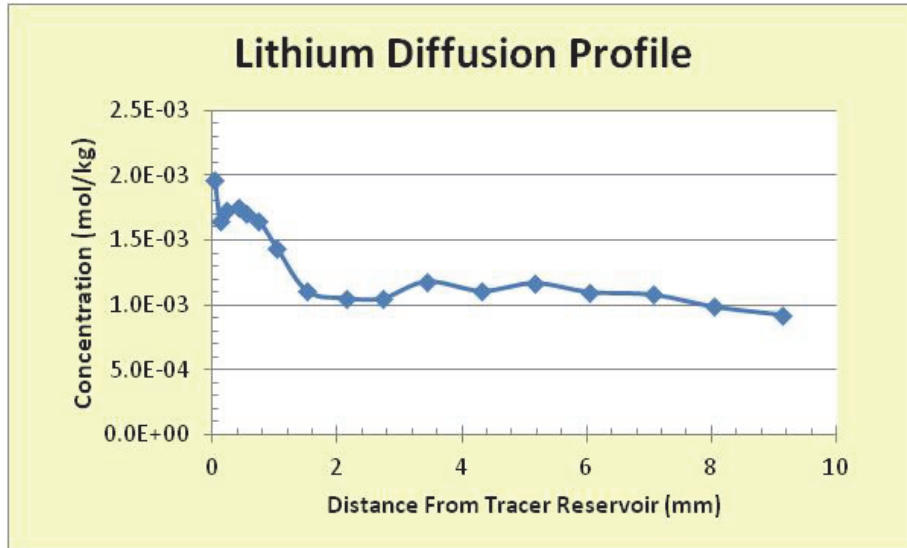


Figure 27: Lithium Diffusion Profile in Shale after 141 Days of Through Diffusion Test

The Ni and Pb diffusion profiles are illustrated in Figure 28 . Both of these two elements have elevated concentrations close to the tracer reservoir, with steep downward slopes with distance within the first 1.5 mm. Nickel appears to decrease with a relatively constant concentration gradient from 2 mm to the end of the core. Compared to Ni, Pb appears to have a steeper concentration gradient from 2 to 5 mm, after which Pb concentration is relatively constant. Remembering that these diffusion profiles include both sorbed tracer and tracer in porewater, the Ni and Pb diffusion profiles reflect Ni and Pb sorption within the shale fairly close to the tracer reservoir. The low Pb and Ni concentrations away from the tracer reservoir indicate that these two elements have diffused to the elution reservoir in small quantities that are too small to be detected in the elution reservoir. Note that the Ni concentration beyond about 5 mm is higher than 0. To check whether this reflects the transport of Ni tracer or represents the background Ni concentration, the Ni concentrations were corrected by the background Ni concentration. The background Ni concentration was taken from a reference tracer-free shale sample and it had a lower Ni concentration than the test shale sample. The U and Cu diffusion profiles (Figure 29) display even steeper profiles with major decrease in concentration within the 1 mm for U and within 0.5 mm for Cu. After 1 mm both of these elements appear to have dropped to background concentrations. These diffusion profiles demonstrated that U and Cu have higher sorption values than the elements Li, Ni, and Pb, with Cu being sorbed most strongly. This is consistent with batch sorption measurements. The Cu diffusion profile also helps to confirm that any Cu concentrations observed in the elution reservoir were not from the diffused Cu tracer. Modelling is required to extract sorption data from these diffusion profiles. This will be addressed in Section 5.

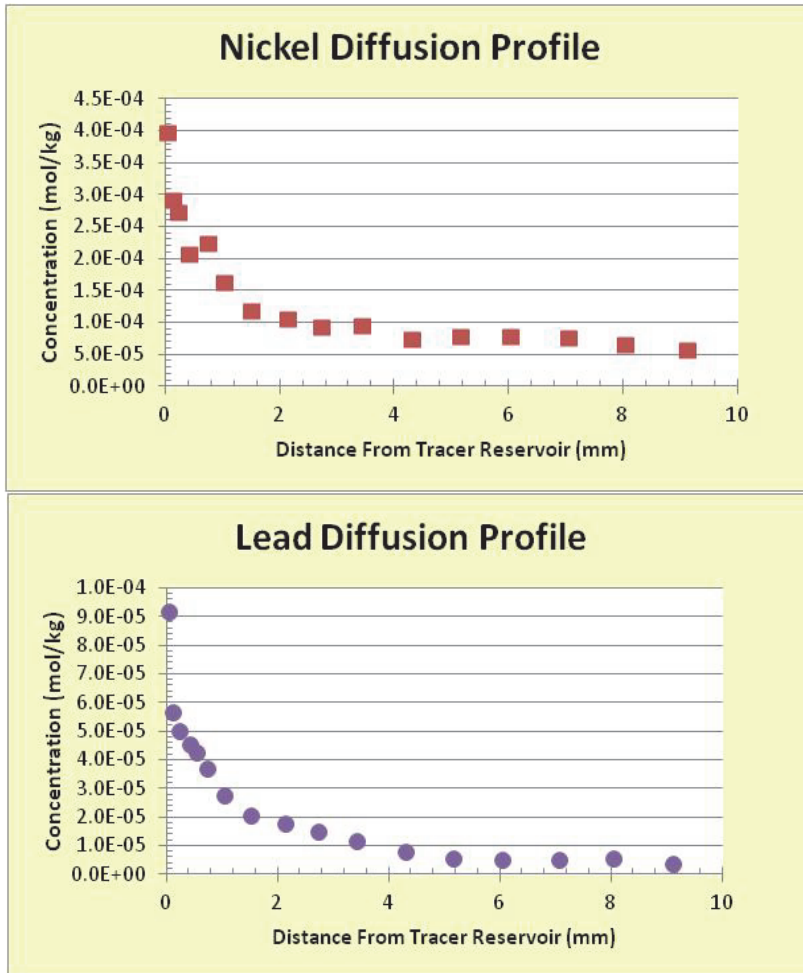


Figure 28: Nickel and Lead Diffusion Profiles in Shale after 141 Days of Through Diffusion Test

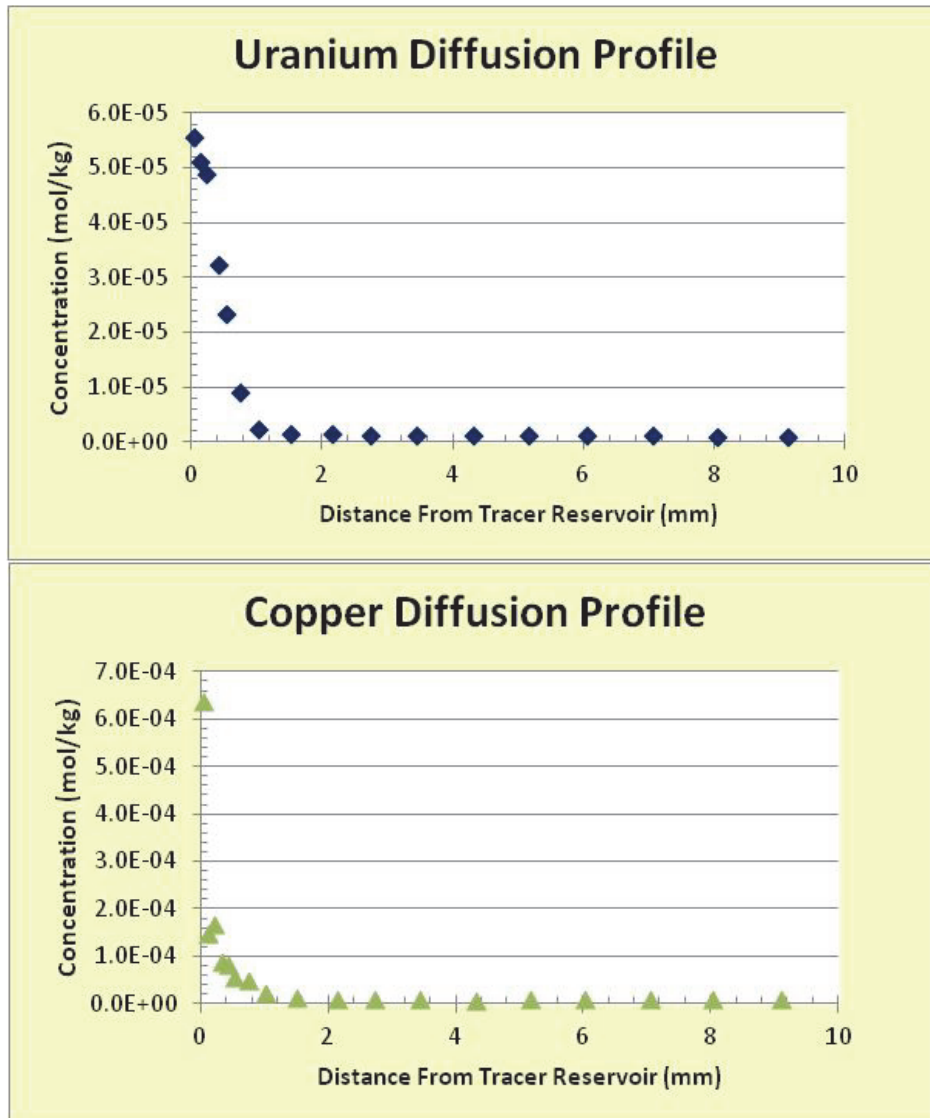


Figure 29: Uranium and Copper Diffusion Profiles in Shale after 141 Days of Through Diffusion Test

5. MASS TRANSPORT MODELLING

5.1 METHOD

The through diffusion transport was simulated to interpret the results of the mass transport experiments. Modelling was performed with AMBER, Version 5.5, a code designed and licensed by Quintessa Ltd., Henley-on-Thames, United Kingdom (www.quintessa.org). AMBER is designed to assist in the building of and solving compartment models. In AMBER, the materials of interest, referred to as 'contaminants', are assumed to be uniformly mixed in a series of compartments between which transfers can take place. Each transfer is 'donor controlled', depending directly on the amount of the material present in the compartment from which the material is moving, and can change with time.

A model was set up to re-create the geometry of the diffusion experiment. Mass transport was considered to occur in only one direction, from the boundary of tracer injection reservoir toward the opposite side of the sample. Compartments were set up to represent either a volume of water (inlet or outlet) or water saturated shale. The thickness of each compartment within shale was 0.1 mm. In general, all compartments are assumed to be well mixed (homogeneous). Transport between two shale compartments is assumed to be from the centre of one compartment to the centre of the next compartment. Transport between the water compartment and shale compartment is assumed to be from the interface between water and shale and the centre of shale compartment. Water compartments have defined volume and concentrations, but a zero thickness to ensure transport is calculated only from the edge of the shale to centre of the first shale compartment. Transport occurs across the entire exposed area of shale sample.

In the diffusion experiment, the tracer and elution reservoirs are very well mixed and assumed to be homogeneous. Any potential losses due to evaporation, degassing or other passive loss mechanisms are assumed negligible.

The fractional diffusive transfer rates from compartment A to compartment B ($\lambda_{Diff A \rightarrow B}$), as well as the back transfer from B to A ($\lambda_{Diff B \rightarrow A}$) are considered. These are determined from the effective diffusion coefficient ($D_{AVG}^{e Diff}$), the porosity of compartment A or B (θ_A, θ_B), transport distance between compartment centers (d_{c-c}), the length of compartment A or B (L_A, L_B), and the retardation factors for compartment A or B (R_A^E, R_B^E):

$$\lambda_{Diff A \rightarrow B} = \frac{D_{AVG}^{e Diff}}{\theta_A \cdot d_{c-c} \cdot L_A \cdot R_A^E} \quad [/\text{day}] \quad (26)$$

$$\lambda_{Diff B \rightarrow A} = \frac{D_{AVG}^{e Diff}}{\theta_B \cdot d_{c-c} \cdot L_B \cdot R_B^E} \quad [/\text{day}] \quad (27)$$

where

$D_{AVG}^{e Diff}$ = effective diffusion coefficient (m²/day);

L_A = length of compartment A (m);

L_B = length of compartment B (m);

d_{c-c} = transport distance between centres of compartment A and B (m);

R_A^E = retardation factor for element E in compartment A (-);

R_B^E = retardation factor for element E in compartment B (-);

θ_A = porosity of compartment A (-); and

θ_B = porosity of compartment A (-).

The retardation factor is calculated from the porosity, the rock density, and the sorption coefficient, K_d :

$$R_A^E = \left(1 + \frac{\rho K_d}{\theta}\right) \quad [\text{no units}] \quad (28)$$

K_d = sorption coefficient of tracer in shale (m^3/kg), and

ρ = density of shale (kg/m^3).

The initial model parameters used to model diffusive transport are summarized in Table 36. The porosity of the shale sample was an average shale porosity (Vilks and Miller, 2007) determined with the water immersion technique. Although the porosity could have been as low as 0.037 (based on iodide rock capacity) or as high as 0.096 (based on tritium rock capacity), the porosity term was not manipulated in the transport simulation. The density was based on average values reported by Vilks and Miller (2007). The tortuosity factor in Table 36 is related to the effective tortuosity (τ_D) by:

$$\text{tortuosity factor} = \frac{1}{\tau_D^2} \quad (29)$$

The tortuosity factor takes into account the effect of pore geometry on diffusive transport, and the tortuosity factor value in Table 36 was calculated from the τ_D value of 9.89, based on iodide diffusion reported by Vilks and Miller (2007). Multiplying the free water diffusion coefficients (D_w) by the tortuosity factor gives porewater diffusion coefficients (D_p) for each tracer (Table 36). The effective diffusion coefficients (D_e) are obtained by multiplying D_p by the rock porosity. Initial simulations were performed with the tortuosity factor in Table 36 and the resulting D_p values for each tracer, on the assumption that the pore geometry used by the tracers was identical to that defined by iodine. In order to test this assumption, simulations were performed with higher and lower tortuosity factors (by adjusting the D_p values) to test the response of simulated diffusion coefficients. The K_d values for each element in initial simulations were based on values that were in the range of values observed in batch sorption experiments. The K_d values were then manipulated to get better fits to measured diffusion profiles.

Table 36: Parameters Used for Diffusive Mass Transport Modelling with AMBER**Shale Properties**

Porosity [-]	0.0663
Density [kg/m ³]	2608
Tortuosity Factor [-]	0.0102
Segment Length [mm]	9.8
# compartments [-]	98
Transport Distance [mm] in Each Compartment	0.1
Radius [mm]	31.25

Water Compartment Properties

Parameter	Tracer reservoir	Elution reservoir
Volume [mL]	950	155
Rate of Water Exchange During Sampling That Reduces Tracer Concentration [mL/sample]	-	5
Transport Distance from Water Compartment to Center of First Shale Layer[mm]	0.05	0.05

Tracer Properties

Element	Initial diffusion inventory (mol)	*Free-water diffusion coefficient D_w (m ² /s)	Porewater diffusion coefficient D_p (m ² /s)	Effective diffusion coefficient D_e (m ² /s)
Li	9.50×10^{-3}	1.0147×10^{-9}	1.035×10^{-11}	6.862×10^{-13}
Ni	9.50×10^{-5}	1.332×10^{-9}	1.358×10^{-11}	9.007×10^{-13}
Cu	9.50×10^{-6}	1.427×10^{-9}	1.455×10^{-11}	9.650×10^{-13}
Pb	4.75×10^{-5}	1.903×10^{-9}	1.941×10^{-11}	1.287×10^{-12}
U	9.50×10^{-6}	8.530×10^{-9}	8.701×10^{-11}	5.768×10^{-12}

*Lide 1994

5.2 DIFFUSIVE TRANSPORT RESULTS

Numerical simulations of tracer diffusion through shale provide an estimate of tracer concentrations in the elution reservoir as a function of time, as well as tracer distribution throughout the shale sample at various times. Since Li was the only tracer that was able to diffuse through the shale sample into the elution reservoir, the modelling of tracer breakthrough does not significantly advance the understanding of diffusion processes that involve sorbing tracers. Instead, the modelling results focus on the development of tracer concentrations throughout the shale sample in the form of diffusion profiles after a transport period of 141 days. As mentioned before, the initial modelling processes starts with factors relating to pore geometry (porosity, tortuosity factor) that were previously determined by Vilks and Miller (2007) using iodide diffusion. The free water diffusion coefficients and the porewater diffusion coefficients (influenced by pore geometry) are unique to each tracer. Initial guesses for K_d values were based on results from batch sorption tests. The K_d values were then adjusted to obtain better fits between simulated and measured diffusion coefficients.

The measured and simulated diffusion profiles for Li are presented in Figure 30 for diffusion times of 141 days. Lithium was used as a conservative tracer in the diffusion test on the assumption that its K_d value would be 0 or close to 0 cm^3/g . The simulation with a K_d value of 0 cm^3/g displays a straight line in Figure 30A that is a factor of 2.8 to 3.8 lower than measured concentrations. If the Li K_d value is increased to 0.065 cm^3/g , the simulated diffusion profile falls in the range of measured concentrations. If the sorption coefficient is increased to higher values, such as 0.8 cm^3/g , the simulated diffusion profile becomes too high. Therefore, modelling of Li diffusion profiles indicates that Li is weakly sorbed, as suspected from the other studies. The tortuosity factor was manipulated to vary the D_p value for Li as a sensitivity analysis of the effect of pore geometry on Li diffusion (Figure 30B). Manipulating the pore geometry had very little effect on simulated diffusion profiles. The simulated Li diffusion profiles are straight lines, while the measured profile displays a dog leg pattern. The likely explanation is that the shale contains heterogeneity, impacting Li diffusion, that was not included in the diffusion model.

The Ni measured and simulated diffusion profiles are presented in Figure 31. The best fit with experimental data was found with a K_d value of 4.0 cm^3/g (Figure 31A). The simulated values matched measured Ni concentrations to a distance of about 2 mm. Simulated curves fall below experimental data beyond 2 mm. It could be that the background Ni concentration in this shale sample was higher than the value of 0 assumed in the numerical model. Figure 31B illustrates the effect of manipulating the tortuosity factor to increase or reduce the porewater diffusion coefficient, D_p , as defined by equation 16. The effective tortuosity value for shale used in the modelling was based on the results of through diffusion experiments using iodide (Vilks and Miller, 2007). However, it is possible that the effective tortuosity will not be the same for cations and anions. Figure 31B presents simulated diffusion profiles in which the Ni D_p value was increased by factors of 2 and 5, and reduced by a factor of 10. Increasing the Ni D_p value reduced the slope of the simulated diffusion profile so that simulated diffusion went further into the shale than was observed with the measured data. Clearly, the tortuosity factor for Ni was not larger than that determined with iodide. Reducing the tortuosity factor by a factor 10 slightly increased the slope, but did not significantly improve the model fit.

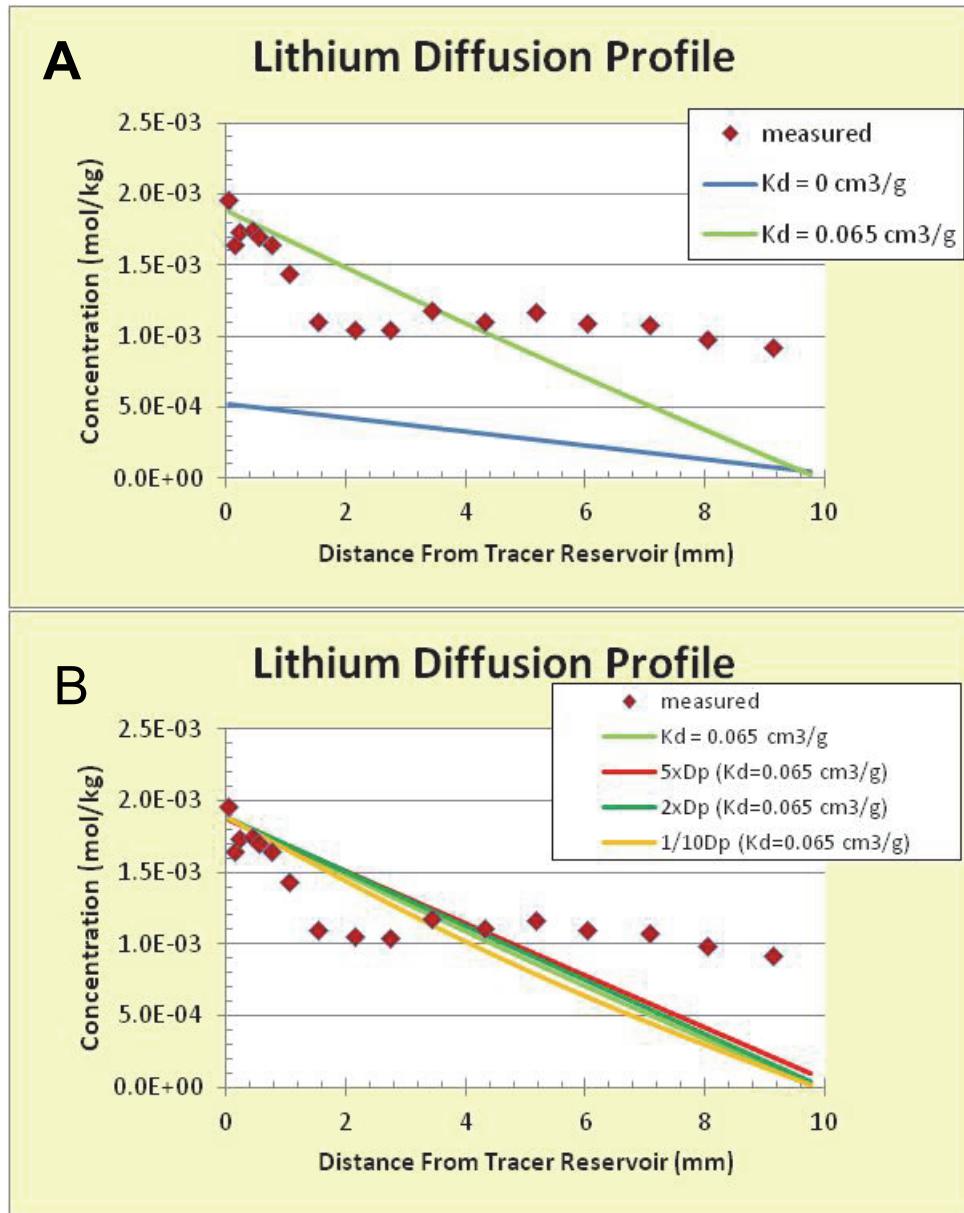


Figure 30: Simulated Lithium Diffusion Profile after 141 Days of Through Diffusion Test

The simulated and measured Pb diffusion profiles are presented in Figure 32. The simulation with a K_d value of $2.0 \text{ cm}^3/\text{g}$ produced the best fit with measured data (Figure 32A). If a higher K_d value, such as $6.1 \text{ cm}^3/\text{g}$ had been used, the simulated concentration of Pb at 0.1 mm would have been about a factor 2.9 higher than the measured value. On the other hand, a K_d value lower than $2.0 \text{ cm}^3/\text{g}$ would have produced a simulated diffusion profile lower than the measured profile for Pb. The effects of manipulating pore geometry on simulated Pb sorption are shown in Figure 32B. Reducing the tortuosity factor (or D_p) by a factor 10 increases the slope of the simulated diffusion profile, but does not produce a significantly better fit. As with Li, there

appears to be heterogeneity in the shale close to the tracer reservoir, that was not included in the diffusion model.

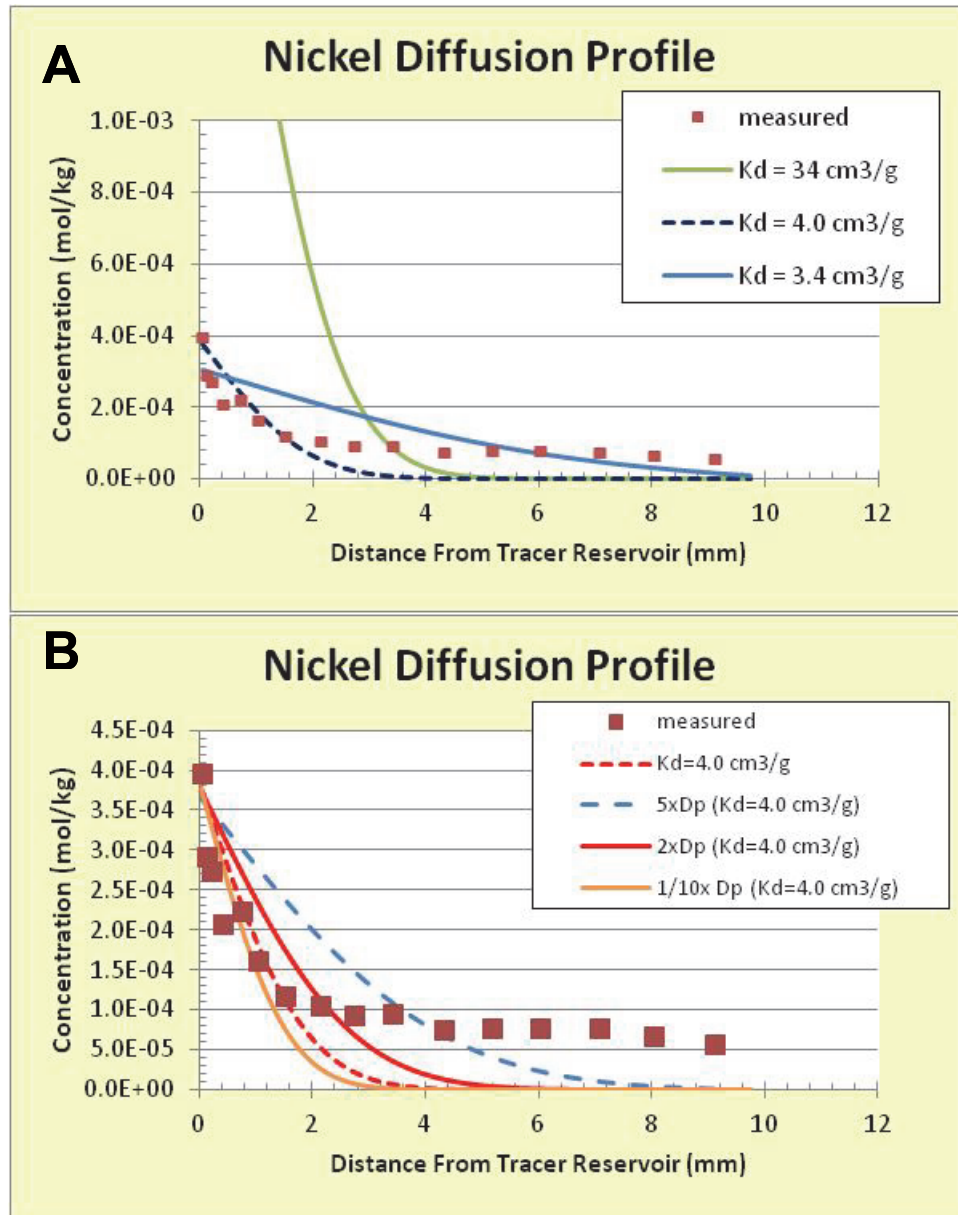


Figure 31: Simulated Nickel Diffusion Profiles after 141 Days of Through Diffusion Test

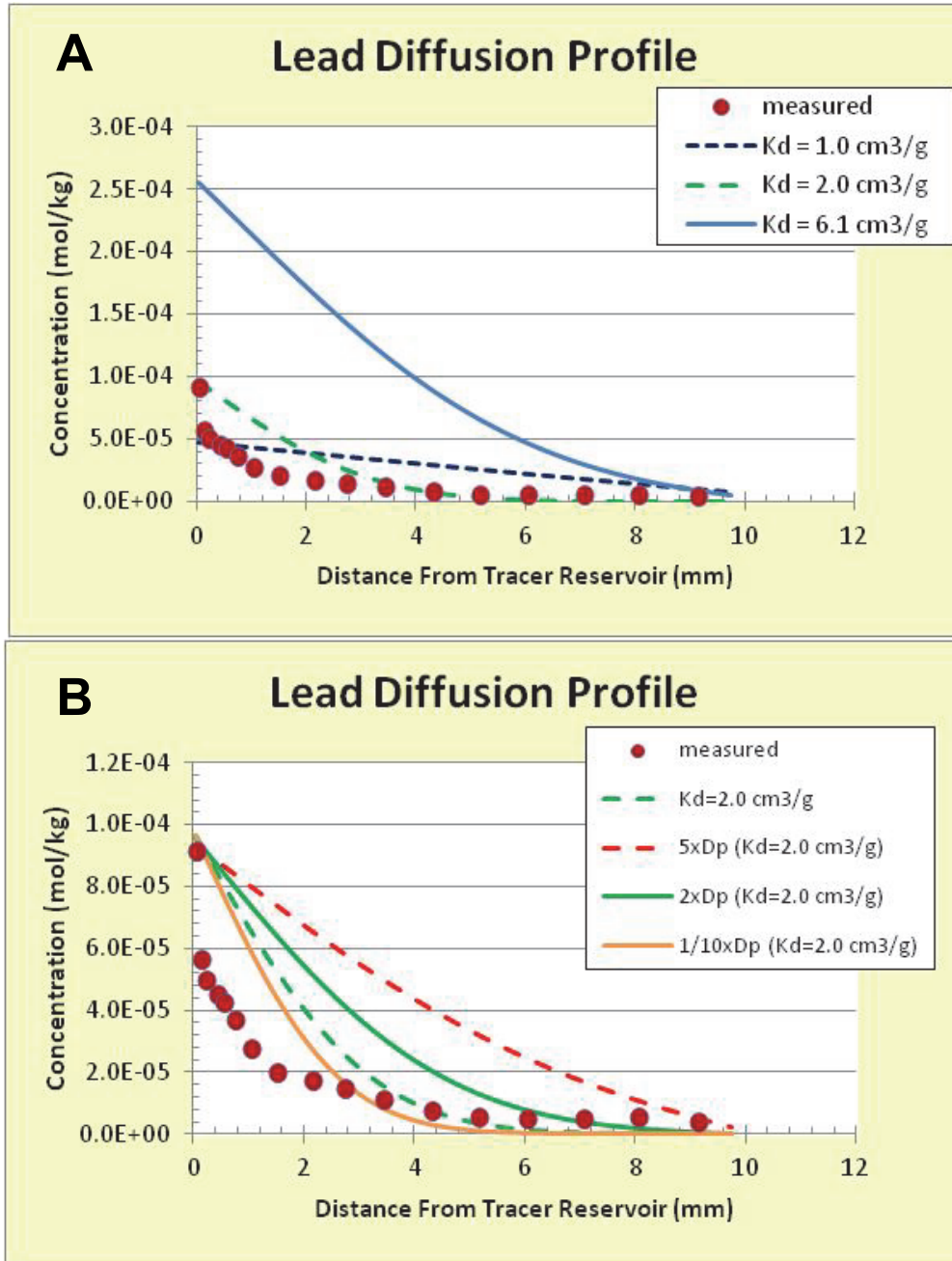


Figure 32: Simulated Lead Diffusion Profiles after 141 Days of Through Diffusion Test

The simulated Cu diffusion profiles for several K_d values are compared to the measured diffusion profile in Figure 33A. The K_d value of $51 \text{ cm}^3/\text{g}$ produced a reasonable fit to the measured diffusion profile. Figure 33B explores the effect of varying the effective tortuosity on simulated diffusion profiles. The tortuosity factor determined from iodide diffusion produces a good fit to the data, and a factor 10 reduction in the tortuosity factor does not significantly

change the simulated diffusion profiles. Increase of the tortuosity factor, or D_p values, clearly did not improve the model fit.

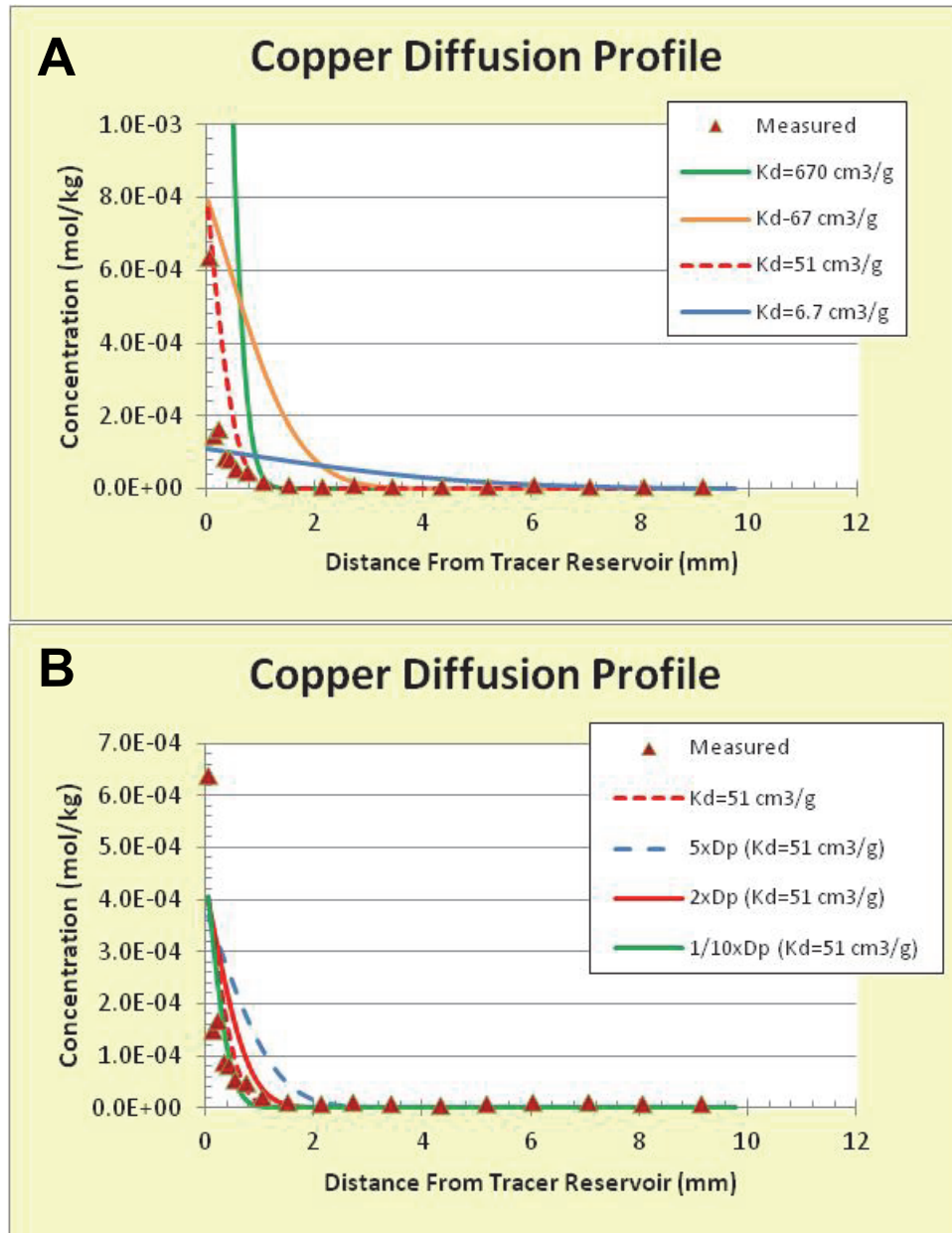


Figure 33: Simulated Copper Diffusion Profiles after 141 Days of Through Diffusion Test

Simulated U diffusion profiles for a number of K_d values are presented in Figure 34A. A K_d value of $20 \text{ cm}^3/\text{g}$ was selected to best represent U diffusion through shale. Figure 34B illustrates the effect of varying the tortuosity factor on simulated U diffusion profiles. Again, using the pore geometry defined by iodide diffusion produces a good fit, and a reduction in the D_p value by a factor of 10 did not make a significant difference to the simulated diffusion profiles.

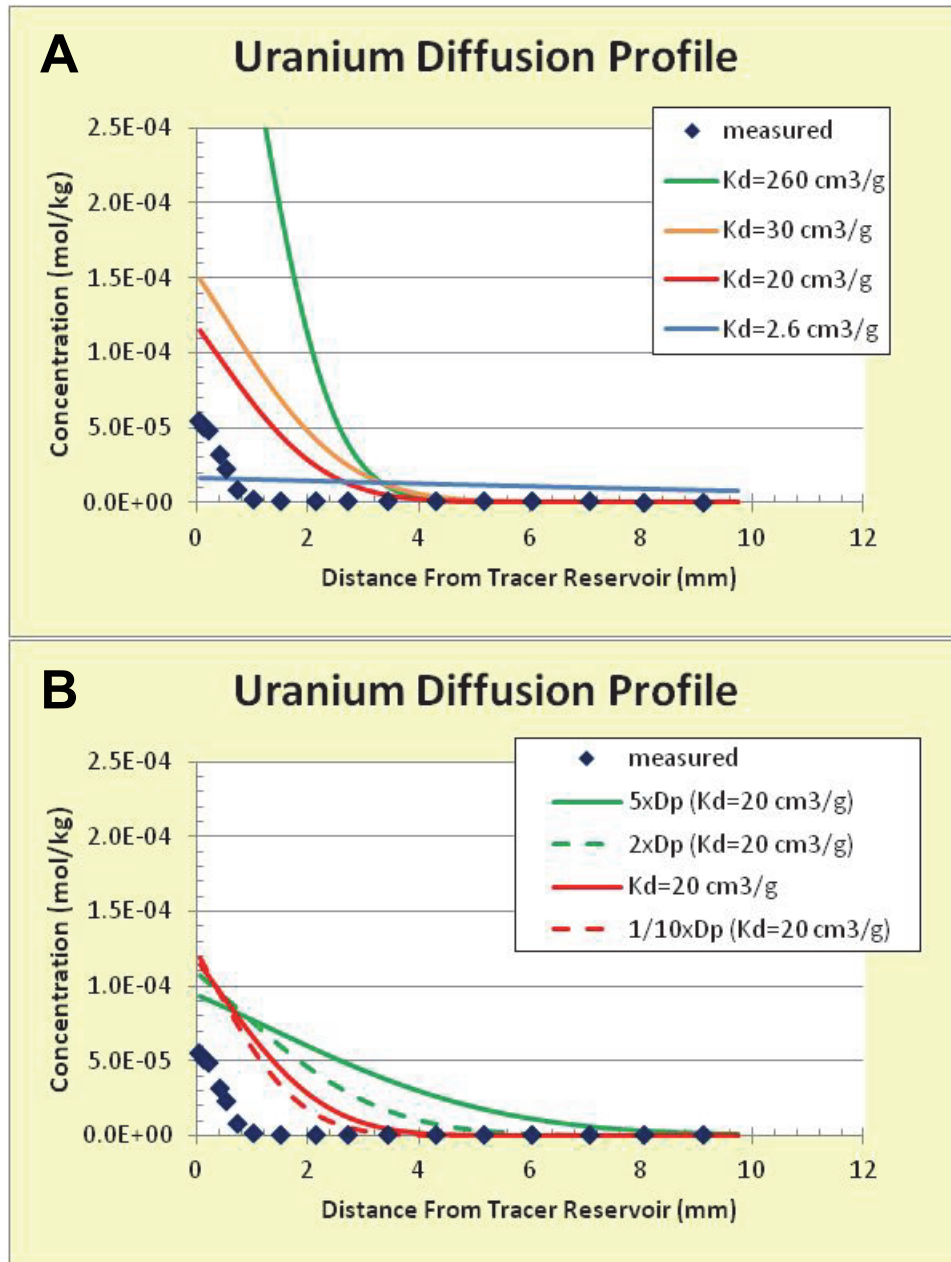


Figure 34: Simulated Uranium Diffusion Profiles after 141 Days of Through Diffusion Test

5.3 SUMMARY

Tracer breakthrough curves and tracer diffusion profiles through the sample can be determined by the diffusive mass transport experiment. For sorbing tracers, the diffusion profiles provide more information because sorbing tracers may not breakthrough in measurable quantities within a practical experimental time frame. Concentration profiles will usually identify how far the tracer has migrated, and when compared to the mass transport model simulations the diffusion profiles may reveal information regarding the pore geometry and sorption parameters controlling the diffusive transport of sorbing tracers.

Lithium was included in the tracer mix because it was assumed that it would have a K_d close to $0 \text{ cm}^3/\text{g}$, making it useful as a conservative tracer. The through diffusion data indicated that Li had a K_d value of $0.016 \text{ cm}^3/\text{g}$, while modelling of the diffusion profile suggested a K_d value of $0.065 \text{ cm}^3/\text{g}$. This is in agreement with the average Li K_d value determined for shale ($2 \pm 3 \text{ cm}^3/\text{g}$) from batch experiments. The very low K_d values indicate that Li is a weakly sorbing element on shale, that could approximate a conservative tracer in some cases.

No information was obtained from Cu breakthrough from the diffusion transport test. However, a comparison of the measured diffusion profile with numerical simulations indicated that a K_d value of $51 \text{ cm}^3/\text{g}$ was able to simulate the Cu diffusion profile in shale. The average measured K_d value on shale in brine solution is $52 \pm 31 \text{ cm}^3/\text{g}$ by batch tests. Therefore, the results of batch sorption tests can be used to simulated Cu diffusive transport in shale.

Breakthroughs of Ni, Pb and U in the diffusion test were not observed. Modelling of the Ni diffusion profile indicated a K_d value of $4.0 \text{ cm}^3/\text{g}$, which is not significantly different from the average measured K_d value of $2 \pm 3 \text{ cm}^3/\text{g}$ for shale in brine solutions by batch experiments. Since Ni sorption in brine solutions is very low, its sorption behavior may be difficult to determine with batch tests because the small changes in Ni concentration due to sorption are difficult to measure due to analytical interferences caused by high salt concentrations in the brine. The diffusion test provided an opportunity to confirm that although Ni K_d values are small, they are definitely higher than $0 \text{ cm}^3/\text{g}$.

As with Ni, Pb is weakly sorbed in brine solutions and due to analytical interferences from the high salt content, its sorption behavior may be difficult to determine with batch tests. The measured Pb diffusion profile indicated that there was very little Pb diffusion beyond 5 mm. Numerical simulations of Pb diffusion indicated that the best fit to measured data was obtained with a K_d value of $2.0 \text{ cm}^3/\text{g}$. The average Pb K_d value for shale in brine solution obtained from batch testing is $3 \pm 3 \text{ cm}^3/\text{g}$, which is consistent with the results of diffusive mass transport tests. The diffusion test in shale demonstrated that Pb sorbs on shale in brine solutions with a K_d value that is higher than $0 \text{ cm}^3/\text{g}$.

The measured U diffusion profile extended only about 1 mm into the shale. A reasonable fit to the observed diffusion profile was obtained using a K_d value of $20 \text{ cm}^3/\text{g}$. The average U K_d value for shale in brine solution obtained from batch testing is $28 \pm 9 \text{ cm}^3/\text{g}$. The U K_d values derived from the diffusion test and batch experiments are not significantly different.

The degree to which the K_d values impact contaminant mass transport can be approximated with the concept of the retardation factor (R), originally developed for advective mass transport through a column of crushed rock, and assuming sorption is reversible. As shown by Equation 30, the retardation factor is a ratio of the average groundwater velocity divided by the

contaminant velocity (Freeze and Cherry, 1979). Therefore, the retardation factor provides an indication of how much slower a sorbing contaminant will be transported compared to the average groundwater velocity. As an example, retardation factors for shale were calculated for a range of K_d values and presented in Table 37.

$$R = \frac{V_{gw}}{V_{con}} = 1 + \frac{\rho K_d}{\varepsilon} \quad (30)$$

where

- V_{gw} = average groundwater velocity (m/s);
 V_{con} = average contaminant velocity (m/s);
 ρ = rock density (2.608 g/cm³ for shale); and
 ε = rock porosity (0.0663 for shale).

Table 37: Sorption Coefficients and Retardation Factors for Shale

K_d (cm ³ /g)	Retardation Factor (dimensionless)	Comment
0.001	1.039	weakly sorbing
0.01	1.39	weakly sorbing
0.016	1.63	weakly sorbing
0.065	3.56	weakly sorbing
0.1	4.93	weakly sorbing
1.0	40	weakly sorbing
2.0	80	weakly sorbing
5.0	198	weakly sorbing
10	394	moderately sorbing
20	788	moderately sorbing
51	2010	moderately sorbing
144	5665	moderately sorbing
250	9800	moderately sorbing
500	19700	strongly sorbing
1000	39300	strongly sorbing

The retardation factor for an element that does not sorb to any degree is 1.0. With increasing K_d values from 0.001 to 10 cm³/g, the retardation factor increases from 1.039 to 394, at which point the contaminant would travel 394 times slower than groundwater. In this report, elements with K_d values of less than 10 cm³/g are considered to be weakly sorbing. Elements with a K_d value of 250 cm³/g would be transported almost 10,000 times slower than groundwater. In this report, moderately sorbing elements are considered to be those with K_d values from 10 to 250 cm³/g. The elements with K_d values greater than 250 cm³/g are classified as strongly sorbing.

Although Li was included in sorption studies on the assumption that it was a conservative tracer, it was discovered that Li is weakly sorbed (K_d values of 0.016 to 0.065 cm³/g on shale) and is

transported 4 to 5 times slower than groundwater in shale. Ni and Pb were also weakly sorbed on shale, while Cu(II) and U(VI) were moderately sorbed onto shale in the SR-270 reference brine under oxidizing conditions.

In summary, the sorption values derived from batch tests are consistent with sorption values estimated from diffusive mass transport experiments in shale. This suggests that the “equilibrium” approach, using sorption coefficients assumed to be equilibrium values, is valid for simulating diffusive mass transport in shale. The potential impact of non-reversible sorption was not significant. Diffusive mass transport test improves our understanding of the role of sorption in mass transport and can be used to estimate sorption coefficients. The effective tortuosity for shale (which affects calculated porewater diffusion coefficients, D_p) was determined by through diffusion tests with iodide. The cation tracers used in this study used a similar pore geometry to that used by the anion I^- . Diffusion tests may be very useful for determining sorption properties of weakly sorbing tracers whose K_d values may be difficult to determine by batch methods in brine solutions. Therefore, the optimum approach to furthering the understanding of sorption in mass transport is to use a combination of batch tests (not affected by transport) and migration experiments.

6. SUMMARY AND CONCLUSIONS

Batch sorption tests and a diffusive mass transport experiment were performed to investigate the sorption behavior of Li(I), Ni(II), Pb(II), Cu(II), Zr(IV) and U(VI) onto sedimentary rocks (shale and limestone) and bentonite. The batch techniques were used to determine sorption coefficient K_d values for Li, Ni, Pb, Cu, Zr, and U in a SR-270 reference brine solution and a reference dilute solution. The diffusive mass transport test was used to estimate K_d values for Li, Ni, Pb, Cu, and U based on the element diffusion through shale under brine conditions. The Li, Ni, Pb, and Zr are not redox sensitive. Although Cu and U are redox sensitive, this study focused on characterizing the sorption behaviour of Cu(II) and U(VI), which are the stable forms of these elements under oxidizing conditions.

Batch sorption experiments were performed using single element (U and Zr) and multiple element (Li, Ni, Pb, Cu and U) tests lasting from 1 h to 127 days. Depending upon the element, the time required to reach steady state, or apparent equilibrium, varied from 1 day to longer than 127 days. Uranium desorption tests, performed by diluting the concentration of the sorbing element U, indicate that although desorption does occur, the sorption process is not completely reversible. When desorption was initiated, the apparent K_d values were factors of 5 to 7 higher than before desorption. After 55 days of desorption, these apparent K_d values remained at a factor 2 higher than before desorption. Comparison sorption tests performed under sterile and normal laboratory conditions confirmed that sorption measurements in brine solution are not affected by the presence of microbes in the laboratory. Sorption values determined on bentonite, shale and limestone in the SR-270 brine reference solution were compared to those measured in the dilute reference solution. The sorption K_d values of divalent elements Ni, Pb and Cu were found to be lower in the brine solution compared to the reference dilute solution by 1 to 3 orders of magnitude, mainly because cation exchange is the dominant sorption mechanism for these elements in the dilute solution. Cation exchange for Ni^{+2} , Pb^{+2} and Cu^{+2} is virtually eliminated in the brine due to the high concentrations of the cations Ca^{2+} and Na^+ , competing for the cation exchange sites. U sorption coefficients in the brine solution were factors of 1.5 to 8 lower than that in the reference dilute water. Short term sorption tests to

check the effect of pH on sorption showed that the sorption of U(VI) increased above pH of 6 with a very sharp rise between pH of 7 and 8. The sorption of Zr(IV) increased with increasing pH. The sorption of Cu(II) on bentonite increased above pH of 7, while the variation of Ni(II) and Pb(II) sorption with pH was inconclusive due to the short duration of the pH experiments.

Using montmorillonite and illite to approximate bentonite and shale, surface complexation modelling was performed for these minerals using a 2-site protolysis non-electrostatic surface complexation and cation exchange model. Nickel surface complexation constants were obtained from the literature, while those for Cu, Pb and Zr were estimated using LFER (linear free energy relationships) and metal hydrolysis constants. Cation exchange selectivity coefficients for Ni and Pb were obtained from the literature, while those for Cu were based on Ni. Competition with Ca^{+2} for surface complexation sites was included for Ni, Cu and Pb, but not Zr. Cation exchange was not included for Zr because its dominant solution species is the neutral species $\text{Zr}(\text{OH})_4$.

In the SR-270 reference brine, where sorption of many elements is dominated by surface complexation, simulated Ni K_d values (using the literature-derived surface complexation constants) matched measured Ni K_d values. In the cases using the surface complexation constants estimated by LFER, simulated Pb sorption values on bentonite and shale were within measured values by factors of 1.2 and 3.4, respectively; simulated Zr sorption values on bentonite and shale were within measured values by factors of 3.0 and 1.6, respectively; while simulated Cu values were within measured values by factors of 1.5 and 1.7, respectively. In dilute solution, where sorption of cations was dominated by cation exchange, simulated K_d values on bentonite and shale for Ni, Cu and Pb were within measured values by factors of 1.5 to 3.3. Keeping in mind that the surface complexation constants used by the models were derived from 0.1 and 0.5 mol/L NaClO_4 solutions, the close agreement between simulated sorption values for montmorillonite and illite with measured values for bentonite and shale (assuming 60% illite content) provides confidence that modelling can be used to extend laboratory derived sorption properties to natural brine solutions and to use LFER to estimate sorption behaviour of elements whose sorption properties have not been measured. Conversely, the close agreement between simulated and measured K_d values provides further confidence that the measured K_d values for Ni and Pb by batch tests are correct. The comparison between simulated and experimental sorption coefficients would be significantly improved if equilibrium sorption measurements were available for a broader pH range (4 to 9) to test the response of the model.

A diffusive mass transport experiment was performed using multiple elements Li, Ni, Cu, Pb, and U to study the effect of sorption on diffusion-only transport in shale in the reference brine solution. Numerical simulations of tracer diffusion through shale were performed to fit the diffusion concentration profiles in order to estimate K_d values and to confirm that reactive transport models can be used to explain diffusive transport in shale. The diffusion test was able to better characterize the sorption properties of weakly sorbing elements (Li, Ni, Pb), whose K_d values determined in brine solutions by batch techniques had a higher level of uncertainty due to analytical interferences from high salt concentrations. In addition to estimating sorption coefficients, the diffusive mass transport test improves our understanding of the role of sorption in mass transport. The optimum approach to furthering the understanding of sorption in mass transport is to use a combination of batch tests (not affected by transport) and migration experiments. The results of the diffusion experiment could be improved by performing replicate tests with each rock type, extending the diffusion time to 1 year, and including another conservative tracer, such as iodide.

Table 38 summarizes sorption coefficients determined in brine solution by batch tests and the diffusive mass transport test, as well as by sorption modelling. The sorption values derived from batch tests are consistent with sorption values estimated from diffusive mass transport experiment in shale. This indicates that the batch sorption test approach used, in which sorption coefficients are assumed to be equilibrium values, is valid for simulating mass transport in shale.

Table 38: Sorption Coefficients (cm^3/g) in Brine Solutions Derived from Different Approaches

Element	Solid	Batch Test		Diffusive Mass Transport Tests	Sorption Modelling
		Average	Range		
Li	bentonite	2 ± 3	0 - 5	-	-
	shale	2 ± 3	0 - 5	0.016 to 0.065	-
	limestone	1 ± 1	0 - 2	-	-
Ni	bentonite	5 ± 5	0 - 10	-	7.0
	shale	2 ± 3	0 - 5	4	1.5
	limestone	1 ± 2	0 - 3	-	-
Cu	bentonite	107 ± 25	82 - 132	-	73
	shale	52 ± 31	21 - 83	51	29
	limestone	11 ± 6	5 - 17	-	-
Pb	bentonite	5 ± 4	1 - 9	-	6.1
	shale	3 ± 3	0 - 6	2	0.9
	limestone	1 ± 1	0 - 2	-	-
Zr	bentonite	454 ± 66	388 - 520	-	1350
	shale	494 ± 0	490	-	810
	limestone	144 ± 31	113 - 175	-	-
U(VI) ^a	bentonite	34 ± 9	25 - 43	-	-
	shale	28 ± 9	19 - 37	20	-
	limestone	10 ± 4	6 - 14	-	-

^aU is a redox sensitive element, it is U(VI) under the experimental conditions.

- Data not available: diffusive mass transport tests were not performed for bentonite and limestone; diffusive mass transport tests were not performed for Zr; sorption modelling was not performed for Li and U.

In this report, elements with K_d values of less than $10 \text{ cm}^3/\text{g}$ (with retardation factor greater than 394) are considered to be weakly sorbing, elements with a K_d value from 10 to $250 \text{ cm}^3/\text{g}$ (with

retardation factor of 394 to 9800) are considered to be moderately sorbing, and elements with K_d values greater than $250 \text{ cm}^3/\text{g}$ are classified as strongly sorbing. In the SR-270 reference brine solution, Li, Ni and Pb are weakly sorbed on bentonite, shale and limestone; Cu(II) and U(VI) are moderately sorbed onto bentonite, shale and limestone; Zr is moderately sorbed on limestone, and strongly sorbed on bentonite and shale with retardation factors of 17,900 to 19,700.

ACKNOWLEDGEMENTS

Jeff Miller set up the mass transport models in AMBER and performed the numeric simulations for diffusive mass transport in shale. Tammy (Tianxiao) Yang (NWMO), Frank Garisto (NWMO), Shinya Nagasaki (McMaster University), and Jeff Miller (AECL) provided fruitful discussion and review.

REFERENCES

- Baeyens, B. and M.H. Bradbury. 2004. Cation exchange capacity measurements of illite using the sodium and cesium isotope dilution technique: Effects of the index-cation, electrolyte concentration and competition: Modeling. *Clays and Clay Minerals*, 52, 421-431.
- Baeyens, B. and M.H. Bradbury. 1997. A mechanistic description of Ni, and Zn sorption on Na-montmorillonite. Part I: Titration and sorption experiments. *Journal of Contaminant Hydrology*, 27, 199-222.
- Barone, F.S, R.K. Rowe and R.M. Quigley. 1990. Laboratory determination of chloride diffusion coefficients in an intact shale. *Can. Geotech.*, 27, 177-184.
- Baumann, E. 1973. Determination of pH in concentrated salt solutions. *Analytica Chimica Acta*, 64, 284-288.
- Bradbury, M.H. and B. Baeyens. 2009a. Sorption modelling on illite Part I: Titration measurements and the sorption of Ni, Co, Eu and Sn. *Geochimica et Cosmochimica Acta*, 73, 990-1003.
- Bradbury, M.H. and B. Baeyens. 2009b. Sorption modelling on illite Part II: Actinide sorption and linear free energy relationships. *Geochimica et Cosmochimica Acta*, 73, 1004-1013.
- Bradbury, M.H. and B. Baeyens. 2005a. Experimental measurements and modeling of sorption competition on montmorillonite. *Geochimica et Cosmochimica Acta*. 69, 4187-4197.
- Bradbury, M.H. and B. Baeyans. 2005b. Modelling the sorption of Mn(II), Co(II), Ni(II), Zn(II), Cd(II), Eu(III), Am(III), Sn(IV), Th(IV), Np(V) and U(VI) on montmorillonite: Linear free energy relationships and estimates of surface binding constants for some selected heavy metals and actinides. *Geochimica et Cosmochimica Acta*, 69, 875-892.
- Bradbury, M.H. and B. Baeyens. 1997. A mechanistic description of Ni and Zn sorption on Na-montmorillonite. Part I: Titration and sorption measurements. *Journal of Contaminant Hydrology*, 27, 199-222.
- Bradbury, M.H. and A. Green. 1985. Measurement of important parameters determining aqueous phase diffusion rates through crystalline rock matrices. *Hydrology* 82, 39-55.
- Bradbury, M.J., D. Lever and D. Kinsey. 1982. Aqueous phase diffusion in crystalline rock. *Materials Research Society Symposium Proceedings* 11, 569-578.
- Choi, J.W. and D.W. Oscarson. 1996. Diffusive transport through compacted Na- and Ca-bentonite. *Contaminant Hydrology*, 22, 189-202.
- Cramer J.J., T.W. Melnyk and H.G. Miller. 1997. In-situ diffusion in granite: Results from scoping experiments. *Atomic Energy of Canada Limited Report, AECL-11756, COG-96-656-I*.
- Freeze, R.A. and J.A. Cherry. 1979. *Groundwater*. Prentice-Hall, Inc., Englewood Cliffs, New Jersey.

- Gimmi, T. and H.N. Waber. 2004. Modelling of profiles of stable water isotopes, chloride and chloride isotopes of pore water in argillaceous rocks in the Benken borehole. Nagra Technical Report, NTB 04-05, Nagra, Wettingen, Switzerland.
- Harvey, K.B. 1996. Measurement of diffusive properties of intact rock. Atomic Energy of Canada Limited Report, AECL-11439, COG-95-456.
- Hinds, G., P. Cooling, A. Wain, S. Zhou and A. Turnbull. 2009. Technical Note: Measurement of pH in concentrated brines. Corrosion, 65, 635-638.
- Johnson, D.A. and T.M. Florence. 1971. Spectrophotometric determination of uranium(VI) with 2-(5-bromo-2-pyridylazo)-5-diethylaminophenol. Analytica Chimica Acta, 53, 73-79.
- Katsube, T.J., T.W. Melnyk and J.P. Hum. 1986. Pore structure from diffusion in granitic rocks. Atomic Energy of Canada Limited Technical Record, TR-381.
- Lajudie, A., J. Raynal, J-C. Petit and P. Toulhoat. 1995. Clay-based materials for engineered barriers: A review. In Materials Research Society Symposium Proceedings, V 353.
- Lide, D.R., (Editor). 1992. CRC Handbook of Chemistry and Physics. CRC Press, New York, NY.
- Liu, J. and I. Neretnieks. 2006. Physical and chemical stability of the bentonite buffer, SKB Report R-06-103.
- Marczenko, Z. and M. Balcerzak. 2000. Separation, preconcentration and spectrophotometry in inorganic analysis. Analytical Spectroscopy Library – 10, Elsevier.
- Melnyk, T.W. and A.M.M. Skeet. 1987. A mathematical study of the influence of pore geometry on diffusion. Atomic Energy of Canada Limited Report, AECL-9075.
- NWMO. 2011. OPG's Deep Geologic Repository for Low & Intermediate Level Waste, Geosynthesis. Nuclear Waste Management Organization Report NWMO DGR-TR-2011-11. Toronto, Canada.
- NWMO. 2005. Choosing a way forward. The future management of Canada's used nuclear fuel. Nuclear Waste Management Organization, Toronto, Canada. (Available at www.nwmo.ca).
- Ohlsson, Y. and I. Neretnieks. 1995. Literature survey of matrix diffusion theory and of experiments and data including natural analogues. SKB Technical Report, 95-12.
- Oscarson, D.W. and H.B. Hume. 1994. Diffusion of ^{14}C in dense saturated bentonite under steady-state conditions. Transport in Porous Media, 14, 73-84.
- Parkhurst, D.L. and C.A.J. Appelo. 1999. User's guide to PHREEQC (version 2) - a computer program for speciation, reaction-path, 1D-transport, and inverse geochemical calculations. US Geol. Surv. Water Resour. Inv. Rep. 99-4259, 312p.

- Skagius, K. and I. Neretnieks. 1982. Diffusion in crystalline rocks of some sorbing and non-sorbing species. SKB Report, 82-12, SKB/KBS, Stockholm, Sweden.
- Stumm, W. and J.J. Morgan. 1981. Aquatic Chemistry An Introduction Emphasizing Chemical Equilibria in Natural Waters. John Wiley & Sons.
- Vilks, P. 2011. Sorption of selected radionuclides on sedimentary rocks in saline conditions – literature review. Nuclear Waste Management Organization Report NWMO TR-2011-12. Toronto, Canada.
- Vilks, P., N.H. Miller and K. Felushko. 2011. Sorption experiments in brine solutions with sedimentary rock and bentonite. Nuclear Waste Management Organization Report NWMO-TR-2011-11. Toronto, Canada.
- Vilks, P. 2009. Sorption in highly saline solutions – State of the science review. Nuclear Waste Management Organization Report NWMO-TR-2009-18, Toronto, Canada.
- Vilks, P. and N.H. Miller. 2007. Evaluation of experimental protocols for characterizing diffusion in sedimentary rocks. Nuclear Waste Management Organization Report NWMO TR-2007-11. Toronto, Canada.
- Vilks, P., N.H. Miller and F.W. Stanchell. 2004. Phase II in-situ diffusion experiment. Ontario Power Generation Report 06819-REP-01200-10128-R00.
- Vilks, P., J.J. Cramer, T.W. Melnyk, F.W. Stanchell, N.H. Miller and H.G. Miller. 1999. In-situ diffusion in granite: Phase I final report. Ontario Power Generation, Nuclear Waste Management Division Report 06819-REP-01200-0087-R00. Toronto, Canada.
- Wadden, M.M. and T.J. Katsube. 1982. Radionuclide diffusion rates in igneous crystalline rocks. *Chemical Geology*, 36, 191.
- Wiesner, A.D., L.E. Katz and C.-C. Chen. 2006. The impact of ionic strength and background electrolyte on pH measurements in metal ion adsorption experiments. *Journal of Colloid and Interface Science*, 301, 329-332.
- Wu, Y.C., W.F. Koch, and R.A. Durst. 1988. Standardization of pH Measurements. NBS Special Publication 260-53, U.S. Department of Commerce / National Bureau of Standards, Gaithersburg, MD, 20899.

APPENDIX A: DATA FROM BATCH SORPTION AND TRANSPORT TESTS

LIST OF TABLES

		<u>Page</u>
A.1	Uranium Sorption Variation with pH.....	99
A.2	Uranium Sorption Variation with Time	100
A.3	Uranium Desorption Variation with Time	102
A.4	Zirconium Sorption Variation with pH and Time	104
A.5	Zirconium Sorption with Time.....	105
A.6	Lithium Sorption with Time in Brine.....	106
A.7	Nickel Sorption with Time in Brine	109
A.8	Copper Sorption with Time in Brine	112
A.9	Lead Sorption with Time in Brine	115
A.10	Uranium Sorption with Time in Brine	118
A.11	Lithium Sorption with Time in Dilute Reference Solution	121
A.12	Nickel Sorption with Time in Dilute Reference Solution.....	123
A.13	Copper Sorption with Time in Dilute Reference Solution.....	125
A.14	Lead Sorption with Time in Dilute Reference Solution.....	127
A.15	Uranium Sorption with Time in Dilute Reference Solution.....	129
A.16	Lithium Sorption with pH in Reference Brine Solution.....	131
A.17	Nickel Sorption with pH in Reference Brine Solution	132
A.18	Copper Sorption with pH in Reference Brine Solution	133
A.19	Lead Sorption with pH in Reference Brine Solution	134
A.20	Uranium Sorption with pH in Reference Brine Solution	135
A.21	Lithium Diffusion Data for Figure 26	136
A.22	Trace Element Diffusion Profiles	137

Table A1: Uranium Sorption Variation with pH

Solid	pH	Dissolved U (mol/L)	Sorbed U (mol/kg)	K_d (cm³/g)	Percent Sorbed	K_a (cm)
bentonite	2.88	4.579E-05	9.20E-04	20	9	8.04E-05
	2.98	4.621E-05	8.42E-04	18	8	7.29E-05
	5.77	4.789E-05	4.99E-04	10	5	4.17E-05
	6.84	4.663E-05	6.67E-04	14	7	5.73E-05
	6.93	4.579E-05	8.38E-04	18	8	7.33E-05
	6.94	4.705E-05	6.71E-04	14	7	5.71E-05
	6.96	4.705E-05	6.69E-04	14	7	5.69E-05
	7.44	3.416E-05	3.25E-03	95	32	3.81E-04
	7.45	3.315E-05	3.42E-03	103	34	4.13E-04
	7.93	4.754E-06	6.81E-03	1432	88	5.73E-03
shale	5.33	4.915E-05	1.26E-04	3	3	2.23E-05
	6.04	4.831E-05	2.09E-04	4	4	3.76E-05
	6.07	4.663E-05	3.77E-04	8	8	7.02E-05
	6.89	4.579E-05	4.18E-04	9	8	7.93E-05
	6.95	4.495E-05	5.04E-04	11	10	9.74E-05
	7.03	4.789E-05	2.52E-04	5	5	4.57E-05
	7.71	2.445E-05	2.25E-03	92	48	7.98E-04
	7.72	2.201E-05	2.50E-03	113	53	9.85E-04
	7.99	1.68E-06	2.98E-03	1775	95	1.54E-02
	8.04	1.885E-06	2.01E-03	1066	91	9.26E-03
limestone	5.47	4.915E-05	5.03E-05	1	3	3.53E-05
	5.50	5.041E-05	0.00E+00	0	0	0.00E+00
	6.00	4.663E-05	1.51E-04	3	8	1.12E-04
	6.04	4.621E-05	1.68E-04	4	8	1.26E-04
	6.82	4.537E-05	1.85E-04	4	9	1.41E-04
	7.08	4.285E-05	3.01E-04	7	15	2.43E-04
	7.15	4.369E-05	2.69E-04	6	13	2.13E-04
	8.01	1.066E-06	1.03E-03	970	96	3.35E-02
	8.03	3.403E-06	1.10E-03	324	89	1.12E-02
8.06	1.271E-06	6.77E-04	533	93	1.84E-02	

Table A2: Uranium Sorption Variation with Time

	pH	Time (day)	Dissolved U (mol/L)	Sorbed U (mole/kg)	K _d (cm ³ /g)	Percent Sorbed
Bentonite	6.18	1	9.56E-05	6.90E-04	7	3
	6.31	1	9.33E-05	1.16E-03	12	6
	6.34	1	8.99E-05	1.83E-03	20	9
	6.26	7	9.11E-05	1.72E-03	19	9
	6.29	7	8.74E-05	2.46E-03	28	12
	6.29	7	8.71E-05	2.51E-03	29	13
	6.32	14	8.76E-05	2.00E-03	23	10
	6.45	14	8.57E-05	2.37E-03	28	12
	6.48	14	8.38E-05	2.74E-03	33	14
	6.46	28	9.03E-05	1.76E-03	19	9
	6.47	28	8.57E-05	2.69E-03	31	14
	6.42	28	8.57E-05	2.68E-03	31	14
	6.39	42	8.95E-05	1.98E-03	22	10
	6.43	42	8.74E-05	2.41E-03	28	12
	6.44	42	8.61E-05	2.65E-03	31	13
	6.36	56	9.03E-05	2.01E-03	22	10
	6.45	56	8.86E-05	2.35E-03	27	12
	6.45	56	8.70E-05	2.68E-03	31	13
	6.41	112	8.86E-05	2.04E-03	23	10
	6.44	112	8.70E-05	2.38E-03	27	12
6.43	112	8.44E-05	2.88E-03	34	15	
Shale	6.22	1	9.30E-05	6.05E-04	7	6
	6.26	1	9.14E-05	7.60E-04	8	8
	6.28	1	9.17E-05	7.34E-04	8	7
	6.26	7	8.91E-05	1.06E-03	12	11
	6.22	7	8.82E-05	1.14E-03	13	11
	6.19	7	8.79E-05	1.17E-03	13	12
	6.31	14	8.54E-05	1.21E-03	14	12
	6.35	14	8.54E-05	1.21E-03	14	12
	6.35	14	8.60E-05	1.16E-03	13	12
	6.32	28	8.61E-05	1.30E-03	15	13
	6.34	28	8.40E-05	1.51E-03	18	15
	6.32	28	8.61E-05	1.30E-03	15	13
	6.28	42	8.61E-05	1.33E-03	15	13
	6.30	42	8.61E-05	1.33E-03	15	13
	6.31	42	8.61E-05	1.33E-03	15	13
	6.28	56	8.65E-05	1.39E-03	16	14
	6.30	56	8.57E-05	1.47E-03	17	15
	6.35	56	8.61E-05	1.43E-03	17	14
	6.25	112	8.36E-05	1.53E-03	18	15
	6.25	112	8.28E-05	1.61E-03	19	16
6.26	112	8.36E-05	1.53E-03	18	15	

	pH	Time (day)	Dissolved U (mol/L)	Sorbed U (mole/kg)	K_d (cm ³ /g)	Percent Sorbed
Limestone	6.24	1	9.66E-05	9.68E-05	1	2
	6.16	7	9.59E-05	1.51E-04	2	4
	6.14	7	9.45E-05	2.08E-04	2	5
	6.15	7	9.39E-05	2.31E-04	2	6
	6.21	14	9.13E-05	2.52E-04	3	6
	6.29	14	9.13E-05	2.52E-04	3	6
	6.30	14	9.13E-05	2.52E-04	3	6
	6.28	28	9.33E-05	2.35E-04	3	6
	6.29	28	9.28E-05	2.52E-04	3	6
	6.24	28	8.91E-05	4.03E-04	5	10
	6.20	42	9.20E-05	2.97E-04	3	7
	6.24	42	9.24E-05	2.80E-04	3	7
	6.26	42	9.28E-05	2.63E-04	3	7
	6.20	56	9.28E-05	3.02E-04	3	8
	6.24	56	9.24E-05	3.19E-04	3	8
	6.25	56	9.24E-05	3.19E-04	3	8
	6.17	112	9.03E-05	3.42E-04	4	9
	6.21	112	9.03E-05	3.42E-04	4	9
	6.20	112	9.03E-05	3.41E-04	4	9

Table A3: Uranium Desorption Variation with Time

pH		Desorption Time (day)	Dissolved U (mol/L)	Sorbed U (mol/kg)	K_d (cm ³ /g)	K_d/K_d^0
/	Bentonite	0.13	1.31E-05	2.04E-03	156	6.77
/		0.13	1.13E-05	2.38E-03	210	7.69
/		0.13	1.36E-05	2.88E-03	212	6.21
6.36		1	2.17E-05	2.04E-03	94	4.09
6.43		1	2.07E-05	2.38E-03	115	4.20
6.43		1	2.24E-05	2.88E-03	128	3.76
6.35		2	2.80E-05	2.04E-03	73	3.16
6.42		2	2.85E-05	2.38E-03	83	3.05
6.42		2	2.83E-05	2.88E-03	102	2.99
6.41		7	3.32E-05	2.04E-03	61	2.67
6.44		7	3.32E-05	2.38E-03	72	2.62
6.44		7	3.35E-05	2.88E-03	86	2.52
6.37		14	3.58E-05	2.04E-03	57	2.48
6.41		14	3.66E-05	2.38E-03	65	2.38
6.41		14	3.58E-05	2.88E-03	80	2.36
6.39		28	3.68E-05	2.04E-03	55	2.41
6.42		28	3.78E-05	2.38E-03	63	2.30
6.42		28	3.70E-05	2.88E-03	78	2.28
6.35		56	3.70E-05	2.04E-03	55	2.39
6.37		56	3.91E-05	2.38E-03	61	2.22
6.37		56	3.86E-05	2.88E-03	75	2.19
/	Shale	0.13	1.71E-05	1.53E-03	89	4.88
/		0.13	1.79E-05	1.61E-03	90	4.63
/		0.13	1.84E-05	1.53E-03	83	4.54
6.33		1	2.98E-05	1.52E-03	51	2.81
6.34		1	2.70E-05	1.61E-03	60	3.06
6.34		1	2.70E-05	1.53E-03	56	3.10
6.31		2	3.60E-05	1.52E-03	42	2.32
6.32		2	3.35E-05	1.61E-03	48	2.47
6.32		2	3.50E-05	1.52E-03	44	2.39
6.3		7	4.25E-05	1.52E-03	36	1.96
6.32		7	4.10E-05	1.61E-03	39	2.02
6.31		7	4.18E-05	1.52E-03	37	2.00
6.26		14	4.40E-05	1.52E-03	35	1.90
6.27		14	4.30E-05	1.61E-03	37	1.93
6.26		14	4.19E-05	1.52E-03	36	1.99
6.24		28	4.18E-05	1.52E-03	37	2.00
6.27		28	4.18E-05	1.61E-03	39	1.98
6.26		28	4.25E-05	1.52E-03	36	1.97
6.19		56	3.99E-05	1.52E-03	38	2.09
6.19		56	4.10E-05	1.61E-03	39	2.02
6.2		56	4.17E-05	1.52E-03	37	2.00

pH		Desorption Time (day)	Dissolved U (mol/L)	Sorbed U (mol/kg)	K_d (cm ³ /g)	K_d/K_d^0
/	Limestone	0.13	1.79E-05	3.42E-04	19	5.05
/		0.13	1.71E-05	3.42E-04	20	5.27
/		0.13	1.81E-05	3.41E-04	19	4.98
6.18		1	2.62E-05	3.41E-04	13	3.44
6.19		1	2.47E-05	3.42E-04	14	3.65
6.21		1	2.52E-05	3.41E-04	14	3.58
6.17		2	2.98E-05	3.41E-04	11	3.03
6.19		2	2.90E-05	3.41E-04	12	3.11
6.19		2	3.09E-05	3.41E-04	11	2.93
6.19		7	3.35E-05	3.41E-04	10	2.70
6.21		7	3.45E-05	3.41E-04	10	2.62
6.2		7	3.42E-05	3.41E-04	10	2.64
6.17		14	3.63E-05	3.41E-04	9	2.49
6.18		14	3.76E-05	3.41E-04	9	2.40
6.18		14	3.78E-05	3.41E-04	9	2.39
6.15		28	3.88E-05	3.41E-04	9	2.33
6.16		28	4.00E-05	3.41E-04	9	2.26
6.16		28	4.05E-05	3.41E-04	8	2.23
6.08		56	4.28E-05	3.41E-04	8	2.11
6.08		56	4.54E-05	3.41E-04	8	1.99
6.08		56	4.62E-05	3.41E-04	7	1.95

Table A4: Zirconium Sorption Variation with pH and Time

	pH	Time (day)	Dissolved Zr (mol/L)	Sorbed Zr (mol/kg)	K_d (cm ³ /g)	Percent Sorbed	K_a (cm)
bentonite	6.52	0.042	1.18E-06	4.07E-05	35	15	1.38E-04
	6.97	0.042	1.10E-06	3.97E-05	36	16	1.44E-04
	7.77	0.042	8.55E-07	5.47E-05	64	25	2.56E-04
	6.61	1	5.21E-07	8.96E-05	172	46	6.88E-04
	6.55	14	7.62E-08	7.46E-05	979	83	3.92E-03
shale	6.48	0.042	7.51E-07	6.12E-05	82	46	7.08E-04
	6.95	0.042	7.13E-07	6.01E-05	84	45	7.32E-04
	7.83	0.042	4.79E-07	6.60E-05	138	58	1.20E-03
	6.54	1	2.09E-07	7.73E-05	370	78	3.21E-03
	6.44	14	2.25E-08	4.42E-05	1967	95	1.71E-02
limestone	6.43	0.042	1.05E-06	1.32E-05	13	24	4.33E-04
	6.91	0.042	9.92E-07	1.23E-05	12	24	4.30E-04
	7.88	0.042	7.95E-07	1.39E-05	18	31	6.06E-04
	6.43	1	4.41E-07	2.06E-05	47	55	1.61E-03
	6.30	14	8.44E-08	1.51E-05	179	82	6.19E-03

Table A5: Zirconium Sorption with Time

	pH	Time (day)	Dissolved Zr (mol/L)	Sorbed Zr (mol/kg)	K_d (cm ³ /g)	Percent Sorbed	K_a (cm)
bentonite	6.43	1	8.82E-07	7.74E-05	88	31	3.51E-04
	6.43	1	9.04E-07	7.30E-05	81	29	3.23E-04
	6.43	1	1.05E-06	4.35E-05	41	17	1.65E-04
	6.48	3	7.45E-07	1.05E-04	141	41	5.62E-04
	6.48	3	7.18E-07	1.10E-04	154	43	6.15E-04
	6.48	3	6.36E-07	1.27E-04	199	50	7.98E-04
	6.55	7	4.93E-07	1.55E-04	314	61	1.26E-03
	6.52	7	4.77E-07	1.58E-04	332	62	1.33E-03
	6.53	7	4.44E-07	1.65E-04	372	65	1.49E-03
	6.56	14	3.62E-07	1.81E-04	501	72	2.01E-03
	6.53	14	3.73E-07	1.79E-04	481	71	1.93E-03
	6.55	14	4.39E-07	1.66E-04	379	65	1.52E-03
Shale	6.38	1	4.49E-07	8.20E-05	182	65	1.58E-03
	6.38	1	2.19E-07	1.05E-04	479	83	4.16E-03
	6.38	1	2.19E-07	1.05E-04	479	83	4.16E-03
	6.4	3	2.74E-07	9.95E-05	363	78	3.15E-03
	6.4	3	3.12E-07	9.57E-05	306	75	2.66E-03
	6.42	3	2.96E-07	9.74E-05	329	77	2.86E-03
	6.41	7	2.14E-07	1.06E-04	494	83	4.29E-03
	6.41	7	2.14E-07	1.06E-04	494	83	4.29E-03
	6.43	7	2.14E-07	1.06E-04	494	83	4.29E-03
	6.44	14	2.14E-07	1.06E-04	494	83	4.29E-03
	6.4	14	2.14E-07	1.06E-04	494	83	4.29E-03
	6.39	14	2.14E-07	1.06E-04	494	83	4.29E-03
Limestone	6.31	1	7.34E-07	2.14E-05	29	42	1.01E-03
	6.3	1	4.77E-07	3.17E-05	67	62	2.30E-03
	6.3	1	4.88E-07	3.13E-05	64	62	2.21E-03
	6.31	3	5.59E-07	2.84E-05	51	56	1.76E-03
	6.31	3	5.7E-07	2.80E-05	49	55	1.70E-03
	6.32	3	5.7E-07	2.80E-05	49	55	1.70E-03
	6.29	7	4.55E-07	3.26E-05	72	64	2.47E-03
	6.3	7	3.84E-07	3.54E-05	92	70	3.19E-03
	6.31	7	3.56E-07	3.65E-05	102	72	3.54E-03
	6.27	14	2.41E-07	4.11E-05	170	81	5.89E-03
	6.27	14	3.4E-07	3.72E-05	109	73	3.78E-03
	6.28	14	2.63E-07	4.02E-05	153	79	5.28E-03

Table A6: Lithium Sorption with Time in Brine

Mineral	pH	Time (day)	Dissolved Li (mol/L)	Sorbed Li (mole/kg)	K_d (cm ³ /g)	Percent Sorbed	K_a (cm)
bentonite	6.52	1	1.85E-02	2.40E-02	1.3	0.6	5.19E-06
not sterile	6.52	1	1.82E-02	9.54E-02	5.3	2.6	2.10E-05
	6.53	1	1.79E-02	1.39E-01	7.7	3.7	3.09E-05
	6.42	3	2.41E-02	0.00E+00	0.0	0.0	0.00E+00
	6.52	3	2.29E-02	1.24E-01	5.4	2.7	2.17E-05
	6.54	3	2.42E-02	0.00E+00	0.0	0.0	0.00E+00
	6.46	7	2.46E-02	0.00E+00	0.0	0.0	0.00E+00
	6.53	7	2.61E-02	0.00E+00	0.0	0.0	0.00E+00
	6.51	7	2.45E-02	1.43E-02	0.6	0.3	2.34E-06
	6.50	16	2.59E-02	0.00E+00	0.0	0.0	0.00E+00
	6.53	16	2.50E-02	0.00E+00	0.0	0.0	0.00E+00
	6.53	16	2.49E-02	0.00E+00	0.0	0.0	0.00E+00
	6.51	71	2.43E-02	0.00E+00	0.0	0.0	0.00E+00
	6.52	71	2.43E-02	0.00E+00	0.0	0.0	0.00E+00
	6.53	71	2.23E-02	1.35E-01	6.1	3.0	2.43E-05
	6.52	99	2.43E-02	0.00E+00	0.0	0.0	0.00E+00
	6.51	99	2.19E-02	8.59E-02	3.9	1.9	1.57E-05
	6.50	99	2.22E-02	2.87E-02	1.3	0.6	5.18E-06
	6.53	127	2.17E-02	6.78E-02	3.1	1.5	1.25E-05
	6.54	127	2.17E-02	6.75E-02	3.1	1.5	1.25E-05
	6.55	127	2.14E-02	1.26E-01	5.9	2.9	2.35E-05
shale	6.49	1	1.81E-02	5.54E-02	3.1	3.0	2.66E-05
not sterile	6.50	1	1.85E-02	1.20E-02	0.6	0.6	5.61E-06
	6.50	1	1.83E-02	3.36E-02	1.8	1.8	1.59E-05
	6.44	3	2.46E-02	0.00E+00	0.0	0.0	0.00E+00
	6.45	3	2.25E-02	1.05E-01	4.7	4.5	4.07E-05
	6.48	3	2.36E-02	0.00E+00	0.0	0.0	0.00E+00
	6.43	7	2.47E-02	0.00E+00	0.0	0.0	0.00E+00
	6.43	7	2.49E-02	0.00E+00	0.0	0.0	0.00E+00
	6.49	7	2.44E-02	1.44E-02	0.6	0.6	5.11E-06
	6.37	16	2.43E-02	4.33E-02	1.8	1.7	1.55E-05
	6.22	16	2.56E-02	0.00E+00	0.0	0.0	0.00E+00
	6.43	16	2.14E-02	3.38E-01	15.8	13.7	1.37E-04
	6.34	71	2.18E-02	1.12E-01	5.1	4.9	4.45E-05
	6.34	71	2.42E-02	0.00E+00	0.0	0.0	0.00E+00
	6.35	71	2.34E-02	0.00E+00	0.0	0.0	0.00E+00
	6.35	99	2.35E-02	0.00E+00	0.0	0.0	0.00E+00
	6.33	99	2.31E-02	0.00E+00	0.0	0.0	0.00E+00
	6.34	99	2.20E-02	2.88E-02	1.3	1.3	1.13E-05
	6.36	127	2.18E-02	1.94E-02	0.9	0.9	7.74E-06
	6.36	127	2.21E-02	0.00E+00	0.0	0.0	0.00E+00
	6.36	127	2.26E-02	0.00E+00	0.0	0.0	0.00E+00

Mineral	pH	Time (day)	Dissolved Li (mol/L)	Sorbed Li (mole/kg)	K_d (cm ³ /g)	Percent Sorbed	Ka (cm)
limestone	6.40	1	1.84E-02	1.06E-02	0.6	1.4	1.99E-05
not sterile	6.42	1	1.87E-02	0.00E+00	0.0	0.0	0.00E+00
	6.42	1	1.90E-02	0.00E+00	0.0	0.0	0.00E+00
	6.31	3	2.35E-02	1.92E-03	0.1	0.2	2.83E-06
	6.31	3	2.35E-02	1.92E-03	0.1	0.2	2.83E-06
	6.36	3	2.35E-02	1.92E-03	0.1	0.2	2.83E-06
	6.27	7	2.31E-02	5.76E-02	2.5	5.9	8.61E-05
	6.32	7	2.58E-02	0.00E+00	0.0	0.0	0.00E+00
	6.31	7	2.44E-02	5.76E-03	0.2	0.6	8.16E-06
	6.24	16	2.58E-02	0.00E+00	0.0	0.0	0.00E+00
	6.28	16	2.46E-02	5.76E-03	0.2	0.6	8.08E-06
	6.32	16	2.18E-02	1.21E-01	5.6	12.2	1.92E-04
	6.25	71	2.27E-02	9.70E-03	0.4	1.1	1.48E-05
	6.26	71	2.44E-02	0.00E+00	0.0	0.0	0.00E+00
	6.26	71	2.26E-02	1.55E-02	0.7	1.7	2.38E-05
	6.25	99	2.29E-02	0.00E+00	0.0	0.0	0.00E+00
	6.26	99	2.22E-02	5.76E-03	0.3	0.6	8.98E-06
	6.26	99	2.20E-02	1.15E-02	0.5	1.3	1.81E-05
	6.28	127	2.18E-02	7.76E-03	0.4	0.9	1.23E-05
	6.28	127	2.18E-02	7.76E-03	0.4	0.9	1.23E-05
	6.27	127	2.23E-02	0.00E+00	0.0	0.0	0.00E+00
bentonite	6.57	1	2.54E-02	0.00E+00	0.0	0.0	0.00E+00
sterile	6.57	1	2.35E-02	0.00E+00	0.0	0.0	0.00E+00
	6.46	3	2.31E-02	0.00E+00	0.0	0.0	0.00E+00
	6.50	3	2.24E-02	7.73E-02	3.4	1.7	1.38E-05
	6.53	3	2.23E-02	1.07E-01	4.8	2.3	1.92E-05
	6.53	7	2.30E-02	0.00E+00	0.0	0.0	0.00E+00
	6.53	7	2.08E-02	0.00E+00	0.0	0.0	0.00E+00
	6.56	16	2.21E-02	0.00E+00	0.0	0.0	0.00E+00
	6.57	16	2.18E-02	1.93E-02	0.9	0.4	3.54E-06
	6.56	16	2.27E-02	0.00E+00	0.0	0.0	0.00E+00
	6.50	64	2.30E-02	2.73E-01	11.9	5.6	4.75E-05
	6.52	64	2.30E-02	2.71E-01	11.8	5.6	4.71E-05
	6.51	64	2.34E-02	1.84E-01	7.9	3.8	3.15E-05
	6.49	93	2.14E-02	0.00E+00	0.0	0.0	0.00E+00
	6.49	93	2.02E-02	2.13E-01	10.5	5.0	4.21E-05
	6.50	93	2.11E-02	3.88E-02	1.8	0.9	7.36E-06
	6.52	121	2.37E-02	0.00E+00	0.0	0.0	0.00E+00
	6.53	121	2.27E-02	1.64E-01	7.2	3.5	2.90E-05
	6.54	121	2.33E-02	4.85E-02	2.1	1.0	8.34E-06

Mineral	pH	Time (day)	Dissolved Li (mol/L)	Sorbed Li (mole/kg)	K_d (cm ³ /g)	Percent Sorbed	K_a (cm)
shale	6.52	1	2.43E-02	0.00E+00	0.0	0.0	0.00E+00
sterile	6.56	1	2.43E-02	0.00E+00	0.0	0.0	0.00E+00
	6.33	3	2.30E-02	0.00E+00	0.0	0.0	0.00E+00
	6.43	3	2.26E-02	2.42E-02	1.1	1.1	9.32E-06
	6.46	3	2.14E-02	1.41E-01	6.6	6.2	5.70E-05
	6.34	7	1.91E-02	1.66E-01	8.7	8.0	7.53E-05
	6.44	7	2.10E-02	0.00E+00	0.0	0.0	0.00E+00
	6.46	7	2.00E-02	7.20E-02	3.6	3.5	3.12E-05
	6.33	16	2.20E-02	0.00E+00	0.0	0.0	0.00E+00
	6.46	16	2.21E-02	0.00E+00	0.0	0.0	0.00E+00
	6.47	16	2.20E-02	0.00E+00	0.0	0.0	0.00E+00
	6.28	64	2.36E-02	7.75E-02	3.3	3.2	2.86E-05
	6.39	64	2.49E-02	0.00E+00	0.0	0.0	0.00E+00
	6.41	64	2.42E-02	1.94E-02	0.8	0.8	6.97E-06
	6.27	93	2.26E-02	0.00E+00	0.0	0.0	0.00E+00
	6.37	93	2.28E-02	0.00E+00	0.0	0.0	0.00E+00
	6.37	93	2.08E-02	4.85E-02	2.3	2.3	2.02E-05
	6.32	121	2.28E-02	6.79E-02	3.0	2.9	2.58E-05
	6.41	121	2.34E-02	9.68E-03	0.4	0.4	3.59E-06
	6.40	121	2.43E-02	0.00E+00	0.0	0.0	0.00E+00
limestone	6.52	1	1.99E-02	1.37E-01	6.9	14.7	2.38E-04
sterile	6.49	1	2.45E-02	0.00E+00	0.0	0.0	0.00E+00
	6.47	1	2.24E-02	3.60E-02	1.6	3.9	5.56E-05
	6.39	3	2.28E-02	0.00E+00	0.0	0.0	0.00E+00
	6.37	3	2.27E-02	3.88E-03	0.2	0.4	5.91E-06
	6.39	3	2.27E-02	3.88E-03	0.2	0.4	5.91E-06
	6.45	7	1.95E-02	4.89E-02	2.5	5.9	8.66E-05
	6.36	7	2.13E-02	0.00E+00	0.0	0.0	0.00E+00
	6.34	7	2.01E-02	2.59E-02	1.3	3.1	4.46E-05
	6.45	16	2.20E-02	0.00E+00	0.0	0.0	0.00E+00
	6.36	16	2.18E-02	3.88E-03	0.2	0.4	6.14E-06
	6.36	16	2.21E-02	0.00E+00	0.0	0.0	0.00E+00
	6.38	64	2.36E-02	3.10E-02	1.3	3.2	4.55E-05
	6.31	64	2.42E-02	7.76E-03	0.3	0.8	1.11E-05
	6.29	64	2.43E-02	1.94E-03	0.1	0.2	2.76E-06
	6.37	93	2.14E-02	0.00E+00	0.0	0.0	0.00E+00
	6.29	93	2.15E-02	0.00E+00	0.0	0.0	0.00E+00
	6.28	93	2.10E-02	1.36E-02	0.6	1.6	2.24E-05
	6.40	121	2.34E-02	3.88E-03	0.2	0.4	5.72E-06
	6.33	121	2.34E-02	3.88E-03	0.2	0.4	5.72E-06
	6.30	121	2.36E-02	0.00E+00	0.0	0.0	0.00E+00

Table A7: Nickel Sorption with Time in Brine

Mineral	pH	Time (day)	Dissolved Ni (mol/L)	Sorbed Ni (mole/kg)	K_d (cm ³ /g)	Percent Sorbed	K_a (cm)
bentonite	6.52	1	9.20E-05	7.94E-04	8.6	4.1	3.45E-05
not sterile	6.52	1	9.20E-05	7.90E-04	8.6	4.1	3.44E-05
	6.53	1	9.37E-05	4.52E-04	4.8	2.4	1.93E-05
	6.42	3	1.20E-04	0.00E+00	0.0	0.0	0.00E+00
	6.52	3	1.20E-04	0.00E+00	0.0	0.0	0.00E+00
	6.54	3	1.20E-04	0.00E+00	0.0	0.0	0.00E+00
	6.46	7	9.54E-05	4.25E-04	4.5	2.2	1.78E-05
	6.53	7	9.80E-05	0.00E+00	0.0	0.0	0.00E+00
	6.51	7	9.37E-05	7.63E-04	8.1	3.9	3.26E-05
	6.50	16	9.28E-05	7.94E-04	8.6	4.1	3.42E-05
	6.53	16	9.28E-05	7.90E-04	8.5	4.1	3.41E-05
	6.53	16	9.28E-05	7.92E-04	8.5	4.1	3.41E-05
	6.51	71	1.03E-04	0.00E+00	0.0	0.0	0.00E+00
	6.52	71	1.03E-04	0.00E+00	0.0	0.0	0.00E+00
	6.53	71	8.60E-05	1.98E-03	23	10	9.21E-05
	6.52	99	1.03E-04	0.00E+00	0.0	0.0	0.00E+00
	6.51	99	1.03E-04	0.00E+00	0.0	0.0	0.00E+00
	6.50	99	1.03E-04	0.00E+00	0.0	0.0	0.00E+00
	6.53	127	1.03E-04	0.00E+00	0.0	0.0	1.05E-19
	6.54	127	1.03E-04	0.00E+00	0.0	0.0	1.04E-19
	6.55	127	1.03E-04	0.00E+00	0.0	0.0	1.05E-19
shale	6.49	1	8.77E-05	8.25E-04	9.4	8.6	8.17E-05
not sterile	6.50	1	9.80E-05	0.00E+00	0.0	0.0	0.00E+00
	6.50	1	9.45E-05	1.42E-04	1.5	1.5	1.30E-05
	6.44	3	1.20E-04	0.00E+00	0.0	0.0	0.00E+00
	6.45	3	1.20E-04	0.00E+00	0.0	0.0	0.00E+00
	6.48	3	1.20E-04	0.00E+00	0.0	0.0	0.00E+00
	6.43	7	9.37E-05	3.84E-04	4.1	3.9	3.56E-05
	6.43	7	9.03E-05	7.21E-04	8.0	7.4	6.94E-05
	6.49	7	9.80E-05	0.00E+00	0.0	0.0	0.00E+00
	6.37	16	9.37E-05	3.13E-04	3.3	3.2	2.90E-05
	6.22	16	9.71E-05	0.00E+00	0.0	0.0	0.00E+00
	6.43	16	9.11E-05	5.67E-04	6.2	5.9	5.40E-05
	6.34	71	1.03E-04	0.00E+00	0.0	0.0	0.00E+00
	6.34	71	1.03E-04	0.00E+00	0.0	0.0	0.00E+00
	6.35	71	1.03E-04	0.00E+00	0.0	0.0	0.00E+00
	6.35	99	1.03E-04	0.00E+00	0.0	0.0	0.00E+00
	6.33	99	1.03E-04	0.00E+00	0.0	0.0	0.00E+00
	6.34	99	1.03E-04	0.00E+00	0.0	0.0	0.00E+00
	6.36	127	1.03E-04	0.00E+00	0.0	0.0	1.14E-19
	6.36	127	1.03E-04	0.00E+00	0.0	0.0	1.14E-19
	6.36	127	1.03E-04	0.00E+00	0.0	0.0	1.14E-19

Mineral	pH	Time (day)	Dissolved Ni (mol/L)	Sorbed Ni (mole/kg)	K_d (cm ³ /g)	Percent Sorbed	K_a (cm)
limestone not sterile	6.40	1	9.37E-05	9.09E-05	1.0	2.4	3.35E-05
	6.42	1	9.20E-05	1.59E-04	1.7	4.1	5.97E-05
	6.42	1	9.54E-05	2.27E-05	0.2	0.6	8.23E-06
	6.31	3	1.20E-04	0.00E+00	0.0	0.0	0.00E+00
	6.31	3	1.20E-04	0.00E+00	0.0	0.0	0.00E+00
	6.36	3	1.20E-04	0.00E+00	0.0	0.0	0.00E+00
	6.27	7	9.80E-05	0.00E+00	0.0	0.0	0.00E+00
	6.32	7	9.45E-05	1.19E-04	1.3	3.1	4.36E-05
	6.31	7	1.02E-04	0.00E+00	0.0	0.0	0.00E+00
	6.24	16	9.45E-05	9.09E-05	1.0	2.3	3.32E-05
	6.28	16	9.54E-05	5.68E-05	0.6	1.5	2.06E-05
	6.32	16	9.54E-05	5.68E-05	0.6	1.5	2.06E-05
	6.25	71	1.03E-04	0.00E+00	0.0	0.0	0.00E+00
	6.26	71	1.03E-04	0.00E+00	0.0	0.0	0.00E+00
	6.26	71	8.60E-05	3.98E-04	4.6	10	1.60E-04
	6.25	99	1.03E-04	0.00E+00	0.0	0.0	0.00E+00
	6.26	99	1.03E-04	0.00E+00	0.0	0.0	0.00E+00
	6.26	99	1.03E-04	0.00E+00	0.0	0.0	0.00E+00
	6.28	127	1.03E-04	0.00E+00	0.0	0.0	1.81E-19
	6.28	127	1.03E-04	0.00E+00	0.0	0.0	1.81E-19
6.27	127	1.03E-04	0.00E+00	0.0	0.0	1.81E-19	
bentonite sterile	6.56	1	8.77E-05	2.28E-04	2.6	1.3	1.04E-05
	6.57	1	9.11E-05	0.00E+00	0.0	0.0	0.00E+00
	6.57	1	9.28E-05	0.00E+00	0.0	0.0	0.00E+00
	6.46	3	1.03E-04	1.15E-03	11	5.3	4.47E-05
	6.50	3	1.03E-04	1.14E-03	11	5.3	4.43E-05
	6.53	3	1.03E-04	1.15E-03	11	5.3	4.45E-05
	6.55	7	8.43E-05	6.27E-04	7.4	3.6	2.98E-05
	6.53	7	8.94E-05	0.00E+00	0.0	0.0	0.00E+00
	6.53	7	8.60E-05	2.84E-04	3.3	1.6	1.32E-05
	6.56	16	1.03E-04	1.15E-03	11	5.3	4.47E-05
	6.57	16	1.03E-04	1.14E-03	11	5.3	4.43E-05
	6.56	16	1.03E-04	1.15E-03	11	5.3	4.45E-05
	6.50	64	7.28E-04	0.00E+00	0.0	0.0	0.00E+00
	6.52	64	7.28E-04	0.00E+00	0.0	0.0	0.00E+00
	6.51	64	7.28E-04	0.00E+00	0.0	0.0	0.00E+00
	6.49	93	1.03E-04	0.00E+00	0.0	0.0	1.06E-19
	6.49	93	8.60E-05	3.43E-03	40	17	1.59E-04
	6.50	93	1.03E-04	0.00E+00	0.0	0.0	1.05E-19
	6.52	121	8.60E-05	1.15E-03	13	6.2	5.36E-05
	6.53	121	8.60E-05	1.14E-03	13	6.2	5.32E-05
6.54	121	8.60E-05	1.15E-03	13	6.2	5.34E-05	

Mineral	pH	Time (day)	Dissolved Ni (mol/L)	Sorbed Ni (mole/kg)	K_d (cm ³ /g)	Percent Sorbed	K_a (cm)
shale	6.50	1	8.52E-05	3.69E-04	4.3	4.2	3.76E-05
sterile	6.52	1	9.03E-05	0.00E+00	0.0	0.0	0.00E+00
	6.56	1	9.63E-05	0.00E+00	0.0	0.0	0.00E+00
	6.33	3	1.03E-04	5.73E-04	5.6	5.3	4.82E-05
	6.43	3	1.03E-04	5.72E-04	5.5	5.3	4.81E-05
	6.46	3	1.03E-04	5.73E-04	5.6	5.3	4.82E-05
	6.34	7	8.69E-05	5.67E-05	0.7	0.6	5.67E-06
	6.44	7	8.52E-05	2.27E-04	2.7	2.6	2.31E-05
	6.46	7	8.77E-05	0.00E+00	0.0	0.0	0.00E+00
	6.33	16	1.03E-04	5.73E-04	5.6	5.3	4.82E-05
	6.46	16	1.03E-04	5.72E-04	5.5	5.3	4.81E-05
	6.47	16	1.20E-04	0.00E+00	0.0	0.0	0.00E+00
	6.28	64	7.28E-04	0.00E+00	0.0	0.0	0.00E+00
	6.39	64	7.28E-04	0.00E+00	0.0	0.0	0.00E+00
	6.41	64	7.28E-04	0.00E+00	0.0	0.0	0.00E+00
	6.27	93	1.03E-04	0.00E+00	0.0	0.0	1.14E-19
	6.37	93	1.03E-04	0.00E+00	0.0	0.0	1.14E-19
	6.37	93	1.03E-04	0.00E+00	0.0	0.0	1.14E-19
	6.32	121	8.60E-05	5.73E-04	6.7	6.2	5.78E-05
	6.41	121	8.60E-05	5.72E-04	6.7	6.2	5.78E-05
	6.40	121	8.60E-05	5.73E-04	6.7	6.2	5.78E-05
limestone	6.52	1	8.26E-05	2.50E-04	3.0	7.0	1.04E-04
sterile	6.49	1	8.94E-05	0.00E+00	0.0	0.0	0.00E+00
	6.47	1	9.37E-05	0.00E+00	0.0	0.0	0.00E+00
	6.39	3	1.03E-04	2.29E-04	2.2	5.3	7.67E-05
	6.37	3	1.03E-04	2.29E-04	2.2	5.3	7.68E-05
	6.39	3	1.03E-04	2.29E-04	2.2	5.3	7.68E-05
	6.45	7	8.35E-05	1.59E-04	1.9	4.5	6.58E-05
	6.36	7	8.26E-05	1.93E-04	2.3	5.5	8.07E-05
	6.34	7	8.52E-05	9.09E-05	1.1	2.6	3.69E-05
	6.45	16	1.03E-04	2.29E-04	2.2	5.3	7.67E-05
	6.36	16	1.03E-04	2.29E-04	2.2	5.3	7.68E-05
	6.36	16	1.20E-04	0.00E+00	0.0	0.0	0.00E+00
	6.38	64	7.28E-04	0.00E+00	0.0	0.0	0.00E+00
	6.31	64	7.28E-04	0.00E+00	0.0	0.0	0.00E+00
	6.29	64	7.28E-04	0.00E+00	0.0	0.0	0.00E+00
	6.37	93	8.60E-05	6.88E-04	8.0	17	2.76E-04
	6.29	93	1.03E-04	0.00E+00	0.0	0.0	1.81E-19
	6.28	93	1.03E-04	0.00E+00	0.0	0.0	1.81E-19
	6.40	121	8.60E-05	2.29E-04	2.7	6.2	9.21E-05
	6.33	121	8.60E-05	2.29E-04	2.7	6.2	9.21E-05
	6.30	121	8.60E-05	2.29E-04	2.7	6.2	9.22E-05

Table A8: Copper Sorption with Time in Brine

Mineral	pH	Time (day)	Dissolved Cu (mol/L)	Sorbed Cu (mole/kg)	K_d (cm ³ /g)	Percent Sorbed	K_a (cm)
bentonite	6.52	1	5.66E-06	3.37E-04	60	23	2.38E-04
not sterile	6.52	1	5.93E-06	2.80E-04	47	19	1.89E-04
	6.53	1	5.92E-06	2.83E-04	48	19	1.91E-04
	6.42	3	6.36E-06	3.17E-04	50	20	2.00E-04
	6.54	3	6.36E-06	3.16E-04	50	20	1.99E-04
	6.46	7	6.45E-06	1.78E-04	28	12	1.11E-04
	6.53	7	6.61E-06	1.46E-04	22	10	8.84E-05
	6.51	7	6.69E-06	1.31E-04	20	9	7.81E-05
	6.50	16	6.77E-06	1.15E-04	17	8	6.82E-05
	6.53	16	6.37E-06	1.93E-04	30	13	1.21E-04
	6.53	16	6.14E-06	2.40E-04	39	16	1.57E-04
	6.51	71	6.36E-06	3.17E-04	50	20	2.00E-04
	6.52	71	6.36E-06	3.16E-04	50	20	1.99E-04
	6.53	71	4.77E-06	6.33E-04	133	40	5.31E-04
	6.51	99	4.77E-06	6.32E-04	132	40	5.30E-04
	6.50	99	4.77E-06	6.33E-04	133	40	5.31E-04
	6.53	127	4.77E-06	6.35E-04	133	40	5.33E-04
	6.54	127	4.77E-06	6.32E-04	132	40	5.30E-04
	6.55	127	4.77E-06	6.33E-04	133	40	5.31E-04
shale	6.49	1	6.09E-06	1.26E-04	21	17	1.79E-04
not sterile	6.50	1	6.82E-06	5.20E-05	8	7	6.62E-05
	6.50	1	6.65E-06	6.94E-05	10	9	9.06E-05
	6.44	3	7.95E-06	0.00E+00	0	0	0.00E+00
	6.45	3	6.36E-06	1.58E-04	25	20	2.16E-04
	6.48	3	7.95E-06	0.00E+00	0	0	0.00E+00
	6.43	7	7.08E-06	2.63E-05	4	4	3.22E-05
	6.43	7	6.22E-06	1.12E-04	18	15	1.57E-04
	6.49	7	6.85E-06	4.97E-05	7	7	6.31E-05
	6.37	16	6.61E-06	7.36E-05	11	10	9.67E-05
	6.22	16	6.69E-06	6.53E-05	10	9	8.48E-05
	6.43	16	5.82E-06	1.52E-04	26	21	2.26E-04
	6.34	71	4.77E-06	3.19E-04	67	40	5.80E-04
	6.34	71	6.36E-06	1.58E-04	25	20	2.16E-04
	6.35	71	4.77E-06	3.17E-04	67	40	5.78E-04
	6.35	99	4.77E-06	3.19E-04	67	40	5.80E-04
	6.33	99	6.36E-06	1.58E-04	25	20	2.16E-04
	6.34	99	4.77E-06	3.17E-04	67	40	5.78E-04
	6.36	127	3.18E-06	4.78E-04	150	60	1.31E-03
	6.36	127	4.77E-06	3.17E-04	66	40	5.77E-04
	6.36	127	4.77E-06	3.17E-04	67	40	5.78E-04

Mineral	pH	Time (day)	Dissolved Cu (mol/L)	Sorbed Cu (mole/kg)	K_d (cm ³ /g)	Percent Sorbed	K_a (cm)
limestone	6.40	1	6.64E-06	2.81E-05	4	10	1.46E-04
not sterile	6.42	1	6.55E-06	3.19E-05	5	11	1.68E-04
	6.42	1	6.84E-06	2.03E-05	3	7	1.02E-04
	6.31	3	7.95E-06	0.00E+00	0	0	0.00E+00
	6.31	3	7.95E-06	0.00E+00	0	0	0.00E+00
	6.36	3	7.95E-06	0.00E+00	0	0	0.00E+00
	6.27	7	7.71E-06	0.00E+00	0	0	0.00E+00
	6.32	7	7.47E-06	0.00E+00	0	0	0.00E+00
	6.31	7	7.87E-06	0.00E+00	0	0	0.00E+00
	6.24	16	7.71E-06	0.00E+00	0	0	0.00E+00
	6.28	16	7.40E-06	0.00E+00	0	0	0.00E+00
	6.32	16	8.42E-06	0.00E+00	0	0	0.00E+00
	6.25	71	7.95E-06	0.00E+00	0	0	0.00E+00
	6.26	71	6.36E-06	6.36E-05	10	20	3.46E-04
	6.26	71	4.77E-06	1.27E-04	27	40	9.22E-04
	6.25	99	6.36E-06	6.36E-05	10	20	3.46E-04
	6.26	99	6.36E-06	6.36E-05	10	20	3.46E-04
	6.26	99	6.36E-06	6.36E-05	10	20	3.46E-04
	6.28	127	6.36E-06	6.36E-05	10	20	3.46E-04
	6.28	127	6.36E-06	6.36E-05	10	20	3.46E-04
	6.27	127	6.36E-06	6.36E-05	10	20	3.46E-04
bentonite	6.56	1	5.19E-06	1.90E-04	37	15	1.46E-04
sterile	6.57	1	5.19E-06	1.88E-04	36	15	1.45E-04
	6.57	1	5.59E-06	1.10E-04	20	9	7.89E-05
	6.46	3	6.36E-06	2.13E-04	33	14	1.34E-04
	6.50	3	4.77E-06	5.28E-04	111	36	4.43E-04
	6.53	3	4.77E-06	5.30E-04	111	36	4.45E-04
	6.55	7	4.48E-06	2.48E-04	55	22	2.21E-04
	6.53	7	4.56E-06	2.30E-04	50	20	2.02E-04
	6.53	7	4.88E-06	1.68E-04	34	15	1.38E-04
	6.56	16	4.77E-06	5.32E-04	111	36	4.47E-04
	6.57	16	4.77E-06	5.28E-04	111	36	4.43E-04
	6.56	16	4.77E-06	5.30E-04	111	36	4.45E-04
	6.52	64	3.18E-06	3.17E-04	100	33	3.99E-04
	6.51	64	3.18E-06	3.18E-04	100	33	4.00E-04
	6.49	93	6.36E-06	6.38E-04	100	33	4.02E-04
	6.49	93	6.36E-06	6.33E-04	100	33	3.99E-04
	6.50	93	6.36E-06	6.36E-04	100	33	4.00E-04
	6.52	121	6.36E-06	6.38E-04	100	33	4.02E-04
	6.53	121	6.36E-06	6.33E-04	100	33	3.99E-04
	6.54	121	6.36E-06	6.36E-04	100	33	4.00E-04

Mineral	pH	Time (day)	Dissolved Cu (mol/L)	Sorbed Cu (mole/kg)	K_d (cm ³ /g)	Percent Sorbed	K_a (cm)
shale	6.50	1	5.74E-06	3.93E-05	7	6	5.94E-05
sterile	6.52	1	5.74E-06	3.93E-05	7	6	5.93E-05
	6.56	1	5.82E-06	3.14E-05	5	5	4.69E-05
	6.33	3	6.36E-06	1.06E-04	17	14	1.45E-04
	6.43	3	6.36E-06	1.06E-04	17	14	1.44E-04
	6.46	3	6.36E-06	1.06E-04	17	14	1.45E-04
	6.34	7	5.59E-06	1.31E-05	2	2	2.04E-05
	6.44	7	5.35E-06	3.66E-05	7	6	5.95E-05
	6.46	7	5.59E-06	1.31E-05	2	2	2.04E-05
	6.33	16	6.36E-06	1.06E-04	17	14	1.45E-04
	6.46	16	4.77E-06	2.64E-04	55	36	4.81E-04
	6.47	16	6.36E-06	1.06E-04	17	14	1.45E-04
	6.28	64	4.77E-06	0.00E+00	0	0	0.00E+00
	6.39	64	1.59E-06	3.17E-04	200	67	1.73E-03
	6.41	64	3.18E-06	1.59E-04	50	33	4.34E-04
	6.27	93	7.95E-06	1.59E-04	20	17	1.74E-04
	6.37	93	6.36E-06	3.17E-04	50	33	4.33E-04
	6.37	93	6.36E-06	3.18E-04	50	33	4.34E-04
	6.32	121	7.95E-06	1.59E-04	20	17	1.74E-04
	6.41	121	6.36E-06	3.17E-04	50	33	4.33E-04
	6.40	121	6.36E-06	3.18E-04	50	33	4.34E-04
limestone	6.52	1	5.43E-06	2.83E-05	5	12	1.80E-04
sterile	6.49	1	5.90E-06	9.44E-06	2	4	5.53E-05
	6.47	1	6.37E-06	0.00E+00	0	0	0.00E+00
	6.39	3	6.36E-06	4.23E-05	7	14	2.30E-04
	6.37	3	6.36E-06	4.24E-05	7	14	2.30E-04
	6.39	3	6.36E-06	4.24E-05	7	14	2.30E-04
	6.45	7	5.19E-06	2.10E-05	4	9	1.39E-04
	6.36	7	5.35E-06	1.47E-05	3	6	9.48E-05
	6.34	7	5.51E-06	8.39E-06	2	4	5.27E-05
	6.45	16	4.77E-06	1.06E-04	22	36	7.67E-04
	6.36	16	6.36E-06	4.24E-05	7	14	2.30E-04
	6.36	16	6.36E-06	4.24E-05	7	14	2.30E-04
	6.38	64	3.18E-06	6.35E-05	20	33	6.90E-04
	6.29	64	4.77E-06	0.00E+00	0	0	0.00E+00
	6.37	93	6.36E-06	1.27E-04	20	33	6.90E-04
	6.29	93	7.95E-06	6.36E-05	8	17	2.76E-04
	6.28	93	7.95E-06	6.36E-05	8	17	2.76E-04
	6.40	121	7.95E-06	6.35E-05	8	17	2.76E-04
	6.33	121	7.95E-06	6.36E-05	8	17	2.76E-04
	6.30	121	7.95E-06	6.36E-05	8	17	2.76E-04

Table A9: Lead Sorption with Time in Brine

Mineral	pH	Time	Dissolved Pb (mol/L)	Sorbed Pb (mole/kg)	K_d (cm ³ /g)	Percent Sorbed	K_a (cm)
bentonite	6.52	1	4.92E-05	0.00E+00	0.0	0.0	0.00E+00
not sterile	6.52	1	4.92E-05	0.00E+00	0.0	0.0	0.00E+00
	6.53	1	4.54E-05	3.84E-04	8.5	4.1	3.39E-05
	6.42	3	4.97E-05	0.00E+00	0.0	0.0	0.00E+00
	6.52	3	4.92E-05	9.69E-05	2.0	1.0	7.88E-06
	6.54	3	4.97E-05	0.00E+00	0.0	0.0	0.00E+00
	6.46	7	4.58E-05	1.44E-04	3.1	1.6	1.26E-05
	6.53	7	4.46E-05	3.83E-04	8.6	4.1	3.44E-05
	6.51	7	4.46E-05	3.84E-04	8.6	4.1	3.44E-05
	6.50	16	4.54E-05	2.41E-04	5.3	2.6	2.12E-05
	6.53	16	4.51E-05	2.87E-04	6.4	3.1	2.55E-05
	6.53	16	4.90E-05	0.00E+00	0.0	0.0	0.00E+00
	6.51	71	4.97E-05	0.00E+00	0.0	0.0	0.00E+00
	6.52	71	4.92E-05	9.69E-05	2.0	1.0	7.88E-06
	6.53	71	4.97E-05	0.00E+00	0.0	0.0	0.00E+00
	6.52	99	5.02E-05	0.00E+00	0.0	0.0	0.00E+00
	6.51	99	4.73E-05	4.75E-04	10	4.8	4.01E-05
	6.50	99	4.87E-05	1.94E-04	4.0	2.0	1.59E-05
	6.53	127	4.72E-05	4.97E-04	11	5.0	4.21E-05
	6.54	127	4.77E-05	3.97E-04	8.3	4.0	3.33E-05
	6.55	127	4.78E-05	3.79E-04	7.9	3.8	3.17E-05
shale	6.49	1	4.85E-05	0.00E+00	0.0	0.0	0.00E+00
not sterile	6.50	1	4.68E-05	2.27E-05	0.5	0.5	4.21E-06
	6.50	1	4.56E-05	1.43E-04	3.1	3.0	2.73E-05
	6.44	3	4.97E-05	0.00E+00	0.0	0.0	0.00E+00
	6.45	3	4.84E-05	1.31E-04	2.7	2.6	2.35E-05
	6.48	3	4.87E-05	9.73E-05	2.0	2.0	1.73E-05
	6.43	7	4.37E-05	2.90E-04	6.6	6.2	5.77E-05
	6.43	7	4.51E-05	1.44E-04	3.2	3.1	2.77E-05
	6.49	7	4.32E-05	3.37E-04	7.8	7.3	6.78E-05
	6.37	16	4.44E-05	1.92E-04	4.3	4.1	3.76E-05
	6.22	16	4.37E-05	2.63E-04	6.0	5.7	5.23E-05
	6.43	16	4.71E-05	0.00E+00	0.0	0.0	0.00E+00
	6.34	71	4.97E-05	0.00E+00	0.0	0.0	0.00E+00
	6.34	71	4.84E-05	1.31E-04	2.7	2.6	2.35E-05
	6.35	71	4.87E-05	9.73E-05	2.0	2.0	1.73E-05
	6.35	99	4.83E-05	1.47E-04	3.0	2.9	2.64E-05
	6.33	99	4.69E-05	2.77E-04	5.9	5.6	5.12E-05
	6.34	99	4.97E-05	0.00E+00	0.0	0.0	0.00E+00
	6.36	127	4.66E-05	3.18E-04	6.8	6.4	5.92E-05
	6.36	127	4.75E-05	2.19E-04	4.6	4.4	3.99E-05
	6.36	127	4.75E-05	2.19E-04	4.6	4.4	4.00E-05

Mineral	pH	Time	Dissolved Pb (mol/L)	Sorbed Pb (mole/kg)	K_d (cm ³ /g)	Percent Sorbed	K_a (cm)
limestone not sterile	6.40	1	5.00E-05	0.00E+00	0.0	0.0	0.00E+00
	6.42	1	4.71E-05	6.78E-06	0.1	0.4	4.98E-06
	6.42	1	4.58E-05	5.51E-05	1.2	2.9	4.15E-05
	6.31	3	5.07E-05	0.00E+00	0.0	0.0	0.00E+00
	6.31	3	4.92E-05	1.95E-05	0.4	1.0	1.37E-05
	6.36	3	4.78E-05	7.61E-05	1.6	3.8	5.50E-05
	6.27	7	4.37E-05	1.16E-04	2.7	6.2	9.16E-05
	6.32	7	4.49E-05	6.75E-05	1.5	3.6	5.20E-05
	6.31	7	4.56E-05	3.86E-05	0.8	2.1	2.92E-05
	6.24	16	4.39E-05	1.03E-04	2.4	5.6	8.13E-05
	6.28	16	4.25E-05	1.61E-04	3.8	8.7	1.31E-04
	6.32	16	4.71E-05	0.00E+00	0.0	0.0	0.00E+00
	6.25	71	5.07E-05	0.00E+00	0.0	0.0	0.00E+00
	6.26	71	4.92E-05	1.95E-05	0.4	1.0	1.37E-05
	6.26	71	4.78E-05	7.61E-05	1.6	3.8	5.50E-05
	6.25	99	4.97E-05	0.00E+00	0.0	0.0	0.00E+00
	6.26	99	4.97E-05	0.00E+00	0.0	0.0	0.00E+00
	6.26	99	4.92E-05	1.95E-05	0.4	1.0	1.37E-05
	6.28	127	4.77E-05	8.19E-05	1.7	4.1	5.94E-05
	6.28	127	4.72E-05	9.95E-05	2.1	5.0	7.28E-05
6.27	127	4.78E-05	7.80E-05	1.6	3.9	5.64E-05	
bentonite sterile	6.56	1	4.80E-05	0.00E+00	0.0	0.0	0.00E+00
	6.57	1	4.46E-05	4.49E-04	10	4.8	4.02E-05
	6.57	1	4.80E-05	0.00E+00	0.0	0.0	0.00E+00
	6.46	3	4.92E-05	1.53E-04	3.1	1.5	1.25E-05
	6.50	3	4.92E-05	1.52E-04	3.1	1.5	1.24E-05
	6.53	3	4.97E-05	5.52E-05	1.1	0.6	4.45E-06
	6.55	7	4.85E-05	0.00E+00	0.0	0.0	0.00E+00
	6.53	7	4.92E-05	0.00E+00	0.0	0.0	0.00E+00
	6.53	7	4.80E-05	0.00E+00	0.0	0.0	0.00E+00
	6.56	16	4.97E-05	5.55E-05	1.1	0.6	4.47E-06
	6.57	16	4.92E-05	1.52E-04	3.1	1.5	1.24E-05
	6.56	16	4.97E-05	5.52E-05	1.1	0.6	4.45E-06
	6.50	64	5.17E-05	0.00E+00	0.0	0.0	0.00E+00
	6.52	64	5.12E-05	0.00E+00	0.0	0.0	0.00E+00
	6.51	64	5.02E-05	0.00E+00	0.0	0.0	0.00E+00
	6.49	93	4.86E-05	2.90E-04	6.0	2.9	2.39E-05
	6.49	93	4.86E-05	2.88E-04	5.9	2.9	2.38E-05
	6.50	93	4.86E-05	2.70E-04	5.5	2.7	2.22E-05
	6.53	121	4.87E-05	2.49E-04	5.1	2.5	2.05E-05
	6.54	121	4.92E-05	1.53E-04	3.1	1.5	1.24E-05

Mineral	pH	Time	Dissolved Pb (mol/L)	Sorbed Pb (mole/kg)	K_d (cm ³ /g)	Percent Sorbed	K_a (cm)
shale	6.50	1	4.71E-05	0.00E+00	0.0	0.0	0.00E+00
sterile	6.52	1	4.66E-05	3.21E-05	0.7	0.7	5.99E-06
	6.56	1	4.78E-05	0.00E+00	0.0	0.0	0.00E+00
	6.33	3	4.87E-05	1.25E-04	2.6	2.5	2.23E-05
	6.43	3	4.78E-05	2.22E-04	4.6	4.5	4.04E-05
	6.46	3	4.92E-05	7.63E-05	1.5	1.5	1.35E-05
	6.34	7	4.83E-05	0.00E+00	0.0	0.0	0.00E+00
	6.44	7	4.73E-05	7.21E-05	1.5	1.5	1.32E-05
	6.46	7	4.95E-05	0.00E+00	0.0	0.0	0.00E+00
	6.33	16	5.22E-05	0.00E+00	0.0	0.0	0.00E+00
	6.46	16	4.83E-05	1.69E-04	3.5	3.4	3.03E-05
	6.47	16	5.07E-05	0.00E+00	0.0	0.0	0.00E+00
	6.28	64	5.07E-05	0.00E+00	0.0	0.0	0.00E+00
	6.39	64	4.83E-05	1.73E-04	3.6	3.5	3.11E-05
	6.41	64	4.82E-05	1.83E-04	3.8	3.7	3.31E-05
	6.27	93	4.69E-05	3.10E-04	6.6	6.2	5.74E-05
	6.37	93	4.59E-05	4.07E-04	8.9	8.2	7.70E-05
	6.37	93	4.77E-05	2.27E-04	4.8	4.5	4.14E-05
	6.32	121	4.97E-05	2.76E-05	0.6	0.6	4.82E-06
	6.41	121	4.87E-05	1.25E-04	2.6	2.5	2.22E-05
	6.40	121	4.97E-05	2.76E-05	0.6	0.6	4.82E-06
limestone	6.52	1	4.71E-05	0.00E+00	0.0	0.0	0.00E+00
sterile	6.49	1	4.58E-05	4.18E-05	0.9	2.2	3.15E-05
	6.47	1	4.71E-05	0.00E+00	0.0	0.0	0.00E+00
	6.39	3	4.77E-05	9.09E-05	1.9	4.5	6.58E-05
	6.37	3	4.79E-05	8.51E-05	1.8	4.3	6.15E-05
	6.39	3	4.74E-05	1.03E-04	2.2	5.1	7.48E-05
	6.45	7	4.78E-05	9.59E-06	0.2	0.5	6.94E-06
	6.36	7	4.75E-05	1.93E-05	0.4	1.0	1.40E-05
	6.34	7	4.85E-05	0.00E+00	0.0	0.0	0.00E+00
	6.45	16	4.81E-05	7.53E-05	1.6	3.8	5.41E-05
	6.36	16	4.97E-05	1.10E-05	0.2	0.6	7.68E-06
	6.36	16	5.07E-05	0.00E+00	0.0	0.0	0.00E+00
	6.38	64	4.97E-05	1.10E-05	0.2	0.6	7.67E-06
	6.31	64	5.12E-05	0.00E+00	0.0	0.0	0.00E+00
	6.29	64	4.83E-05	6.94E-05	1.4	3.5	4.97E-05
	6.37	93	4.82E-05	7.34E-05	1.5	3.7	5.26E-05
	6.29	93	4.72E-05	1.10E-04	2.3	5.5	8.08E-05
	6.28	93	4.92E-05	3.06E-05	0.6	1.5	2.14E-05
	6.40	121	5.07E-05	0.00E+00	0.0	0.0	0.00E+00
	6.33	121	4.87E-05	5.00E-05	1.0	2.5	3.55E-05
	6.30	121	4.97E-05	1.11E-05	0.2	0.6	7.68E-06

Table A10: Uranium Sorption with Time in Brine

Mineral	pH	Time	Dissolved U (mol/L)	Sorbed U (mole/kg)	K_d (cm ³ /g)	Percent Sorbed	K_a (cm)
bentonite	6.52	1	7.52E-06	0.00E+00	0.0	0.0	0.00E+00
not sterile	6.52	1	7.52E-06	0.00E+00	0.0	0.0	0.00E+00
	6.53	1	7.02E-06	9.06E-05	13	6.1	5.17E-05
	6.42	3	7.64E-06	5.65E-05	7.4	3.6	2.96E-05
	6.52	3	7.64E-06	5.62E-05	7.4	3.6	2.95E-05
	6.54	3	7.64E-06	5.63E-05	7.4	3.6	2.95E-05
	6.53	7	6.18E-06	5.01E-05	8.1	3.9	3.25E-05
	6.51	7	6.32E-06	2.09E-05	3.3	1.6	1.32E-05
	6.50	16	6.15E-06	2.20E-04	36	15	1.43E-04
	6.53	16	6.09E-06	2.31E-04	38	16	1.52E-04
	6.53	16	7.08E-06	3.49E-05	4.9	2.4	1.97E-05
	6.51	71	6.36E-06	2.54E-04	40	17	1.60E-04
	6.52	71	6.36E-06	2.53E-04	40	17	1.59E-04
	6.53	71	6.79E-06	1.69E-04	25	11	9.96E-05
	6.52	99	6.79E-06	1.70E-04	25	11	9.99E-05
	6.51	99	6.36E-06	2.53E-04	40	17	1.59E-04
	6.50	99	6.79E-06	1.69E-04	25	11	9.96E-05
	6.53	127	5.94E-06	2.54E-04	43	18	1.71E-04
	6.54	127	6.36E-06	1.69E-04	26	12	1.06E-04
	6.55	127	5.94E-06	2.53E-04	43	18	1.71E-04
shale	6.49	1	7.39E-06	7.72E-06	1.0	1.0	9.07E-06
not sterile	6.50	1	7.04E-06	4.32E-05	6.1	5.8	5.34E-05
	6.50	1	6.93E-06	5.38E-05	7.8	7.2	6.74E-05
	6.44	3	7.64E-06	2.84E-05	3.7	3.6	3.22E-05
	6.45	3	7.21E-06	7.05E-05	10	8.9	8.48E-05
	6.48	3	7.64E-06	2.82E-05	3.7	3.6	3.21E-05
	6.43	7	5.90E-06	5.26E-05	8.9	8.2	7.74E-05
	6.43	7	5.92E-06	5.02E-05	8.5	7.8	7.36E-05
	6.49	7	5.92E-06	5.03E-05	8.5	7.8	7.38E-05
	6.37	16	5.80E-06	1.46E-04	25	20	2.19E-04
	6.22	16	5.90E-06	1.35E-04	23	19	1.98E-04
	6.43	16	6.45E-06	8.04E-05	12	11	1.08E-04
	6.34	71	5.94E-06	1.70E-04	29	22	2.49E-04
	6.34	71	6.36E-06	1.27E-04	20	17	1.73E-04
	6.35	71	5.94E-06	1.69E-04	29	22	2.48E-04
	6.35	99	5.94E-06	1.70E-04	29	22	2.49E-04
	6.33	99	5.94E-06	1.69E-04	28	22	2.47E-04
	6.34	99	6.36E-06	1.27E-04	20	17	1.73E-04
	6.36	127	5.52E-06	1.70E-04	31	24	2.68E-04
	6.36	127	5.52E-06	1.69E-04	31	24	2.66E-04
	6.36	127	5.52E-06	1.69E-04	31	24	2.67E-04

Mineral	pH	Time	Dissolved U (mol/L)	Sorbed U (mole/kg)	K_d (cm ³ /g)	Percent Sorbed	K_a (cm)
limestone not sterile	6.40	1	7.75E-06	0.00E+00	0.0	0.0	0.00E+00
	6.42	1	7.12E-06	1.40E-05	2.0	4.7	6.80E-05
	6.42	1	7.14E-06	1.32E-05	1.8	4.4	6.37E-05
	6.31	3	7.64E-06	1.13E-05	1.5	3.6	5.12E-05
	6.31	3	7.21E-06	2.83E-05	3.9	8.9	1.36E-04
	6.36	3	7.64E-06	1.13E-05	1.5	3.6	5.12E-05
	6.27	7	6.15E-06	1.09E-05	1.8	4.2	6.13E-05
	6.32	7	6.22E-06	8.40E-06	1.4	3.3	4.67E-05
	6.31	7	6.26E-06	6.72E-06	1.1	2.6	3.71E-05
	6.24	16	5.88E-06	5.49E-05	9.3	19	3.23E-04
	6.28	16	5.84E-06	5.66E-05	10	19	3.35E-04
	6.32	16	6.74E-06	2.04E-05	3.0	7.0	1.05E-04
	6.25	71	6.36E-06	5.09E-05	8.0	17	2.76E-04
	6.26	71	6.36E-06	5.09E-05	8.0	17	2.76E-04
	6.26	71	6.36E-06	5.09E-05	8.0	17	2.76E-04
	6.25	99	6.36E-06	5.09E-05	8.0	17	2.76E-04
	6.26	99	6.36E-06	5.09E-05	8.0	17	2.76E-04
	6.26	99	6.36E-06	5.09E-05	8.0	17	2.76E-04
	6.28	127	5.94E-06	5.09E-05	8.6	18	2.96E-04
	6.28	127	5.94E-06	5.09E-05	8.6	18	2.96E-04
6.27	127	5.94E-06	5.09E-05	8.6	18	2.96E-04	
bentonite sterile	6.56	1	7.21E-06	6.33E-05	8.8	4.2	3.52E-05
	6.57	1	6.62E-06	1.80E-04	27	12	1.09E-04
	6.57	1	7.25E-06	5.46E-05	7.5	3.6	3.02E-05
	6.46	3	7.21E-06	1.70E-04	24	11	9.46E-05
	6.50	3	7.21E-06	1.69E-04	23	11	9.38E-05
	6.53	3	7.21E-06	1.70E-04	24	11	9.42E-05
	6.55	7	6.60E-06	1.88E-04	28	12	1.14E-04
	6.53	7	6.83E-06	1.40E-04	21	9.3	8.22E-05
	6.53	7	6.66E-06	1.74E-04	26	12	1.05E-04
	6.56	16	6.79E-06	2.56E-04	38	16	1.51E-04
	6.57	16	7.21E-06	1.69E-04	23	11	9.38E-05
	6.56	16	6.79E-06	2.55E-04	38	16	1.50E-04
	6.50	64	6.36E-06	3.12E-04	49	20	1.97E-04
	6.52	64	6.36E-06	3.10E-04	49	20	1.95E-04
	6.51	64	6.36E-06	3.11E-04	49	20	1.96E-04
	6.49	93	6.36E-06	2.56E-04	40	17	1.61E-04
	6.49	93	6.36E-06	2.54E-04	40	17	1.59E-04
	6.50	93	6.36E-06	2.55E-04	40	17	1.60E-04
	6.52	121	6.36E-06	1.99E-04	31	13	1.25E-04
	6.53	121	5.94E-06	2.82E-04	47	19	1.90E-04
6.54	121	5.94E-06	2.83E-04	48	19	1.91E-04	

Mineral	pH	Time	Dissolved U (mol/L)	Sorbed U (mole/kg)	K_d (cm ³ /g)	Percent Sorbed	K_a (cm)
shale	6.50	1	7.14E-06	3.78E-05	5.3	5.0	4.59E-05
sterile	6.52	1	6.93E-06	5.87E-05	8.5	7.8	7.35E-05
	6.56	1	7.29E-06	2.31E-05	3.2	3.1	2.75E-05
	6.33	3	7.64E-06	4.24E-05	5.6	5.3	4.82E-05
	6.43	3	7.21E-06	8.47E-05	12	11	1.02E-04
	6.46	3	7.21E-06	8.48E-05	12	11	1.02E-04
	6.34	7	7.02E-06	5.14E-05	7.3	6.8	6.36E-05
	6.44	7	6.64E-06	8.91E-05	13	12	1.17E-04
	6.46	7	7.86E-06	0.00E+00	0.0	0.0	0.00E+00
	6.33	16	7.64E-06	4.24E-05	5.6	5.3	4.82E-05
	6.46	16	6.79E-06	1.27E-04	19	16	1.62E-04
	6.47	16	6.79E-06	1.27E-04	19	16	1.63E-04
	6.28	64	6.36E-06	1.55E-04	24	20	2.12E-04
	6.39	64	5.94E-06	1.98E-04	33	25	2.89E-04
	6.41	64	5.94E-06	1.98E-04	33	25	2.89E-04
	6.27	93	5.52E-06	2.12E-04	38	28	3.34E-04
	6.37	93	5.52E-06	2.12E-04	38	28	3.33E-04
	6.37	93	5.52E-06	2.12E-04	38	28	3.34E-04
	6.32	121	5.52E-06	1.84E-04	33	25	2.89E-04
	6.41	121	5.52E-06	1.83E-04	33	25	2.89E-04
	6.40	121	5.09E-06	2.26E-04	44	31	3.86E-04
limestone	6.52	1	7.08E-06	1.76E-05	2.5	5.9	8.61E-05
sterile	6.49	1	7.04E-06	1.93E-05	2.7	6.4	9.49E-05
	6.47	1	7.10E-06	1.68E-05	2.4	5.6	8.18E-05
	6.39	3	7.21E-06	3.39E-05	4.7	11	1.62E-04
	6.37	3	7.21E-06	3.39E-05	4.7	11	1.63E-04
	6.39	3	7.21E-06	3.40E-05	4.7	11	1.63E-04
	6.45	7	6.64E-06	3.57E-05	5.4	12	1.86E-04
	6.36	7	6.83E-06	2.81E-05	4.1	9.3	1.42E-04
	6.34	7	7.18E-06	1.39E-05	1.9	4.6	6.67E-05
	6.45	16	6.79E-06	5.09E-05	7.5	16	2.59E-04
	6.36	16	7.21E-06	3.39E-05	4.7	11	1.63E-04
	6.36	16	7.21E-06	3.40E-05	4.7	11	1.63E-04
	6.38	64	5.94E-06	7.91E-05	13	25	4.60E-04
	6.31	64	5.94E-06	7.92E-05	13	25	4.61E-04
	6.29	64	6.36E-06	6.22E-05	10	20	3.38E-04
	6.37	93	5.52E-06	8.48E-05	15	28	5.31E-04
	6.29	93	5.52E-06	8.49E-05	15	28	5.32E-04
	6.28	93	5.94E-06	6.79E-05	11	22	3.95E-04
	6.40	121	5.52E-06	7.35E-05	13	25	4.60E-04
	6.33	121	5.52E-06	7.35E-05	13	25	4.61E-04
	6.30	121	5.94E-06	5.66E-05	10	19	3.29E-04

Table A11: Lithium Sorption with Time in Dilute Reference Solution

Mineral	pH	Time (day)	Dissolved Li (mol/L)	Sorbed Li (mole/kg)	K_d (cm ³ /g)	Percent Sorbed	K_a (cm)
bentonite	8.12	0.042	2.01E-02	1.58E-02	0.8	0.4	3.15E-06
	8.20	0.042	2.00E-02	4.75E-02	2.4	1.2	9.52E-06
	8.11	1	1.82E-02	1.06E-01	5.8	2.8	2.32E-05
	8.14	1	1.73E-02	2.96E-01	17.1	7.9	6.85E-05
	8.13	1	1.85E-02	4.22E-02	2.3	1.1	9.11E-06
	8.19	2	1.98E-02	1.16E-01	5.9	2.8	2.35E-05
	8.21	2	2.00E-02	8.45E-02	4.2	2.1	1.69E-05
	8.20	2	1.92E-02	2.43E-01	12.7	6.0	5.07E-05
	8.15	7	2.01E-02	3.17E-02	1.6	0.8	6.30E-06
	8.15	7	1.95E-02	1.58E-01	8.1	3.9	3.25E-05
	8.17	7	1.97E-02	1.27E-01	6.4	3.1	2.58E-05
	8.16	14	2.01E-02	0.00E+00	0.0	0.0	0.00E+00
	8.17	14	1.84E-02	3.03E-01	16.5	7.6	6.60E-05
	8.13	14	1.92E-02	1.45E-01	7.5	3.6	3.02E-05
	8.13	63	2.04E-02	1.58E-01	7.7	3.7	3.10E-05
	8.14	63	1.98E-02	2.85E-01	14.4	6.7	5.76E-05
8.13	63	2.01E-02	2.22E-01	11.0	5.2	4.41E-05	
shale	8.05	0.042	2.03E-02	0.00E+00	0.0	0.0	0.00E+00
	8.03	0.042	2.04E-02	0.00E+00	0.0	0.0	0.00E+00
	8.07	1	1.79E-02	8.46E-02	4.7	4.5	4.10E-05
	8.05	1	1.84E-02	3.69E-02	2.0	2.0	1.74E-05
	8.13	2	1.93E-02	1.06E-01	5.5	5.2	4.75E-05
	8.11	2	2.03E-02	1.06E-02	0.5	0.5	4.52E-06
	8.08	7	2.00E-02	3.17E-02	1.6	1.6	1.38E-05
	8.10	7	2.06E-02	0.00E+00	0.0	0.0	0.00E+00
	8.09	14	2.08E-02	0.00E+00	0.0	0.0	0.00E+00
	8.09	14	2.17E-02	0.00E+00	0.0	0.0	0.00E+00
	8.05	63	2.01E-02	1.11E-01	5.5	5.2	4.79E-05
	8.02	63	2.12E-02	0.00E+00	0.0	0.0	0.00E+00

Mineral	pH	Time (day)	Dissolved Li (mol/L)	Sorbed Li (mole/kg)	K_d (cm ³ /g)	Percent Sorbed	K_a (cm)
limestone	8.08	0.042	1.92E-02	4.12E-02	2.1	5.1	7.42E-05
	8.05	0.042	1.85E-02	6.65E-02	3.6	8.2	1.24E-04
	8.14	0.042	1.97E-02	2.22E-02	1.1	2.7	3.90E-05
	8.11	1	1.85E-02	8.45E-03	0.5	1.1	1.57E-05
	8.04	1	1.81E-02	2.75E-02	1.5	3.7	5.25E-05
	8.06	1	1.93E-02	0.00E+00	0.0	0.0	0.00E+00
	8.16	2	1.97E-02	2.96E-02	1.5	3.6	5.20E-05
	8.14	7	2.08E-02	0.00E+00	0.0	0.0	0.00E+00
	8.11	7	2.03E-02	0.00E+00	0.0	0.0	0.00E+00
	8.12	7	2.06E-02	0.00E+00	0.0	0.0	0.00E+00
	8.09	14	2.12E-02	0.00E+00	0.0	0.0	0.00E+00
	8.13	14	1.93E-02	2.26E-02	1.2	2.8	4.04E-05
	8.09	14	2.11E-02	0.00E+00	0.0	0.0	0.00E+00
	8.14	63	2.14E-02	0.00E+00	0.0	0.0	0.00E+00
	8.08	63	2.08E-02	1.90E-02	0.9	2.2	3.16E-05
	8.10	63	2.14E-02	0.00E+00	0.0	0.0	0.00E+00

Table A12: Nickel Sorption with Time in Dilute Reference Solution

Mineral	pH	Time (day)	Dissolved Ni (mol/L)	Sorbed Ni (mole/kg)	K_d (cm ³ /g)	Percent Sorbed	K_a (cm)
bentonite	8.19	0.042	4.50E-05	1.21E-02	270	57	1.08E-03
	8.12	0.042	4.31E-05	1.25E-02	290	59	1.16E-03
	8.20	0.042	4.31E-05	1.25E-02	290	59	1.16E-03
	8.11	1	3.37E-05	1.17E-02	348	64	1.39E-03
	8.14	1	3.00E-05	1.25E-02	416	68	1.67E-03
	8.13	1	3.19E-05	1.21E-02	380	66	1.52E-03
	8.19	2	3.37E-05	1.44E-02	426	68	1.71E-03
	8.21	2	3.37E-05	1.44E-02	426	68	1.71E-03
	8.20	2	4.12E-05	1.29E-02	312	61	1.25E-03
	8.15	7	2.62E-05	1.48E-02	566	74	2.27E-03
	8.15	7	2.44E-05	1.52E-02	625	76	2.50E-03
	8.17	7	2.25E-05	1.56E-02	694	78	2.78E-03
	8.16	14	2.06E-05	1.70E-02	824	80	3.30E-03
	8.17	14	2.06E-05	1.70E-02	825	80	3.30E-03
	8.13	14	2.06E-05	1.70E-02	824	80	3.30E-03
	8.13	63	9.37E-06	1.85E-02	1971	91	7.89E-03
	8.14	63	7.50E-06	1.89E-02	2515	93	1.01E-02
	8.13	63	7.50E-06	1.88E-02	2513	93	1.01E-02
shale	8.05	0.042	7.31E-05	3.26E-03	45	31	3.88E-04
	8.03	0.042	7.68E-05	2.88E-03	38	27	3.26E-04
	8.07	1	4.31E-05	4.94E-03	115	53	9.95E-04
	8.05	1	4.31E-05	4.93E-03	114	53	9.93E-04
	8.13	2	3.56E-05	7.01E-03	197	66	1.71E-03
	8.11	2	3.75E-05	6.81E-03	182	65	1.58E-03
	8.08	7	1.69E-05	8.37E-03	496	83	4.31E-03
	8.10	7	1.69E-05	8.36E-03	496	83	4.30E-03
	8.09	14	9.37E-06	9.64E-03	1028	91	8.93E-03
	8.09	14	9.37E-06	9.62E-03	1027	91	8.92E-03
	8.05	63	3.56E-06	9.83E-03	2761	97	2.40E-02
	8.02	63	3.56E-06	9.81E-03	2757	97	2.39E-02
	8.04	63	3.56E-06	9.83E-03	2760	97	2.40E-02

Mineral	pH	Time (day)	Dissolved Ni (mol/L)	Sorbed Ni (mole/kg)	K_d (cm ³ /g)	Percent Sorbed	K_a (cm)
limestone	8.08	0.042	8.62E-05	7.79E-04	9	18	3.12E-04
	8.05	0.042	8.81E-05	7.05E-04	8	17	2.77E-04
	8.14	0.042	8.81E-05	7.05E-04	8	17	2.77E-04
	8.11	1	6.18E-05	1.22E-03	20	33	6.84E-04
	8.04	1	6.00E-05	1.30E-03	22	35	7.48E-04
	8.06	1	6.18E-05	1.22E-03	20	33	6.84E-04
	8.16	2	5.25E-05	2.13E-03	41	50	1.40E-03
	8.14	7	4.31E-05	2.30E-03	53	57	1.84E-03
	8.11	7	3.94E-05	2.45E-03	62	61	2.15E-03
	8.12	7	4.31E-05	2.30E-03	53	57	1.84E-03
	8.09	14	3.37E-05	2.88E-03	85	68	2.95E-03
	8.13	14	3.19E-05	2.95E-03	93	70	3.20E-03
	8.09	14	3.37E-05	2.88E-03	85	68	2.95E-03
	8.14	63	9.37E-06	3.70E-03	394	91	1.36E-02
	8.08	63	9.37E-06	3.70E-03	395	91	1.36E-02
	8.10	63	1.12E-05	3.62E-03	322	89	1.11E-02

Table A13: Copper Sorption with Time in Dilute Reference Solution

Mineral	pH	Time (day)	Dissolved Cu (mol/L)	Sorbed Cu (mole/kg)	K_d (cm ³ /g)	Percent Sorbed	K_a (cm)
bentonite	8.19	0.042	1.56E-06	1.46E-03	940	82	3.76E-03
	8.12	0.042	1.56E-06	1.46E-03	940	82	3.76E-03
	8.20	0.042	1.56E-06	1.46E-03	940	82	3.76E-03
	8.11	1	1.38E-06	1.26E-03	907	82	3.63E-03
	8.14	1	1.21E-06	1.29E-03	1066	84	4.27E-03
	8.13	1	1.38E-06	1.26E-03	907	82	3.63E-03
	8.19	2	1.38E-06	1.66E-03	1198	86	4.80E-03
	8.21	2	1.56E-06	1.63E-03	1044	84	4.18E-03
	8.20	2	1.38E-06	1.66E-03	1198	86	4.80E-03
	8.15	7	1.38E-06	1.69E-03	1223	86	4.90E-03
	8.15	7	1.38E-06	1.70E-03	1224	86	4.90E-03
	8.17	7	1.38E-06	1.69E-03	1223	86	4.90E-03
	8.17	14	5.19E-07	1.66E-03	3198	94	1.28E-02
	8.13	14	5.19E-07	1.66E-03	3196	94	1.28E-02
	8.13	63	3.46E-07	1.04E-03	2996	94	1.20E-02
	8.14	63	3.46E-07	1.04E-03	2998	94	1.20E-02
	8.13	63	3.46E-07	1.04E-03	2996	94	1.20E-02
	shale	8.05	0.042	1.56E-06	7.33E-04	471	82
8.03		0.042	1.73E-06	7.15E-04	413	81	3.59E-03
8.07		0.042	1.38E-06	7.50E-04	542	84	4.70E-03
8.07		1	1.38E-06	6.29E-04	454	82	3.95E-03
8.05		1	1.38E-06	6.28E-04	454	82	3.94E-03
8.07		1	1.38E-06	6.29E-04	454	82	3.94E-03
8.13		2	1.56E-06	8.14E-04	522	84	4.54E-03
8.11		2	1.38E-06	8.30E-04	599	86	5.20E-03
8.15		2	1.38E-06	8.31E-04	600	86	5.21E-03
8.08		7	1.38E-06	8.49E-04	613	86	5.32E-03
8.10		7	1.38E-06	8.47E-04	612	86	5.31E-03
8.12		7	1.38E-06	8.48E-04	613	86	5.32E-03
8.09		14	6.92E-07	8.14E-04	1175	92	1.02E-02
8.09		14	5.19E-07	8.30E-04	1598	94	1.39E-02
8.13		14	5.19E-07	8.31E-04	1600	94	1.39E-02
8.05		63	3.46E-07	5.19E-04	1501	94	1.30E-02
8.02		63	3.46E-07	5.19E-04	1498	94	1.30E-02
8.04		63	3.46E-07	5.19E-04	1500	94	1.30E-02

Mineral	pH	Time (day)	Dissolved Cu (mol/L)	Sorbed Cu (mole/kg)	K_d (cm ³ /g)	Percent Sorbed	K_a (cm)
limestone	8.08	0.042	1.90E-06	2.79E-04	147	79	5.06E-03
	8.05	0.042	2.25E-06	2.65E-04	118	75	4.07E-03
	8.14	0.042	1.90E-06	2.79E-04	147	79	5.07E-03
	8.11	1	1.56E-06	2.44E-04	157	80	5.42E-03
	8.04	1	1.38E-06	2.52E-04	182	82	6.28E-03
	8.06	1	1.38E-06	2.52E-04	182	82	6.28E-03
	8.15	2	1.56E-06	3.25E-04	209	84	7.21E-03
	8.15	2	1.38E-06	3.32E-04	240	86	8.29E-03
	8.16	2	1.56E-06	3.25E-04	209	84	7.22E-03
	8.14	7	1.38E-06	3.39E-04	245	86	8.46E-03
	8.11	7	1.38E-06	3.39E-04	245	86	8.46E-03
	8.12	7	1.38E-06	3.39E-04	245	86	8.47E-03
	8.09	14	5.19E-07	3.32E-04	640	94	2.21E-02
	8.13	14	6.92E-07	3.25E-04	470	92	1.62E-02
	8.09	14	5.19E-07	3.32E-04	640	94	2.21E-02
	8.14	63	3.46E-07	2.08E-04	600	94	2.07E-02
	8.08	63	3.46E-07	2.08E-04	600	94	2.07E-02
	8.10	63	3.46E-07	2.08E-04	600	94	2.07E-02

Table A14: Lead Sorption with Time in Dilute Reference Solution

Mineral	pH	Time	Dissolved Pb (mol/L)	Sorbed Pb (mole/kg)	K_d (cm ³ /g)	Percent Sorbed	K_a (cm)
bentonite	8.19	0.042	2.18E-07	7.85E-05	361	64	1.44E-03
	8.12	0.042	1.96E-07	8.28E-05	421	68	1.69E-03
	8.20	0.042	2.02E-07	8.17E-05	405	67	1.62E-03
	8.11	1	2.07E-07	7.32E-05	353	64	1.41E-03
	8.14	1	2.02E-07	7.43E-05	368	65	1.47E-03
	8.13	1	1.86E-07	7.74E-05	417	68	1.67E-03
	8.19	2	1.96E-07	9.38E-05	477	71	1.91E-03
	8.21	2	1.96E-07	9.38E-05	478	71	1.91E-03
	8.20	2	2.02E-07	9.27E-05	460	70	1.84E-03
	8.15	7	1.96E-07	0.000104	529	73	2.12E-03
	8.15	7	1.91E-07	0.000105	550	73	2.20E-03
	8.17	7	1.96E-07	0.000104	529	73	2.12E-03
	8.16	14	1.65E-07	0.000103	623	76	2.49E-03
	8.17	14	1.65E-07	0.000103	623	76	2.49E-03
	8.13	14	1.65E-07	0.000103	623	76	2.49E-03
	8.13	63	2.71E-07	6.33E-05	234	54	9.35E-04
	8.14	63	1.54E-07	8.67E-05	563	74	2.25E-03
	8.13	63	1.49E-07	8.77E-05	590	75	2.36E-03
shale	8.05	0.042	1.96E-07	4.14E-05	211	68	1.83E-03
	8.03	0.042	1.96E-07	4.14E-05	211	68	1.83E-03
	8.07	0.042	1.91E-07	4.19E-05	219	69	1.91E-03
	8.07	1	2.07E-07	3.66E-05	177	64	1.54E-03
	8.05	1	2.02E-07	3.71E-05	184	65	1.60E-03
	8.07	1	1.96E-07	3.77E-05	192	66	1.67E-03
	8.13	2	1.96E-07	4.7E-05	239	71	2.08E-03
	8.11	2	1.91E-07	4.74E-05	248	71	2.16E-03
	8.15	2	1.91E-07	4.75E-05	248	71	2.16E-03
	8.08	7	2.02E-07	5.15E-05	255	72	2.22E-03
	8.10	7	1.96E-07	5.2E-05	265	73	2.30E-03
	8.12	7	1.96E-07	5.2E-05	265	73	2.30E-03
	8.09	14	1.70E-07	5.08E-05	299	75	2.60E-03
	8.09	14	1.81E-07	4.97E-05	275	73	2.39E-03
	8.13	14	1.65E-07	5.13E-05	312	76	2.71E-03
	8.05	63	1.54E-07	4.34E-05	282	74	2.45E-03
	8.02	63	1.49E-07	4.38E-05	295	75	2.56E-03
	8.04	63	1.49E-07	4.39E-05	295	75	2.56E-03

Mineral	pH	Time	Dissolved Pb (mol/L)	Sorbed Pb (mole/kg)	K_d (cm ³ /g)	Percent Sorbed	K_a (cm)
limestone	8.08	0.042	2.02E-07	1.63E-05	81	67	2.80E-03
	8.05	0.042	2.02E-07	1.63E-05	81	67	2.80E-03
	8.14	0.042	2.02E-07	1.64E-05	81	67	2.80E-03
	8.11	1	2.12E-07	1.44E-05	68	63	2.35E-03
	8.04	1	2.07E-07	1.46E-05	71	64	2.44E-03
	8.06	1	1.96E-07	1.51E-05	77	66	2.65E-03
	8.15	2	2.92E-07	1.5E-05	51	56	1.77E-03
	8.15	2	2.02E-07	1.86E-05	92	70	3.18E-03
	8.16	2	1.96E-07	1.88E-05	96	71	3.30E-03
	8.14	7	1.96E-07	2.08E-05	106	73	3.66E-03
	8.11	7	2.12E-07	2.02E-05	95	70	3.28E-03
	8.12	7	1.96E-07	2.08E-05	106	73	3.66E-03
	8.09	14	1.65E-07	2.05E-05	125	76	4.31E-03
	8.13	14	1.65E-07	2.05E-05	125	76	4.31E-03
	8.09	14	2.44E-07	1.73E-05	71	64	2.45E-03
	8.14	63	1.49E-07	1.75E-05	118	75	4.08E-03
	8.08	63	1.65E-07	1.69E-05	103	72	3.55E-03
	8.10	63	1.65E-07	1.69E-05	103	72	3.55E-03

Table A15: Uranium Sorption with Time in Dilute Reference Solution

Mineral	pH	Time	Dissolved U (mol/L)	Sorbed U (mole/kg)	K_d (cm ³ /g)	Percent Sorbed	K_a (cm)
bentonite	8.19	0.042	7.58E-06	1.14E-04	15	7	6.02E-05
	8.12	0.042	7.21E-06	1.88E-04	26	12	1.04E-04
	8.20	0.042	7.16E-06	1.97E-04	28	12	1.10E-04
	8.11	1	6.79E-06	2.74E-04	40	17	1.61E-04
	8.14	1	6.65E-06	3.02E-04	45	18	1.81E-04
	8.13	1	6.61E-06	3.11E-04	47	19	1.88E-04
	8.19	2	6.75E-06	2.80E-04	42	17	1.66E-04
	8.21	2	6.75E-06	2.80E-04	42	17	1.66E-04
	8.20	2	6.24E-06	3.82E-04	61	23	2.45E-04
	8.15	7	6.19E-06	3.02E-04	49	20	1.95E-04
	8.15	7	5.96E-06	3.48E-04	58	23	2.34E-04
	8.17	7	5.78E-06	3.85E-04	67	25	2.67E-04
	8.16	14	6.01E-06	4.15E-04	69	26	2.77E-04
	8.17	14	6.01E-06	4.16E-04	69	26	2.77E-04
	8.13	14	5.92E-06	4.34E-04	73	27	2.94E-04
	8.13	63	6.15E-06	2.65E-04	43	18	1.72E-04
	8.14	63	6.01E-06	2.92E-04	49	20	1.95E-04
	8.13	63	5.82E-06	3.29E-04	57	22	2.26E-04
shale	8.05	0.042	6.70E-06	1.45E-04	22	18	1.88E-04
	8.03	0.042	6.98E-06	1.17E-04	17	14	1.46E-04
	8.07	1	5.36E-06	2.80E-04	52	34	4.54E-04
	8.05	1	5.55E-06	2.62E-04	47	32	4.10E-04
	8.13	2	4.76E-06	3.39E-04	71	42	6.19E-04
	8.11	2	4.76E-06	3.39E-04	71	42	6.18E-04
	8.08	7	3.47E-06	4.24E-04	122	55	1.06E-03
	8.10	7	3.47E-06	4.23E-04	122	55	1.06E-03
	8.09	14	3.19E-06	4.90E-04	154	61	1.33E-03
	8.09	14	3.28E-06	4.80E-04	146	59	1.27E-03
	8.05	63	3.10E-06	4.38E-04	141	59	1.23E-03
	8.02	63	3.19E-06	4.28E-04	134	57	1.16E-03

Mineral	pH	Time	Dissolved U (mol/L)	Sorbed U (mole/kg)	K_d (cm ³ /g)	Percent Sorbed	K_a (cm)
limestone	8.08	0.042	7.39E-06	3.02E-05	4	9	1.41E-04
	8.05	0.042	7.02E-06	4.50E-05	6	14	2.21E-04
	8.14	0.042	7.35E-06	3.21E-05	4	10	1.51E-04
	8.11	1	6.05E-06	8.44E-05	14	26	4.82E-04
	8.04	1	5.78E-06	9.55E-05	17	29	5.71E-04
	8.06	1	6.10E-06	8.26E-05	14	25	4.68E-04
	8.16	2	5.59E-06	1.02E-04	18	31	6.32E-04
	8.14	7	4.02E-06	1.47E-04	37	48	1.26E-03
	8.11	7	3.70E-06	1.60E-04	43	52	1.50E-03
	8.12	7	3.97E-06	1.49E-04	38	48	1.30E-03
	8.09	14	3.51E-06	1.83E-04	52	57	1.80E-03
	8.13	14	3.23E-06	1.94E-04	60	60	2.07E-03
	8.09	14	3.51E-06	1.83E-04	52	57	1.80E-03
	8.14	63	2.31E-06	2.06E-04	89	69	3.08E-03
	8.08	63	2.26E-06	2.08E-04	92	70	3.18E-03
	8.10	63	2.45E-06	2.01E-04	82	67	2.83E-03

Table A16: Lithium Sorption with pH in Reference Brine Solution

Mineral	pH	Time (day)	Dissolved Li (mol/L)	Sorbed Li (mole/kg)	K_d (cm ³ /g)	Percent Sorbed	K_a (cm)
bentonite	4.99	0.042	2.23E-02	0.00E+00	0.0	0.0	0.00E+00
	5.01	0.042	2.17E-02	5.04E-02	2.3	2.3	9.31E-06
	6.01	0.042	1.96E-02	1.04E-01	5.3	5.3	2.11E-05
	6.01	0.042	1.96E-02	1.04E-01	5.3	5.3	2.13E-05
	6.59	0.042	1.91E-02	1.19E-01	6.2	6.1	2.50E-05
	6.60	0.042	2.04E-02	0.00E+00	0.0	0.0	0.00E+00
	7.18	0.042	2.33E-02	7.15E-02	3.1	3.0	1.23E-05
	7.18	0.042	2.34E-02	5.81E-02	2.5	2.4	9.93E-06
	7.61	0.042	2.04E-02	0.00E+00	0.0	0.0	0.00E+00
	7.75	0.042	2.23E-02	4.28E-02	1.9	1.9	7.69E-06
	7.96	0.042	2.90E-02	1.23E-01	4.3	4.3	1.70E-05
shale	5.80	0.042	2.23E-02	0.00E+00	0.0	0.0	0.00E+00
	5.83	0.042	2.18E-02	1.82E-02	0.8	1.6	7.23E-06
	5.99	0.042	2.01E-02	3.23E-02	1.6	3.2	1.40E-05
	5.99	0.042	2.08E-02	0.00E+00	0.0	0.0	0.00E+00
	6.53	0.042	2.04E-02	0.00E+00	0.0	0.0	0.00E+00
	6.54	0.042	2.12E-02	0.00E+00	0.0	0.0	0.00E+00
	7.15	0.042	2.37E-02	1.44E-02	0.6	1.2	5.27E-06
	7.16	0.042	2.36E-02	2.14E-02	0.9	1.8	7.89E-06
	7.64	0.042	2.08E-02	0.00E+00	0.0	0.0	0.00E+00
	7.70	0.042	2.14E-02	6.48E-02	3.0	5.8	2.63E-05
7.72	0.042	2.23E-02	2.18E-02	1.0	1.9	8.51E-06	
limestone	5.81	0.042	2.20E-02	4.36E-03	0.2	1.0	6.86E-06
	5.82	0.042	2.30E-02	0.00E+00	0.0	0.0	0.00E+00
	5.99	0.042	2.05E-02	4.36E-03	0.2	1.1	7.35E-06
	6.00	0.042	1.92E-02	3.05E-02	1.6	7.4	5.49E-05
	6.43	0.042	2.05E-02	0.00E+00	0.0	0.0	0.00E+00
	6.44	0.042	1.92E-02	2.19E-02	1.1	5.4	3.93E-05
	7.18	0.042	2.31E-02	1.73E-02	0.7	3.6	2.59E-05
	7.19	0.042	2.40E-02	0.00E+00	0.0	0.0	0.00E+00
	7.77	0.042	1.92E-02	0.00E+00	0.0	0.0	0.00E+00
	7.78	0.042	2.08E-02	0.00E+00	0.0	0.0	0.00E+00
	7.80	0.042	2.11E-02	3.18E-02	1.5	7.1	5.21E-05
	7.99	0.042	2.81E-02	4.31E-02	1.5	7.2	5.31E-05

Table A17: Nickel Sorption with pH in Reference Brine Solution

Mineral	pH	Time (day)	Dissolved Ni (mol/L)	Sorbed Ni (mole/kg)	K_d (cm ³ /g)	Percent Sorbed	K_a (cm)
bentonite	4.99	0.042	1.03E-04	0.00E+00	0.0	0.0	0.00E+00
	5.01	0.042	1.03E-04	0.00E+00	0.0	0.0	0.00E+00
	6.01	0.042	8.60E-05	0.00E+00	0.0	0.0	0.00E+00
	6.01	0.042	8.60E-05	0.00E+00	0.0	0.0	0.00E+00
	6.59	0.042	8.60E-05	0.00E+00	0.0	0.0	0.00E+00
	6.60	0.042	8.60E-05	0.00E+00	0.0	0.0	0.00E+00
	7.18	0.042	1.03E-04	0.00E+00	0.0	0.0	0.00E+00
	7.18	0.042	1.03E-04	0.00E+00	0.0	0.0	0.00E+00
	7.61	0.042	8.60E-05	0.00E+00	0.0	0.0	0.00E+00
	7.75	0.042	8.60E-05	0.00E+00	0.0	0.0	0.00E+00
	7.96	0.042	1.03E-04	1.08E-03	10.5	10.0	4.18E-05
shale	5.80	0.042	1.03E-04	0.00E+00	0.0	0.0	0.00E+00
	5.83	0.042	1.03E-04	0.00E+00	0.0	0.0	0.00E+00
	5.99	0.042	8.60E-05	0.00E+00	0.0	0.0	0.00E+00
	5.99	0.042	8.60E-05	0.00E+00	0.0	0.0	0.00E+00
	6.53	0.042	8.60E-05	0.00E+00	0.0	0.0	0.00E+00
	6.54	0.042	8.60E-05	0.00E+00	0.0	0.0	0.00E+00
	7.15	0.042	1.03E-04	0.00E+00	0.0	0.0	0.00E+00
	7.16	0.042	1.03E-04	0.00E+00	0.0	0.0	0.00E+00
	7.64	0.042	8.60E-05	0.00E+00	0.0	0.0	0.00E+00
	7.70	0.042	8.60E-05	0.00E+00	0.0	0.0	0.00E+00
	7.72	0.042	8.60E-05	0.00E+00	0.0	0.0	0.00E+00
limestone	5.81	0.042	1.03E-04	0.00E+00	0.0	0.0	0.00E+00
	5.82	0.042	1.03E-04	0.00E+00	0.0	0.0	0.00E+00
	5.99	0.042	8.60E-05	0.00E+00	0.0	0.0	0.00E+00
	6.00	0.042	8.60E-05	0.00E+00	0.0	0.0	0.00E+00
	6.43	0.042	8.60E-05	0.00E+00	0.0	0.0	0.00E+00
	6.44	0.042	8.60E-05	0.00E+00	0.0	0.0	0.00E+00
	7.18	0.042	1.03E-04	0.00E+00	0.0	0.0	0.00E+00
	7.19	0.042	1.03E-04	0.00E+00	0.0	0.0	0.00E+00
	7.77	0.042	8.60E-05	0.00E+00	0.0	0.0	0.00E+00
	7.78	0.042	8.60E-05	0.00E+00	0.0	0.0	0.00E+00
	7.80	0.042	8.60E-05	0.00E+00	0.0	0.0	0.00E+00
	7.99	0.042	1.03E-04	2.27E-04	2.2	10	7.58E-05

Table A18: Copper Sorption with pH in Reference Brine Solution

Mineral	pH	Time (day)	Dissolved Cu (mol/L)	Sorbed Cu (mole/kg)	K_d (cm ³ /g)	Percent Sorbed	K_a (cm)
bentonite	4.99	0.042	1.11E-05	1.58E-04	14	13	5.69E-05
	5.01	0.042	9.54E-06	3.15E-04	33	25	1.32E-04
	6.01	0.042	9.54E-06	3.02E-04	32	25	1.27E-04
	6.01	0.042	9.54E-06	3.04E-04	32	25	1.28E-04
	6.59	0.042	7.95E-06	3.06E-04	38	29	1.54E-04
	7.18	0.042	1.27E-05	0.00E+00	0	0	0.00E+00
	7.18	0.042	1.11E-05	0.00E+00	0	0	0.00E+00
	7.61	0.042	7.95E-06	0.00E+00	0	0	0.00E+00
	7.75	0.042	6.36E-06	4.67E-04	73	43	2.94E-04
	7.96	0.042	9.54E-06	4.98E-04	52	36	2.09E-04
shale	5.80	0.042	9.54E-06	1.58E-04	17	25	1.44E-04
	5.83	0.042	9.54E-06	1.59E-04	17	25	1.45E-04
	5.99	0.042	9.54E-06	1.57E-04	16	25	1.43E-04
	5.99	0.042	1.11E-05	7.94E-05	7.1	13	6.19E-05
	6.53	0.042	7.95E-06	1.59E-04	20	29	1.73E-04
	7.70	0.042	7.95E-06	1.57E-04	20	29	1.72E-04
	7.72	0.042	7.95E-06	1.59E-04	20	29	1.74E-04
limestone	5.81	0.042	9.54E-06	6.35E-05	6.7	25	2.30E-04
	5.82	0.042	9.54E-06	6.32E-05	6.6	25	2.29E-04
	5.99	0.042	1.11E-05	3.18E-05	2.9	13	9.87E-05
	6.00	0.042	1.11E-05	3.17E-05	2.9	13	9.86E-05
	6.43	0.042	9.54E-06	3.16E-05	3.3	14	1.14E-04
	6.44	0.042	9.54E-06	3.18E-05	3.3	14	1.15E-04
	7.77	0.042	6.36E-06	3.14E-05	4.9	20	1.71E-04
	7.80	0.042	7.95E-06	6.32E-05	7.9	29	2.75E-04
	7.99	0.042	9.54E-06	1.05E-04	11.0	36	3.79E-04

Table A19: Lead Sorption with pH in Reference Brine Solution

Mineral	pH	Time	Dissolved Pb (mol/L)	Sorbed Pb (mole/kg)	K_d (cm ³ /g)	Percent Sorbed	K_a (cm)
bentonite	4.99	0.042	4.84E-05	2.43E-05	0.5	0.5	2.01E-06
	5.01	0.042	4.68E-05	1.79E-04	3.8	3.7	1.53E-05
	6.01	0.042	4.44E-05	3.29E-04	7.4	7.2	2.97E-05
	6.01	0.042	4.55E-05	2.28E-04	5.0	5.0	2.01E-05
	6.59	0.042	4.46E-05	1.87E-04	4.2	4.2	1.68E-05
	6.6	0.042	4.37E-05	2.74E-04	6.3	6.1	2.52E-05
	7.18	0.042	5.18E-05	0.00E+00	0.0	0.0	0.00E+00
	7.18	0.042	5.13E-05	4.86E-05	0.9	0.9	3.80E-06
	7.61	0.042	4.28E-05	0.00E+00	0.0	0.0	0.00E+00
	7.75	0.042	4.73E-05	4.77E-06	0.1	0.1	4.04E-07
	7.96	0.042	6.25E-05	6.41E-05	1.0	1.1	4.10E-06
shale	5.8	0.042	4.73E-05	6.31E-05	1.3	2.6	1.16E-05
	5.83	0.042	4.73E-05	6.33E-05	1.3	2.6	1.16E-05
	5.99	0.042	4.79E-05	0.00E+00	0.0	0.0	0.00E+00
	5.99	0.042	4.79E-05	0.00E+00	0.0	0.0	0.00E+00
	6.53	0.042	4.61E-05	1.95E-05	0.4	0.8	3.67E-06
	6.54	0.042	4.70E-05	0.00E+00	0.0	0.0	0.00E+00
	7.15	0.042	5.03E-05	7.24E-05	1.4	2.8	1.25E-05
	7.16	0.042	5.08E-05	4.78E-05	0.9	1.9	8.17E-06
	7.64	0.042	4.30E-05	0.00E+00	0.0	0.0	0.00E+00
	7.7	0.042	4.44E-05	1.49E-04	3.4	6.4	2.93E-05
	7.72	0.042	4.57E-05	8.53E-05	1.9	3.6	1.62E-05
limestone	5.81	0.042	4.79E-05	1.46E-05	0.3	1.5	1.05E-05
	5.82	0.042	4.88E-05	0.00E+00	0.0	0.0	0.00E+00
	5.99	0.042	4.88E-05	0.00E+00	0.0	0.0	0.00E+00
	6	0.042	4.66E-05	2.43E-05	0.5	2.5	1.80E-05
	6.43	0.042	4.56E-05	1.84E-05	0.4	2.0	1.40E-05
	6.44	0.042	4.53E-05	2.44E-05	0.5	2.6	1.86E-05
	7.18	0.042	5.08E-05	1.93E-05	0.4	1.9	1.32E-05
	7.19	0.042	5.23E-05	0.00E+00	0.0	0.0	0.00E+00
	7.77	0.042	4.10E-05	0.00E+00	0.0	0.0	0.00E+00
	7.78	0.042	4.45E-05	0.00E+00	0.0	0.0	0.00E+00
	7.8	0.042	4.45E-05	5.81E-05	1.3	6.2	4.52E-05
7.99	0.042	5.86E-05	9.05E-05	1.5	7.3	5.34E-05	

Table A20: Uranium Sorption with pH in Reference Brine Solution

Mineral	pH	Time	Dissolved U (mol/L)	Sorbed U (mole/kg)	K_d (cm ³ /g)	Percent Sorbed	K_a (cm)
bentonite	4.99	0.042	6.36E-06	1.69E-04	27	21	1.06E-04
	5.01	0.042	5.94E-06	2.10E-04	35	26	1.42E-04
	6.01	0.042	7.64E-06	4.03E-05	5.3	5.3	2.11E-05
	6.01	0.042	7.64E-06	4.06E-05	5.3	5.3	2.13E-05
	6.59	0.042	7.21E-06	8.16E-05	11	11	4.53E-05
	6.6	0.042	7.64E-06	4.12E-05	5.4	5.3	2.16E-05
	7.18	0.042	7.21E-06	0.00E+00	0.0	0.0	0.00E+00
	7.18	0.042	7.21E-06	0.00E+00	0.0	0.0	0.00E+00
	7.61	0.042	2.55E-06	0.00E+00	0.0	0.0	0.00E+00
	7.75	0.042	2.55E-06	0.00E+00	0.0	0.0	0.00E+00
	7.96	0.042	2.55E-06	7.98E-05	31	25	1.26E-04
shale	5.8	0.042	7.64E-06	2.11E-05	2.8	5.3	2.40E-05
	5.83	0.042	8.06E-06	0.00E+00	0.0	0.0	0.00E+00
	5.99	0.042	8.06E-06	0.00E+00	0.0	0.0	0.00E+00
	5.99	0.042	8.49E-06	0.00E+00	0.0	0.0	0.00E+00
	6.53	0.042	7.64E-06	2.12E-05	2.8	5.3	2.41E-05
	6.54	0.042	8.06E-06	0.00E+00	0.0	0.0	0.00E+00
	7.15	0.042	6.79E-06	1.04E-05	1.5	3.0	1.33E-05
	7.16	0.042	6.79E-06	1.03E-05	1.5	3.0	1.32E-05
	7.64	0.042	1.70E-06	2.11E-05	12	20	1.08E-04
	7.7	0.042	1.27E-06	6.30E-05	49	50	4.29E-04
7.72	0.042	1.27E-06	6.36E-05	50	50	4.34E-04	
limestone	5.81	0.042	8.06E-06	0.00E+00	0.0	0.0	0.00E+00
	5.82	0.042	8.06E-06	0.00E+00	0.0	0.0	0.00E+00
	5.99	0.042	8.49E-06	0.00E+00	0.0	0.0	0.00E+00
	6	0.042	8.06E-06	0.00E+00	0.0	0.0	0.00E+00
	6.43	0.042	8.06E-06	0.00E+00	0.0	0.0	0.00E+00
	6.44	0.042	7.64E-06	8.50E-06	1.1	5.3	3.84E-05
	7.18	0.042	5.94E-06	2.10E-05	3.5	15	1.22E-04
	7.19	0.042	5.94E-06	2.09E-05	3.5	15	1.22E-04
	7.77	0.042	4.24E-07	3.35E-05	79	80	2.73E-03
	7.78	0.042	4.24E-07	3.39E-05	80	80	2.76E-03
	7.8	0.042	8.49E-07	3.37E-05	40	67	1.37E-03
	7.99	0.042	8.49E-07	5.03E-05	59	75	2.05E-03

Table A21: Lithium Diffusion Data For Figure 26

Time (day)	C/C₀	Integrated Mass Li (mol)	Used in Trend Plot
1	0.0000	0	
6	0.0070	2.36E-05	
10	0.0070	2.43E-05	
22	0.0070	2.51E-05	
38	0.0140	4.91E-05	
57	0.0140	5.06E-05	
63	0.0140	5.20E-05	
65	0.0140	5.35E-05	
70	0.0140	5.50E-05	
84	0.0209	7.97E-05	yes
90	0.0209	8.19E-05	yes
100	0.0278	1.07E-04	yes
104	0.0209	8.70E-05	yes
111	0.0278	1.12E-04	yes
120	0.0278	1.15E-04	yes
132	0.0347	1.42E-04	yes
139	0.0347	1.45E-04	yes
141	0.0278	1.26E-04	yes

Table A22: Trace Element Diffusion Profiles

Sample	mid point Distance From Tracer (mm)	Corrected for Background Concentration				
		Li (mol/kg)	Ni (mol/kg)	Cu (mol/kg)	Pb (mol/kg)	U (mol/kg)
DS1S	0.040	1.87E-03	3.92E-04	6.36E-04	9.09E-05	5.54E-05
DS2S	0.128	1.56E-03	2.86E-04	1.47E-04	5.58E-05	5.09E-05
DS3S	0.227	1.65E-03	2.68E-04	1.66E-04	4.93E-05	4.87E-05
DS4S	0.333	-	-	8.54E-05	-	-
DS5S	0.428	1.66E-03	2.02E-04	8.03E-05	4.45E-05	3.22E-05
DS6S	0.547	1.62E-03	-	5.34E-05	4.19E-05	2.31E-05
DS7S	0.747	1.56E-03	2.19E-04	4.53E-05	3.59E-05	8.80E-06
DS8S	1.035	1.35E-03	1.57E-04	1.89E-05	2.68E-05	2.00E-06
DS9S	1.517	1.02E-03	1.12E-04	9.18E-06	1.94E-05	1.30E-06
DS10S	2.145	9.64E-04	9.99E-05	7.66E-06	1.66E-05	1.20E-06
DS11S	2.733	9.64E-04	8.80E-05	8.97E-06	1.40E-05	1.11E-06
DS12S	3.435	1.09E-03	8.94E-05	6.24E-06	1.07E-05	1.13E-06
DS13S	4.318	1.02E-03	6.90E-05	4.76E-06	6.81E-06	9.81E-07
DS14S	5.170	1.08E-03	7.26E-05	7.08E-06	4.62E-06	9.70E-07
DS15S	6.038	1.01E-03	7.28E-05	8.70E-06	4.10E-06	9.73E-07
DS16S	7.062	9.92E-04	7.14E-05	8.50E-06	4.37E-06	9.54E-07
DS17S	8.047	8.98E-04	6.14E-05	7.49E-06	4.89E-06	8.28E-07
DS18S	9.125	8.36E-04	5.14E-05	7.21E-06	2.99E-06	7.03E-07